5-2018

Exploiting Treg Plasticity and Immune Cell Metabolism to Control Stromal Keratitis

Siva Karthik Varanasi
University of Tennessee, svaranas@vols.utk.edu

To the Graduate Council:

I am submitting herewith a dissertation written by Siva Karthik Varanasi entitled "Exploiting Treg Plasticity and Immune Cell Metabolism to Control Stromal Keratitis." I have examined the final electronic copy of this dissertation for form and content and recommend that it be accepted in partial fulfillment of the requirements for the degree of Doctor of Philosophy, with a major in Life Sciences.

Barry T. Rouse, Major Professor

We have read this dissertation and recommend its acceptance:

Stephen J Kennel, Albrecht G. Vonarnim, Jonathan S. Wall

Accepted for the Council:

Dixie L. Thompson

Vice Provost and Dean of the Graduate School

(Original signatures are on file with official student records.)

Exploiting Treg Plasticity and Immune Cell Metabolism to Control Stromal Keratitis

A Dissertation Presented for the
Doctor of Philosophy
Degree
The University of Tennessee, Knoxville

Siva Karthik Varanasi
May 2018

DEDICATION

I dedicate my thesis to my family and to my future better half Sushmitha Vijaya Kumar who loved me unconditionally and supported me throughout this journey.

ACKNOWLEDGEMENTS

This work would not be possible without the help from many people to whom I am ever obliged. First and foremost, I would like to thank Dr. Barry Rouse for his continued support and motivation throughout my PhD. You are a tremendous mentor and a great inspiration to me. I have thoroughly enjoyed all our scientific discussion and appreciate all his efforts in helping me become better researcher.

I would like to also express my gratitude to all my committee member that include Dr. Jonathan Wall, Dr. Albrecht von Arnim and Dr. Stephen Kennel for all their encouragement and support. Dr. Sarah Lebis for her helpful discussions. All of them played a vital role in shaping my scientific career. My sincere thanks to my collaborators Dr. Dallas Donohoe and Dr. Igor Nosonkin without whom I would not have had the opportunity to conduct such elegant research.

I would also thank my colleagues Pradeep, Fernanda, Sid, Naveen, Ujjal, Leon, Pranay and Joseph. All of them were a great support system and helped me stay sane through this interesting ride. The endless cups of coffee and scientific debates with Sid have truly shaped by PhD. Many thanks to all my friends in the GST program. My sincere thanks to GST department to recruit me and Terrie Yates for all her help.

Last but not the least, I would like to thank my parents and my girlfriend Sushmitha who have always been my pillars of support. To my sisters, Sirisha and Anusha who were always encouraging and proud of my accomplishments. I am truly blessed to have such a supportive family.

ABSTRACT

Ocular infections with Herpes Simplex virus (HSV) can have damaging consequences one of which is the loss of vision due to a chronic inflammatory reaction. T cells of the Th1 subset appear to be the main orchestrators of the inflammatory reaction. Certain components of the host immunity help to suppress the severity of lesions. My research focuses on one such protective component - CD4 regulatory T cells (Treg). We showed that Treg can initially function to suppress lesion development but this function can be lost and become pro-inflammatory. This provided the challenge of why this so-called plasticity occurred and how might it be prevented from developing. I was able to show that inhibiting the epigenetic modification occurring within the Foxp3 gene curbed the Treg plasticity. This reversal of plasticity was sufficient to enhance the control of SK lesion severity.

Another focus of my research was to find ways to rebalance immune subsets in SK lesions. We pioneered a new approach which exploited different metabolic requirements for the pro-inflammatory and regulatory T cells in lesions. Pro-inflammatory T cells such as Th1 use glucose for its function, whereas Treg rely on fatty acid oxidation and to a lesser extent on glucose. Using 2-Deoxyglucose which inhibits glucose utilization, the pro-inflammatory Th1 were affected but not Treg thereby reducing lesion severity. It was important not to impair glucose utilization when replicating virus was present since this could result in virus spreading to the brain to cause encephalitis.

We also evaluated if Treg were involved in repairing SK lesions. We could show that Treg within the cornea made a tissue repair molecule called Amphiregulin peaking during lesion development. This expression of Amphiregulin was partly dependent on the cytokines IL-18 and IL-12 which acted together to induce the expression of Amphiregulin. Moreover, enhancing the levels of IL-18 in the cornea using an expression plasmid helped resolve SK lesion severity, an effect which correlated with increased Amphiregulin expression by Treg.

In conclusion, my studies revealed several innovative approaches which might be moved to the clinic to help minimize the consequence of an important cause of human blindness.

TABLE OF CONTENTS

LIST OF FIGURES

ABBREVIATIONS

HSV-1 Herpes Simplex virus type 1
SK Herpes Stromal Keratitis
Treg Regulatory T cells
Th1 T helper 1 cells (Interferon producing CD4 T cells)
Aza Azacytidine
RA Retinoid acid
2DG 2-Deoxy Glucose
DNMT3a DNA methyltransferase 3a
DLN Draining lymph node
FACS Fluorescence activated cell sorting
Th17 T helper 17 cells (IL-17 producing CD4+ T cells)
IFNγ Interferon gamma
HSE-Herpes Simplex Encephatitis
Amp-Amphiregulin
IL-18R Interleukin 18 Receptor
STAT Signal transducer and activator of transcription
TSDR-Treg Specific Demethylating region
Q-RT-PCR Quantitative RT-PCR
PFU Plaque Forming Units
MOI multiplicity of Infection
IL Interleukin
TGFβ Transforming Growth Factor
EGFR Epidermal Growth Factor
WT Wildtype
KO Knockout
PMA phorbol 12-myristate 13-acetate
TG Trigeminal ganglion
H&E Hematoxylin and eosin
i.p Intraperitoneal
i.v Intravenous
µl microliter
ml milliliter
ng nanogram

CHAPTER 1
BACKGROUND AND OVERVIEW

Some of the Information in this chapter is reproduced from a publication accepted in Current opinion in virology by Siva Karthik Varanasi, Barry T Rouse.

Siva Karthik Varanasi, Barry T Rouse. How host metabolism impacts on virus pathogenesis. Current opinion in virology. 2018 Feb 28

Herpes simplex virus Infection

Herpes viruses are a group of large enveloped DNA viruses that contribute to one of the most common virus infections in the world. Herpes simplex virus belongs to the alpha herpes virus subfamily which primarily targets neurons for their long-term residency . While Herpes Simplex Virus type 1 (HSV-1) is often transmitted and associated with facial lesions or cold sores, type 2 (HSV-2) is sexually transmitted and usually shows genital lesions . Herpes simplex viruses develop an intricate relationship with the host and upon infection the virus replicates in the mucosal epithelia while gaining access to the sensory ganglion to set up latency. Periodically, the virus reactivates in the sensory ganglion and sheds back to the mucosal surface causing lesions. Although there are multiple reasons for why and when the virus reactivates, dysregulation of immune signaling has been implicated to be one of the mechanisms involved . With HSV-1 infection, reactivation of virus in the trigeminal ganglion can lead to three main outcomes depending on the location of shedding. 1. Virus can shed to the oral mucosa to cause cold sores. 2. Virus can shed to the cornea to cause keratitis 3. Rarely virus can enter the brain to cause encephalitis .

Herpes stromal keratitis

With more than 500,000 people infected with ocular herpes, Herpes stromal keratitis (SK) is one of the leading causes of infectious blindness in developed countries . Stromal keratitis in humans is usually a consequence of an overt immune inflammatory response to repeated virus reactivation episodes in the cornea resulting in the corneal tissue damage. Both primary infection and reactivation mouse models have provided valuable information on mechanisms involved in SK pathogenesis. In the primary infection mouse model the initial phase of virus replication results in a robust immune response that results both in viral clearance as well as triggering a chronic inflammation that causes tissue damage . The innate and adaptive immune contributions to SK are briefly described below.

Innate immune responses

Innate immune responses are critical for the control of virus replication in the cornea. Various innate immune cells such as dendritic cells, macrophages, natural killer cells, neutrophils and monocytes have been identified during the acute phase of infection. Viral components trigger innate immune cells to secrete various inflammatory components that include various cytokines like IFN-α/β, IL-1β, IL-6 and TNF-α and chemokines such as MIP-1α, MIP-1β, MIP-2 and MCP-1. Together, these molecules help clear virus but in doing so they also bring in more inflammatory cells of both innate and adaptive immune origin that contributes to tissue damage . Defects in these innate immune responses results in uncontrolled virus replication and often lead to virus induced encephalitis as observed in humans and mouse models .

Adaptive immune responses

The initial wave of innate immune responses causes the release of various chemokines and activation of adaptive immune cells, mainly T cells and B cells. Although, the contribution of B cell responses to SK lesion severity is not yet clear, B cells play a protective role by controlling virus replication. Thus, B-cell deficient mice were shown to be more susceptible to virus induced encephalitis compared to wild type animals . The SK lesion is mainly orchestrated by T cells, particularly CD4 T cells . CD8 T cells appear

to be more relevant in the trigeminal ganglion where they play a protective role and may help sustain latency . Thus mice showing defective CD8 T cells responses show increased susceptibility to HSV infection which can result in the encephalitis . On the contrary, CD4 T cells that are primary orchestrators in corneal inflammation, play a helper hand in TG .

CD4 T cells

Upon antigen presentation by antigen presenting cells (APC), naive CD4 T cells quickly differentiate into at least four T cell subsets (lineages) depending on the cytokine environment. For example, IL-12 induces IFN-gamma secreting Th1, IL-6 and TGF-beta induces IL-17A secreting Th17 cells, IL-4 induces IL-4 secreting Th2 cells and TGF-beta induces Foxp3 expressing regulatory T cells (Treg) . Various transcription factors are associated with and are critical for the differentiation of individual T cell subsets. For instance the transcription factor T-bet mediates the differentiation of Th1 cells, the transcription factor RORgt for the differentiation of Th17 cells, the transcription factor GATA3 for the differentiation of Th2 subsets and the transcription factor Foxp3 for Treg differentiation. While Th1, Th17 and Th2 subset of T cells have pro-inflammatory functions, Treg play an anti-inflammatory role, however, functional and phenotypic plasticity within lineages do exist . Both Th1 and Th17 cells were shown to orchestrate lesion development by inducing the recruitment of inflammatory innate immune cells such as neutrophils and macrophages to cause tissue damage. In contrast, Treg play a protective role. For instance, depletion of Treg or reduction in their function results in increased lesion severity .

Regulatory T cells

Regulatory T cells (Treg) are a subset of T cells that have both anti-inflammatory and tissue reparative properties. Treg are characterized by their expression of the transcription factor Foxp3 which is critical for maintenance of the anti-inflammatory functions that include expression of surface molecules such as CTLA-4, GITR, OX-40, NRP-1, CD39, Lag-3, CD25, secretory molecules such as IL-10, ROS TGF-beta, granzymes, and IL-35 . Based on their developmental origin, Treg can be classified into natural Treg (nTreg) if they derive from the thymus or referred to as induced Treg (iTreg) if the Treg originate in the periphery. While the expression of molecules such as Neuropilin-1, Helios, IKAROS and IL-2ra (CD25) has been associated with nTreg in an unimmunized host, inflammation drives the expression of these molecules (CD25, Nrp1, Helios etc.) in iTreg. Another significant difference between nTreg and iTreg is in their differential CpG DNA methylation pattern within the Foxp3 gene locus especially in the intron-2 region also referred to as Treg Specific Demethylated Region (TSDR) . While, the TSDR is methylated in the iTreg population, TSDR stays demethylated in the nTreg. Thus the methylation status of TSDR acts as a good marker to distinguish nTreg and iTreg population. . TSDR methylation patterns are not only important to distinguish Treg populations but also indicate the stable nature of Foxp3 gene expression and thus the maintenance Treg specific anti-inflammatory functions. For instance, Treg that have a methylated TSDR (iTreg), lose their Foxp3 expression when exposed to pro-inflammatory cytokines and attain the characteristics of effector T cells (Th1/Th17/Th2). However, Treg whose TSDR region is demethylated (nTreg) are resistant to such plasticity . Hence,

approaches that inhibits the methylation or promotes demethylation of TSDR region may enhance the stability of Treg and can be likely useful to control SK.

Besides anti-inflammatory functions, Treg also perform tissue reparative functions to maintain tissue homeostasis. Studies on various tissues such as intestines, skin, lungs and muscles have shown that Treg can be involved in tissue repair and promote wound healing . Although the complete list of tissue repair molecules secreted by Treg is yet to be identified, two molecules were shown to initiate the tissue reparative process are Amphiregulin (Areg) and Jag-1. While the role of Jag-1 signaling in cornea and other tissues remain elusive, Areg has long been studied for its role wound healing in various tissues. However, the role of Treg in promoting tissue repair or wound healing during HSV induced damage is currently being studied.

Host-Immune metabolism

Few if any viruses kill all the hosts they infect but instead cause a broad range of consequences. The outcome is affected by properties of the virus itself, the circumstances of infection (such as dose and route of delivery) and several variables within the host which include genetics, age, and previous experience with other agents and the makeup of microbes that inhabit the gut and other locations . A poorly studied variable that could affect the outcome of virus infections is host metabolism, the topic of this brief review. We strive to answer a number of questions and speculate if manipulating the metabolic status of infected persons could be a useful strategy to shape the consequences of a virus infection.

Some lessons to be learned

Immunologists rediscovered their biochemistry of metabolism quite recently and several informative reviews have been written . Basically, cellular components of both innate and adaptive immunity adopt different primary means of generating energy and biosynthetic products to support their immune functions. In addition, activated cells responding to immune stimuli reprogram their metabolism and use different pathways compared to those adopted by resting cells. As elegantly recounted by Luke O'Neil, there are six major metabolic pathways which immune cells differentially employ to sub-serve their functions . These pathways include glycolysis, oxidative phosphorylation, pentose phosphate pathway, fatty acid oxidation, fatty acid synthesis and amino acid metabolism. To date, most investigations have focused on pathways that provide cells with energy, biosynthesis, and redox balance. For instance, naïve T cells, memory T cells and some T cells with regulatory function (Treg) require few nutrients and all use oxidative phosphorylation (oxphos) supported by oxidation of fatty acids to supply their energy. However, activated immune cells that are involved in pathogen clearance and inflammation, such as CD4, CD8 T cells and M1 type macrophages, derive their energy mainly from glucose via aerobic glycolysis . These effectors also take up amino acids, such as glutamine, to generate intermediates which enter the tricarboxylic acid cycle. This generates products that include coenzymes and fatty acids which provide metabolic precursors for energy and biosynthesis (see Fig 1.1). Hence, nutrient availability and how they are used by an immune cell becomes a critical issue which helps determine the efficacy of an immune response. A major interest has been to explore how manipulating the balance of oxphos and glycolytic metabolism can be used to shape the course of

immune events in autoimmunity and cancers , but few studies have related metabolic events to the outcome of infectious diseases. We demonstrate that host metabolism can have a major effect on virus infections and speculate about the value of metabolic profiling to predict the outcome of infections.

Does nutrient availability influence the outcome of virus infection?

It seems logical to assume that malnutrition could affect the outcome of a virus infection and observations have linked starvation, obesity or dietary deficiencies to changes in responses to some virus infections . However, at least with human virus infections, the cause and effect evidence is scanty and usually provides no mechanistic explanation for observed changes in susceptibility. It is known that nutritional effects such as increased sugars and fat intake can change the number and function of immune cell types , but how this relates to the expression of virus infection requires further investigation. One of the more complete studies on nutritional consequences to infections was reported by the Medzhitov group . They evaluated the effects of calorie deprivation and supplementation on the outcome of some viral and bacterial infections in mice. They showed that deprivation increased susceptibility to a neurotropic strain of influenza virus, yet increased resistance to bacterial infections. In addition, force-feeding with extra glucose saved the mice from virus infection, but made them more susceptible to bacteria. They associated these effects with glucose metabolism, since inhibiting glucose utilization with 2-deoxy glucose (2DG) led to virus-induced lethality, but survival from bacterial infection. This outcome did not correlate with effects of 2DG on immune responsiveness, but was attributed to effects on ER stress responses in the brain to virus–induced interferon induction. This uncontrolled ER stress response resulted in neuronal apoptosis through induction of a pro-apoptotic protein - CHOP. Thus, inhibition of glucose utilization during virus infection led to CHOP dependent death of mice. Additionally, in a system using poly (I:C) to mimic a virus infection, animals treated with 2DG also succumbed to a similar ER stress mediated apoptotic response in the CNS .

Another example where inhibition of glucose utilization led to severe consequences was observed following ocular HSV infection in mice . When treated with 2DG during acute infection, the majority of animals developed lethal encephalitis and virus was present in the CNS. The outcome was proposed to result from inadequate control of virus replication at the infection site because of suppressed innate immunity, along with less efficacious CD8 T cell control of virus in the local nerve ganglia.

There are situations where impaired glucose utilization can limit the damage caused by a virus infection. Such a circumstance was observed where virus caused tissue lesions by an immunopathological mechanism . Accordingly, animals ocularly infected with HSV develop chronic inflammatory lesions of stromal keratitis (SK) and express mild hyperglycemia. However, if given 2DG when lesions were initiating these were minimized and animals recovered. This 2DG therapy appeared to act by inhibitory effects on the lesion orchestrating pro-inflammatory T cells, but spared the function of the anti-inflammatory Treg population known to constrain SK severity .

Another nutritional situation suspected to influence viral pathogenesis is protein deprivation. For example, mice fed a low protein diet experienced increased mortality to influenza, LCMV as well as Sendai virus infections . The diet was associated with higher viral titers and reduced numbers and function of virus specific CD8 T cells and NK cells. In addition, total number of IFN-γ, TNF-α and IL-2 producing memory CD8 T cells were

reduced likely accounting for less protection from reinfection . More studies are needed at a mechanistic level to explain how protein deprivation results in heightened susceptibility to virus infection.

Other essential components of nutrition are fatty acids, but few studies have linked lipid availability, or its utilization, to effects on viral pathogenesis. One study in mice did associate a diet rich in omega-3 fatty acids (considered anti-inflammatory) with increased susceptibility to influenza virus infection . The outcome was associated with reduced NK cell and neutrophil responses as well as reduced CD8 T cell activity which together resulted in diminished antiviral and immunopathological responses in the lungs. The dietary intake of both saturated and polyunsaturated fatty acids are also likely to affect virus infections. Saturated fatty acids are usually pro-inflammatory, whereas some polyunsaturated fatty acids and short chain fatty acids are usually anti-inflammatory . In one study, mice unable to use long chain polyunsaturated fatty acids, because the receptor-Fatty acid binding protein 5 (FABP5) was genetically deleted, became more susceptible to influenza infection . Although such animals controlled virus replication more effectively, the increased disease severity was attributed to more severe inflammatory responses in the lungs involving increased numbers of macrophages, neutrophils and pro-inflammatory T cells. Since FABP5 is also robustly expressed on other cell types such as lung epithelial cells and fibroblasts in addition to immune cells, a direct link between FABP5 knockdown and immunopathology still needs to be formally demonstrated.

Another potential mechanism, by which the dietary intake and utilization of fatty acids affect the antiviral response, is their surprising influence on the persistence of CD8+ resident memory T cells (TRM). In fact, a key metabolic difference between the two subsets of memory cells (central vs TRM) is the source of fatty acids they use to power fatty acid oxidation. While central memory T cells rely on cell intrinsic lipolysis to generate intracellular fatty acids , resident memory T cells take up fatty acids from the environment . Thus, knockdown of FABP5, or inhibition of fatty acid-oxidation in vivo with the drug etomoxir, resulted in a significantly reduced TRM response in the skin following dermal infection with vaccinia virus . Exactly how inhibition of FABP5 or etomoxir treatment led to the reduced TRM response requires further study.

The effect of dietary components on the expression of a virus infection is likely to be mediated at least in part by the balance of microbes in the gut. This balance can influence numerous systemic diseases that include cancers, autoimmunity and allergies, as well as responses to infections and vaccines. For example, dietary intake which favored the dominance of a particular species of *Clostridium* was protective against severe influenza virus infections in mice . The proposed mechanism involved was breakdown by Clostridia species of naturally occurring compounds called flavonoids (commonly found in certain foodstuffs like cranberries) to produce the metabolite desaminotyrosine (DAT). This molecule was proposed to enter the lungs and protect against influenza infection by enhancing type I IFN signaling . However, if levels of DAT were elevated once infection was already underway then the outcome was immunopathology and lethality. Thus, timing is relevant since some nutrients that potentially prevent virus infections might make matters worse if given at a different time.

What effect do metabolic diseases have on virus infections?

Based on the evidence presented above, one might expect that metabolic diseases should influence susceptibility to virus infections, but the issue is far from settled. Most reports focus on diabetes with some associating human diabetes with increased risk to influenza infection , but others finding no such association . Diabetic patients also have additional conditions not involving glucose metabolism, such as physical changes in several organs that could influence susceptibility to infection. The issue of relating metabolic changes in diabetes to susceptibility to virus infection should be resolvable using animal models of diabetes. The favored models have been induction of insulin dependent type one diabetes in mice using the drug streptozotocin, as well as a leptin receptor deficient mouse model which spontaneously develops a type two form of diabetes . Multiple observations indicate that diabetes in both models increased susceptibility to influenza ; but how this occurs and if it is the direct consequence of altered glucose metabolism remains unclear. Direct effects of hyperglycemia are perhaps unlikely, at least if the Medzhitov observations are generalizable. Thus in those studies, supplementing glucose levels made mice more resistant to influenza infection . It is possible that the increased susceptibility of diabetic mice to virus infections has non-metabolic explanations. These could include reduced antigen presentation , structural changes in the lung such as collapsed alveolar epithelia, increased vascular permeability , changes in fat tissues and effects on the gut microbiota . Thus, ascribing a cause for the increased susceptibility will be challenging.

The other metabolic disease with apparent association with susceptibility to virus infections is obesity with obese patients being prone to influenza-related hospitalizations and death. In fact, obese patients have many changes which could make them susceptible to infection. These include hyperglycemia, dyslipidemia, excess glucocorticoids and hyperinsulinemia , but how these signs might explain virus susceptibility is uncertain. Mouse models are being used to resolve the issues which include diet induced obesity (DIO) mice which suffer greater mortality during both primary and secondary influenza infections. In this instance, the reduced resistance was attributed to higher antigen specific CD8 T IFN-gamma responses that mediated lung immunopathology . Defective memory responses were advocated to explain susceptibility to secondary challenge . In obese mice, influenza infections may be more severe as a consequence of reduced wound healing of the lungs . However how metabolic events that occur during obesity explain increased viral susceptibility needs further study especially to identify the mechanisms involved.

Can metabolism be manipulated to influence the outcome of virus infection?

As mentioned before, the idea of manipulating metabolic events to counteract diseases has so far focused on cancer and autoimmunity. However, metabolic manipulation to control some virus disease syndromes is ripe for the taking although the topic at present largely represents unharvested fruit. We already discussed the potential of manipulating glucose metabolism since immune cells with different functions may differ on how they use glucose. Hence targeting glucose metabolism represents an approach to rebalance immune responsiveness. So far, the completed studies have focused on preventing glucose metabolism of aerobic glycolysis using 2DG therapy, but other approaches should be explored. For example, a potential target in the glucose metabolism field is the gene PFKFB3 (encoding 6-phosphofructo-2-kinase/fructose-2,6-

biphosphatase3) involved in glycolysis. Type I IFN driven expression of PFKFB3 is responsible for the hyperglycolytic state and the antiviral function of macrophages . Accordingly, inhibition of macrophage PFKFB3 resulted in poor control of RSV infection in mice . Expression of PFKFB3 may also be needed for T cell activation and pro-inflammatory function . In consequence, if a convenient way is found to increase PFKFB3 this could be a useful therapy against many virus infections.

Another potential approach to strengthen immunity against multiple viruses could be to augment the expression and activity of Hypoxia inducible factor 1a (HIF-1a). This molecule activates several glycolytic genes that include Glut1, PFKFB3, PGK1 and PKM2. Small molecule activators of HIF-1a are already available but these may not have been tested for antiviral effects. However, a recent study has shown that genetic ablation of VHL, a negative regulator of HIF-1a, selectively in CD8 T cells provided more effective control of chronic LCMV. However, increased mortality occurred which was associated with the enhanced function of immunopathological CD8+ T cells Thus, as with HSV pathogenesis, timing of procedures that modulate metabolism can be a critical issue . An alternative to targeting glucose for metabolic therapy is to use the amino acid glutamine which as mentioned before provides an alternate source of energy. Recently, a report showed that glutamine supplementation acted to stabilize HSV latency in mice . Thus, reactivation from latency was inhibited in mice fed glutamine, an outcome correlated with enhanced HSV specific CD8 T cell responses. Such responses act to prevent neurons in local nerve ganglia from replicating virus .

The hot topic of immune exhaustion might also benefit from therapies that target metabolism. Several chronic viral infections remain uncontrolled because their T cells fail to function adequately . Recently, it became evident that antiviral exhausted CD8 T cells displayed extensive mitochondrial changes that included elevated mitochondrial ROS production and reduced levels of PPARα co-activator 1α (PGC1α), a key transcriptional regulator controlling energy metabolism and mitochondrial biogenesis. Conceivably, these metabolic consequences could be reversed chemically which should be a far more economical approach than counteracting exhausted T cells with monoclonal antibodies (Fig 1.2).

References

1. Nicoll MP, Proença JT, Efstathiou S: The molecular basis of herpes simplex virus latency. *FEMS microbiology reviews* 2012, 36:684-705.
2. Grinde B: Herpesviruses: latency and reactivation–viral strategies and host response. *Journal of oral microbiology* 2013, 5:22766.
3. Rozenberg F, Deback C, Agut H: Herpes simplex encephalitis: from virus to therapy. *Infectious Disorders-Drug Targets (Formerly Current Drug Targets-Infectious Disorders)* 2011, 11:235-250.
4. Nahmias AJ, Roizman B: Infection with herpes-simplex viruses 1 and 2. *New England Journal of Medicine* 1973, 289:781-789.
5. Rouse BT, Sehrawat S: Immunity and immunopathology to viruses: what decides the outcome? *Nature reviews. Immunology* 2010, 10:514.
6. Rosato PC, Leib DA: Neurons versus herpes simplex virus: the innate immune interactions that contribute to a host–pathogen standoff. *Future virology* 2015, 10:699-714.
7. Halford WP, Gebhardt BM, Carr D: Mechanisms of herpes simplex virus type 1 reactivation. *Journal of virology* 1996, 70:5051-5060.
8. Du T, Zhou G, Roizman B: Modulation of reactivation of latent herpes simplex virus 1 in ganglionic organ cultures by p300/CBP and STAT3. *Proceedings of the National Academy of Sciences* 2013, 110:E2621-E2628.
9. Preston CM, Efstathiou S: Molecular basis of HSV latency and reactivation. 2007.
10. Fraser NW, Valyi-Nagy T: Viral, neuronal and immune factors which may influence herpes simplex virus (HSV) latency and reactivation. *Microbial pathogenesis* 1993, 15:83-91.
11. Lairson DR, Begley CE, Reynolds TF, Wilhelmus KR: Prevention of herpes simplex virus eye disease: a cost-effectiveness analysis. *Archives of ophthalmology* 2003, 121:108-112.
12. Liesegang TJ: Epidemiology of ocular herpes simplex. *Arch Ophthalmol* 1989, 107.
13. Dawson CR, Togni B: Herpes simplex eye infections: clinical manifestations, pathogenesis and management. *Survey of ophthalmology* 1976, 21:121-135.
14. Farooq AV, Shukla D: Herpes simplex epithelial and stromal keratitis: an epidemiologic update. *Survey of ophthalmology* 2012, 57:448-462.
15. Rouse BT: *Herpes simplex virus: pathogenesis, immunobiology and control*, vol 179: Springer Science & Business Media; 2012.
16. Giménez F, Suryawanshi A, Rouse BT: Pathogenesis of herpes stromal keratitis–a focus on corneal neovascularization. *Progress in retinal and eye research* 2013, 33:1-9.
17. Biswas PS, Rouse BT: Early events in HSV keratitis—setting the stage for a blinding disease. *Microbes and infection* 2005, 7:799-810.
18. Sarangi PP, Rouse BT: Herpetic keratitis. In *Ocular Disease*. Edited by: Elsevier; 2010:91-97.
19. Chew T, Taylor KE, Mossman KL: Innate and adaptive immune responses to herpes simplex virus. *Viruses* 2009, 1:979-1002.

20. Bryant-Hudson KM, Gurung HR, Zheng M, Carr DJ: Tumor necrosis factor alpha and interleukin-6 facilitate corneal lymphangiogenesis in response to herpes simplex virus 1 infection. *Journal of virology* 2014, 88:14451-14457.
21. Keadle TL, Usui N, Laycock KA, Miller JK, Pepose JS, Stuart PM: IL-1 and TNF-α are important factors in the pathogenesis of murine recurrent herpetic stromal keratitis. *Investigative ophthalmology & visual science* 2000, 41:96-102.
22. Azher TN, Yin X-T, Stuart PM: Understanding the role of chemokines and cytokines in experimental models of herpes simplex keratitis. *Journal of immunology research* 2017, 2017.
23. Casrouge A, Zhang S-Y, Eidenschenk C, Jouanguy E, Puel A, Yang K, Alcais A, Picard C, Mahfoufi N, Nicolas N: Herpes simplex virus encephalitis in human UNC-93B deficiency. *Science* 2006, 314:308-312.
24. Unterholzner L, Keating SE, Baran M, Horan KA, Jensen SB, Sharma S, Sirois CM, Jin T, Latz E, Xiao TS: IFI16 is an innate immune sensor for intracellular DNA. *Nature immunology* 2010, 11:997.
25. Zhang S-Y, Jouanguy E, Ugolini S, Smahi A, Elain G, Romero P, Segal D, Sancho-Shimizu V, Lorenzo L, Puel A: TLR3 deficiency in patients with herpes simplex encephalitis. *science* 2007, 317:1522-1527.
26. Sancho-Shimizu V, de Diego RP, Lorenzo L, Halwani R, Alangari A, Israelsson E, Fabrega S, Cardon A, Maluenda J, Tatematsu M: Herpes simplex encephalitis in children with autosomal recessive and dominant TRIF deficiency. *The Journal of clinical investigation* 2011, 121:4889-4902.
27. Guo Y, Audry M, Ciancanelli M, Alsina L, Azevedo J, Herman M, Anguiano E, Sancho-Shimizu V, Lorenzo L, Pauwels E: Herpes simplex virus encephalitis in a patient with complete TLR3 deficiency: TLR3 is otherwise redundant in protective immunity. *Journal of Experimental Medicine* 2011, 208:2083-2098.
28. Kurt-Jones EA, Chan M, Zhou S, Wang J, Reed G, Bronson R, Arnold MM, Knipe DM, Finberg RW: Herpes simplex virus 1 interaction with Toll-like receptor 2 contributes to lethal encephalitis. *Proceedings of the National Academy of Sciences of the United States of America* 2004, 101:1315-1320.
29. Wang JP, Bowen GN, Zhou S, Cerny A, Zacharia A, Knipe DM, Finberg RW, Kurt-Jones EA: Role of specific innate immune responses in herpes simplex virus infection of the central nervous system. *Journal of virology* 2012, 86:2273-2281.
30. Mansur DS, Kroon EG, Nogueira ML, Arantes RM, Rodrigues SC, Akira S, Gazzinelli RT, Campos MA: Lethal encephalitis in myeloid differentiation factor 88-deficient mice infected with herpes simplex virus 1. *The American journal of pathology* 2005, 166:1419-1426.
31. Daheshia M, Deshpande S, Chun S, Kuklin NA, Rouse BT: Resistance to herpetic stromal keratitis in immunized B-cell-deficient mice. *Virology* 1999, 257:168-176.
32. Lepisto AJ, Frank GM, Xu M, Stuart PM, Hendricks RL: CD8 T cells mediate transient herpes stromal keratitis in CD4-deficient mice. *Investigative ophthalmology & visual science* 2006, 47:3400-3409.
33. Niemialtowski M, Rouse B: Phenotypic and functional studies on ocular T cells during herpetic infections of the eye. *The Journal of Immunology* 1992, 148:1864-1870.

34. Russell R, Nasisse M, Larsen H, Rouse B: Role of T-lymphocytes in the pathogenesis of herpetic stromal keratitis. *Investigative ophthalmology & visual science* 1984, 25:938-944.
35. Leger AJS, Hendricks RL: CD8+ T cells patrol HSV-1-infected trigeminal ganglia and prevent viral reactivation. *Journal of neurovirology* 2011, 17:528-534.
36. Liu T, Khanna KM, Chen X, Fink DJ, Hendricks RL: CD8+ T cells can block herpes simplex virus type 1 (HSV-1) reactivation from latency in sensory neurons. *Journal of Experimental Medicine* 2000, 191:1459-1466.
37. Koyanagi N, Imai T, Shindo K, Sato A, Fujii W, Ichinohe T, Takemura N, Kakuta S, Uematsu S, Kiyono H: Herpes simplex virus-1 evasion of CD8+ T cell accumulation contributes to viral encephalitis. *The Journal of clinical investigation* 2017, 127:3784-3795.
38. Bhela S, Mulik S, Reddy PB, Richardson RL, Gimenez F, Rajasagi NK, Veiga-Parga T, Osmand AP, Rouse BT: Critical role of microRNA-155 in herpes simplex encephalitis. *The Journal of Immunology* 2014, 192:2734-2743.
39. Frank GM, Lepisto AJ, Freeman ML, Sheridan BS, Cherpes TL, Hendricks RL: Early CD4+ T cell help prevents partial CD8+ T cell exhaustion and promotes maintenance of herpes simplex virus 1 latency. *The journal of immunology* 2010, 184:277-286.
40. Zhu J, Yamane H, Paul WE: Differentiation of effector CD4 T cell populations. *Annual review of immunology* 2009, 28:445-489.
41. Caza T, Landas S: Functional and Phenotypic Plasticity of CD4. *BioMed research international* 2015, 2015.
42. Suryawanshi A, Veiga-Parga T, Rajasagi NK, Reddy PBJ, Sehrawat S, Sharma S, Rouse BT: Role of IL-17 and Th17 cells in herpes simplex virus-induced corneal immunopathology. *The Journal of Immunology* 2011, 187:1919-1930.
43. Niemialtowski M, Rouse B: Predominance of Th1 cells in ocular tissues during herpetic stromal keratitis. *The Journal of Immunology* 1992, 149:3035-3039.
44. Suvas S, Azkur AK, Kim BS, Kumaraguru U, Rouse BT: CD4+ CD25+ regulatory T cells control the severity of viral immunoinflammatory lesions. *The Journal of Immunology* 2004, 172:4123-4132.
45. Efimova O, Szankasi P, Kelley TW: Ncf1 (p47phox) is essential for direct regulatory T cell mediated suppression of CD4+ effector T cells. *PloS one* 2011, 6:e16013.
46. Schmidt A, Oberle N, Krammer PH: Molecular mechanisms of treg-mediated T cell suppression. *Frontiers in immunology* 2012, 3:51.
47. Sakaguchi S, Wing K, Onishi Y, Prieto-Martin P, Yamaguchi T: Regulatory T cells: how do they suppress immune responses? *International immunology* 2009, 21:1105-1111.
48. Sakaguchi S, Yamaguchi T, Nomura T, Ono M: Regulatory T cells and immune tolerance. *Cell* 2008, 133:775-787.
49. Lin X, Chen M, Liu Y, Guo Z, He X, Brand D, Zheng SG: Advances in distinguishing natural from induced Foxp3+ regulatory T cells. *International journal of clinical and experimental pathology* 2013, 6:116.
50. Lal G, Zhang N, Van Der Touw W, Ding Y, Ju W, Bottinger EP, Levy DE, Bromberg JS: Epigenetic regulation of Foxp3 expression in regulatory T cells by DNA methylation. *The Journal of Immunology* 2009, 182:259-273.

51. Chen Q, Kim YC, Laurence A, Punkosdy GA, Shevach EM: IL-2 controls the stability of Foxp3 expression in TGF-β–induced Foxp3+ T cells in vivo. *The Journal of Immunology* 2011, 186:6329-6337.
52. Polansky JK, Schreiber L, Thelemann C, Ludwig L, Krüger M, Baumgrass R, Cording S, Floess S, Hamann A, Huehn J: Methylation matters: binding of Ets-1 to the demethylated Foxp3 gene contributes to the stabilization of Foxp3 expression in regulatory T cells. *Journal of molecular medicine* 2010, 88:1029-1040.
53. Floess S, Freyer J, Siewert C, Baron U, Olek S, Polansky J, Schlawe K, Chang H-D, Bopp T, Schmitt E: Epigenetic control of the foxp3 locus in regulatory T cells. *PLoS biology* 2007, 5:e38.
54. Ohkura N, Kitagawa Y, Sakaguchi S: Development and maintenance of regulatory T cells. *Immunity* 2013, 38:414-423.
55. Panduro M, Benoist C, Mathis D: Tissue tregs. *Annual review of immunology* 2016, 34:609-633.
56. Vasanthakumar A, Kallies A: The regulatory T cell: jack-of-all-trades. *Trends in immunology* 2015, 36:756-758.
57. Arpaia N, Green JA, Moltedo B, Arvey A, Hemmers S, Yuan S, Treuting PM, Rudensky AY: A distinct function of regulatory T cells in tissue protection. *Cell* 2015, 162:1078-1089.
58. Burzyn D, Kuswanto W, Kolodin D, Shadrach JL, Cerletti M, Jang Y, Sefik E, Tan TG, Wagers AJ, Benoist C: A special population of regulatory T cells potentiates muscle repair. *Cell* 2013, 155:1282-1295.
59. Ali N, Zirak B, Rodriguez RS, Pauli ML, Truong H-A, Lai K, Ahn R, Corbin K, Lowe MM, Scharschmidt TC: Regulatory T cells in skin facilitate epithelial stem cell differentiation. *Cell* 2017, 169:1119-1129. e1111.
60. Pearce EL, Pearce EJ: Metabolic pathways in immune cell activation and quiescence. *Immunity* 2013, 38:633-643.
61. O'Neill LA, Pearce EJ: Immunometabolism governs dendritic cell and macrophage function. *Journal of Experimental Medicine* 2016, 213:15-23.
62. O'Neill LA, Kishton RJ, Rathmell J: A guide to immunometabolism for immunologists. *Nature Reviews Immunology* 2016.
63. O'Sullivan D, Pearce EL: Targeting T cell metabolism for therapy. *Trends in immunology* 2015, 36:71-80.
64. Ritz BW, Gardner EM: Malnutrition and energy restriction differentially affect viral immunity. *The Journal of nutrition* 2006, 136:1141-1144.
65. Soares MP, Teixeira L, Moita LF: Disease tolerance and immunity in host protection against infection. *Nature Reviews Immunology* 2017, 17:83-96.
66. Buck MD, Sowell RT, Kaech SM, Pearce EL: Metabolic Instruction of Immunity. *Cell* 2017, 169:570-586.
67. Balmer ML, Hess C: Starving for survival—how catabolic metabolism fuels immune function. *Current Opinion in Immunology* 2017, 46:8-13.
68. Wang A, Huen SC, Luan HH, Yu S, Zhang C, Gallezot J-D, Booth CJ, Medzhitov R: Opposing effects of fasting metabolism on tissue tolerance in bacterial and viral inflammation. *Cell* 2016, 166:1512-1525. e1512.

69. Varanasi SK, Donohoe D, Jaggi U, Rouse BT: Manipulating Glucose Metabolism during Different Stages of Viral Pathogenesis Can Have either Detrimental or Beneficial Effects. *The Journal of Immunology* 2017, 199:1748-1761.
70. Veiga-Parga T, Sehrawat S, Rouse BT: Role of regulatory T cells during virus infection. *Immunological reviews* 2013, 255:182-196.
71. Chatraw JH, Wherry EJ, Ahmed R, Kapasi ZF: Diminished primary CD8 T cell response to viral infection during protein energy malnutrition in mice is due to changes in microenvironment and low numbers of viral-specific CD8 T cell precursors. *The Journal of nutrition* 2008, 138:806-812.
72. Taylor AK, Cao W, Vora KP, Cruz JDL, Shieh W-J, Zaki SR, Katz JM, Sambhara S, Gangappa S: Protein energy malnutrition decreases immunity and increases susceptibility to influenza infection in mice. *The Journal of infectious diseases* 2012, 207:501-510.
73. Pena-Cruz V, Reiss C, McIntosh K: Sendai virus infection of mice with protein malnutrition. *Journal of virology* 1989, 63:3541-3544.
74. Iyer SS, Chatraw JH, Tan WG, Wherry EJ, Becker TC, Ahmed R, Kapasi ZF: Protein energy malnutrition impairs homeostatic proliferation of memory CD8 T cells. *The Journal of Immunology* 2012, 188:77-84.
75. Schwerbrock NM, Karlsson EA, Shi Q, Sheridan PA, Beck MA: Fish oil-fed mice have impaired resistance to influenza infection. *The Journal of nutrition* 2009, 139:1588-1594.
76. Haghikia A, Jörg S, Duscha A, Berg J, Manzel A, Waschbisch A, Hammer A, Lee D-H, May C, Wilck N: Dietary fatty acids directly impact central nervous system autoimmunity via the small intestine. *Immunity* 2015, 43:817-829.
77. Angela M, Endo Y, Asou HK, Yamamoto T, Tumes DJ, Tokuyama H, Yokote K, Nakayama T: Fatty acid metabolic reprogramming via mTOR-mediated inductions of PPARγ directs early activation of T cells. *Nature communications* 2016, 7:13683.
78. Gally F, Kosmider B, Weaver MR, Pate KM, Hartshorn KL, Oberley-Deegan RE: FABP5 deficiency enhances susceptibility to H1N1 influenza A virus-induced lung inflammation. *American Journal of Physiology-Lung Cellular and Molecular Physiology* 2013, 305:L64-L72.
79. Guthmann F, Hohoff C, Fechner H, Humbert P, Börchers T, Spener F, Rüstow B: Expression of fatty-acid-binding proteins in cells involved in lung-specific lipid metabolism. *The FEBS Journal* 1998, 253:430-436.
80. O'Sullivan D, van der Windt GJ, Huang SC-C, Curtis JD, Chang C-H, Buck MD, Qiu J, Smith AM, Lam WY, DiPlato LM: Memory CD8+ T cells use cell-intrinsic lipolysis to support the metabolic programming necessary for development. *Immunity* 2014, 41:75-88.
81. Pan Y, Tian T, Park CO, Lofftus SY, Mei S, Liu X, Luo C, O'Malley JT, Gehad A, Teague JE: Survival of tissue-resident memory T cells requires exogenous lipid uptake and metabolism. *Nature* 2017, 543:252-256.
82. Maslowski KM, Mackay CR: Diet, gut microbiota and immune responses. *Nature immunology* 2011, 12:5-9.
83. Van Den Elsen LW, Poyntz HC, Weyrich LS, Young W, Forbes-Blom EE: Embracing the gut microbiota: the new frontier for inflammatory and infectious diseases. *Clinical & translational immunology* 2017, 6:e125.

84. Steed AL, Christophi GP, Kaiko GE, Sun L, Goodwin VM, Jain U, Esaulova E, Artyomov MN, Morales DJ, Holtzman MJ: The microbial metabolite desaminotyrosine protects from influenza through type I interferon. *Science* 2017, 357:498-502.
85. Allard R, Leclerc P, Tremblay C, Tannenbaum T-N: Diabetes and the severity of pandemic influenza A (H1N1) infection. *Diabetes care* 2010, 33:1491-1493.
86. Jiménez-García R, Hernández-Barrera V, Rodríguez-Rieiro C, Lopez de Andres A, de Miguel-Diez J, Jimenez-Trujillo I, Gil de Miguel A, Carrasco-Garrido P: Hospitalizations from pandemic Influenza [A (H1N1) pdm09] infections among type 1 and 2 diabetes patients in Spain. *Influenza and other respiratory viruses* 2013, 7:439-447.
87. King AJ: The use of animal models in diabetes research. *British journal of pharmacology* 2012, 166:877-894.
88. Hulme KD, Gallo LA, Short KR: Influenza Virus and Glycemic Variability in Diabetes: A Killer Combination? *Frontiers in microbiology* 2017, 8.
89. Jansen A, van Hagen M, Drexhage HA: Defective maturation and function of antigen-presenting cells in type 1 diabetes. *The Lancet* 1995, 345:491-492.
90. Pitocco D, Fuso L, Conte EG, Zaccardi F, Condoluci C, Scavone G, Incalzi RA, Ghirlanda G: The diabetic lung-a new target organ? *The review of diabetic studies: RDS* 2012, 9:23.
91. Musso G, Gambino R, Cassader M: Obesity, diabetes, and gut microbiota. *Diabetes care* 2010, 33:2277-2284.
92. Zhang Y, Zhang H: Microbiota associated with type 2 diabetes and its related complications. *Food Science and Human Wellness* 2013, 2:167-172.
93. Morgan OW, Bramley A, Fowlkes A, Freedman DS, Taylor TH, Gargiullo P, Belay B, Jain S, Cox C, Kamimoto L: Morbid obesity as a risk factor for hospitalization and death due to 2009 pandemic influenza A (H1N1) disease. *PloS one* 2010, 5:e9694.
94. Jung UJ, Choi M-S: Obesity and its metabolic complications: the role of adipokines and the relationship between obesity, inflammation, insulin resistance, dyslipidemia and nonalcoholic fatty liver disease. *International journal of molecular sciences* 2014, 15:6184-6223.
95. Smith AG, Sheridan PA, Harp JB, Beck MA: Diet-induced obese mice have increased mortality and altered immune responses when infected with influenza virus. *The Journal of nutrition* 2007, 137:1236-1243.
96. Milner JJ, Rebeles J, Dhungana S, Stewart DA, Sumner SC, Meyers MH, Mancuso P, Beck MA: Obesity increases mortality and modulates the lung metabolome during pandemic H1N1 influenza virus infection in mice. *The Journal of Immunology* 2015, 194:4846-4859.
97. Karlsson EA, Sheridan PA, Beck MA: Diet-induced obesity impairs the T cell memory response to influenza virus infection. *The Journal of Immunology* 2010, 184:3127-3133.
98. O'Brien KB, Vogel P, Duan S, Govorkova EA, Webby RJ, McCullers JA, Schultz-Cherry S: Impaired wound healing predisposes obese mice to severe influenza virus infection. *Journal of Infectious Diseases* 2011, 205:252-261.
99. Jiang H, Shi H, Sun M, Wang Y, Meng Q, Guo P, Cao Y, Chen J, Gao X, Li E: PFKFB3-driven macrophage glycolytic metabolism is a crucial component of innate antiviral defense. *The Journal of Immunology* 2016, 197:2880-2890.

100. Telang S, Clem BF, Klarer AC, Clem AL, Trent JO, Bucala R, Chesney J: Small molecule inhibition of 6-phosphofructo-2-kinase suppresses t cell activation. *Journal of translational medicine* 2012, 10:95.
101. Liu W, Shen S-M, Zhao X-Y, Chen G-Q: Targeted genes and interacting proteins of hypoxia inducible factor-1. *International journal of biochemistry and molecular biology* 2012, 3:165.
102. Doedens AL, Phan AT, Stradner MH, Fujimoto JK, Nguyen JV, Yang E, Johnson RS, Goldrath AW: Hypoxia-inducible factors enhance the effector responses of CD8+ T cells to persistent antigen. *Nature immunology* 2013, 14:1173-1182.
103. Wang K, Hoshino Y, Dowdell K, Bosch-Marce M, Myers TG, Sarmiento M, Pesnicak L, Krause PR, Cohen JI: Glutamine supplementation suppresses herpes simplex virus reactivation. *The Journal of Clinical Investigation* 2017, 127.
104. Kahan SM, Wherry EJ, Zajac AJ: T cell exhaustion during persistent viral infections. *Virology* 2015, 479:180-193.
105. Fisicaro P, Barili V, Montanini B, Acerbi G, Ferracin M, Guerrieri F, Salerno D, Boni C, Massari M, Cavallo MC: Targeting mitochondrial dysfunction can restore antiviral activity of exhausted HBV-specific CD8 T cells in chronic hepatitis B. *Nature Medicine* 2017, 23:327-336.
106. Bengsch B, Johnson AL, Kurachi M, Odorizzi PM, Pauken KE, Attanasio J, Stelekati E, McLane LM, Paley MA, Delgoffe GM: Bioenergetic insufficiencies due to metabolic alterations regulated by the inhibitory receptor PD-1 are an early driver of CD8+ T cell exhaustion. *Immunity* 2016, 45:358-373.

APPENDIX

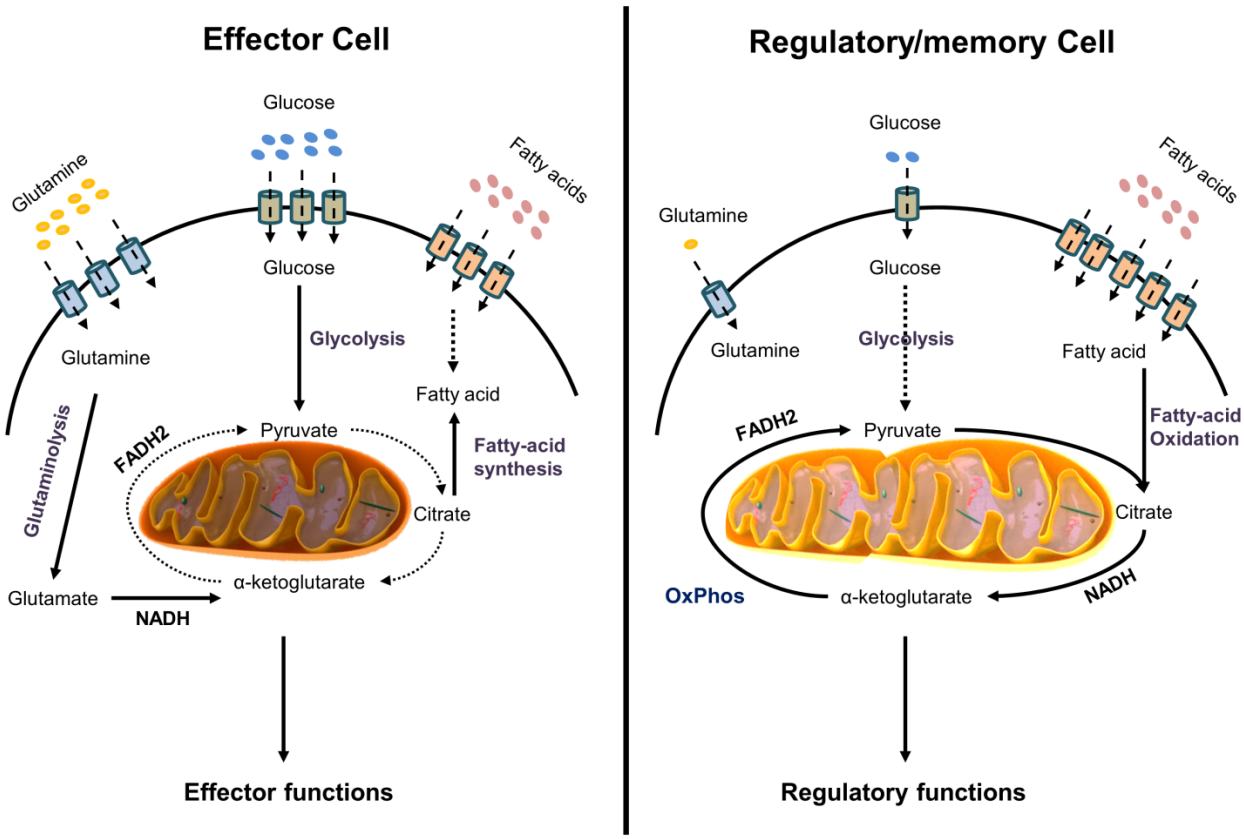

Figure 1. Metabolic differences in immune cells with effector functions versus cells with regulatory or memory functions.
(1) Effector immune cells take up glutamine and glucose to generate ATP and intermediates for amino acids and fatty acid synthesis (2) Regulatory and memory immune cells take up less glucose and glutamine molecules but instead take up more fatty acids that power mitochondria to generate ATP. Dominant metabolic pathways are shown in solid lines; less critical or studied pathways are shown in dotted lines.

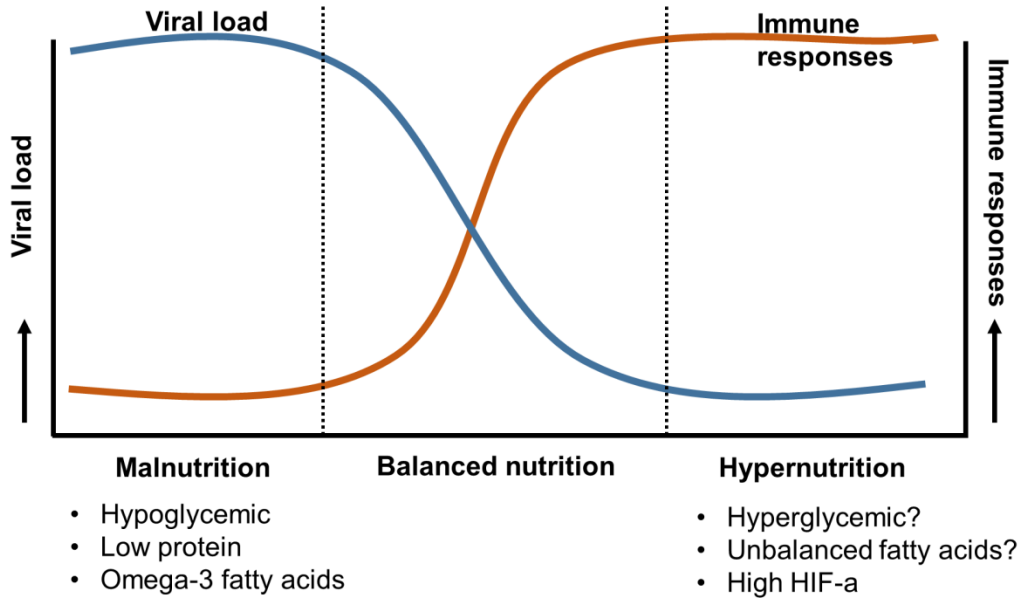

Figure 2. Proposed model of link between nutrition and immune responses to virus infection.
Both Hyper-nutrition and malnutrition have effects on immune function. Thus malnutrition can suppress immune functions and increase susceptibility to infections. Hyper-nutrition or dysregulated nutrition may cause overt immune responses and cause immunopathology. Thus, optimal nutritional and metabolic homeostasis is an important part of appropriate immune function and good health.

CHAPTER 2
THE PLASTICITY AND STABILITY OF REGULATORY T CELLS DURING VIRAL-INDUCED INFLAMMATORY LESIONS

Research described in this chapter is reproduced from a publication accepted in Journal of Immunology by Siddheshvar Bhela, Siva Karthik Varanasi, Ujjaldeep Jaggi, Sarah S Sloan, Naveen K Rajasagi, Barry T Rouse.

Abstract

Ocular infection with Herpes Simplex Virus causes a chronic T-cell mediated inflammatory lesion in the cornea. Lesion severity is affected by the balance of different CD4 T-cell subsets with greater severity occurring when the activity of regulatory T-cells is compromised. In the present report, fate-mapping mice were used to assess the stability of Treg function in ocular lesions. We show that cells that were once FoxP3+ functional Treg may lose FoxP3 and become Th1 cells which themselves could contribute to lesion expression. The instability mostly occurred with IL-2 receptor low Treg and was shown to be in part the consequence of exposure to IL-12. Lastly, in-vitro generated iTreg were shown to be highly plastic and capable of inducing SK when adoptively transferred into Rag1-/- mice, with 95% of iTreg converting into ex-Treg in the cornea. This plasticity of iTreg could be prevented when they were generated in the presence of Vitamin-C and Retinoic acid. Importantly, adoptive transfer of these stabilized iTreg to HSV-1 infected mice more effectively prevented the development of SK lesions than did the control iTreg. Our results demonstrate that CD25lo Treg and iTreg instability occurs during a viral immuno-inflammatory lesion and that its control may help avoid lesion chronicity.

Introduction

Ocular infection with herpes simplex virus type 1 (HSV-1) can result in a chronic immuno-inflammatory reaction in the cornea, which represents a common cause of human blindness . Studies in animal models have revealed that stromal keratitis (SK) lesions are orchestrated mainly by IFN-γ–producing CD4+ T cells (Th1) cells . The lesions are less severe and can even resolve if regulatory T cells (Treg), such as CD4 Foxp3 T cells, dominate over the proinflammatory CD4 T cell subsets . Lesions become far more severe if Treg are depleted prior to infection or even if suppressed in the face of ongoing infection . Thus lesions can be limited in severity if Treg function is optimized. Recent studies on some experimental models of autoimmunity have revealed that the function of Treg may be unstable in the face of an inflammatory environment . In fact Treg may lose their regulatory function and even take on proinflammatory activity and contribute to lesion expression. So far it is not known if Treg plasticity happens during a viral immune-inflammatory lesion and if the event helps explain why lesions become chronic and eventually fail to resolve. This issue is evaluated in the present report using a fate mapping mouse model system.

Reasons for plasticity are thought to be the consequence of either epigenetic modifications or posttranslational modifications . Several studies have shown that DNA demethylation of the Foxp3 conserved noncoding sequence 2 (CNS2), also named Treg-specific demethylated region (TSDR), is critical for stable expression of FoxP3 . Demethylation of CpG motifs allows critical transcription factors, such as Foxp3 itself and Runx1–Cbf-β complex, to bind to the TSDR region and keep the transcription of Foxp3 active in the progeny of dividing Treg . Another layer of epigenetic control involves the acetylation of the Foxp3 gene, which enforces FoxP3 expression and stability . Several other external stimuli such as proinflammatory cytokines can also influence Treg stability either by influencing the epigenetic status of the FoxP3 gene or by making posttranslational modification . Accordingly, activation of Treg in the presence of IL-6

leads to a STAT3-dependent decrease in Foxp3 protein and message accompanied by increased DNA Methyltransferase 1 (DNMT1) expression. These effects lead to methylation of the TSDR region of the Foxp3 gene, as well as reduced acetylation of histone 3 at the upstream promoter region of the gene . Another important cytokine that influences Treg stability is IL-2 . Accordingly, several recent studies correlate robust surface expression of the high affinity IL-2 receptor (CD25) with enhanced Foxp3 expression, suppressive function, and stability of the Treg phenotype .

In this report we use fate mapping mice to show that Treg plasticity occurs in a virus induced inflammatory reaction and might contribute to stromal keratitis lesion severity and chronicity by secreting proinflammatory cytokine IFN-γ. This plasticity of Treg occurred more readily in the CD25lo population of Treg and was in part due to proinflammatory cytokine IL-12. Additionally, we also show that iTreg are highly plastic in the SK microenvironment. Lastly of therapeutic interest we could limit iTreg plasticity both in-vitro and in-vivo by generating induced Treg in the presence of Vitamin C and Retinoic acid. Moreover these stabilized iTreg could reduce SK lesions more effectively compared to unstable iTreg when adoptively transferred to HSV infected mice. All these results suggest that stabilizing Treg might represent a process to be targeted to minimize lesion expression and their chronicity.

Results

Treg lose FoxP3 expression in the cornea after ocular HSV-1 infection and acquire a Th1 cell phenotype

To directly examine Treg plasticity in the cornea after HSV-1 ocular infection in-vivo, FoxP3Cre-GFP: Rosa26lsl-Td-Tomato mice (now referred to as fate mapping mice (FM mice)) were used. These mice allow Treg fate mapping and the ability to distinguish between cells that currently express from the cells that once expressed FoxP3 but now lack its expression (ex-Treg). FM mice have cells that can be distinguished by flow cytometric analysis into three main T cell populations that participate in SK lesions. Accordingly, Treg are (CD4+ GFP+ Tomato+), ex-Treg are (CD4+ Tomato+ GFP-) and lastly effector CD4 T cells are (CD4+ Tomato- GFP-) (Supplementary figure S2.1). It was evident that after HSV-1 ocular infection of FM mice that some of the Treg lineage cells in the cornea lost their GFP expression indicating their likely loss of Treg function. Such ex-Treg accounted for 38% of the total Treg population at day 8, 60% at day 15 and 35% at day 21 pi (Figure 2.1A). Curiously, the peak numbers of ex-Treg were evident in day 15 pi samples, which is the usual time when lesions are at their peak (Figure 2.1B).

To quantify the cytokine producing abilities of these ex-Treg, single cell suspensions of 3-4 collagen-digested pooled corneas from ocularly HSV-1 infected FM mice were stimulated at different times pi with PMA/ionomycin, followed by an intracellular cytokine detection assay. As shown in figure 2.1C at days 8 and 21 pi 33% of the ex-Treg became IFN- γ producers but at day 15, which is the peak of the disease, 80% of the ex-Treg were IFN-γ producers. Additionally, similar to ex-Treg numbers, the IFN- γ producing ex-Treg cells peaked at day 15 pi. Of particular interest, the percentage of exFoxp3 cells was increased particularly in the corneas (approx. 50%), as compared to DLN and spleen (approx. 19% and 25% respectively) at day 15pi (Supplementary figure 2.2A). The frequencies of IFN- γ produced by exFoxp3 cells were also higher in corneas (approx. 80

%) as compared to DLN and spleen (approx. 7% and 16% respectively) when measured at the same time pi (Supplementary figure 2.2B). Furthermore, intracellular cytokine production by corneal cells stimulated with a UV-inactivated viral Ag revealed a high percentage of ex-Treg (approx. 22%) that were HSV-specific Th1 cells at day 15pi (Figure 2.1E). All these results indicate that a substantial proportion of corneal Treg convert into Th1 ex-Treg after HSV-1 ocular infection. Of interest, some of the ex-Treg were HSV antigen specific indicating that such ex-Treg may have derived from the HSV specific Treg population.

CD25lo Foxp3+CD4+ Treg generate ex-Treg during HSV-1 induced inflammation

Several reports suggest that Treg are comprised of Foxp3-stable CD25hi and Foxp3-unstable CD25lo populations. These reports also show that CD25lo Treg have defective suppression, express less Foxp3 expression and had a moderately less demethylated TSDR compared to the CD25hi Treg. Similarly, in our system we could show that HSV-1 immune FACS sorted CD25lo Treg at day 15pi were less suppressive. and had a moderately less demethylated TSDR as compared to the CD25hi Treg (Figure 2.2A and B). Additionally, CD25lo Treg also showed less Foxp3 expression as compared to the CD25hi Treg, as measured by MFI (Figure 2.2C). These results led us to hypothesize that CD25lo Treg might be the main population that harbored uncommitted Treg in SK lesions. To evaluate if such CD25lo Treg were unstable in-vitro, CD4+ GFP+ T cells were sorted into CD25lo and CD25hi cells with purity >95% (Supplementary figure 2.3) from HSV-1 infected FoxP3-GFP mice at day 15pi and stimulated with anti-CD3/CD28+IL-2 (control) or CD3/CD28+IL-12 for 5 days. As shown in figure 2.2D, in the presence of pro-inflammatory cytokines IL-12, 25% of the CD25lo, but only 10% of the CD25hi Treg lost FoxP3 expression. However, in the control cultures that received IL-2 alone, minimal loss of FoxP3 expression was observed (approx. 10%). These results indicate that pro-inflammatory cytokine IL-12 can promote the conversion of antigen experienced CD25lo Treg into ex-Treg.

To evaluate FoxP3 stability of the two CD25lo and CD25hi Treg populations in vivo, FACS sorted HSV-1 immune Thy1.2 CD25lo and CD25hi Treg (gated on GFP+ cells) from FM mice were adoptively transferred into congenic Thy1.1 mice and these were infected via the footpad with HSV-1 24 hours later. The recipient mice were analyzed for the presence of donor T cells in the popliteal lymph node (PLN) and spleen at day 5 pi by reacting with anti-CD4 and anti-Thy1.2. As is evident from Figure 2.2E, 50% of the donor CD25lo Treg lost GFP expression and converted into ex-Treg. This compared to only 16.4% in the donor CD25hi Treg in the PLN of recipient animals (Figure 2.2E). Similar results were found in the spleen (data not shown).

To determine if ex-Treg could be derived from activated conventional T cells that transiently express Foxp3 or if ex-Treg could be converted back into Treg. The same experimental setup as above was used. Accordingly, similar numbers of FACS sorted effector T cells or ex-Treg cells from immunized FM mice were adoptively transferred into congenic Thy1.1 mice and these were infected via the footpad with HSV-1 24 hours later. The recipient mice were analyzed for the presence of donor T cells in the PLN and spleen at day 5 pi by reacting with anti-CD4 and anti-Thy1.2. As is evident from figure 2.2F, none of effector T cells or the ex-Treg cells showed any conversion into Treg. This suggests that transient upregulation of FoxP3 on effector T cells is not contaminating the ex-Treg population and that the ex-Treg population does not convert back into Treg during HSV-

1 induced inflammation. Taken together, our results show that HSV-1 immune CD25lo Treg showed defective suppression, had a partially methylated TSDR and were highly unstable cells that convert to ex-Treg under inflammatory conditions.

CD25lo Treg were increased in the cornea after HSV-1 ocular infection

To determine if the population of unstable CD25lo Treg increased in the cornea after HSV-1 ocular infection, FoxP3-GFP mice were ocularly infected with HSV-1 and corneas were collected, collagen digested and the recovered cells reacted with anti-CD4 and anti-CD25 antibodies at days 8, 15 and 21 pi. As shown in figure 2.3A, the frequency of CD25lo Treg remained stable over time, but the numbers of CD25lo Treg increased as the disease progressed and reached a peak at day 15 pi. These results suggest that unstable CD25lo Treg population is present in the cornea at different days post infection and could contribute to the generation of ex-Treg in corneal lesions.

Ex-Treg are pathogenic and can cause SK

Previous results showed the presence of ex-Treg, Treg as well as conventional effector T cells in corneal lesions. To measure and compare the pathogenicity of ex-Treg, Treg and CD44hi T effectors, ex-Treg, CD25hi Treg and CD44hi FoxP3- T effectors were FACS sorted from DLNs and spleens of day 15 post infected FM mice. Equal numbers of each cell population were then transferred into T cell and B cell deficient Rag1-/-, which were infected ocularly 24h later with HSV-1. The recipients were monitored clinically over the next 10 days. Because HSV-1 infected Rag1-/- mice usually develop lethal herpetic encephalitis, infected recipient mice were given a source of anti-HSV-1 antibody (human IVIG) 2 days after infection, which allows mice to survive beyond day 6 pi and ensures optimal HSK development in surviving mice . Using this protocol our results showed that CD44hi T effectors and ex-Treg induced similar levels of SK severity (lesion score < 2.5) at day 10 pi (Figure 2.4A), while the control animals that received no cells or CD25hi Treg showed minimal lesions. In addition, T effectors and ex-Treg cells in subpools of collagen-digested corneas produced similar levels of IFN-γ (approx. 70%) as seen by the ICS assay after PMA/ionomycin stimulation (Figure 2.4B), while the control animals that received CD25hi Treg showed minimal IFN-γ production (approx. 15%). These results demonstrate that ex-Treg cells can function as pathogenic effector cells producing IFN-γ in the cornea and that these ex-Treg can induce SK with a similar severity to that caused by CD44hi T effector cells.

iTreg covert into ex-Treg and induce SK disease in Rag1-/- recipients

Previous reports show that naive T cells converted in-vitro into iTreg cells by TCR stimulation in the presence of IL-2 and TGF-β had methylated CpG sites in the FoxP3 CNS2 region, but could lose Foxp3 expression rapidly . However, whether or not FoxP3 instability of in-vitro induced iTreg results in pathogenic ex-Treg during HSV-1 infection remains to be substantiated. To test this possibility iTreg were generated from sorted naïve CD4+T cells from FM mice by stimulating them with anti-CD3/CD28 in the presence of IL-2 and TGF-β for 5 days. Tomato+ GFP+ iTreg cells were then FACS sorted and adoptively transferred into T cell and B cell deficient Rag1-/- mice 24 hours after ocular infection with HSV-1. Recipients were monitored clinically over the next 10 days. These mice were also given IVIG at day 2pi to protect them from lethal encephalitis as described in the previous section. At day 10 pi typical HSK lesions (score ≥2.5) were evident in the iTreg recipients at the time of sacrifice whereas only minimal lesions were evident at the same time in control animals that were infected but received no cell transfer (Figure 2.5A).

More importantly, 95% of the cells recovered from the corneas of the iTreg recipients lost FoxP3 expression and converted into ex-Treg in the SK lesions (Figure 2.5B). Moreover, 26% of the infiltrating CD4 T cells in the cornea produced IFN-γ as measured by the ICS assay after PMA/ionomycin stimulation (Figure 2.5C). This supports the notion that the iTreg had converted into Th1 cells in the SK microenvironment. Taken together our data show that iTreg were highly unstable and could convert into Th1 ex-Treg in an SK inflammatory micro- environment and that these cells contributed to SK expression.

iTreg generated in the presence of Vitamin C and RA were highly stable and resistant to conversion into ex-Treg.

A previous report had indicated that iTreg generated in the presence of Vitamin C and RA could substantially stabilize FoxP3 expression both in-vitro and in- vivo . This occurred in part by demethylating the TSDR region of the Foxp3 locus. Similarly, we could show that iTreg generated in the presence of Vitamin C + RA had an almost completely demethylated TSDR region (90%), whereas, in the control iTreg (without Vitamin C + RA) the TSDR was only minimally demethylated (12%) (Figure 2.6A). Furthermore, to show that Vitamin C + RA could stabilize iTreg in the face of inflammatory cytokines in the SK system, splenocytes from DO11.10 RAG2-/- animals (ova peptide specific and 98% naïve CD4+ T cells) were cultured in the presence of Treg differentiating conditions (anti-CD3/CD28 stimulation +IL-2 and TGF-β) either in the presence or absence of Vitamin C + RA. After 5 days of culture a few cells were harvested and cell numbers that expressed Foxp3 were recorded. The remaining cells were exposed either to IL-2 or IL-12 (Th1 condition) or IL-6 and TGF-beta (Th17 conditions) for an additional 3 days. FoxP3 expression was analyzed again at this time point and the % Foxp3 expression lost was calculated. In these experiments, IL-2 alone led to minimal loss of Foxp3 expression (approx. 8%), whereas exposure to IL-12 and IL-6 +TGF-β resulted in a significant loss of Foxp3 expression (approx. 30%) in control iTreg. In contrast, iTreg generated in the presence of Vitamin C + RA were significantly more stable and lost minimal (5-10%) Foxp3 expression when exposed to either Th1 or Th17 differentiating conditions (Figure 2.6B).

To evaluate in vivo stability of Foxp3 expression of iTreg cells generated in the presence of Vitamin C + RA, naive CD4+ T cells from FM mice were cultured in the presence of Treg differentiating conditions (anti-CD3/CD28 stimulation +IL-2 and TGF-β) either in the presence or absence of Vitamin C + RA. The control iTreg and Vitamin C + RA generated iTreg were adoptively transferred into congenic, HSV-1 ocularly infected Thy1.1 mice at 72hpi. Recipient mice were then analyzed for the presence of donor T cells in the DLN and spleen at day 15 pi by reacting with anti-CD4 and anti-Thy1.2. As evident from Figure 2.6C, 26-28% of the donor control iTreg lost GFP expression and converted into ex-Treg. This compared to a loss of only 3-7% in the recipients of Vitamin C + RA generated iTreg.

These results demonstrate that HSV-1 induced inflammation and pro-inflammatory cytokines IL-12 and IL-6 could promote the conversion of iTreg into ex-Treg and this conversion could be markedly inhibited when iTreg were generated in the presence of Vitamin C and RA.

Vitamin C+ RA stabilized iTreg more efficiently suppress SK lesions than do control iTreg

To evaluate if iTreg populations stabilized in vitro by induction in the presence of Vitamin C + RA were more effective at controlling SK lesions than un-stabilized iTreg, adoptive experiments were performed. The donor cell populations used to generate the both stabilized iTreg and control unstable iTreg were from DO11.10 RAG2-/- (OVA specific) mice as described in materials and methods. These mice were used because they provide a highly enriched naïve CD4 T cell population . Groups of Balb/c mice received the adoptive transfer 3 days after ocular infection and disease severity were followed until termination on day 15 pi. As shown in Figure 2.7A mice that received the stabilized iTreg population expressed significantly reduced lesions compared to those that received no iTreg. Similarly, mice that received the stabilized iTreg population showed a trend of reduced lesions compared to those that received unstable control iTreg population although no significance was achieved. Additionally, there were 1.8 fold reduced number of CD4+T cells and Th1 cells infiltrating the cornea in the mice that received the stabilized iTreg compared to those that received no iTreg (Figure 2.7B). Taken together, our data demonstrate that stabilized Vitamin C +RA generated iTreg were better at suppressing SK lesions compared to un-stabilized control iTreg.

Discussion

In this report, using fate mapping mice, we showed that Treg present in the cornea during a viral induced inflammatory reaction are unstable and can become ex-Treg with a Th1 phenotype. We also showed that the CD25lo Treg were highly plastic and converted into ex-Treg more readily than the stable CD25hi Treg subpopulation. Interestingly, the unstable CD25lo Treg were present in the cornea and this population increased with the progression of disease and followed the same pattern as the appearance of ex-Treg. The pro-inflammatory cytokine IL-12 and IL-6 was in part responsible for the generation of ex-Treg during SK development. Furthermore, ex-Treg displayed equivalent disease causing potential as effector T cells when cells were adoptively transferred in HSV-1 infected Rag1-/- animals. We also showed that the population of Treg generated in vitro from naïve CD4 T cells were highly unstable when transferred into lymphopenic Rag1-/- recipients with almost 95% of the iTreg converting into ex-Treg. Finally, we could show that Treg generated in-vitro in the presence of Vitamin C and RA produced a population with increased stability when exposed to an inflammatory environment either in-vitro or in-vivo. More importantly, the stabilized iTreg population was more efficient at reducing SK lesions as compared to control unstable iTreg when adoptively transferred in day 3 HSV-1 infected mice. Taken together our results demonstrate that instability of Treg function occurs in the inflammatory environment of a virus-induced lesion and that the converted ex-Treg can also participate in tissue damage, an event that may help explain chronicity.

It is becoming increasingly evident that diverse environmental stimuli can affect Treg stability acting by modulating epigenetic programing or posttranslational modifications . For example, proinflammatory cytokines such as IL-12, IL-6 and IL-1β could trigger a signaling pathway through their receptors on Treg. This could cause a loss of Foxp3 expression by several mechanisms. Thus, IL-1β induces the ubiquitinase

enzyme Stub1 that permits the ubiquitination of FoxP3 and its degradation . In addition, IL-6 leads to a STAT3-dependent decrease in Foxp3 protein and mRNA accompanied by increased DNMT1 expression. This effect results in methylation of the TSDR region of the Foxp3 gene, as well as diminished acetylation of histone 3 at the upstream promoter region of the gene . Additionally, IL-12 can activate the IL-12R-β2/STAT4-mediated signaling pathway, which causes the polarization towards the Th1 type Treg and loss of FoxP3 expression . In our report we showed that IL-12 and IL-6 could cause the loss of FoxP3 expression especially in CD25lo Treg and iTreg populations. A cytokine that has been shown to stabilize Treg is IL-2 by signaling through the IL-2R (CD25) on the Treg cells . Accordingly, several recent studies in mice and humans showed that robust CD25 expression on Treg correlated with enhanced FoxP3 expression, suppressive function and stability of the Treg phenotype . Similarly, we observed that the CD25lo population of Treg in SK system were less suppressive and were highly unstable with 50% of them losing FoxP3 expression when adoptively transferred into HSV-1 footpad infected WT mice.

An interesting observation was that CD25lo Treg infiltration into the cornea mirrored the appearance of ex-Treg which could mean that the ex-Treg generated in the cornea were derived mainly from the CD25loTreg population. However, some question whether ex-Treg observed in some autoimmune settings represent the loss of Foxp3 by bonafide Treg, or whether they represent conventional proinflammatory T cells that transiently induced endogenous FoxP3 and so induced FoxP3-Cre recombinase, leading to activation of the lineage tracer (Tomato) expression. We favor the notion that in our system of SK the ex-Treg represents true ex-Treg and not proinflammatory T cells that transiently expressed FoxP3 based largely on the results of adoptive transfer experiments. Accordingly, adoptive transfer of Foxp3-CD4+ T cells from FM mice into HSV-1 infected WT mice did not show any conversion to ex-Treg (Figure 2.1F), thus showing that T conv cells transiently expressing FoxP3 did not occur in our system or that the transient expression of Foxp3 was not enough to induce FoxP3-Cre recombinase. In addition, adoptive transfer of FACS sorted CD25lo Treg from HSV-1 infected FM mice into Thy1.1 mice that were infected with HSV-1 in the footpad showed conversion of these Treg into ex-Treg. This would support the idea that the conversion of Treg to ex-Treg is occurring in the infectious disease system we investigated.

Explanations for Treg plasticity include epigenetic and posttranslational modifications . Accordingly, demethylation of CpG islands in the TSDR region of the Foxp3 locus is considered a hallmark of Treg stability and functionality . Demethylation of the CpG islands in the TSDR region ensures that critical transcription factors such as Foxp3 and Runx1–Cbf-β complex, to bind to the TSDR region and maintain Foxp3 activity in the progeny of dividing Treg . Epigenetic regulation of stable Foxp3 expression is also regulated by FoxP3 acetylation . Previous reports show that the TSDR region is demethylated in thymic Treg expressing Foxp3, but in iTreg TSDR region is fully methylated making them unstable . We could also show that iTreg have a fully methylated TSDR and displayed plasticity when adoptively transferred in Rag1-/- mice. Moreover, almost 95% of these iTreg lost FoxP3 expression and became ex-Treg with the Th1 phenotype. Post-translation modifications that regulate Treg plasticity include phosphorylation and ubiquitination of FoxP3 and these events are being further explored in our system.

It is important from a lesion management perspective to find appropriate measures to limit or prevent Treg plasticity. Approaches under consideration include agents that cause demethylation of the TSDR region of the FoxP3 gene such as Azacytidine, which was investigated for its effects on SK lesion severity . The results showed that Azacytidine therapy after disease process had been initiated effectively diminished lesions. Other agents that prevent methylation of the TSDR region or promote acetylation of the FoxP3 gene may also show therapeutic promise to contain Treg plasticity . Vitamin C induces CNS2 demethylation in iTreg in a ten-eleven-translocation 2 (Tet2)/Tet3-dependent manner to increase the stability of Foxp3 expression . Similarly, RA also has a stabilizing effect on Foxp3 protein expression. It acts by suppressing IL-1 receptor upregulation, and accelerating IL-6 receptor downregulation along with increasing histone acetylation of the FoxP3 TSDR without affecting the methylation status of the TSDR region .

In the present communication we explored the value of Vitamin C and RA and could show that iTreg generated in the presence of Vitamin C and RA were more stable both in-vitro and in-vivo. Accordingly, when iTreg were adoptively transferred into WT HSV-1 ocularly infected mice at day 3 pi (a time at which levels of pro-inflammatory cytokines is high in the DLN), almost 30% of these iTreg lost Foxp3 expression. In contrast when iTreg were generated in the presence of Vitamin C and RA conversion was minimal (3-7%). Similar stabilizing effects were observed when iTreg generated with Vitamin C and RA, were exposed to proinflammatory cytokines IL-6 or IL-12 in-vitro. Moreover, these results might also explain previous findings that adoptive transfer of iTreg before infection effectively controlled SK lesion development yet transfers given later when the proinflammatory cytokines such as IL-6 were highly elevated were without notable lesion control . Our current finding explains this phenomenon since many iTreg converted and become ex-Treg without regulatory activity. Interestingly, we could stop this plasticity by generating iTreg in the presence of Vitamin C + RA and more importantly adoptive transfer of stabilized Vitamin C+ RA generated Treg suppressed SK lesions more efficiently than the control unstable iTreg when transferred to day 3 HSV-1 infected mice. It remains to be evaluated if Vitamin C + RA could stabilize CD25lo Treg and if the combination of Vitamin C and RA treatment in-vivo might hold promise as a therapeutic means of controlling virus induced inflammatory lesions.

Our results indicate that conversion of Treg or iTreg into Th1 cells may have a critical role in the severity of viral induced inflammatory lesions. Blocking pathways to prevent the conversion of these Treg into pathogenic T cells could represent a useful approach to control an important cause of human blindness.

Materials and methods

Mice

Female 6 to 8 week old C57BL/6 and Balb/c mice were purchased from Harlan Sprague Dawley Inc. (Indianapolis, IN). CD45.1 congenic (B6.SJL-*Ptprc*^{a} *Pepc*^{b}/BoyJ), Rag1-deficient (B6.129S7-*Rag1*^{tm1Mom}/J) and B6 ROSA26-Td Tomato reporter mice were purchased from Jackson Laboratory. Foxp3-GFP-Cre mice were provided by Dr. Jeffery Bluestone (San Francisco, CA). To generate Treg fate mapping mice Foxp3-GFP-Cre were crossed with B6 ROSA26-Td Tomato mice. Foxp3-GFP (C57BL/6 background) mice were a kind gift from M.Oukka (Brigham and Women's Hospital, Harvard Medical School), BALB/c DO11.10 RAG2 -/- mice were purchased from Taconic and kept in

pathogen free facility where food, water, bedding and instruments were autoclaved. All mice were housed in facilities at the University of Tennessee (Knoxville, TN) approved by the American Association of Laboratory Animal Care. All investigations followed guidelines of the Institutional Animal Care and Use Committee.

Ethics Statement

This study was carried out in strict accordance with the recommendations in the Guide for the Care and Use of Laboratory Animals of the National Institutes of Health. The protocol was approved by the University of Tennessee Animal Care and Use committee (protocol approval numbers 1253-0412 and 1244-0412). All procedures were performed under tribromoethanol (avertin) anesthesia, and all efforts were made to minimize suffering.

Virus

HSV-1 strain RE Tumpey and HSV-1 KOS was propagated in Vero cell monolayers (number CCL81; ATCC, Manassas, VA), titrated, and stored in aliquots at –80°C until used. Ultraviolet (UV) inactivation of the HSV-1 RE virus was performed for 10 minutes.

Corneal HSV-1 Infection and Scoring

Corneal infections of mice were performed under deep anesthesia. The mice were lightly scarified on their corneas with a 27-gauge needle, and a 3-µL drop that contained 104 plaque-forming units of HSV-1 RE was applied to one eye. Mock-infected mice were used as controls. These mice were monitored for the development of SK lesions. The SK lesion severity and angiogenesis in the eyes of mice were examined by slit-lamp biomicroscopy (Kowa Company, Nagoya, Japan). The scoring system was as follows: 0, normal cornea; +1, mild corneal haze; +2, moderate corneal opacity or scarring; +3, severe corneal opacity but iris visible; +4, opaque cornea and corneal ulcer; and +5, corneal rupture and necrotizing keratitis.

Flow Cytometric Analysis

At day 15 pi, corneas were excised, pooled group-wise, and digested with liberase (Roche Diagnostics Corporation, Indianapolis, IN) for 45 minutes at 37°C in a humidified atmosphere of 5% CO2. After incubation, the corneas were disrupted by grinding with a syringe plunger on a cell strainer and a single-cell suspension was made in complete RPMI 1640 medium. The single-cell suspensions obtained from corneal samples were stained for different cell surface molecules for fluorescence-activated cell sorting (FACS) analyses. All steps were performed at 4°C. Briefly, cells were stained with respective surface fluorochrome-labeled Abs in FACS buffer for 30 minutes, then stained for intracellular Abs. Finally, the cells were washed three times with FACS buffer and resuspended in 1% paraformaldehyde. The stained samples were acquired with a FACS LSR II (BD Biosciences, San Jose, CA) and the data were analyzed using FlowJo software (Tree Star, Inc., Ashland, OR).

To determine the number of IFN-γ producing T cells, intracellular cytokine staining was performed. In brief, corneal cells were either stimulated with Phorbol myristate acetate (PMA) (50ng) and Ionomycin (500ng) for 4 hours in the presence of brefeldin A (10 µg/mL) or stimulated with UV-inactivated HSV-1 RE (1 MOI) overnight followed by 5 hour brefeldin A (10 µg/mL) in U-bottom 96-well plates. After this period, Live/Dead staining was performed followed by cell surface and intracellular cytokine staining using Foxp3 intracellular staining kit (ebioscience) in accordance with the manufacturer's recommendations.

Reagents and antibodies.
CD4 (RM4-5), IFN-γ (XMG1.2), CD25 (PC61, 7D4), CD44 (IM7), Foxp3 (FJK-16S), anti-CD3 (145-2C11), anti-CD28 (37.51), GolgiPlug (brefeldin A) from either ebiosciences or BD biosciences. PMA and Ionomycin from sigma. Cell Trace Violet and Live/Dead Fixable Violet Dead Cell Stain Kit from Life Technologies. Recombinant IL-2, IL-12, IL-6 and TGF-β from R&D systems.

TSDR assay
A quantitative real-time PCR method was used as described by Floess et al., 2007 . Briefly, two subsets of Treg (CD4+ Foxp3+ GFP+ CD25lo and CD4+ Foxp3+ GFP+ CD25hi) from HSV-1 ocularly infected Foxp3-GFP male mice (day 15 pi) or iTreg generated with or without the supplementation of Vitamin C +RA from naïve CD4 + T cells isolated from the spleens of Foxp3 GFP male mice as described above (2×10^5 each) were sorted and processed using the EZ DNA Methylation-Direct kit (Zymo Research) according to the manufacturer's protocol. Purified bisulfite-treated DNA was used in a quantitative PCR reaction. Primers and probes sequences used were the following: forward primer, 5′-GGTTTATATTTGGGTTTTGTTGTTATAATTT-3′; and reverse primer, 5′-CCCCTTCTCTTCCTCCTTATTACC-3′. Probe sequences were: methylated (CG) probe, 5′-TGACGTTATGGCGGTCG-3′; and unmethylated (TG) probe, 5′-ATTGATGTTATGGTGGTTGGA-3′. PCR was performed with 10 µl Universal Master Mix II (Applied Biosystems), 1 µl eluted DNA, primer/probe mix, and enough water to bring the total volume to 20 µl. Final concentration of primers were 900 nM and concentration of probes were 150 nM. Reactions were run for 10 min at 95°C for 10 min and 50 cycles of 95°C for 15 s and 61°C for 1.5 min (7500 Real-Time PCR System; Applied Biosystems). Percent demethylation was calculated using the formula percent demethylation = 100/[1 + 2(CtTG−CtCG)], where CtTG represents the threshold cycle of the TG (unmethylated) probe and CtCG represents the threshold cycle of the CG (methylated) probe .

T cell isolation, sorting and adoptive transfer experiments
Single-cell suspensions were obtained from DLNs and the spleens from footpad or ocular HSV-1 infected mice at day 5 and day 15 pi respectively. Splenic erythrocytes were eliminated with red blood cell lysis buffer (Sigma-Aldrich). To purify the peripheral CD4+ T cell subpopulation obtained from FM mice, pooled spleen and DLN cells were isolated using a mouse CD4+ T cell isolation kit according to the manufacturer's instructions (Miltenyi Biotec, Auburn, CA). Cells were then stained and subject to FACS sorting. The purity of all the sorted cells was >95%. The sorted cells were subsequently used for adoptive transfer experiments.

For adoptive transfer experiments in Balb/c mice, splenocytes isolated from DO11.10 RAG2 -/- mice were used as a precursor population for the induction of Foxp3+ in CD4+ T cells as described elsewhere . Briefly, (1×10^6/ml) splenocytes after RBC lysis and several washings were cultured in RPMI media containing rIL-2 (100 U/ml) and TGFβ (5ng/ml) in the presence or absence of Vitamin C and RA with plate bound anti-CD3/28 Ab (1 µg/ml) for 5 days at 37°C in a 5% CO2 incubator. After 5 days, a few cells were characterized for Foxp3 intracellular staining (ebioscience staining kit) analyzed by flow cytometry. Based on the frequency of Live Foxp3+ cells generated in the different cultures conditions 10 x 10^6 Vitamin C + RA stabilized iTreg or control unstable iTreg were adoptively transferred i.v into HSV-1 infected Balb/c mice at day 3 pi.

Administration of IVIGs

Intravenous immunoglobulins (IVIGs; Gammagard Liquid) was obtained from Baxter (Deerfield, IL). Rag1-/- mice were intraperitoneally injected with IVIG (3.75 mg per mouse) at day 2 after infection. The dose of IVIG was chosen to be 3.75 mg per mouse, based on previous studies .

In vitro Treg and Treg stability assays

Splenocytes isolated from DO11.10 RAG2 -/- or Foxp3 GFP mice were used as a precursor population for the induction of Foxp3+ in CD4+ T cells. Briefly, 1×10^6 splenocytes after RBC lysis and several washings were cultured in 1ml RPMI media containing rIL-2 (100 U/ml) and TGFβ (5ng/ml) in the presence or absence of Vitamin C and RA with plate bound anti-CD3/28 Ab (1 µg/ml) for 5 days at 37°C in a 5% CO2 incubator. After 5 days, samples were characterized for Foxp3 intracellular staining (ebioscience staining kit) or GFP expression (Foxp3 GFP mice) analyzed by flow cytometry. Treg were either sorted (TSDR methylation analysis) or cultured in 96-well round bottom plate in the presence of IL-2 (100U/ml) or IL-12 (5ng/ml) or IL-6 (25ng/ml) +TGF-β (1ng/ml) for 3 days followed by flow cytometry analysis of Live CD4+ Foxp3+ cells.

In vitro suppression assay

To measure the suppressor function of CD25lo and CD25hi Treg, FACS sorted CD25lo, CD25hi GFP+ cells and naïve CD4+ cells (CD62L+ CD44-) from DLN and spleens (day 15 pi) of HSV-1 ocularly infected FM mice were cultured with anti-CD3 (1 µg/well) and anti-CD28 (0.5 µg/well) antibodies in a U-bottom 96-well plate. The suppressive capacity of the subsets of Treg was measured by co-culturing Treg and T conventional cells (Tconv) at different ratios (Treg/Tconv, 1:1 to 1:8). After 3 days of incubation, the extent of CTV dilution was measured in CD4+ cells by flow cytometry. Percent suppression by different subsets of Treg was calculated by using the formula 100 − [(frequency of cells proliferated at a particular Treg/effector T cell ratio)/(frequency of cells proliferated in the absence of Treg)].

Statistical Analysis

Statistical significance was determined by Student t test unless otherwise specified. A P value of <0.05 was regarded as a significant difference between groups: *P ≤ 0.05, **P ≤ 0.01, ***P ≤ 0.001. GraphPad Prism software (GraphPad Software, Inc., La Jolla, CA) was used for statistical analysis.

References

1.Liesegang, T. J. 2001. Herpes simplex virus epidemiology and ocular importance. *Cornea* 20: 1-13.

2.Niemialtowski, M. G., and B. T. Rouse. 1992. Predominance of Th1 cells in ocular tissues during herpetic stromal keratitis. *J Immunol* 149: 3035-3039.

3.Hendricks, R. L., T. M. Tumpey, and A. Finnegan. 1992. IFN-gamma and IL-2 are protective in the skin but pathologic in the corneas of HSV-1-infected mice. *J Immunol* 149: 3023-3028.

4.Suvas, S., A. K. Azkur, B. S. Kim, U. Kumaraguru, and B. T. Rouse. 2004. CD4+CD25+ regulatory T cells control the severity of viral immunoinflammatory lesions. *J Immunol* 172: 4123-4132.

5.Sehrawat, S., S. Suvas, P. P. Sarangi, A. Suryawanshi, and B. T. Rouse. 2008. In vitro-generated antigen-specific CD4+ CD25+ Foxp3+ regulatory T cells control the severity of herpes simplex virus-induced ocular immunoinflammatory lesions. *J Virol* 82: 6838-6851.

6.Veiga-Parga, T., A. Suryawanshi, S. Mulik, F. Gimenez, S. Sharma, T. Sparwasser, and B. T. Rouse. 2012. On the role of regulatory T cells during viral-induced inflammatory lesions. *J Immunol* 189: 5924-5933.

7.Zhou, X., S. L. Bailey-Bucktrout, L. T. Jeker, C. Penaranda, M. Martinez-Llordella, M. Ashby, M. Nakayama, W. Rosenthal, and J. A. Bluestone. 2009. Instability of the transcription factor Foxp3 leads to the generation of pathogenic memory T cells in vivo. *Nat Immunol* 10: 1000-1007.

8.Bailey-Bucktrout, S. L., and J. A. Bluestone. 2011. Regulatory T cells: stability revisited. *Trends in immunology* 32: 301-306.

9.Miyao, T., S. Floess, R. Setoguchi, H. Luche, H. J. Fehling, H. Waldmann, J. Huehn, and S. Hori. 2012. Plasticity of Foxp3(+) T cells reflects promiscuous Foxp3 expression in conventional T cells but not reprogramming of regulatory T cells. *Immunity* 36: 262-275.

10.Sujino, T., M. London, D. P. Hoytema van Konijnenburg, T. Rendon, T. Buch, H. M. Silva, J. J. Lafaille, B. S. Reis, and D. Mucida. 2016. Tissue adaptation of regulatory and intraepithelial CD4(+) T cells controls gut inflammation. *Science* 352: 1581-1586.

11.Sakaguchi, S., D. A. Vignali, A. Y. Rudensky, R. E. Niec, and H. Waldmann. 2013. The plasticity and stability of regulatory T cells. *Nat Rev Immunol* 13: 461-467.

12.Floess, S., J. Freyer, C. Siewert, U. Baron, S. Olek, J. Polansky, K. Schlawe, H. D. Chang, T. Bopp, E. Schmitt, S. Klein-Hessling, E. Serfling, A. Hamann, and J. Huehn. 2007. Epigenetic control of the foxp3 locus in regulatory T cells. *PLoS biology* 5: e38.

13.Huehn, J., J. K. Polansky, and A. Hamann. 2009. Epigenetic control of FOXP3 expression: the key to a stable regulatory T-cell lineage? *Nat Rev Immunol* 9: 83-89.

14.Zheng, Y., S. Josefowicz, A. Chaudhry, X. P. Peng, K. Forbush, and A. Y. Rudensky. 2010. Role of conserved non-coding DNA elements in the Foxp3 gene in regulatory T-cell fate. *Nature* 463: 808-812.

15.van Loosdregt, J., Y. Vercoulen, T. Guichelaar, Y. Y. Gent, J. M. Beekman, O. van Beekum, A. B. Brenkman, D. J. Hijnen, T. Mutis, E. Kalkhoven, B. J. Prakken, and P. J. Coffer. 2010. Regulation of Treg functionality by acetylation-mediated Foxp3 protein stabilization. *Blood* 115: 965-974.

16. Barbi, J., D. Pardoll, and F. Pan. 2014. Treg functional stability and its responsiveness to the microenvironment. *Immunol Rev* 259: 115-139.
17. Hodge, D. R., E. Cho, T. D. Copeland, T. Guszczynski, E. Yang, A. K. Seth, and W. L. Farrar. 2007. IL-6 enhances the nuclear translocation of DNA cytosine-5-methyltransferase 1 (DNMT1) via phosphorylation of the nuclear localization sequence by the AKT kinase. *Cancer genomics & proteomics* 4: 387-398.
18. Samanta, A., B. Li, X. Song, K. Bembas, G. Zhang, M. Katsumata, S. J. Saouaf, Q. Wang, W. W. Hancock, Y. Shen, and M. I. Greene. 2008. TGF-beta and IL-6 signals modulate chromatin binding and promoter occupancy by acetylated FOXP3. *Proc Natl Acad Sci U S A* 105: 14023-14027.
19. Lal, G., and J. S. Bromberg. 2009. Epigenetic mechanisms of regulation of Foxp3 expression. *Blood* 114: 3727-3735.
20. Chen, Q., Y. C. Kim, A. Laurence, G. A. Punkosdy, and E. M. Shevach. 2011. IL-2 controls the stability of Foxp3 expression in TGF-beta-induced Foxp3+ T cells in vivo. *J Immunol* 186: 6329-6337.
21. Komatsu, N., M. E. Mariotti-Ferrandiz, Y. Wang, B. Malissen, H. Waldmann, and S. Hori. 2009. Heterogeneity of natural Foxp3+ T cells: a committed regulatory T-cell lineage and an uncommitted minor population retaining plasticity. *Proc Natl Acad Sci U S A* 106: 1903-1908.
22. Huynh, A., M. DuPage, B. Priyadharshini, P. T. Sage, J. Quiros, C. M. Borges, N. Townamchai, V. A. Gerriets, J. C. Rathmell, A. H. Sharpe, J. A. Bluestone, and L. A. Turka. 2015. Control of PI(3) kinase in Treg cells maintains homeostasis and lineage stability. *Nat Immunol* 16: 188-196.
23. Komatsu, N., K. Okamoto, S. Sawa, T. Nakashima, M. Oh-hora, T. Kodama, S. Tanaka, J. A. Bluestone, and H. Takayanagi. 2014. Pathogenic conversion of Foxp3+ T cells into TH17 cells in autoimmune arthritis. *Nat Med* 20: 62-68.
24. Bhela, S., S. Mulik, P. B. Reddy, R. L. Richardson, F. Gimenez, N. K. Rajasagi, T. Veiga-Parga, A. P. Osmand, and B. T. Rouse. 2014. Critical role of microRNA-155 in herpes simplex encephalitis. *J Immunol* 192: 2734-2743.
25. Yue, X., S. Trifari, T. Aijo, A. Tsagaratou, W. A. Pastor, J. A. Zepeda-Martinez, C. W. Lio, X. Li, Y. Huang, P. Vijayanand, H. Lahdesmaki, and A. Rao. 2016. Control of Foxp3 stability through modulation of TET activity. *J Exp Med* 213: 377-397.
26. Sasidharan Nair, V., M. H. Song, and K. I. Oh. 2016. Vitamin C Facilitates Demethylation of the Foxp3 Enhancer in a Tet-Dependent Manner. *J Immunol* 196: 2119-2131.
27. Chen, Z., J. Barbi, S. Bu, H. Y. Yang, Z. Li, Y. Gao, D. Jinasena, J. Fu, F. Lin, C. Chen, J. Zhang, N. Yu, X. Li, Z. Shan, J. Nie, Z. Gao, H. Tian, Y. Li, Z. Yao, Y. Zheng, B. V. Park, Z. Pan, J. Zhang, E. Dang, Z. Li, H. Wang, W. Luo, L. Li, G. L. Semenza, S. G. Zheng, K. Loser, A. Tsun, M. I. Greene, D. M. Pardoll, F. Pan, and B. Li. 2013. The ubiquitin ligase Stub1 negatively modulates regulatory T cell suppressive activity by promoting degradation of the transcription factor Foxp3. *Immunity* 39: 272-285.
28. Lal, G., N. Zhang, W. van der Touw, Y. Ding, W. Ju, E. P. Bottinger, S. P. Reid, D. E. Levy, and J. S. Bromberg. 2009. Epigenetic regulation of Foxp3 expression in regulatory T cells by DNA methylation. *J Immunol* 182: 259-273.

29. Koch, M. A., K. R. Thomas, N. R. Perdue, K. S. Smigiel, S. Srivastava, and D. J. Campbell. 2012. T-bet(+) Treg cells undergo abortive Th1 cell differentiation due to impaired expression of IL-12 receptor beta2. *Immunity* 37: 501-510.
30. Hall, A. O., D. P. Beiting, C. Tato, B. John, G. Oldenhove, C. G. Lombana, G. H. Pritchard, J. S. Silver, N. Bouladoux, J. S. Stumhofer, T. H. Harris, J. Grainger, E. D. Wojno, S. Wagage, D. S. Roos, P. Scott, L. A. Turka, S. Cherry, S. L. Reiner, D. Cua, Y. Belkaid, M. M. Elloso, and C. A. Hunter. 2012. The cytokines interleukin 27 and interferon-gamma promote distinct Treg cell populations required to limit infection-induced pathology. *Immunity* 37: 511-523.
31. Hori, S. 2010. Developmental plasticity of Foxp3+ regulatory T cells. *Curr Opin Immunol* 22: 575-582.
32. Miyara, M., Y. Yoshioka, A. Kitoh, T. Shima, K. Wing, A. Niwa, C. Parizot, C. Taflin, T. Heike, D. Valeyre, A. Mathian, T. Nakahata, T. Yamaguchi, T. Nomura, M. Ono, Z. Amoura, G. Gorochov, and S. Sakaguchi. 2009. Functional delineation and differentiation dynamics of human CD4+ T cells expressing the FoxP3 transcription factor. *Immunity* 30: 899-911.
33. Rudra, D., T. Egawa, M. M. Chong, P. Treuting, D. R. Littman, and A. Y. Rudensky. 2009. Runx-CBFbeta complexes control expression of the transcription factor Foxp3 in regulatory T cells. *Nat Immunol* 10: 1170-1177.
34. Li, B., A. Samanta, X. Song, K. T. Iacono, K. Bembas, R. Tao, S. Basu, J. L. Riley, W. W. Hancock, Y. Shen, S. J. Saouaf, and M. I. Greene. 2007. FOXP3 interactions with histone acetyltransferase and class II histone deacetylases are required for repression. *Proc Natl Acad Sci U S A* 104: 4571-4576.
35. Tao, R., E. F. de Zoeten, E. Ozkaynak, C. Chen, L. Wang, P. M. Porrett, B. Li, L. A. Turka, E. N. Olson, M. I. Greene, A. D. Wells, and W. W. Hancock. 2007. Deacetylase inhibition promotes the generation and function of regulatory T cells. *Nat Med* 13: 1299-1307.
36. Varanasi, S. K., P. B. Reddy, S. Bhela, U. Jaggi, F. Gimenez, and B. T. Rouse. 2017. Azacytidine treatment inhibits the progression of Herpes Stromal Keratitis by enhancing regulatory T cell function. *J Virol*.
37. Lu, L., Q. Lan, Z. Li, X. Zhou, J. Gu, Q. Li, J. Wang, M. Chen, Y. Liu, Y. Shen, D. D. Brand, B. Ryffel, D. A. Horwitz, F. P. Quismorio, Z. Liu, B. Li, N. J. Olsen, and S. G. Zheng. 2014. Critical role of all-trans retinoic acid in stabilizing human natural regulatory T cells under inflammatory conditions. *Proc Natl Acad Sci U S A* 111: E3432-3440.
38. Cottrell, S., K. Jung, G. Kristiansen, E. Eltze, A. Semjonow, M. Ittmann, A. Hartmann, T. Stamey, C. Haefliger, and G. Weiss. 2007. Discovery and validation of 3 novel DNA methylation markers of prostate cancer prognosis. *The Journal of urology* 177: 1753-1758.
39. Veiga-Parga, T., A. Suryawanshi, and B. T. Rouse. 2011. Controlling viral immuno-inflammatory lesions by modulating aryl hydrocarbon receptor signaling. *PLoS Pathog* 7: e1002427.
40. Bhela, S., S. Mulik, F. Gimenez, P. B. Reddy, R. L. Richardson, S. K. Varanasi, U. Jaggi, J. Xu, P. Y. Lu, and B. T. Rouse. 2015. Role of miR-155 in the Pathogenesis of Herpetic Stromal Keratitis. *Am J Pathol*.

APPENDIX

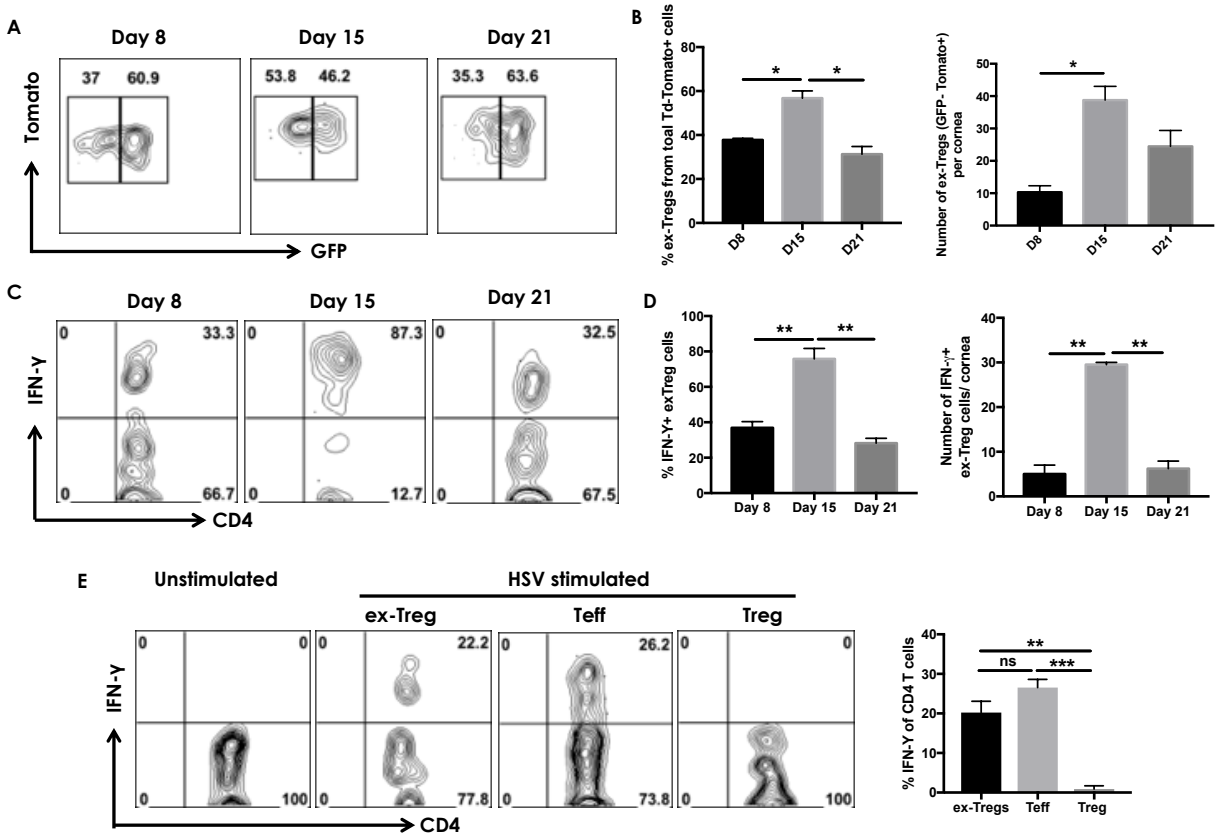

Figure 2.1. Kinetic analysis of ex-Treg in the corneas of HSV-infected mice.
FM mice were infected ocularly with 1× 10^4 PFU of HSV, and at each time point (d8, 15 and day 21) three to four corneas were collected, pooled, and digested with Liberase and analyzed for various cell types. **A)** Representative FACS plots, frequencies and average numbers of corneal ex-Treg cells at each time point pi. **B)** Intracellular staining was conducted to quantify Th1 and Th17 ex-Treg cells by stimulating them with PMA/ionomycin. Representative FACS plots, frequencies and average numbers of ex-Treg cells producing IFN-g or IL-17A after stimulation with PMA/ionomycin. Plots shown were gated on ex-Treg cells. **C)** For quantification of Ag-specific ex-Treg cells, corneal single cell suspensions were stimulated for 16 h with UV-inactivated HSV-KOS, with the addition of brefeldin A for the last 5 h of stimulation. Representative FACS plots shown are gated on ex-Treg cells. The level of significance was determined by a Student t test (unpaired). Error bars represent means ± SEM (n = 8 – 10 mice). Experiments were repeated at least three times. P≤0.0001(****), P≤0.01(**), P≤0.05(*).

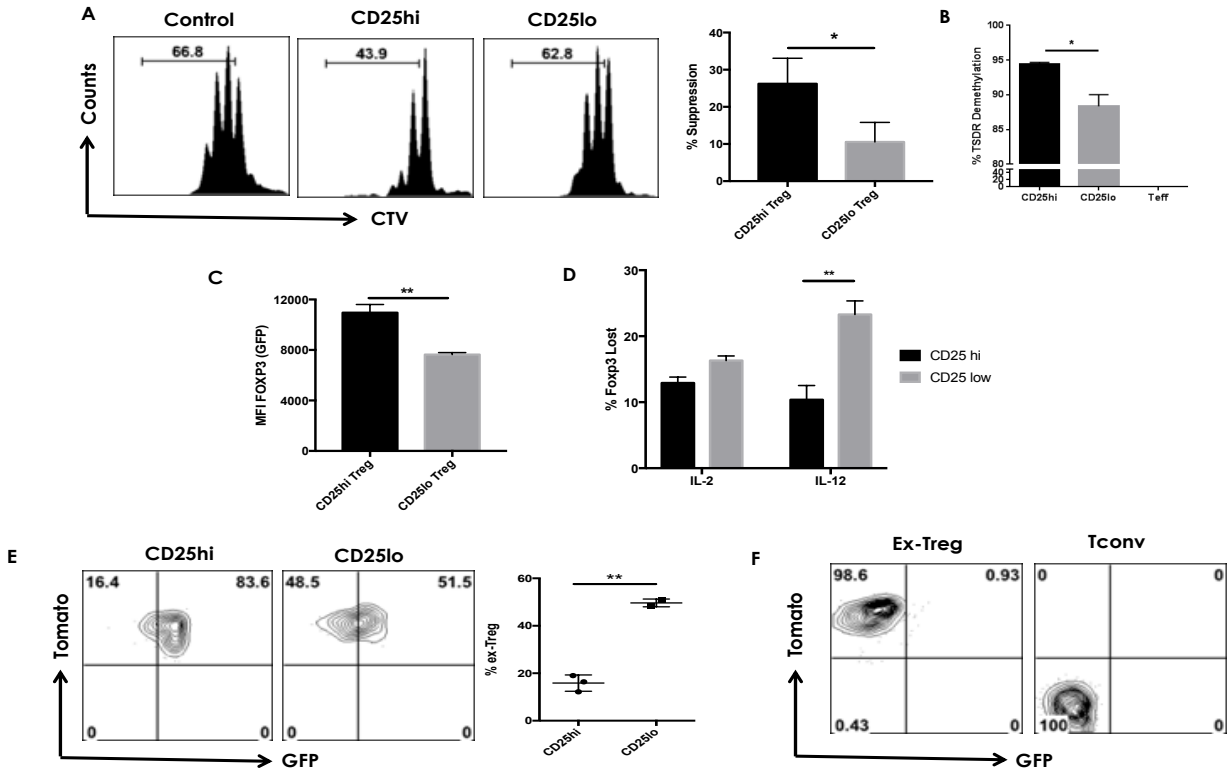

Figure 2.2. CD25loFoxp3+CD4+ Treg are unstable Treg cells that convert into ex-Treg in an inflammatory environment.

(A-E) FM mice were infected ocularly with 1× 10^4 PFU of HSV**.** DLNs and spleens were collected at day 14 pi and CD25lo and CD25hi Treg cells were sorted. **A)** An equal number of each population (1 x 10^5 cells) was cultured with CTV-labeled sorted effector T cells (Treg/Teff, 1:1) in the presence of anti-CD3 and anti-CD28 antibodies. Representative histograms show the extent of CTV dilution at a 1:1 Treg/Teff ratio. Bar graphs show the percent suppression of CD25lo Treg and CD25 Treg at 1:1 ratio to Teff. **B)** Demethylation of TSDR region at Foxp3 locus of the sorted CD25lo and CD25hi Treg was determined as described in materials and methods. **C)** Bar graph shows the MFI of FoxP3 expression on CD25lo and CD25hi Treg. **D)** Sorted CD25lo and CD25hi Treg were exposed to 100U/ml IL-2 or 5ng/ml IL-12 or 25ng/ml IL-6 and 1ng/ml TGF-beta for 3 days. Cells were measured for ex-Treg cells before exposure and after exposure. Histograms represent the frequency of Foxp3 lost by CD25lo and CD25hi Treg exposed to different conditions. **E)** Sorted CD25lo and CD25hi Treg were adoptively transferred into HSV-1 footpad infected congenic Thy1.1 mice at 24hpi and transferred cells were analyzed for ex-Treg. Representative FACS plots show the frequency of ex-Treg after adoptive transfer. Plots are gated on CD4+Thy1.2+Tomato+ cells. **F)** Sorted effector T cells and ex-Treg from immunized FM mice were adoptively transferred into HSV-1 footpad infected congenic Thy1.1 mice at 24h pi and transferred cells were analyzed for Treg. Representative FACS plots show the frequency of Treg after adoptive transfer. Plots are gated on CD4+Thy1.2 + cells. Each experiment was repeated at least two times with at least 3 mice per group. Statistical significance was calculated by one-way ANOVA with Tukey multiple-comparison test. P≤0.01(**), P≤0.05(*).

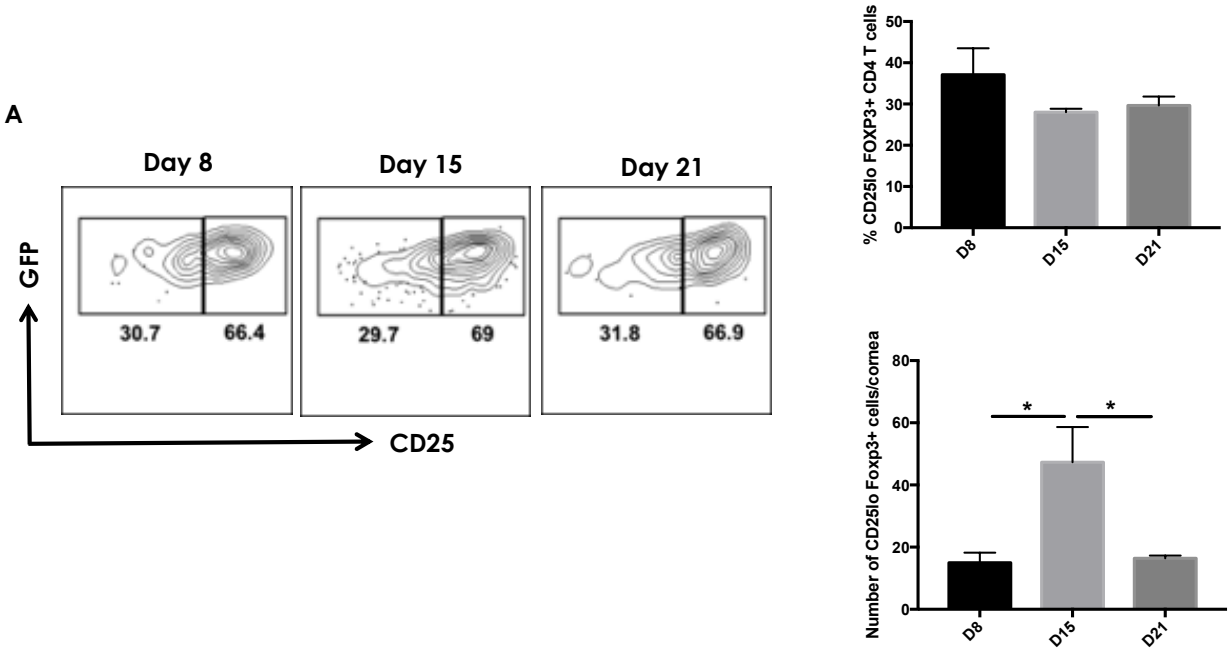

Figure 2.3. Unstable CD25lo Treg increase with the progression of disease. Foxp3 GFP mice were infected ocularly with 1× 10^4 PFU of HSV and at each time point (d8, 15 and 21) three to four corneas were collected, pooled, and digested with Liberase and analyzed for CD25lo Treg. **A)** Representative FACS plots, frequencies and average numbers of corneal CD25lo Treg cells at each time point pi. The level of significance was determined by a Student t test (unpaired). Error bars represent means ± SEM (n = 8 – 10 mice). Experiments were repeated at least three times. P≤0.05(*).

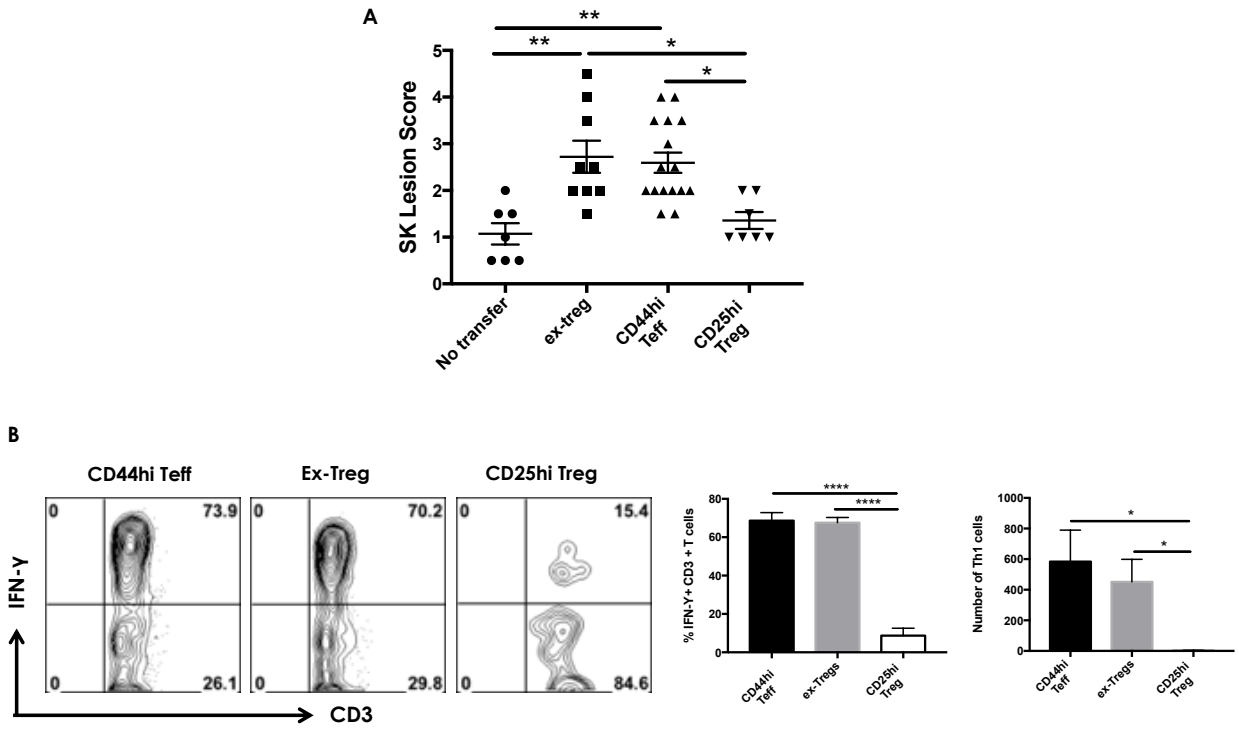

Figure 2.4. ex-Treg are pathogenic in-vivo.

FM mice were infected ocularly with 1× 10^4 PFU of HSV**.** DLNs and spleens were collected at day 15 pi and ex-Treg and CD44hi FoxP3- T effectors cell were FACS sorted. Rag1-/- were ocularly infected with HSV-1 and were divided into groups. One group of mice received 5 x 10^5 ex-Treg cell at 24hpi. One group of mice received 5 x 10^5 CD44hi FoxP3- T effectors cell 24h pi and one group received no cells. All mice were treated with IVIG at day 2 pi. **A)** SK lesion severity at day 10 after infection is shown. **B)** Mice were sacrificed on day 10 after infection, and corneas were harvested and pooled group wise for the analysis of various cell types. Intracellular staining was conducted to quantify Th1 cells by stimulating them with PMA/ionomycin. Representative FACS plots, frequencies and average numbers of CD4 T cells producing IFN-γ after stimulation with PMA/ionomycin. Plots shown were gated on CD3+CD4+ T cells. Data compiled from two separate experiments consisting of 3-4 animals in each group. The level of significance was determined by a Student t test (unpaired). Error bars represent means ± SEM. P≤0.01(**).

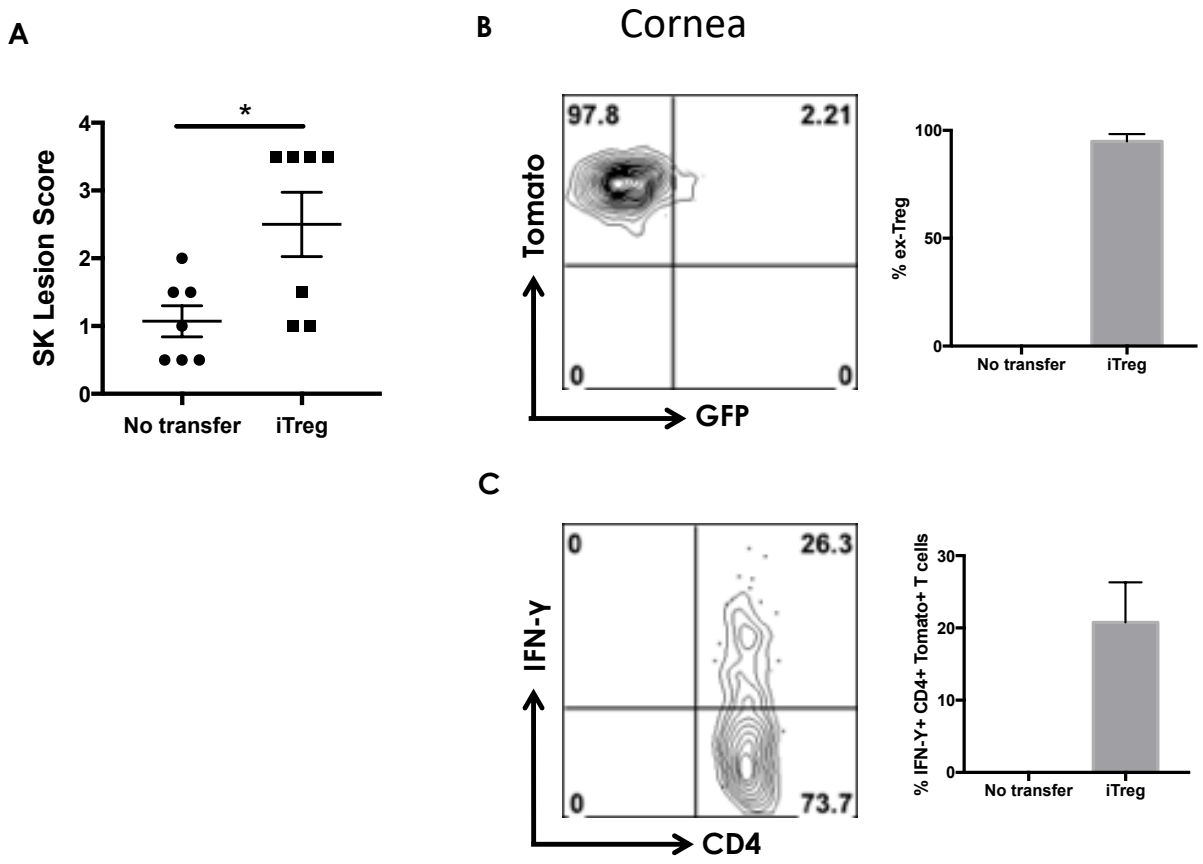

Figure 2.5. iTreg are pathogenic in-vivo.
(A) Naive CD4 T cells purified from FM mice were cultured (1x10^6 cells/well) with 100U/ml IL-2, 5ng/ml TGFβ and 1μg/ml anti-CD3/CD28, for up to 5 days. Foxp3 GFP+ Tomato+ T cells (iTreg) were FACS sorted. Rag1-/- were ocularly infected with HSV-1 and were divided into two groups. One group of mice received 5 x 10^5 iTreg cells at 24h pi and one group received no cells. All mice were treated with IVIG at day 2 pi. **A)** SK lesion severity at day 10 after infection is shown. **B)** Mice were sacrificed on day 10 after infection, and corneas were harvested and pooled group wise for the analysis of various cell types. Intracellular staining was conducted to quantify Th1 cells by stimulating them with PMA/ionomycin. Representative FACS plots show frequency of ex-Treg and CD4 T cells producing IFN-g after stimulation with PMA/ionomycin. Plots shown were gated on CD3+CD4+Tomato+ T cells. Data compiled from two separate experiments consisting of 3-4 animals in each group. The level of significance was determined by a Student t test (unpaired). Error bars represent means ± SEM. P≤0.05(*).

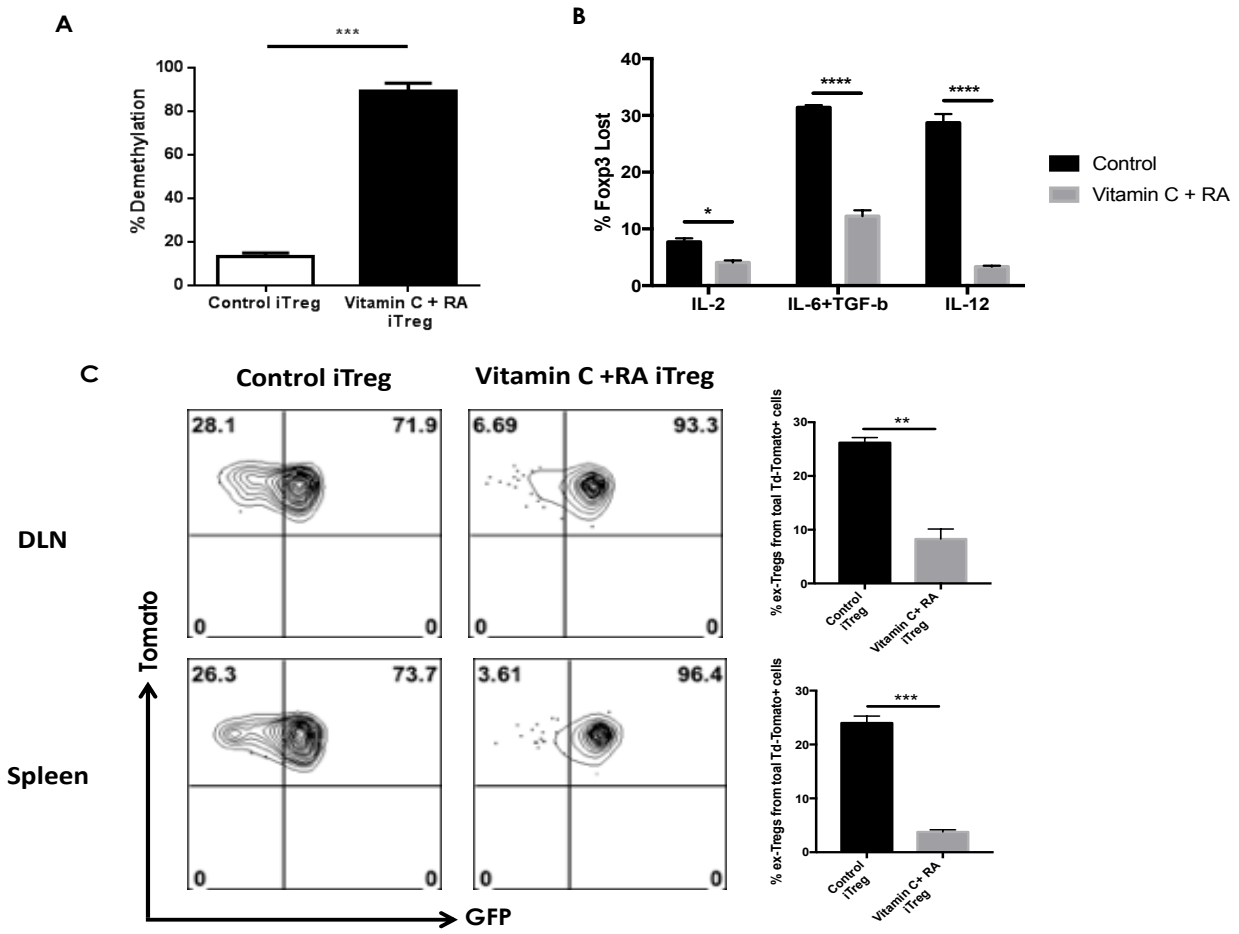

Figure 2.6. Vitamin C + RA generated iTreg are highly stable.
(**A)** Naive CD4 T cells purified from Foxp3 GFP male mouse were cultured (500,000 cells/well) with 100U/ml IL-2, 1µg/ml anti-CD3/CD28, 5ng/ml TGFβ and in the presence or absence of Vitamin C and RA for up to 5 days. Foxp3 GFP+ T cells were FACS sorted. Demethylation of TSDR region at Foxp3 locus was determined as described in Materials and methods. **B)** Splenocytes from DO11.10 RAG2-/- animals were cultured in the presence of 1µg/ml anti-CD3/CD28, 100 U/ml IL-2, 5ng/ml TGF-β in the presence or absence of Vitamin C and RA for 5 days. Then exposed to 100U/ml IL-2 or 5ng/ml IL-12 or 25ng/ml IL-6 and 1ng/ml TGF-beta for another 3 days. Cells were measured for Live CD4+ Foxp3+ cells before exposure and after exposure. Bar graphs show the frequency of Foxp3 lost by cells of control and Vitamin C and RA induced iTreg exposed to different conditions. **C)** Naive CD4 T cells purified from FM mice were cultured (1 x 10^6 cells/well) with 100U/ml IL-2, 1µg/ml anti-CD3/CD28, 5ng/ml TGFβ and in the presence or absence of Vitamin C and RA for 5 days. Cells Control iTreg and Vitamin C + RA generated Treg were adoptively transferred into HSV-1 ocularly infected congenic Thy1.1 mice at 72hpi and transferred cells were analyzed for ex-Treg cells. Representative FACS plots show the frequency of ex-Treg after adoptive transfer. Plots are gated on CD4+Thy1.2+Tomato+ cells. Each experiment was repeated at least two times with at least 3 mice per group. Statistical significance was calculated by one-way ANOVA with Tukey multiple-comparison test P≤ 0.0001(****),P≤0.001 (***),P≤0.01(**), P≤0.05(*).

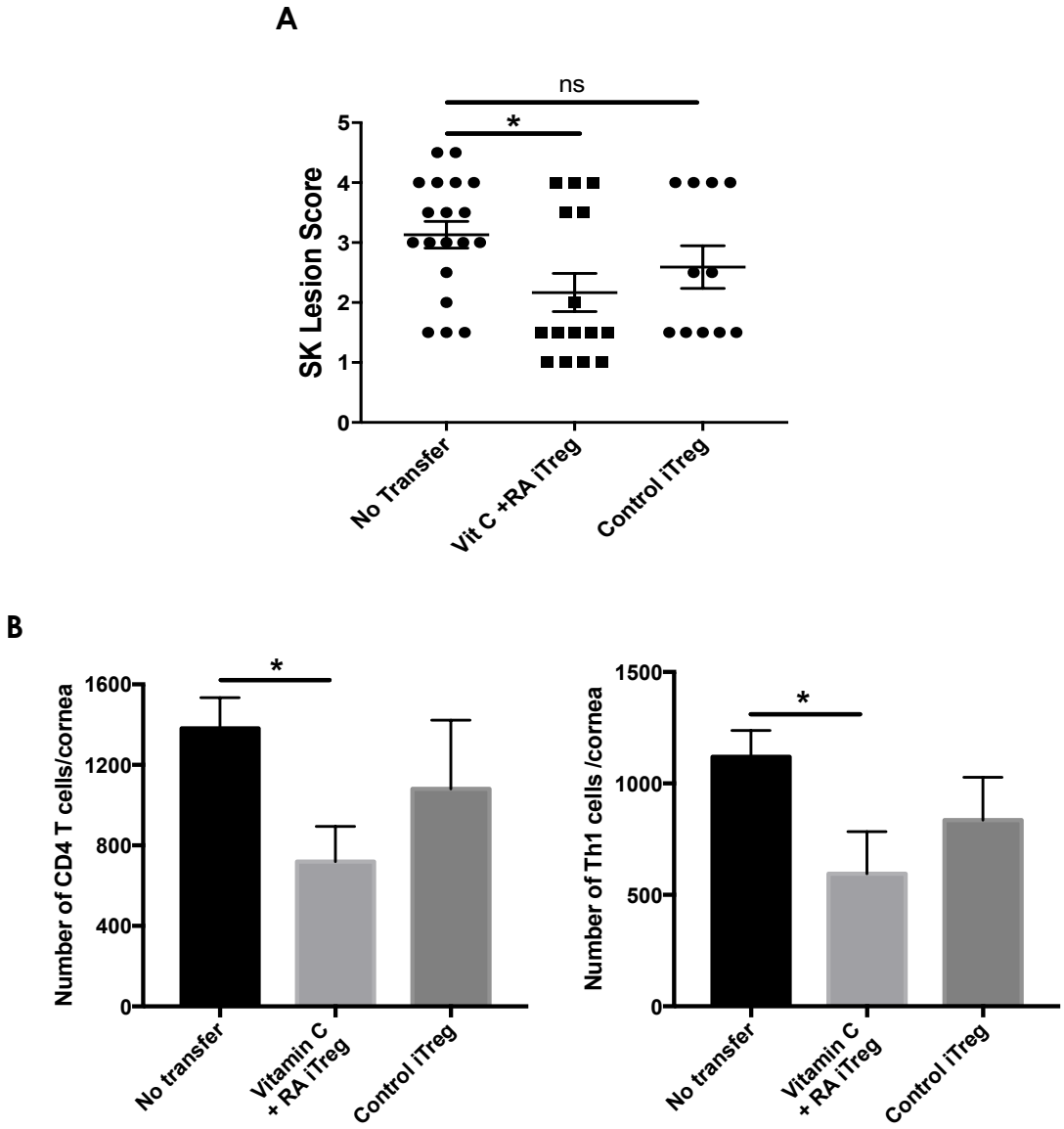

Figure 2.7. Vitamin C+ RA generated Treg suppress SK lesions better than control iTreg.

Balb/c mice ocularly infected with $1x10^5$ PFU of HSV-1 were divided into groups. One group of mice received stabilized Vitamin C + RA generated iTreg (10×10^6) at day 3 after infection. One group of mice received control unstable iTreg (10×10^6) at day 3 after infection, and one group of mice received no transfer of cells. Disease severity and immune indicators in the cornea were evaluated at day 15 after infection. **A)** SK lesion severity at day 15 after infection are shown. **B)** Mice were sacrificed on day 15 after infection, and corneas were harvested and pooled group wise for the analysis of various cell types. Intracellular staining was conducted to quantify Th1 cells by stimulating them with PMA/ionomycin. The bar graph represents total numbers of corneal infiltrating CD4+ T cells, and Th1cells of mice that received no transfer, control iTreg or Vitamin C + RA generated iTreg. Each experiment was repeated at least two times with at least 8 mice per group. Statistical significance was calculated by one-way ANOVA with Tukey multiple-comparison test. Error bars represent means ± SEM. $P \leq 0.05$(*)

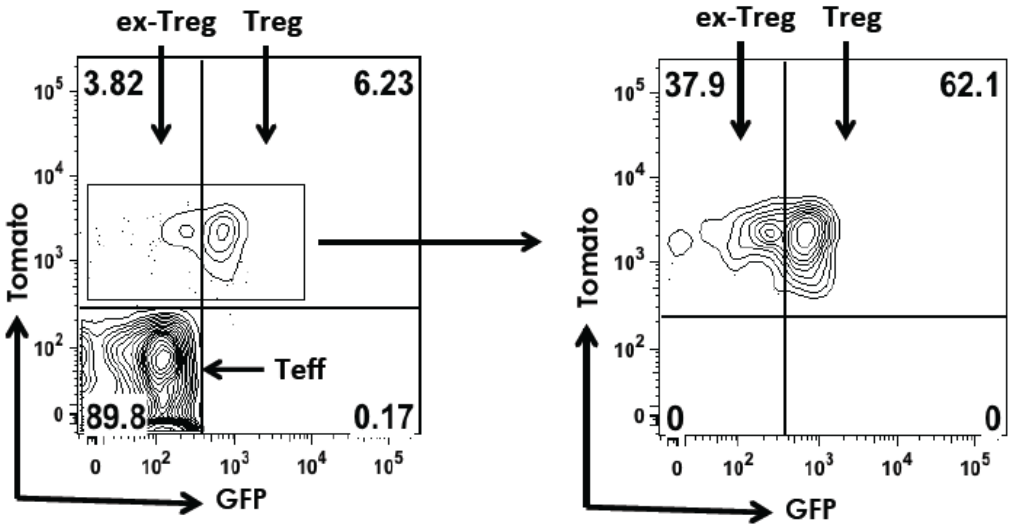

Figure S2.1. Analysis of corneal CD4 T cells.
Graph shows frequencies of ex-Treg, Treg and T effectors in ocularly HSV-1 infected FM mice at day 8 pi (left) and ex-Treg and Treg frequency after gating on Tomato+ cell (right).

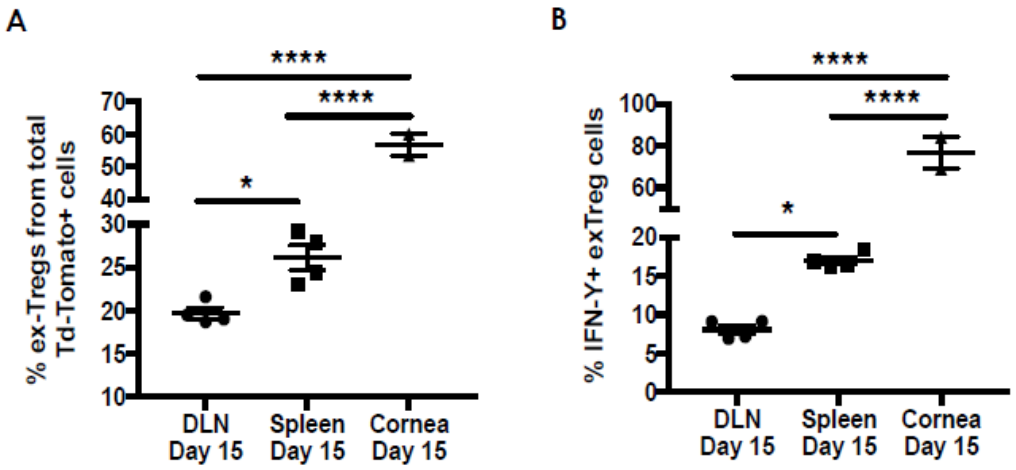

Figure S2.2. ex-Treg in lymphoid tissues and cornea after ocular HSV-1 infection. (A) Graph shows ex-Treg frequencies in DLN, spleen and corneas of day 15 ocularly HSV-1 infected FM mice. B) Intracellular staining was conducted to quantify Th1 ex-Treg cells by stimulating them with PMA/ionomycin. Graph shows frequency of IFN-γ producing ex-Treg in DLN, spleen and cornea of day 15 HSV-1 infected FM mice. Statistical significance was calculated by one-way ANOVA with Tukey multiple - comparison test. Error bars represent means ± SEM. P≤ 0.0001(****), P≤0.05(*).

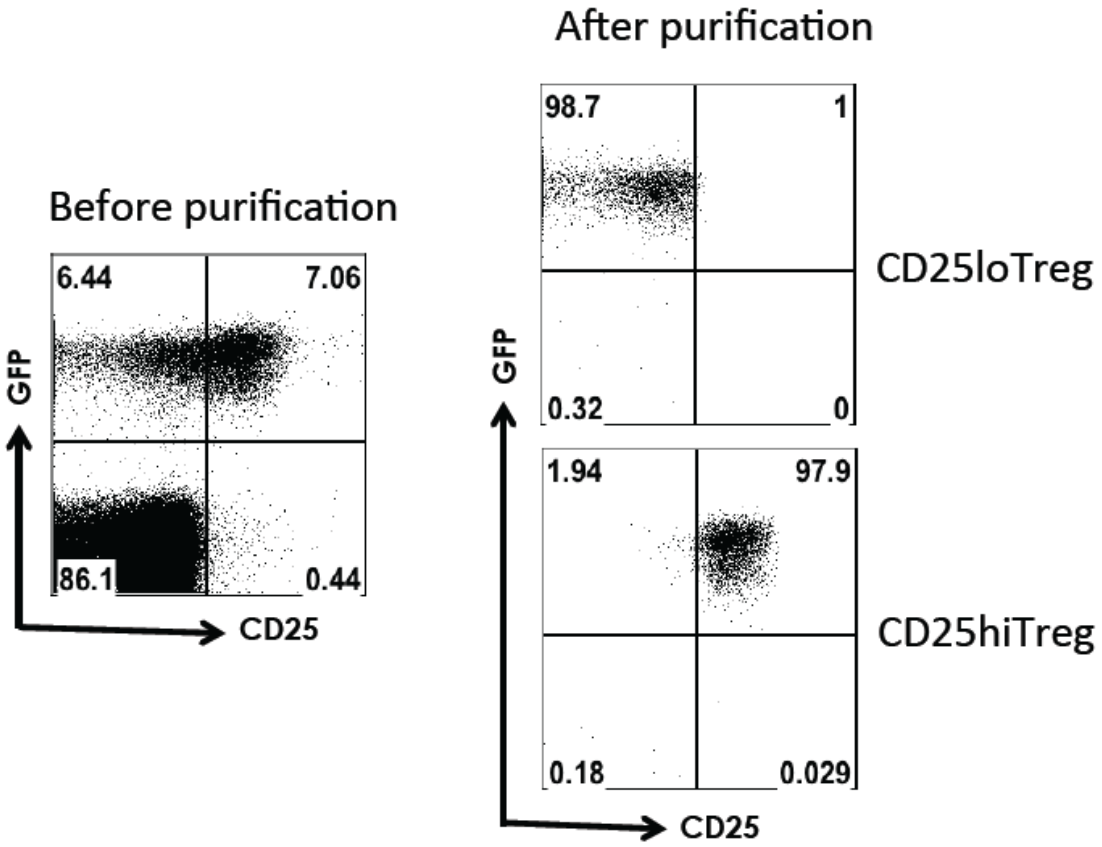

Figure S2.3. Purity of sorted CD25lo and CD25hi Treg cells.
Flow cytometric analysis of CD4 and CD25 expression by cells from spleen and lymph nodes of day 15 ocularly HSV-1 infected FM mice before FACS purification (left) and after purification (right).

CHAPTER 3
AZACYTIDINE TREATMENT INHIBITS THE PROGRESSION OF HERPES STROMAL KERATITIS BY ENHANCING REGULATORY T CELL FUNCTION

Research described in this chapter is reproduced from a publication accepted in Journal of Virology by Siva Karthik Varanasi, Pradeep BJ Reddy, Siddheshvar Bhela, Ujjaldeep Jaggi, Fernanda Gimenez, Barry T Rouse

Abstract

Ocular infection with Herpes Simplex Virus type 1 (HSV-1) sets off an inflammatory reaction in the cornea which leads to both virus clearance as well as chronic lesions that are orchestrated by CD4 T cells. Approaches that enhance the function of regulatory T cells (Treg) and dampen effector T cells can be effective to limit Stromal Keratitis (SK) lesion severity. In this report, we have explored the novel approach of inhibiting DNA methyltransferase activity using 5-Azacytidine (cytosine analog) to limit HSV-1 induced ocular lesions. We show that therapy begun after infection when virus was no longer actively replicating resulted in the pronounced reduction in lesion severity with markedly diminished numbers of T cells and non-lymphoid inflammatory cells along with reduced cytokine mediators. The remaining inflammatory reactions had a change in ratio of CD4 Foxp3+Treg to effector Th1 CD4 T cells in ocular lesions and lymphoid tissues with Treg becoming predominant over the effectors. In addition, compared to controls, Treg from Aza treated mice showed more suppressor activity in vitro and expressed higher levels of activation molecules. Additionally, cells induced in vitro in the presence of Aza showed epigenetic differences in the Treg Specific Demethylated Region (TSDR) of Foxp3 and were more stable when exposed to inflammatory cytokines. Our results show that therapy with Aza is an effective means of controlling a virus-induced inflammatory reaction and may act mainly by the effects on Treg.

Introduction

Once a viral infection becomes established its removal largely depends on the activity of T lymphocytes. Multiple functional subsets of T cells can participate with the outcome dependent on the nature of the virus, its location in the body and the types of T cells that become activated and expanded by the infection (1,2). Chronic tissue damaging inflammatory reactions can occur when elimination of infection is difficult to achieve, or the balance of T cell responsiveness emphasizes pro-inflammatory cells that contribute to tissue damage (3). For example, in stromal keratitis (SK) resulting from ocular infection by herpes simplex virus (HSV), a chronic inflammatory reaction occurs in the corneal stroma which is orchestrated mainly by pro-inflammatory CD4 Th1 and Th17 T cells (4-6). The lesion is less severe and can even resolve if regulatory T cells (Treg), such as Foxp3+ CD4 T cells, dominant over the other pro-inflammatory CD4 T cell subsets (7-11). Accordingly, therapies aimed at increasing Treg numbers and/or improving their regulatory activity is of high relevance.

It is becoming evident that the balance between inflammatory and regulatory T cells is not fixed, but can change as a consequence of one or the other cell type changing in number or altering their functional activity (12). For example, functional changes were observed in vitro when Treg were exposed to some inflammatory mediators (13,14). Similar functional changes may occur during auto-inflammatory lesions in vivo with Treg losing their regulatory activity (15,16). Of more concern, these Treg may change and take on a pro-inflammatory function and then contribute to the severity of tissue damage (15-18). The changes in functional phenotype that occur is likely explained by epigenetic changes that affect expression of the Treg transcription factor Foxp3 (19,20). These epigenetic changes usually occur in the highly conserved intron-2 also known as Treg

specific demethylation region (TSDR), which harbors cytosine-phospho-guanine (CpG) sites subject to methylation (21,22). Thus, when TSDR is demethylated the transcription factors Ets-1 and Creb can bind and act as enhancers for the continuous transcription of the Foxp3 gene (23,24). However, when the TSDR is methylated, the enhancer activity is diminished and only transient expression of Foxp3 occurs. Consequently, for the stable expression of the Foxp3 gene, demethylation of TSDR is required (25,26). In fact, natural Treg that derive from the thymus are stable and their TSDR is invariably demethylated (22). In contrast, in vitro or in vivo induced Treg have a TSDR which is methylated and such cells show plasticity of both phenotype and function (22,25,27,28).

Approaches to promote the stability of induced Treg are to block TSDR methylation or to generate Treg that have a demethylated TSDR profile. The later can be achieved by inhibiting DNA methyltransferase as occurs when 5-Azacytidine (Aza) is used for therapy (22,25,61). This FDA approved drug is used to treat myelodysplastic syndrome (29), and is also an effective therapy against some inflammatory disease models (30-32). The treatment has also been proposed to act by increasing the potency of the Treg response (31-33), and we further evaluate this notion using an infectious disease model of inflammation.

In this report, we show that the therapeutic administration of Aza was highly effective at suppressing the severity of ocular immuno-inflammatory lesions that result from corneal infection with HSV. The beneficial outcome of the Aza therapy appeared to be the consequence of restricted infiltration of pro-inflammatory immune cells to the cornea. The cells that did enter had increased number of Treg in comparison to CD4+ gamma interferon-producing (IFN-γ+) effector T cells. This increased representation of Treg in Aza treated animals was also evident in the blood and lymphoid tissues. Significant differences in suppressive efficacy of Treg from control and treated groups was also observed, with Treg from Aza treated animals being more suppressive, a property explained at least in part by higher expression levels of Reactive Oxygen Species (ROS) and activation markers. Furthermore, Treg generated in vitro in the presence of Aza expressed a fully demethylated TSDR and these cells also displayed enhanced suppressive activity which correlated with enhanced ROS production and activation markers. Overall, our results emphasize that the epigenetic modifying drug Aza may represent a novel approach to control HSV-1 induced ocular immuno-pathological lesions, the most common infectious cause of blindness in humans in the USA.

Results

Azacytidine reduces SK lesion severity and diminishes pro-inflammatory cytokines and chemokines after HSV-1 infection

To assess the efficacy of Aza on the extent of ocular lesions caused by HSV infection, animals were given either Aza or PBS (control) daily starting day 5 post infection (pi). This is the time point when there is at best minimal replicating virus detectable in the infected corneas and early inflammatory reactions start to become evident (36). Animals were examined at intervals to record the severity of SK lesions. The results were clear cut with animals receiving Aza therapy showing significantly ($P < 0.001$) reduced SK lesion severity compared to PBS treated control animals (Fig. 3.1A) Treatment effects were first evident by day 10, and by day 15, 10% of Aza-treated animals showed a lesion

score of ≥ 3 compared to 60% in control PBS treated animals (Fig. 3.1B). This pattern of reduced inflammatory reaction in Aza treated animals was also evident in histological sections of corneas taken from animals terminated at day 15pi (10 days after treatment) (Fig.3.1C).

At the termination of the experiments on day 15 pi, pools of 4 corneas were collected and processed to identify their cellular composition by FACS analysis. There was a reduction in inflammatory cell numbers including neutrophils (>500 fold), macrophages (10 fold), and CD4 T cells (> 10 fold) in Aza treated animals compared to controls (Fig 3.2A-C). In separate experiments of the same design, pools of corneas were processed to quantify mRNA of selected cytokines (IL-1β, TNF-α, IL-6 and IL-12) and chemokines (CCL3, CCL2, CXCL1and MMP1) by quantitative real time PCR (Q-RTPCR). As shown in Fig 3.3, those treated with Aza showed a reduction in the level of several pro-inflammatory cytokines and chemokines compared to controls. However, there was also a reduction in the expression levels of anti-inflammatory IL-10 and TGF-β (Fig 3.3), likely explained by reduced numbers of infiltrating immune cells. Taken together, our results show that daily administration of Aza, 5 days after virus infection significantly diminished HSV-1 induced immunopathology.

Aza treatment changes the balance of Treg to Th1 effectors

Since it is known that the outcome of SK lesion severity is dependent on the ratio of Treg to Th1 (37), the ratio of the cell types was compared in corneas, blood and DLN in Aza treated and control infected animals. Pools of corneas were collected at 15 days p.i from Aza treated and control animals and the infiltrating cell population was recovered after collagen digestion. These cells were then stimulated in vitro for 4 hours with PMA and ionomycin and the CD4 T cells were enumerated that were either IFN-γ producers or expressed the transcription factor Foxp3. (Fig. 3.2D). Changes in representation of the two cell types occurred as a consequence of Aza therapy. Thus in the corneas of Aza treated animals, the ratio favored Foxp3+ CD4 T cells to Th1 cells being around 2:1, but in controls the ratio was around 1:7 (Fig.3.2E). Approximately, 7% of the total CD4 T cells in the corneas of control animals expressed Foxp3, but in Aza treated animals around 35% were Foxp3+ cells (Fig. 3.2D). As with the corneas, blood from Aza treated mice displayed an increased Treg frequency with 12% of the CD4 T cells being Foxp3+ compared to only 5% in PBS treated controls at day 15pi (Fig. 3.4A). The total number of CD4 T cells (per 1 million cells) in the blood was decreased by 2-fold in the Aza treated animals (Fig. 3.4B). Although less in magnitude similar reduction in Th1 frequency and number (Fig. 3.4D,E) along with changes in Treg to Th1 ratio occurred in the DLN at day 15pi (Fig. 3.4F). The number of total CD4 T cells and Treg cells in the DLN of the Aza treated animals were reduced by 1.8 and 1.4 fold respectively (Fig. 3.4C,G). Reduction in Treg numbers may be as a consequence of reduced inflammatory response. Additionally, single cell suspensions of DLNs isolated at day 15 pi from control and Aza treated animals were stimulated overnight with UV-inactivated HSV-1 followed by ICS assay to measure antigen specific Th1 responses. Results indicated that there was more than 2-fold reduction in frequency and number of Th1 cells (CD4+ IFN-γ+ cells) in DLN samples from Aza treated animals that were specific for HSV-1 (Fig. 3.4H). In conclusion, upon Aza treatment there was a change in the balance in CD4 T cell responses with an increased representation of Treg which could in part contribute to the reduced lesion severity.

Azacytidine increased Treg suppressive function and activation markers

Since Aza treatment of HSV ocularly infected mice resulted in diminished lesions and increased representation of Foxp3+ CD4 T cells, the question arose as to whether or not the Treg population showed any changes in regulatory function in response to Aza therapy. To measure the suppressive activity, Foxp3 GFP mice were infected with HSV-1 and Foxp3+ T cells were recovered by FACS sorting from the pools of DLN and spleens of control and Aza treated animals at day 15 pi. Equal numbers of Foxp3+ T cells were cultured at different ratios with naïve responders stimulated with anti-CD3/CD28. The results indicate that Treg from HSV-1 infected Aza treated mice displayed more suppressive activity against stimulated naïve responders (>20 fold at 1:8 ratio) compared to Treg from infected controls (Fig.3.5A). Suppression with Treg from Aza treated animals could be observed in cultures with 1 Treg to 16 responders, whereas with control Treg a ratio of 1 to 4 was needed to demonstrate significant levels of suppression (Fig. 3.5B).

To provide an explanation for the greater suppressive activity of cells from Aza treated infected animals, a number of measurements were made. To determine if differences in IL-10 production was an explanation, DLNs from Aza treated and control animals were isolated at day 15 pi and 1 million single cell suspensions were stimulated with PMA/Ionomycin and supernatants were compared for levels of IL-10 using ELISA. No significant differences were detectable between the cells from Aza treated and control groups (data not shown). Comparisons were also made between Treg in control and Aza treated animals for activation markers as well as ROS production, since the latter has been advocated to be involved in suppressive activity (38). In the DLNs from Aza treated animals isolated at day 15 pi, Treg displayed only a modest increase in expression (ranging from 1.3 to 1.6 fold) of activation markers. These included CD25, OX40, GITR, CD103, FR4 and CD44 on Foxp3+ CD4 T cells (Fig. 3.5C). Differences between the two Treg populations were greatest in the case of expression of intracellular ROS. Thus the Treg in DLN from Aza treated animals had around 3-fold increase in ROS activity as compared to the cells from controls (Fig. 3.5D,E). Additionally, expression of genes involved in ROS production i.e NOX-2 and NCF-1 genes (components of NADPH oxidase complex) (39) were also increased 3 and 2.5 fold respectively in the Treg of Aza treated compared to control animals**,** as measured by QRT-PCR (Fig. 3.5F). The expression of IL-10 and TGF-beta was also measured in Treg from Aza treated and control animals using QRT-PCR. The results indicate similar expression levels of IL-10 and TGF-beta in both samples (Fig. 3.5G). Based on the above results, we could show that Aza treatment protected the phenotype and function of Treg cells. In conclusion, Treg show enhanced suppressive activity after Aza treatment and this may be explained at least in part by their increased activation markers and ROS producing ability.

Effect of Azacytidine on the lesion severity was dependent on the presence of Treg

Since Aza treatment reduced lesion severity which correlated with changes in Treg number and function, experiments were done to determine the outcome of Aza treatment wherein Treg were depleted prior to infection. Depletion was achieved by administration of mAb against the IL-2 receptor (CD25) given on day 0 of infection. The depletion procedure, as measured at day 15 pi, was shown to be around 50% effective at reducing total Foxp3+ T cells in DLN (Fig. 3.6A). SK lesion severity was measured at day 15 pi and the results indicate that Aza treatment to Treg intact animals led to reduced lesion severity with an average SK score of 1.7. This compared to an average score of 3.1 in the control

groups. However, in animals depleted of Treg and Aza treated, the inhibitory effects on SK severity were no longer apparent with an average score of 3.8 (Fig. 3.6B). To measure any effect of Aza therapy on the magnitude of CD4 Th1 response, the numbers of IFN-γ producing CD4 T cells in the DLNs at day 15pi were measured. Unlike in Treg intact animals where Aza treatment resulted in reduced effector T cells numbers, Aza treatment to Treg depleted animals displayed no significant difference in effector responses compared to PBS treated controls. (Fig. 3.6C).

Next, to evaluate the effect of Aza on proliferation of Treg and effectors, DLN were isolated at day 15pi from Treg depleted and control animals treated with or without Aza. Single cell suspensions were stained for CD4, Foxp3 and Ki-67 (proliferation marker). Results indicated that after Aza treatment, the proliferation of effector T cells was reduced by 1.5 fold in the Treg intact animals compared to the untreated controls. Whereas, Aza treatment in Treg depleted animals resulted in a 1.5-fold increase in the proliferation of effector T cells compared to untreated controls (Fig. 3.6D), the proliferation of Treg were unchanged after Aza treatment in both cases (Fig. 3.6E). Consistent with the role of Treg in controlling effector cell proliferation, Aza treatment in the Treg depleted animals increased the proliferation of effector cells, whereas in the presence of Treg Aza treatment led to reduced proliferation. Accordingly, our results imply that Aza may act preferentially on the Treg subset that likely express high level of CD25.

Azacytidine promotes differentiation and stability of Treg in vitro

To evaluate the direct effect of Aza on Treg and T effectors (Th1), in vitro differentiation experiments were performed. For this purpose, naïve splenocytes from DO11.10 RAG2-/- animals (ova peptide specific and 98% naïve CD4+ T cells) were cultured in the presence of Treg differentiating conditions (IL-2 and TGF-β) as well as in the presence or absence of graded amounts of Aza (from 1 μM to 15 μM). The results show a dose dependent enhancement in Treg differentiation compared to control cells without Aza with the maximal effect evident at 5μM (Fig. 3.7A). This dose yielded an approximately 2-fold increase in the frequency of Foxp3+ CD4 T cells induced in cultures (Fig. 3.7B). Similarly, when naïve DO11.10 RAG2-/- splenocytes were cultured in the presence of 5μM Aza and Th1 differentiating conditions (IL-12 and anti-IL-4), Aza increased the frequency of IFN-γ by 2-fold (Fig 3.7C). To provide a possible explanation for the Aza enhancement effects on Treg induction, experiments were done to record epigenetic changes in the TSDR region of Treg induced in the presence or absence of Aza. Although, Aza might affect the global methylation status of several other genes with CpG sites such as Gitr, Ctla4, Ikzf4 and CD25 (27), the methylation status of only the TSDR region of Foxp3 gene was evaluated, as this region is known to be an indicator of Treg stability and function (25-27, 55,56). Naïve CD4 T cells isolated from Foxp3 GFP mice were differentiated into Treg in the presence or absence of Aza (5μM) and equal numbers of Foxp3 GFP+ cells were harvested 5 d post culture by FACS sorting. The DNA was bisulfite converted after which the TSDR region was PCR amplified, cloned and sequence analyzed for methylated CpG sites. Dramatic differences were evident between cells induced in the presence or absence of Aza. In the presence of Aza, the TSDR region was demethylated about 80%. In contrast, without Aza the TSDR was only minimally demethylated (about 5%) (Fig. 3.7D). These methylation differences could have consequences in terms of Treg stability.

Since the Treg induced in the presence of Aza displayed a demethylated TSDR region, the effects of exposing the Treg population induced in the presence or absence of Aza to inflammatory cytokines which are known to destabilize Treg were measured (25,40). The two Treg populations were harvested and Foxp3 expression was determined following exposure for 3 days to IL-2 or IL-12 (Th1 condition) or IL-6 and TGF-β (Th17 conditions). In agreement with previous reports (41), IL-2 alone under non-stimulating conditions did not cause a change of Foxp3 expression. However, exposure to IL-12 for 3 d resulted in loss of Foxp3 expression in around 40% of cells. In contrast, the Treg induced in the presence of Aza lost only 20% of their Foxp3 expression after exposure to IL-12. Similar differences, but less in magnitude, were observed when the two populations were exposed to Th17 conditions (IL-6 and TGF-β). In those experiments, control induced Treg lost around 25% of their Foxp3 expression whereas Aza induced Treg lost around 12% (Fig. 3.7E). In conclusion, Treg induced in vitro in the presence of Aza had TSDR that was demethylated and such cells were more stable in the presence of inflammatory cytokines (IL-12 or IL-6) than were Treg induced without Aza.

Aza promotes Treg suppressive function and activation markers

To evaluate if enhanced Treg stability may lead to enhanced Treg function, experiments were done to measure functional differences in Treg induced in vitro in the presence or absence of Aza. For these experiments, naïve CD4 T cells isolated from Foxp3 GFP mice were used. The Foxp3 GFP+ cells were harvested 5 d post culture, FACS sorted and in vitro suppression assays were performed. Equal numbers of Foxp3+ T cells were cultured at different ratios with naïve responders stimulated with anti-CD3/CD28. The results indicate that Treg differentiated in the presence of Aza showed more than 2 fold higher suppressive activity compared to that of control Tregs (Fig. 3.8 A,B). In separate experiments, Treg were differentiated in the presence or absence of Aza (5μM) to yield a similar frequency of Foxp3+CD4 T cells between the two groups (high concentration of TGF-β) (Fig. 3.8C). The expression of ROS and the activation markers was compared. The Treg generated in the presence of Aza displayed around 1.3-1.8 fold increase in the expression of CD25, GITR, FR4, OX40 and ROS compared to that of control Treg (Fig. 3.8D,E). In conclusion, exposure of Aza during Treg induction resulted in enhanced Treg suppressive function which could be partly explained by enhanced activation markers and ROS production in vitro.

Discussion

Ocular infection with HSV sets off an inflammatory cytokine reaction in the cornea which leads to both virus clearance as well as chronic lesions that are orchestrated by CD4 T cells (4,36). Approaches that enhance the function of Treg cells and dampen effector T cells can be effective to limit SK lesion severity (7-10). In this report, we have explored the novel approach of inhibiting DNA methyltransferase activity using 5-Azacytidine (cytosine analog) to limit HSV induced ocular lesions. We show that therapy begun after infection when virus was no longer actively replicating resulted in the pronounced reduction in lesion severity with markedly diminished numbers of inflammatory T cells and non-lymphoid inflammatory cells along with reduced cytokine mediators. The remaining inflammatory reactions had a change in ratio of CD4 Foxp3+Treg to effector Th1 CD4 T cells in ocular lesions with Treg becoming predominant

over the effectors. We also show that a consequence of Aza therapy was an increased suppressive activity of Treg, an effect which correlated with their increased expression of ROS. Hence treatment with Azacytidine during early stages of lesion development represents an effective and novel therapy for a lesion that is a common cause of human blindness (42).

Our results clearly showed markedly reduced lesions in response to HSV-1 infection in Aza treated animals. In the model we used, SK lesions are immunopathological and are orchestrated mainly by IFN-γ producing CD4 T cells. However, the tissue damage is mediated largely by neutrophils and to lesser extent macrophages which are recruited to the corneal site of inflammation by signals generated by the T cells (43,44). In consequence, the inhibitory effects of Aza might be directed against multiple cell types in the SK response. In fact, some reports have indicated that Aza therapy can inhibit the generation of neutrophils (45) and pro-inflammatory (M1) macrophages (46), but we argue that the anti-inflammatory effects of Aza in the SK system may be explained mainly by its effects on T cells, particularly Treg. Thus whereas all cell types were reduced in number in Aza treated animals, there was a differential effect on Th1 effectors and Treg. In fact, in treated animals the ratio of Treg to Th1 cells was increased substantially in corneal lesions (a change from 1:7 to 2:1) and similar but less dramatic changes of ratios occurred in the blood and DLN. Our results indicate that the ratio change may be more the consequence of direct effects on Treg rather than on T effectors. In fact, our working hypothesis is that Aza serves to stabilize, expand or change the regulatory potency of Treg and this acts to inhibit the function or perhaps transport of effectors to the corneal site of inflammation. Support of these ideas came from the observation that antigen specific effectors were reduced in number in the DLN of Aza treated animals, an effect likely the consequence of enhanced Treg function. Thus we observed that Treg induced in the presence of Aza had significantly enhanced suppressive activity in vitro compared to cells from control animals.

With regard to why the Treg from Aza treated animals were more suppressive compared to Treg from control animals, we could show that the activation markers such as CD25, GITR, OX40 and FR4 levels along with ROS were significantly increased as a consequence of Aza therapy. A possible involvement of ROS activity in Treg function was noted in models of autoimmune arthritis and colitis, where inhibition of ROS producing enzyme system, such as NCF-1 or NOX2, led to loss of Treg suppressor function, enhanced effector responses and aggravated inflammatory lesions (51-53). Conceivably, increased ROS expression by Treg makes them more inhibitory against T effectors by inducing T cell death (57,58). However, since Aza induces DNA demethylation across several genes leading to their increased transcriptional activity, whether or not changes in ROS expression is the most critical event that explains why Treg after Aza treatment were more effective to control the inflammatory reactions in the SK system needs further study. One line of studies we are pursuing is that the promoter, or the intron regions, of the Treg associated genes such as CD25, GITR, NCF-1 and NOX-2 might be hypomethylated upon Aza treatment which leads to their increased gene expression.

An alternative potential explanation for increased Treg representation over Th1 effectors in Aza treated animals could be that Aza might render Treg resistant to the destabilization effects of pro-inflammatory cytokines that are highly expressed at the lesion and DLN sites (36,59). Although this destabilization phenomenon was not

evaluated in vivo, we could show that Treg induced in vitro in the presence of Aza, but not control Treg, displayed enhanced stability when exposed to the pro-inflammatory cytokines IL-12 and IL-6. The increased stability was explained likely by epigenetic differences caused by Aza therapy which inhibited DNA methyltransferase that were induced as downstream signaling events of pro-inflammatory cytokines. Such events result in methylation of the TSDR and only transient Foxp3 expression (25,60). Evidence for epigenetic differences in the TSDR region between Treg generated in the presence or absence of Aza were shown by in vitro studies. Thus Treg generated in the presence of Aza had a demethylated TSDR region and showed stability when exposed to pro-inflammatory cytokines, unlike the non Aza exposed Treg which had a methylated TSDR and lost Foxp3 expression in the presence of pro-inflammatory cytokines.

The final line of evidence implicating Treg as a critical cell type affected by Aza therapy came from the observation that the anti-inflammatory effects of Aza were blunted if Treg were depleted from animals prior to infection and subsequent Aza therapy. This observation also makes it unlikely that Aza acts to cause suppressed lesions via direct inhibitory effects on effector T cells or on non-lymphoid inflammatory cells such as neutrophils. Supporting this notion, no inhibitory effects of Aza on effectors were observed in vitro and in fact when Aza was present during in vitro induction, both Treg and Th1 cells were increased in frequency. This observation that Aza therapy did not limit the lesion severity and effector responses when Treg were depleted came as a surprise, since the anti-CD25 mAb depletion procedure was only around 50% effective at depleting Treg. However, the depletion procedure is known to preferentially deplete Treg with high expression of the IL-2 receptor (CD25) (54,62) and this population is likely the one from which antigen specific induced Treg are generated and which regulate the effectors involved in SK. In fact, in prior studies, we had shown that anti-CD25 depletion results in enhanced effector function along with more severe lesions of SK (47). Moreover, some studies have shown CD25 hi Treg are in fact the precursors of antigen-specific Treg (48-50), but we lacked the necessary reagents to formally demonstrate the antigen specific Treg in our system. Nevertheless, Treg without HSV antigen specificity can also express modulatory effects in the SK system (7), although their CD25 expression level has not been evaluated. Overall, we take our observations to indicate that Aza therapy acts to stabilize and increase the regulatory function of Treg, an effect which likely acts in lymphoid tissue as well as at the corneal inflammatory site to limit the magnitude of effector T cell responses.

In conclusion, our results are consistent with the observation that inhibiting DNA methyltransferase activity through the use of Azacytidine plays a role in influencing the expression of SK lesions. The mechanisms involved to explain the outcome were multiple, and involve a change in the balance between effector and regulatory T cells. We anticipate that inhibiting DNA methyltransferase, could represent a useful approach to control an important cause of human blindness.

Materials and Methods

Mice and Virus

Female C57BL/6 mice and congenic Thy1.1+ mice were purchased from Harlan Sprague-Dawley, Inc. (Indianapolis, IN), Foxp3-GFP (C57BL/6 background) mice were a kind gift from M.Oukka (Brigham and Womens hospital, Harvard Medical School), BALB/c DO11.10 RAG2-/- mice were purchased from Taconic and kept in pathogen free facility where food, water, bedding and instruments were autoclaved. All the animals were housed in American Association of Laboratory Animal Care–approved facilities at the University of Tennessee, Knoxville, Tennessee. All investigations followed guidelines of the Institutional Animal Care and Use Committee, and adhered to the ARVO Statement for the Use of Animals in Ophthalmic and Vision Research. HSV-I RE strain was used in all procedures. Virus was grown in Vero cell monolayers (American Type Culture Collection, Manassas, VA), titrated, and stored in aliquots at −80°C until used.

HSV-1 ocular infection and clinical scoring

Corneal infections of C57BL/6 and Foxp3 GFP mice were conducted under deep anesthesia induced by intra peritoneal (i.p) injection of tribromoethanol (Avertin). Mice were scarified on cornea with a 27-gauge needle, and a 3 μl drop containing $1x10^5$ PFU of HSV in 3 μl volume was applied to the eye. The eyes were examined on different days post infection (dpi) with a slit-lamp biomicroscope (Kowa Company, Nagoya, Japan), and the clinical severity of keratitis of individually scored mice was recorded as previously described (34). Briefly, the scoring system was as follows: 0, normal cornea; +1, mild corneal haze; +2, moderate corneal opacity or scarring; +3, severe corneal opacity but iris visible; +4, opaque cornea and corneal ulcer; +5, corneal rupture and necrotizing keratitis.

Aza Administration

The 5-Azacytidine (MP BIOMEDICALS) was dissolved in PBS and administered intraperitoneally at 2mg/kg starting from day 5 post infection until day 14 after infection. The control group either received an equal volume of PBS or left untreated. The dose of Aza was chosen based on our preliminary studies (data not shown) and previous reports (35). Most of the experiments were repeated at least three times.

Histopathology

Eyes from control and TCDD treated mice were extirpated on day 15 pi and snap frozen in OCT compound (Miles, Elkart, IN). Six micron thick sections were cut, air dried in a desiccation box. Staining was performed with hematoxylin and eosin (Richard Allen Scientific, Kalamazoo, MI).

Flow Cytometric Analysis

At day 15 pi, corneas were excised, pooled group-wise, and digested with liberase (Roche Diagnostics Corporation, Indianapolis, IN) for 45 minutes at 37°C in a humidified atmosphere of 5% CO2. After incubation, the corneas were disrupted by grinding with a syringe plunger on a cell strainer and a single-cell suspension was made in complete RPMI 1640 medium. The single-cell suspensions obtained from corneal samples were stained for different cell surface molecules for fluorescence-activated cell sorting (FACS) analyses. Draining cervical lymph nodes were obtained from mice sacrificed at 15 days post infection and single cell suspensions were used. Blood samples were collected at intervals from Aza treated or control C57BL/6 Foxp3-GFP mice (HSV infected) to record

the percentage of CD4+ T cells that were Foxp3 positive. All steps were performed at 4°C. Briefly; cells were stained with respective surface fluorochrome-labeled Abs in FACS buffer for 30 minutes, then stained for intracellular Abs. Finally, the cells were washed three times with FACS buffer and resuspended in 1% paraformaldehyde. The stained samples were acquired with a FACS LSR II (BD Biosciences, San Jose, CA) and the data were analyzed using FlowJo software (Tree Star, Inc., Ashland, OR).

To determine the number of IFN-γ producing T cells, intracellular cytokine staining was performed. In brief, corneal cells were either stimulated with PMA (50ng) and Ionomycin (500ng) for 4 hours in the presence of brefeldin A (10 μg/mL) or stimulated with UV-inactivated HSV-1 RE (1 MOI) overnight followed by 5 hour brefeldin A (10 μg/mL) in U-bottom 96-well plates (6). After this period, Live/Dead staining was performed followed by cell surface and intracellular cytokine staining using Foxp3 intracellular staining kit (ebioscience) in accordance with the manufacturer's recommendations.

Reagents and antibodies.

CD4 (RM4-5), CD45 (53-6.7), CD11b (M1/70), Ly6G (1A8), F4/80 (BM8), IFN-γ (XMG1.2), CD103 (M290), CD25 (PC61, 7D4), GITR (DTA-1), FR4 (eBio12A5), CD44 (IM7), OX40 (OX-86), annexin-V, Foxp3 (FJK-16S), anti-CD3 (145-2C11), anti-CD28 (37.51), GolgiPlug (brefeldin A) from either ebiosciences or BD biosciences. Phorbol myristate acetate (PMA) and Ionomycin from sigma. Cell Trace Violet, Live/Dead Fixable Violet Dead Cell Stain Kit and CMH2DCFDA from Life Technologies. Recombinant IL-2, IL-12, IL-6 and TGF-β from R&D systems.

Quantitative PCR (qPCR)

At day 15 post ocular infection with HSV-1, the corneas were isolated and four corneas were pooled per sample/group. Regulatory T cells and effector cells were FACS sorted using Foxp3 GFP mice. Total mRNA from corneal and sorted T cell populations was isolated using mirVana miRNA isolation kit (Ambion). cDNA was made with 500ng of RNA (corneal samples) and entire RNA (isolated T cells) by using oligo(dT) primer and ImProm-II Reverse Transcription system (Promega). Taqman gene expression assays for cytokines (IL-10, TGF- β, IL-1β, TNF-α, IL-6, IL-12), chemokines (CCL3, CXCL1, CCL2, and MMP1) and NADPH oxidase components (NCF-1, NOX2) were purchased from Applied biosystems and quantified using 7500 Fast Real-Time PCR system (Applied Biosystems). The expression levels of different molecules were normalized to β-actin using ΔCt calculation. Relative expression between control and experimental groups was calculated using the $2^{-\Delta\Delta Ct}$ X 1000 formula.

Depletion of regulatory T cells in vivo

C57BL/6 mice were given i.p injection of 500 μg of Anti-CD25 monoclonal antibody (clone: PC61 rIgG1,BioXcell, West Lebanon, NH, USA) or control rat IgG1 (BioXcell) on same day of infection (day 0). Depletion efficiency was quantified by measuring percentage of Foxp3+ CD4 T cells after 15 days post infection.

Purification of CD4+ T cells.

CD4+ T cells (total or naïve) were purified from single cell suspension of pooled draining cervical lymph nodes (DLNs) and spleen from HSV-infected or naïve Foxp3 GFP and Thy1.1+ B6 (H-2b) mice using a mouse total or naïve CD4+ T cell isolation kit according to the manufacturer's instructions (Miltenyi Biotec, Auburn, CA). The purity was achieved at least to an extent of 90%. For methylation studies and suppression assays, Treg cultures were sorted based on foxp3 GFP using FACS sorter to achieve high purity.

In vitro suppression assay.

Treg suppression assay was done as previously described (9). Briefly, Foxp3-GFP mice infected with HSV-1 were divided into multiple groups. Mice in one group were injected with Aza on day 5 p.i., and control groups were injected with PBS. At day 15 p.i., single-cell suspensions from draining cervical lymph nodes (DLN) and spleen were prepared and CD4+ Foxp3+ T cells were sorted on a FACSAria cell sorter to 99% purity. To measure the suppressor function of Treg differentiated in vitro, naïve CD4 T cells from Foxp3 GFP mice were differentiated to Tregs in the presence or absence of Aza and Foxp3 GFP+ cells FACS sorted. CD4+ Foxp3+ T cells were then cultured with anti-CD3 (1 μg/well) and anti-CD28 (0.5 μg/well) antibodies and cell Trace violet (CTV) labeled naïve CD4+ Thy1.1 responder cells (purified by a Miltenyi biotech kit) in a 96-well round bottom plate. The suppressive capacity of Tregs was measured by coculturing Tregs and T conventional cells (Tconv) at different ratios (Treg/Tconv, 1:1 to 1:16). After 3 days of incubation, the extent of CTV dilution was measured in Thy1.1 CD4+ cells by flow cytometry. Percent suppression by Tregs was calculated by using the formula 100 − [(frequency of cells proliferated at a particular Treg/effector T cell ratio)/(frequency of cells proliferated in the absence of Tregs)]100 .

In vitro Treg and Th1 differentiation and Treg stability assays

Splenocytes isolated from DO11.10 RAG2 -/- or Foxp3 GFP mice were used as a precursor population for the induction of Foxp3+ in CD4+ T cells as previously described (8). Briefly, 1×10^6 splenocytes after RBC lysis and several washings were cultured in 1ml RPMI media containing rIL-2 (100 U/ml) and TGFβ (1-5ng/ml) in the presence or absence of various concentrations of Aza (1-15μM) with plate bound anti-CD3/CD28 Ab (1 μg/ml) for 5 days at 37°C in a 5% CO2 incubator. After 5 days, samples were characterized for Foxp3 intracellular staining (ebioscience staining kit) or GFP expression (Foxp3 GFP mice) analyzed by flow cytometry. Treg were either sorted (TSDR methylation analysis) or cultured in 96-well round bottom plate in the presence of IL-2 (100U/ml) or IL-12 (5ng/ml) or IL-6 (25ng/ml) +TGF-β (1ng/ml) for 3 days followed by flow cytometry analysis of Live CD4+ Foxp3+ cells.

For Th1 differentiation, splenocytes from DO11.10 RAG2 -/- mice were stimulated with plate bound anti-CD3/CD28 Ab (1 μg/ml) in the presence of recombinant mouse IL-12 (5-10ng/ml) and anti-IL-4 (10 μg/ml) and in the presence or absence of varying concentrations of Aza (1-15μM). After 5-days samples were re-stimulated with PMA/Ionomycin and analyzed for the production of IFN-γ by intracellular cytokine staining kit (BD biosciences) using flow cytometer.

TSDR methylation assay

Foxp3 GFP+ Cells were FACS sorted and genomic DNA was isolated (Qiagen) and was bisulfite-converted with an EZ DNA Methylation-Direct kit according to the manufacturer's protocol (Zymo Research). TSDR region (corresponding to Foxp3 conserved noncoding sequence 2) was PCR amplified using primer sequences 5′-GGGTTTTTTTGGTATTTAAG-3′ (forward) and 5′-CCTAAACTTAACCAAATTTT-3′ (reverse). PCR products were sub-cloned into pGEM-T Easy vectors (Promega) and transformed into bacterial clones. Plasmid DNA samples from each bacterial colony were sequenced separately at the UTK core facility (at least 10 sequences per sample).

Detection of intracellular redox state

Single suspension of cells from draining lymph nodes (DLNs) from both Aza treated and control HSV-infected C57BL/6 or in vitro differentiated Tregs were incubated with 1μM of CM-H2DCFDA (6- chloromethyl-2′,7′-dichlorodihyrofluorescin diacetate, acetyl ester) for 30 min at 37°C, followed by washing with PBS and surface staining for live CD4+ CD25+ cells. Oxidation of dye was detected by FITC fluorescence.

References

1. Swain, S. L., K. K. McKinstry, and T. M. Strutt. 2012. Expanding roles for CD4+ T cells in immunity to viruses. Nat Rev Immunol.
2. Sant, A. J., and A. McMichael. 2012. Revealing the role of CD4 + T cells in viral immunity:. The Journal of Experimental Medicine 209: 1391-1395.
3. Rouse, B. T., and S. Sehrawat. 2010. Immunity and immunopathology to viruses: what decides the outcome? Nat Rev Immunol 10: 514-526.
4. Niemialtowski, M., and B. T. Rouse. 1992. Predominance of Th1 cells in ocular tissues during herpetic stromal keratitis. The Journal of Immunology 149: 3035-3039.
5. Hendricks, R. L., T. M. Tumpey, and A. Finnegan. 1992. IFN-gamma and IL-2 are protective in the skin but pathologic in the corneas of HSV-1-infected mice. The Journal of Immunology 149: 3023-3028.
6. Suryawanshi, A., T. Veiga-Parga, N. K. Rajasagi, P. B. J. Reddy, S. Sehrawat, S. Sharma, and B. T. Rouse. 2011. Role of IL-17 and Th17 Cells in Herpes Simplex Virus-Induced Corneal Immunopathology. The Journal of Immunology 187: 1919-1930.
7. Sehrawat, S., S. Suvas, P. P. Sarangi, A. Suryawanshi, and B. T. Rouse. 2008. In Vitro-Generated Antigen-Specific CD4+ CD25+ Foxp3+ Regulatory T Cells Control the Severity of Herpes Simplex Virus-Induced Ocular Immunoinflammatory Lesions. Journal of Virology 82: 6838-6851.
8. Veiga-Parga, T., A. Suryawanshi, and B. T. Rouse. 2011. Controlling Viral Immuno-Inflammatory Lesions by Modulating Aryl Hydrocarbon Receptor Signaling. PLoS Pathog 7: e1002427.
9. J Reddy, P. B., T. H. Schreiber, N. K. Rajasagi, A. Suryawanshi, S. Mulik, T. Veiga-Parga, T. Niki, M. Hirashima, E. R. Podack, and B. T. Rouse. 2012. TNFRSF25 Agonistic Antibody and Galectin-9 Combination Therapy Controls Herpes Simplex Virus-Induced Immunoinflammatory Lesions. Journal of Virology 86: 10606-10620.
10. Gaddipati, S., K. Estrada, P. Rao, A. D. Jerome, and S. Suvas. 2014. IL-2/Anti-IL-2 Antibody Complex Treatment Inhibits the Development but Not the Progression of Herpetic Stromal Keratitis. The Journal of Immunology 194: 273-282.
11. Veiga-Parga, T., S. Sehrawat, and B. T. Rouse. 2013. Role of regulatory T cells during virus infection. Immunol Rev 255: 182-196.
12. Wohlfert, E., and Y. Belkaid. 2010. Plasticity of Treg at infected sites. Mucosal Immunol 3: 213-215.
13. Hoffmann, P., T. J. Boeld, R. Eder, J. Huehn, S. Floess, G. Wieczorek, S. Olek, W. Dietmaier, R. Andreesen, and M. Edinger. 2009. Loss of FOXP3 expression in natural human CD4 + CD25 + regulatory T cells upon repetitive in vitro stimulation. European Journal of Immunology 39: 1088-1097.
14. Yang, X. O., R. Nurieva, G. J. Martinez, H. S. Kang, Y. Chung, B. P. Pappu, B. Shah, S. H. Chang, K. S. Schluns, S. S. Watowich, X.-H. Feng, A. M. Jetten, and C. Dong. 2008. Molecular Antagonism and Plasticity of Regulatory and Inflammatory T Cell Programs. Immunity 29: 44-56.
15. Zhou, X., S. L. Bailey-Bucktrout, L. T. Jeker, C. Penaranda, M. Martínez-Llordella, M. Ashby, M. Nakayama, W. Rosenthal, and J. A. Bluestone. 2009. Instability of the transcription factor Foxp3 leads to the generation of pathogenic memory T cells in vivo. Nature Immunology 10: 1000-1007.

16. Bailey-Bucktrout, Samantha L., M. Martinez-Llordella, X. Zhou, B. Anthony, W. Rosenthal, H. Luche, Hans J. Fehling, and Jeffrey A. Bluestone. 2013. Self-antigen-Driven Activation Induces Instability of Regulatory T Cells during an Inflammatory Autoimmune Response. Immunity 39: 949-962.
17. Oldenhove, G., N. Bouladoux, E. A. Wohlfert, J. A. Hall, D. Chou, L. Dos santos, S. O'Brien, R. Blank, E. Lamb, S. Natarajan, R. Kastenmayer, C. Hunter, M. E. Grigg, and Y. Belkaid. 2009. Decrease of Foxp3+ Treg Cell Number and Acquisition of Effector Cell Phenotype during Lethal Infection. Immunity 31: 772-786.
18. Komatsu, N., K. Okamoto, S. Sawa, T. Nakashima, M. Oh-hora, T. Kodama, S. Tanaka, J. A. Bluestone, and H. Takayanagi. 2013. Pathogenic conversion of Foxp3+ T cells into TH17 cells in autoimmune arthritis. Nature Medicine 20: 62-68.
19. van Loosdregt, J., Y. Vercoulen, T. Guichelaar, Y. Y. J. Gent, J. M. Beekman, O. van Beekum, A. B. Brenkman, D. J. Hijnen, T. Mutis, E. Kalkhoven, B. J. Prakken, and P. J. Coffer. 2009. Regulation of Treg functionality by acetylation-mediated Foxp3 protein stabilization. Blood 115: 965-974.
20. Baron, U., S. Floess, G. Wieczorek, K. Baumann, A. Grützkau, J. Dong, A. Thiel, T. J. Boeld, P. Hoffmann, M. Edinger, I. Türbachova, A. Hamann, S. Olek, and J. Huehn. 2007. DNA demethylation in the humanFOXP3 locus discriminates regulatory T cells from activated FOXP3+ conventional T cells. European Journal of Immunology 37: 2378-2389.
21. Floess, S., J. Freyer, C. Siewert, U. Baron, S. Olek, J. Polansky, K. Schlawe, H.-D. Chang, T. Bopp, E. Schmitt, S. Klein-Hessling, E. Serfling, A. Hamann, and J. Huehn. 2007. Epigenetic Control of the foxp3 Locus in Regulatory T Cells. PLoS Biology 5: e38.
22. Polansky, J. K., K. Kretschmer, J. Freyer, S. Floess, A. Garbe, U. Baron, S. Olek, A. Hamann, H. von Boehmer, and J. Huehn. 2008. DNA methylation controls Foxp3 gene expression. European Journal of Immunology 38: 1654-1663.
23. Kim, H.-P., and W. J. Leonard. 2007. CREB/ATF-dependent T cell receptor–induced FoxP3 gene expression: a role for DNA methylation. The Journal of Experimental Medicine 204: 1543-1551.
24. Polansky, J. K., L. Schreiber, C. Thelemann, L. Ludwig, M. Krüger, R. Baumgrass, S. Cording, S. Floess, A. Hamann, and J. Huehn. 2010. Methylation matters: binding of Ets-1 to the demethylated Foxp3 gene contributes to the stabilization of Foxp3 expression in regulatory T cells. Journal of Molecular Medicine 88: 1029-1040.
25. Lal, G., N. Zhang, W. van der Touw, Y. Ding, W. Ju, E. P. Bottinger, S. P. Reid, D. E. Levy, and J. S. Bromberg. 2008. Epigenetic Regulation of Foxp3 Expression in Regulatory T Cells by DNA Methylation. The Journal of Immunology 182: 259-273.
26. Ohkura, N., Y. Kitagawa, and S. Sakaguchi. 2013. Development and Maintenance of Regulatory T cells. Immunity 38: 414-423.
27. Ohkura, N., M. Hamaguchi, H. Morikawa, K. Sugimura, A. Tanaka, Y. Ito, M. Osaki, Y. Tanaka, R. Yamashita, N. Nakano, J. Huehn, H. J. Fehling, T. Sparwasser, K. Nakai, and S. Sakaguchi. 2012. T Cell Receptor Stimulation-Induced Epigenetic Changes and Foxp3 Expression Are Independent and Complementary Events Required for Treg Cell Development. Immunity 37: 785-799.
28. Miyao, T., S. Floess, R. Setoguchi, H. Luche, Hans J. Fehling, H. Waldmann, J. Huehn, and S. Hori. 2012. Plasticity of Foxp3+ T Cells Reflects Promiscuous Foxp3 Expression in Conventional T Cells but Not Reprogramming of Regulatory T Cells. Immunity 36: 262-275.

29. Kaminskas, E. 2005. FDA Drug Approval Summary: Azacitidine (5-azacytidine, VidazaTM) for Injectable Suspension. The Oncologist 10: 176-182.
30. Goodyear, O. C., M. Dennis, N. Y. Jilani, J. Loke, S. Siddique, G. Ryan, J. Nunnick, R. Khanum, M. Raghavan, M. Cook, J. A. Snowden, M. Griffiths, N. Russell, J. Yin, C. Crawley, G. Cook, P. Vyas, P. Moss, R. Malladi, and C. F. Craddock. 2012. Azacitidine augments expansion of regulatory T cells after allogeneic stem cell transplantation in patients with acute myeloid leukemia (AML). Blood 119: 3361-3369.
31. Wu, C.-J., C.-Y. Yang, Y.-H. Chen, C.-M. Chen, L.-C. Chen, and M.-L. Kuo. 2013. The DNA Methylation Inhibitor 5-Azacytidine Increases Regulatory T Cells and Alleviates Airway Inflammation in Ovalbumin-Sensitized Mice. Int Arch Allergy Immunol 160: 356-364.
32. Zheng, Q., Y. Xu, Y. Liu, B. Zhang, X. Li, F. Guo, and Y. Zhao. 2009. Induction of Foxp3 demethylation increases regulatory CD4+CD25+ T cells and prevents the occurrence of diabetes in mice. Journal of Molecular Medicine 87: 1191-1205.
33. Singer, B. D., J. R. Mock, N. R. Aggarwal, B. T. Garibaldi, V. K. Sidhaye, M. A. Florez, E. Chau, K. W. Gibbs, P. Mandke, A. Tripathi, S. Yegnasubramanian, L. S. King, and F. R. D'Alessio. 2015. Regulatory T Cell DNA Methyltransferase Inhibition Accelerates Resolution of Lung Inflammation. American Journal of Respiratory Cell and Molecular Biology 52: 641-652.
34. Rajasagi, N. K., A. Suryawanshi, S. Sehrawat, P. B. J. Reddy, S. Mulik, M. Hirashima, and B. T. Rouse. 2012. Galectin-1 Reduces the Severity of Herpes Simplex Virus-Induced Ocular Immunopathological Lesions. The Journal of Immunology 188: 4631-4643.
35. Choi, J., J. Ritchey, J. L. Prior, M. Holt, W. D. Shannon, E. Deych, D. R. Piwnica-Worms, and J. F. DiPersio. 2010. In vivo administration of hypomethylating agents mitigate graft-versus-host disease without sacrificing graft-versus-leukemia. Blood 116: 129-139.
36. Biswas, P. S., and B. T. Rouse. 2005. Early events in HSV keratitis—setting the stage for a blinding disease. Microbes and Infection 7: 799-810.
37. Suvas, S., A. K. Azkur, B. S. Kim, U. Kumaraguru, and B. T. Rouse. 2004. CD4+CD25+ Regulatory T Cells Control the Severity of Viral Immunoinflammatory Lesions. The Journal of Immunology 172: 4123-4132.
38. Kim, H.-R., A. Lee, E.-J. Choi, M.-P. Hong, J.-H. Kie, W. Lim, H. K. Lee, B.-I. Moon, and J.-Y. Seoh. 2014. Reactive Oxygen Species Prevent Imiquimod-Induced Psoriatic Dermatitis through Enhancing Regulatory T Cell Function. PLoS ONE 9: e91146.
39. Jackson, S. H., S. Devadas, J. Kwon, L. A. Pinto, and M. S. Williams. 2004. T cells express a phagocyte-type NADPH oxidase that is activated after T cell receptor stimulation. Nature Immunology 5: 818-827.
40. Thomas, R. M., C. J. Gamper, B. H. Ladle, J. D. Powell, and A. D. Wells. 2012. De Novo DNA Methylation Is Required to Restrict T Helper Lineage Plasticity. Journal of Biological Chemistry 287: 22900-22909.
41. Chen, Q., Y. C. Kim, A. Laurence, G. A. Punkosdy, and E. M. Shevach. 2011. IL-2 Controls the Stability of Foxp3 Expression in TGF-β-Induced Foxp3+ T Cells In Vivo. The Journal of Immunology 186: 6329-6337.
42. Streilein, J. W., M. R. Dana, and B. R. Ksander. 1997. Immunity causing blindness: five different paths to herpes stromal keratitis. Immunology Today 18: 443-449.

43. Thomas, J., S. Gangappa, S. Kanangat, and B. T. Rouse. 1997. On the essential involvement of neutrophils in the immunopathologic disease: herpetic stromal keratitis. The Journal of Immunology 158: 1383-1391.
44. Griffin, G. K., G. Newton, M. L. Tarrio, D. x. Bu, E. Maganto-Garcia, V. Azcutia, P. Alcaide, N. Grabie, F. W. Luscinskas, K. J. Croce, and A. H. Lichtman. 2012. IL-17 and TNF- Sustain Neutrophil Recruitment during Inflammation through Synergistic Effects on Endothelial Activation. The Journal of Immunology 188: 6287-6299.
45. Platzbecker, U., M. Wermke, J. Radke, U. Oelschlaegel, F. Seltmann, A. Kiani, I. M. Klut, H. Knoth, C. Röllig, J. Schetelig, B. Mohr, X. Graehlert, G. Ehninger, M. Bornhäuser, and C. Thiede. 2011. Azacitidine for treatment of imminent relapse in MDS or AML patients after allogeneic HSCT: results of the RELAZA trial. Leukemia 26: 381-389.
46. Kim, Y. S., W. S. Kang, J. S. Kwon, M. H. Hong, H.-y. Jeong, H. C. Jeong, M. H. Jeong, and Y. Ahn. 2014. Protective role of 5-azacytidine on myocardial infarction is associated with modulation of macrophage phenotype and inhibition of fibrosis. J. Cell. Mol. Med. 18: 1018-1027.
47. Zhao, J., J. Zhao, and S. Perlman. 2014. Virus-Specific Regulatory T Cells Ameliorate Encephalitis by Repressing Effector T Cell Functions from Priming to Effector Stages. PLoS Pathog 10: e1004279.
48. Kasagi, S., P. Zhang, L. Che, B. Abbatiello, T. Maruyama, H. Nakatsukasa, P. Zanvit, W. Jin, J. E. Konkel, and W. Chen. 2014. In Vivo-Generated Antigen-Specific Regulatory T Cells Treat Autoimmunity Without Compromising Antibacterial Immune Response. Science Translational Medicine 6: 241ra278-241ra278.
49. Tang, Q., K. J. Henriksen, M. Bi, E. B. Finger, G. Szot, J. Ye, E. L. Masteller, H. McDevitt, M. Bonyhadi, and J. A. Bluestone. 2004. In Vitro–expanded Antigen-specific Regulatory T Cells Suppress Autoimmune Diabetes. The Journal of Experimental Medicine 199: 1455-1465.
50. Bonertz, A., J. Weitz, D.-H. K. Pietsch, N. N. Rahbari, C. Schlude, Y. Ge, S. Juenger, I. Vlodavsky, K. Khazaie, D. Jaeger, C. Reissfelder, D. Antolovic, M. Aigner, M. Koch, and P. Beckhove. 2009. Antigen-specific Tregs control T cell responses against a limited repertoire of tumor antigens in patients with colorectal carcinoma. Journal of Clinical Investigation.
51. Efimova, O., P. Szankasi, and T. W. Kelley. 2011. Ncf1 (p47phox) Is Essential for Direct Regulatory T Cell Mediated Suppression of CD4+ Effector T Cells. PLoS ONE 6: e16013.
52. Rodrigues-Sousa, T., A. F. Ladeirinha, A. R. Santiago, H. Carvalheiro, B. Raposo, A. Alarcão, A. Cabrita, R. Holmdahl, L. Carvalho, and M. M. Souto-Carneiro. 2014. Deficient Production of Reactive Oxygen Species Leads to Severe Chronic DSS-Induced Colitis in Ncf1/p47phox-Mutant Mice. PLoS ONE 9: e97532.
53. Lee, K., H. Y. Won, M. A. Bae, J. H. Hong, and E. S. Hwang. 2011. Spontaneous and aging-dependent development of arthritis in NADPH oxidase 2 deficiency through altered differentiation of CD11b+ and Th/Treg cells. Proceedings of the National Academy of Sciences 108: 9548-9553.
54. Couper, K. N., D. G. Blount, J. B. de Souza, I. Suffia, Y. Belkaid, and E. M. Riley. 2007. Incomplete Depletion and Rapid Regeneration of Foxp3+ Regulatory T Cells

Following Anti-CD25 Treatment in Malaria-Infected Mice. The Journal of Immunology 178: 4136-4146.
55. Zheng, Y., S. Josefowicz, A. Chaudhry, X. P. Peng, K. Forbush, and A. Y. Rudensky. 2010. Role of conserved non-coding DNA elements in the Foxp3 gene in regulatory T-cell fate. Nature 463: 808-812.
56. Li, X., Y. Liang, M. LeBlanc, C. Benner, and Y. Zheng. 2014. Function of a Foxp3 cis-element in protecting regulatory T cell identity. Cell 158: 734-748.
57. Hildeman, D. A., T. Mitchell, J. Kappler, and P. Marrack. 2003. T cell apoptosis and reactive oxygen species. Journal of Clinical Investigation 111: 575-581.
58. Hildeman, D. A., T. Mitchell, T. K. Teague, P. Henson, B. J. Day, J. Kappler, and P. C. Marrack. 1999. Reactive oxygen species regulate activation-induced T cell apoptosis. Immunity 10: 735-744.
59. Thomas, J., S. Kanangat, and B. T. Rouse. 1998. Herpes Simplex Virus Replication-Induced Expression of Chemokines and Proinflammatory Cytokines in the Eye: Implications in Herpetic Stromal Keratitis. Journal of Interferon & Cytokine Research 18: 681-690.
60. Samanta, A., B. Li, X. Song, K. Bembas, G. Zhang, M. Katsumata, S. J. Saouaf, Q. Wang, W. W. Hancock, Y. Shen, and M. I. Greene. 2008. TGF-β and IL-6 signals modulate chromatin binding and promoter occupancy by acetylated FOXP3. Proceedings of the National Academy of Sciences 105: 14023-14027.
61. DuPage, M., and J. A. Bluestone. 2016. Harnessing the plasticity of CD4+ T cells to treat immune-mediated disease. Nat Rev Immunol 16: 149-163.
62. Setiady, Y. Y., Coccia, J. A., Park, P. U. 2010. In vivo depletion of CD4+ FOXP3+ Treg cells by the PC61 anti-CD25 monoclonal antibody is mediated by FcγRIII+ phagocytes. European journal of immunology, 40(3): 780-786.
63. Dantal, J., Jacques, Y., Soulillou, J.P. 1991. Cluster-function relationship of rat-antimouse p55 il-2 receptor monoclonal antibodies in vitro studies of the ctl-l2 mouse cell line and in vivo studies in a delayed-type hypersensitivity model in mice. Transplantation, 52(1): 110-115.

APPENDIX

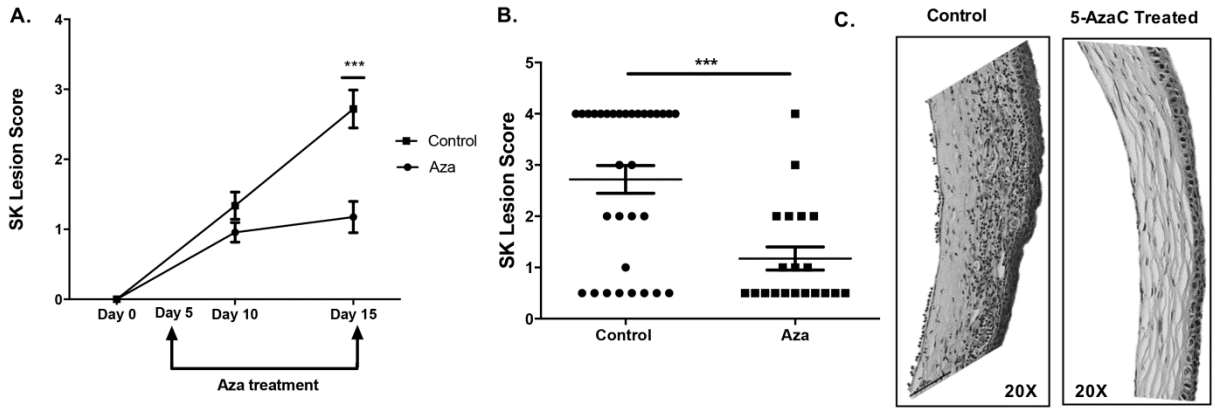

Figure 3.1. Therapeutic administration of Aza diminishes SK severity.
C57BL/6 animals infected with 1 x 10^4 PFU of HSV-RE were given either Aza or PBS from day 5 pi to day 14 pi. The disease progression was analyzed throughout time in a blinded manner using a scale described in materials and methods. (A) Kinetics of SK severity is shown. The progression of SK lesion severity was significantly reduced in the group of mice treated with Aza as compared with control mice. (B) Individual eye scores of SK lesion severity on day 15 pi. (C) Eyes were processed for cryo-sections on day 15 pi. Hematoxylin and eosin staining was carried out on 6-µm sections and pictures were taken at different microscope augmentations at ×20 magnification. Data represents the mean ± SEM of more than 3 independent experiments (n=10 mice/group). All the data were analyzed with student's t test and Mann-Whitney U test. P≤0.001(***)

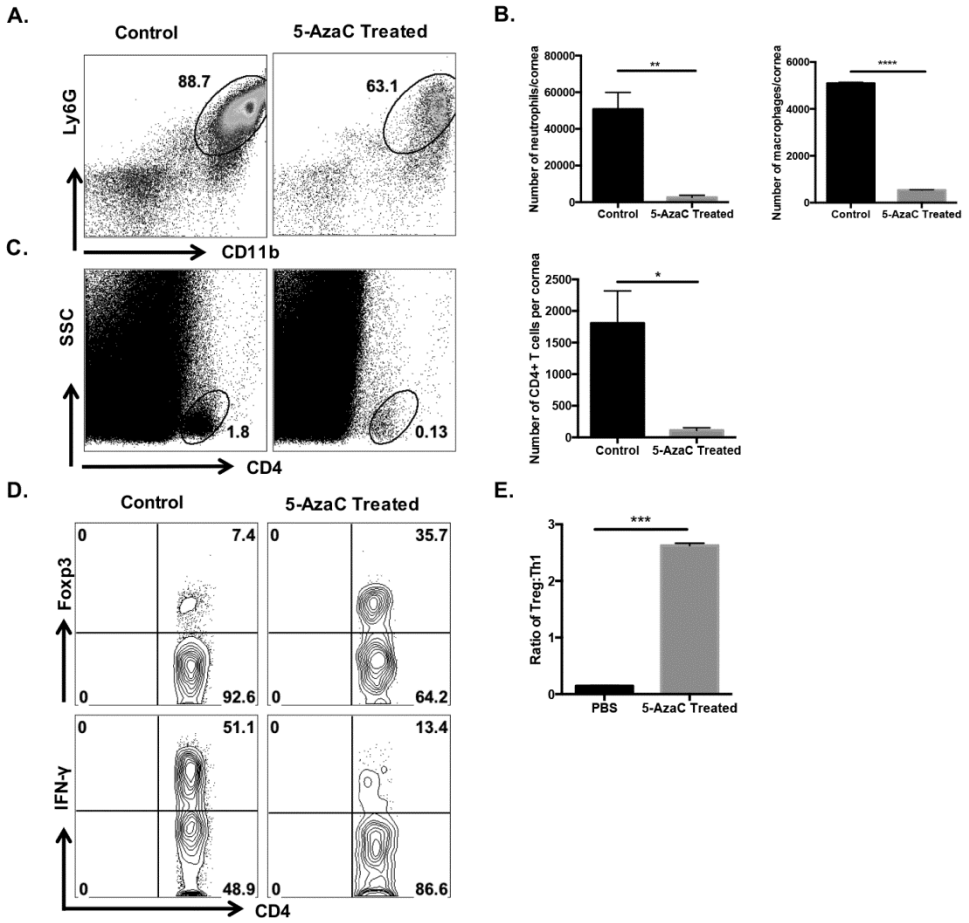

Figure 3.2. Aza administration diminishes infiltration of both lymphoid and non-lymphoid cells.

C57BL/6 animals infected with 1 x 10^4 PFU of HSV-RE were given either Aza or PBS from day 5 pi to day 14 pi. (A) Representative FACS plots showing frequency of neutrophils (CD45+CD11b+Ly6G+) infiltrating the cornea at day 15 p.i (B) Representative histogram showing the number of neutrophils and macrophages (CD45+CD11b+F4/80+) infiltrating the cornea at day 15 p.i (C) Representative FACS plots and histogram depicting the frequencies and number of total $CD4^+$ T cells infiltrating the cornea at day 15 p.i (D) Pool of corneas were stimulated with PMA/Ionomycin, representative FACS plots showing Treg (CD4+ Foxp3+) and Th1 (CD4+ IFN-γ) cells in the cornea at day 15pi cells were gated on CD4+ T cells (E) Histogram representing ratio of Treg to Th1 in the cornea at day 15pi. Data are the combination of atleast 3 independent experiments and show mean values ± SEM (n=3). The level of significance was determined by Student's t test (unpaired). P≤ 0.0001 (****), P≤0.001(***), P≤0.01(**), P≤0.05(*).

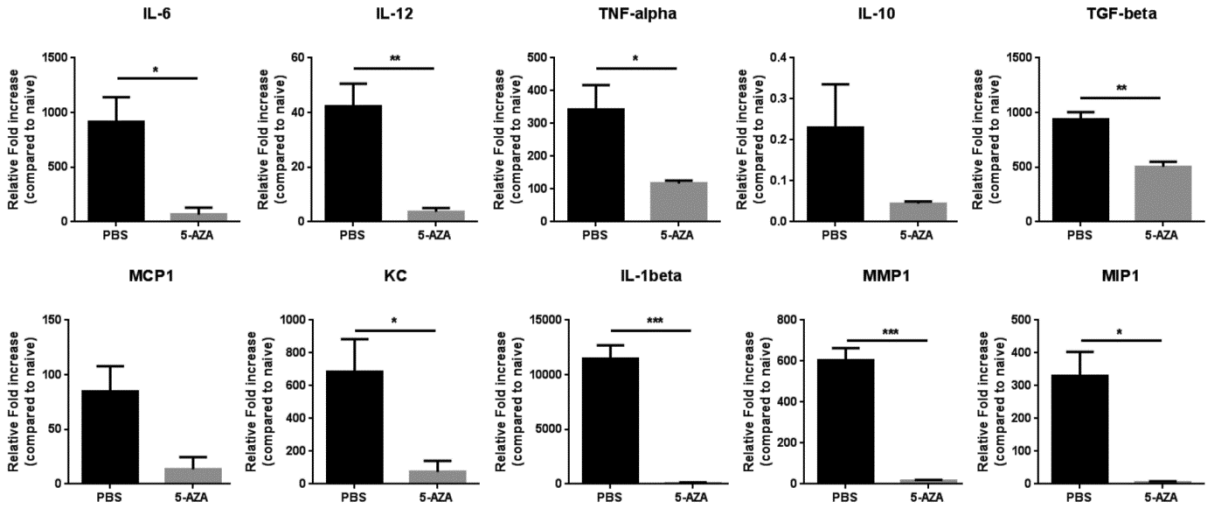

Figure 3.3. Effect of Aza treatment on cytokines and chemokines in the corneas of HSV-1 infected animals

C57BL/6 mice infected with 1×10^4 PFU of HSV-1 RE were given AZA once daily starting from day 5 until day 14 post infection. Mice were sacrificed at day 15 post infection and corneas were collected for measuring relative fold change in the mRNA expression using QRT-PCR of various cytokines and chemokines (TNF-α, IL-1β, IL-6, IL-12, IL-10, TGF-β MIP-1(CCL3), KC(CXCL1), MCP1(CCL2), MMP1) in pooled corneal samples each consisting of four cornea in control and Aza treated animals. Data represents means ± SEM from two different independent experiments (n=3/group) The level of significance was determined by Student's t test (unpaired). P≤0.001(***), P≤0.01(**), P≤0.05(*).

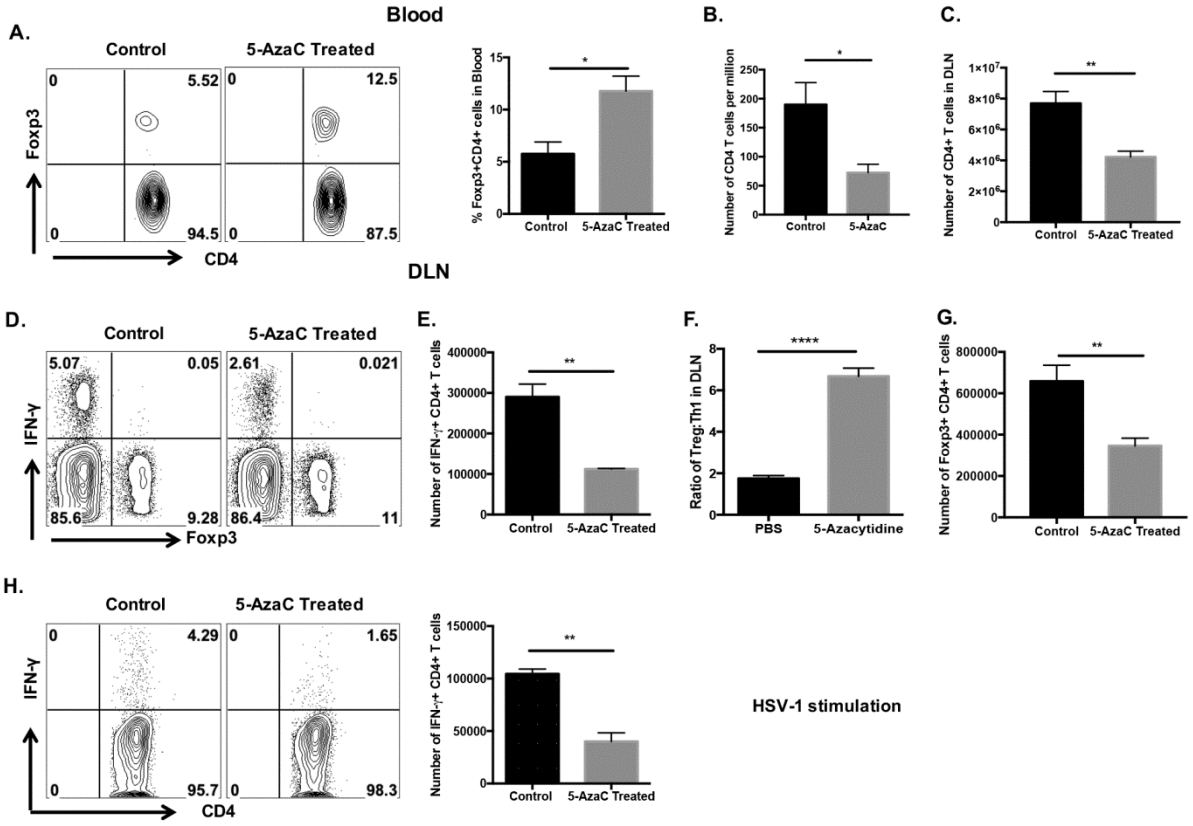

Figure 3.4. Aza administration changes the balance towards Tregs in the blood and draining lymph nodes

C57BL/6 or Foxp3 GFP mice infected with 1×10^4 PFU of HSV-1 RE were treated with Aza once daily starting from day 5 until day 14 post infection and terminated at day 15 p.i. (A) FACS and histograms showing frequency of Tregs (Foxp3 GFP+) cells in blood gated on CD4+ T cells. (B) Histogram representing the total number of CD4 T cells per 1 million of cells recorded in the blood. (C) DLN from day 15pi were stimulated with PMA/Ionomycin and histogram showing the total number of CD4 T cells (D) Representative FACS plots showing frequency of Treg (CD4+ Foxp3+) and Th1 (CD4+ IFN-γ) (E) Histogram representing number of Th1 cells in DLN (F) Histogram representing the ratio of number of Treg to Th1 in DLN (G) Histogram representing number of Treg cells in DLN (H) DLN were stimulated with UV-inactivated HSV-1, representative FACS plots and histogram showing frequency and number of antigen specific Th1 (CD4+ IFN-γ+) gated on live population. Data represents means ± SEM from three different independent experiments (n=3/group) and the level of significance was determined by Student's t test (unpaired). P≤ 0.0001 (****), P≤0.01(**), P≤0.05(*).

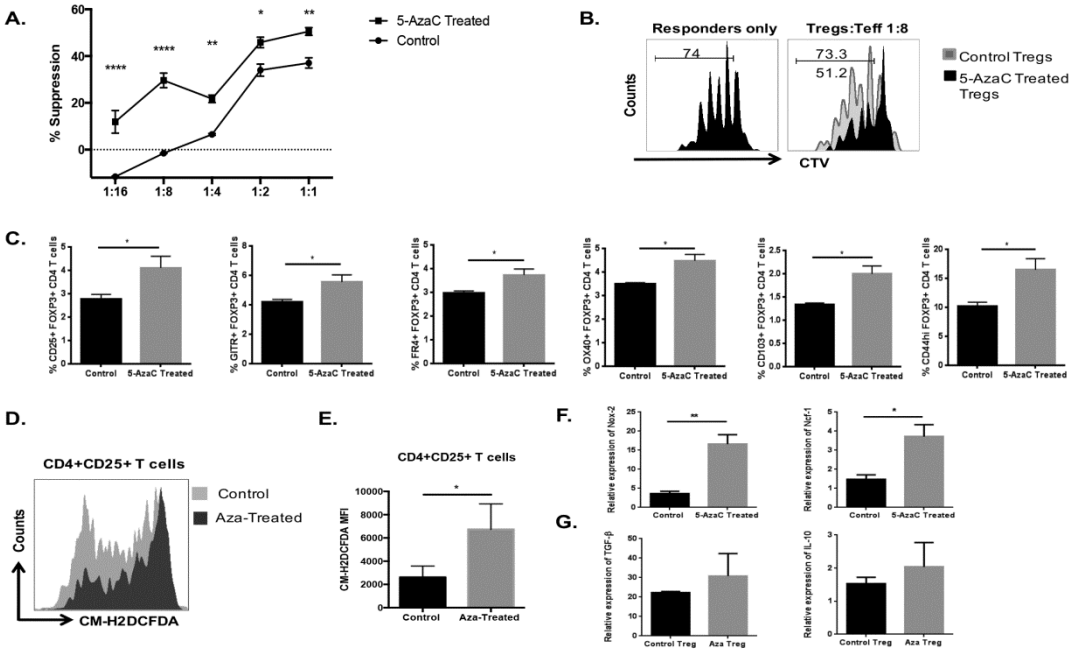

Figure 3.5. Aza treatment increases suppressor activity of Tregs

(A-B) Foxp3-GFP mice infected with HSV-1 were treated with Aza on day 5 p.i. until day 14 p.i. CD4+ Foxp3+ T cells were sorted at day 15pi and equal number (1 x 10^5cells) were cultured with CTV-labeled CD4+ CD25− Thy1.1 responder cells (Treg/Tconv, 1:1 to 1:16) in the presence of anti-CD3/CD28 antibodies. (A) Line graphs showing the percent suppression of Tregs from control and Aza treated groups at different ratio of naïve responders. (B) Representative FACS plots showing the extent of CTV dilution at a 1:8 Treg/effector T cell (Teff) ratio. Each experiment was repeated at least two times with at least 3 replicates per group. Statistical significance was calculated by one-way ANOVA with Tukey's multiple-comparison test P≤0.0001(****), P≤0.01(**), P≤0.05(*). (C) C57BL/6 mice infected with 1×10^4 PFU of HSV-1 RE were treated with Aza once daily starting from day 5 until day 14 post infection and terminated at day 15 p.i. Histogram showing the proportion Tregs in DLN expressing CD25, GITR, FR4, OX40, CD103 and CD44 at day 15pi gated on CD4+ Foxp3+ cells Data represent means ± SEMs of at least two independent experiments and the level of significance was determined by Student's t test (unpaired) P≤0.05(*). (D-E) DLNs from C57BL/6 HSV-1 infected control and Aza treated animals were isolated at day 15pi and stained with ROS indicator dye CM-H2DCFDA. (D) Representative FACS plot showing the expression of CM-H2DCFDA (E) Histogram showing MFI of CM-H2DCFDA from control and Aza treated mice gated live CD4+ CD25+ T cells. (F) Foxp3 GFP+ T cells were FACS sorted from HSV-1 infected control and Aza treated Foxp3 GFP mice and mRNA expression levels were measured by QRT-PCR. Bar graphs representing relative expression levels of Nox-2 and NCF-1 genes. (G) Bar graphs representing relative expression levels of TGF-β and IL-10 genes. Relative expression was calculated compared to expression of beta-actin. Data represents means ± SEM from two independent experiments (n=3/group). The level of significance was determined by Student's t test (unpaired) P≤0.01(**), P≤0.05(*).

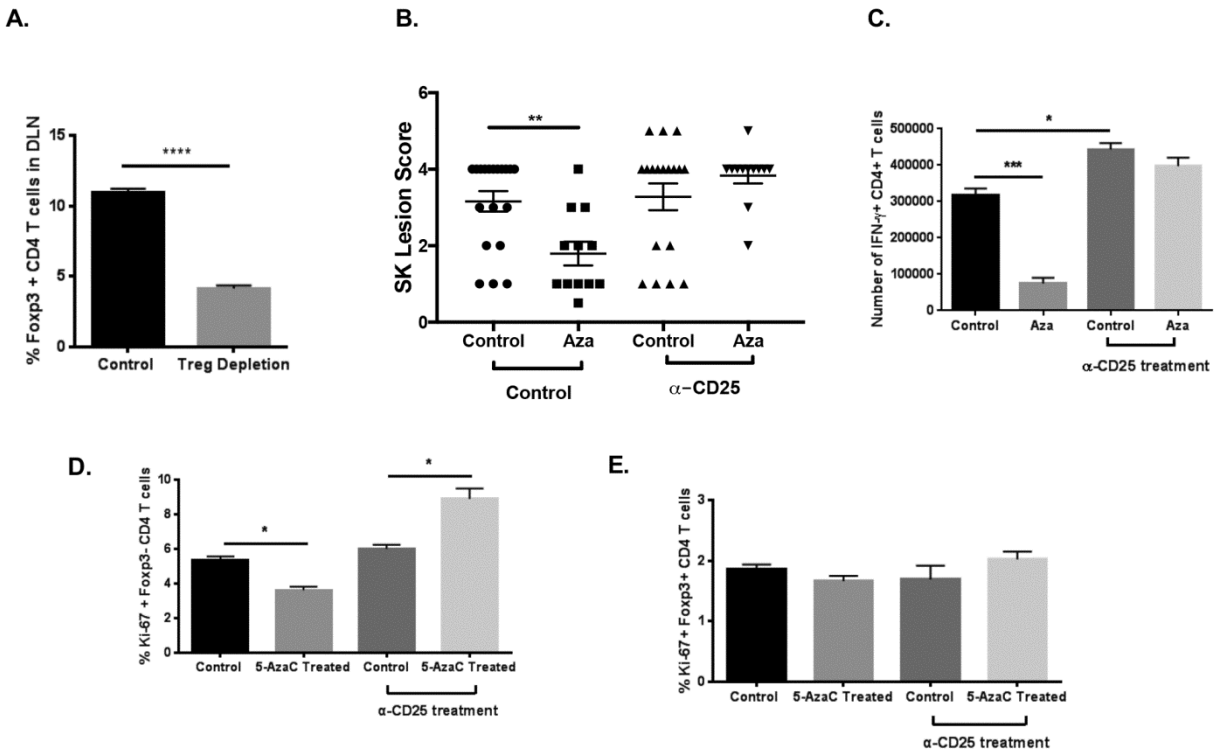

Figure 3.6. Depletion of CD25+ cells during Aza treatment did not ameliorate lesion severity

C57BL/6 mice infected with 1×10^4 PFU of HSV-1 RE were given either anti-CD25 depleting antibody (PC61) or control (IgG) antibody on day 0 and given either AZA or PBS daily starting from day 5 until day 14 post infection and were terminated at day 15 p.i (A) Histogram showing 50% reduction in Foxp3+ CD4+ T cells in DLN of Treg depleted animals compared to control animals at day 15p.i (B) Individual eye scores of SK lesion severity on day 15 pi. (C) DLNs were isolated and single cell suspensions stimulated with PMA/Ionomycin and representative histogram showing number of Th1 (CD4+ IFN-γ+) in DLN. (D,E) DLNs were isolated and single cell suspensions were surface stained for CD4 and intracellular stained for Foxp3 and Ki-67. (D) Histogram showing proliferation of effector T cells (CD4+ Foxp3-) (E) Histogram showing proliferation of Treg (CD4+ Foxp3+). Experiments were repeated at least two times and the level of significance was determined by Student's t test (unpaired) and Mann-Whitney U test. Error bars represent mean ± S.E.M. P≤ 0.0001 (****), P≤0.001(***), P≤0.01(**), P≤0.05(*).

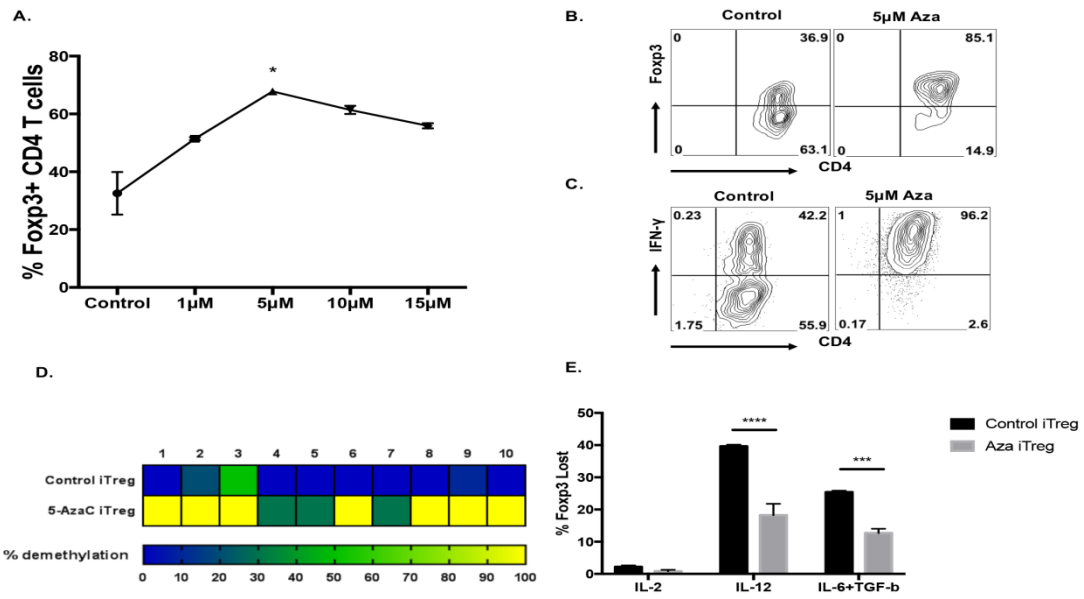

Figure 3.7. Aza promotes stability of Tregs in vitro (A-C) Splenocytes from DO11.10 RAG2−/− mice were cultured (1 million cells) in the presence of 1 μg/ml of anti-CD3/CD28 antibody with either Treg or Th1 differentiating conditions. (A,B) Treg differentiation was performed in the presence of 100 U/ml of recombinant IL-2, 1ng/ml TGF-β and varying concentrations of Aza (1μM-15-μM). After 5 days of culture, cells were analyzed for the expression of CD4 and Foxp3. Dose-response curve for Foxp3 induction with various concentrations of 5-Azacytidine (Aza) were indicated. (A) Line graph representing the Live CD4+ Foxp3+ cells at various concentrations of Aza. (B) Representative FACS plots showing Foxp3 expression in cells differentiated under Treg differentiating conditions in the presence or absence of 5μM Aza (C) Representative FACS plots showing the expression of IFN-γ in cells differentiated under Th1 differentiating conditions (5ng/ml IL-12 and 10μg/ml anti-IL-4) in the presence or absence of Aza 5μM (D) Naive CD4 T cells purified from Foxp3 GFP male mouse were cultured (1 million cells) with 100U/ml IL-2, 1μg/ml anti-CD3/CD28, 5ng/ml TGFβ and in the presence or absence of Aza (5μM) for up to 4 days. Foxp3 GFP+ T cells were FACS sorted. Methylation status of CpG motifs of the Foxp3 locus was assessed by bisulfite sequencing as described in Materials and methods. Numbers above boxes (1–10) indicate the 10 CpG islands in CNS2 of the Foxp3 locus (TSDR), from 5′ to 3′. Data are from one experiment with at least 10 bacterial colonies containing the plasmid encoding TSDR region were sequenced and average values were represented (E) Splenocytes from DO11.10 RAG2−/− animals were cultured in the presence of 1μg/ml anti-CD3/CD28, 100 U/ml IL-2, 5ng/ml TGF-β in the presence or absence of Aza (5μM) for 5 days. Later, exposed to 100U/ml IL-2 or 5ng/ml IL-12 or 25ng/ml IL-6 and 1ng/ml TGF-beta for another 3 days. Cells were measured for Live CD4+ Foxp3+ cells before exposure and after exposure. Histogram represents the frequency of Foxp3 lost by cells of control and Aza induced iTreg exposed to different conditions. Experiments were repeated at least three times. The level of significance was determined by Student's t test (unpaired) and error bars represent mean ± S.E.M. P≤ 0.0001 (****), P≤0.001(***), P≤0.01(**), P≤0.05(*).

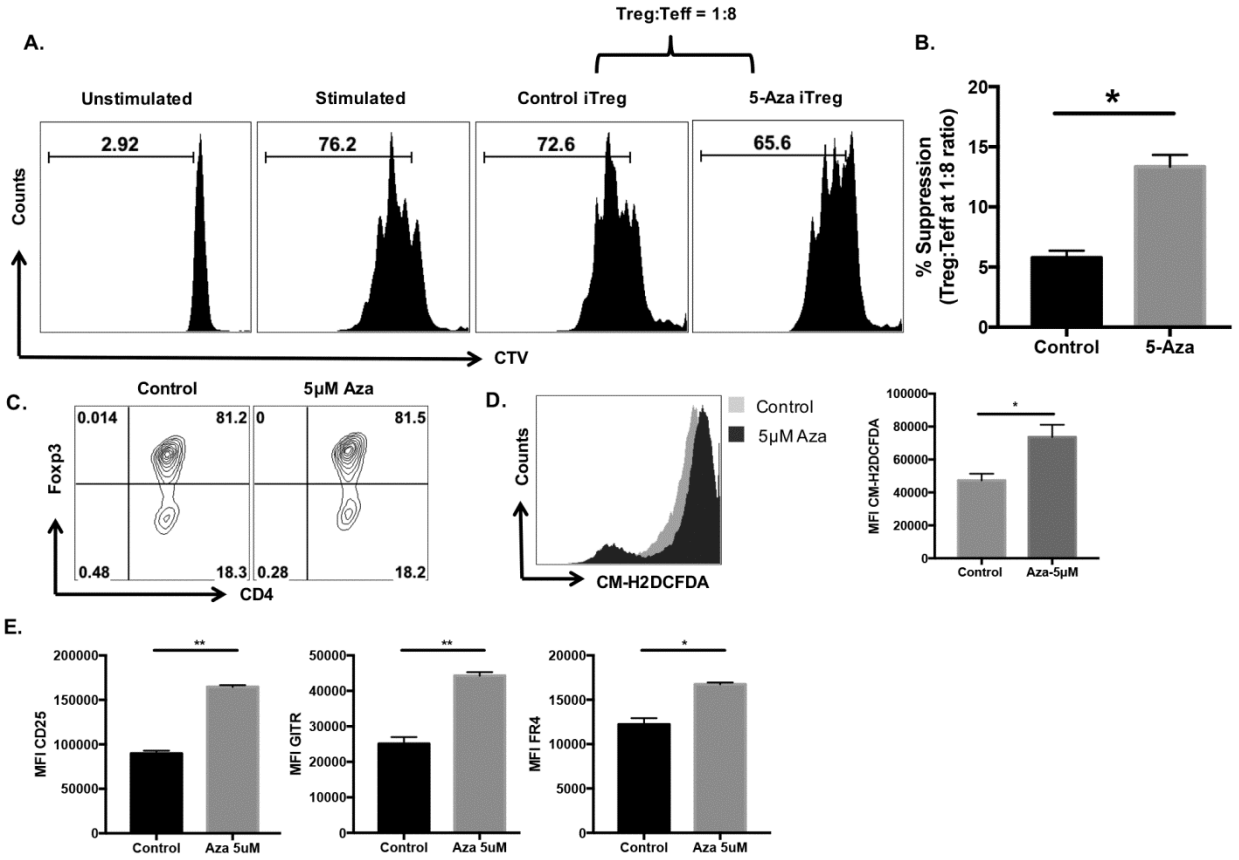

Figure 3.8. Aza promotes Treg suppressive function (A) Naive CD4 T cells purified from Foxp3 GFP mice were cultured (500,000 cells/well) with 100U/ml IL-2, 1μg/ml anti-CD3/CD28, 5ng/ml TGFβ and in the presence or absence of 5μM Aza for up to 5 days. Foxp3 GFP+ T cells were FACS sorted and in vitro Treg suppression assay was performed on both control iTreg and Aza iTregs. CD4+ Foxp3+ T cells were sorted and equal number of cells (1 x 10^5) were cultured with CTV-labeled naïve CD4+ Thy1.1 responder cells (Treg/Tconv, 1:1 to 1:8) in the presence of anti-CD3/CD28 antibodies. (A) Representative histograms showing the extent of CTV dilution at 1:8 Treg/effector T cell (Teff) ratio. (B) Bar graphs showing the percent suppression by Treg at 1:8 ratio. (C-D) Splenocytes from DO11.10 RAG2−/− mice were cultured in 1μg/ml anti-CD3/CD28, 100 U/ml IL-2, 5ng/ml TGF-β in the presence or absence of Aza (5μM). After 5 days of culture, cells were either measured for intracellular Foxp3 expression or surface stained with ROS indicator dye CM-H2DCFDA for measuring ROS expression. (C) Representative FACS plots showing the similar Foxp3 expression (gated on Live CD4+ T cells) (D) Representative FACS plots and histogram showing ROS expression (CM-H2DCFDA) in cells induced in the presence or absence of Aza (5μM). (E) Representative bar graph showing expression of CD25, GITR and FR4 in the Treg induced cells in the presence or absence of Aza (5μM). Data represent means ± SEMs of and representative of two independent experiments with n=3/group. Statistical significance was calculated by Student's t test (unpaired) (P≤0.01(**), P≤0.05 (*)).

CHAPTER 4
ROLE OF IL-18 INDUCED AMPHIREGULIN EXPRESSION BY TREG ON VIRUS INDUCED LESIONS

Research described in this chapter is reproduced from a publication submitted to Mucosal Immunology by Siva Karthik Varanasi, Naveen Rajasagi, Ujjaldeep Jaggi, and Barry T Rouse.

Siva Karthik Varanasi, Naveen Rajasagi, Ujjaldeep Jaggi, and Barry T Rouse. Role of IL-18 Induced Amphiregulin Expression by Treg on Virus Induced Lesions. Mucosal Immunology. 2018

Abstract

This report deals with the possible mechanism by which regulatory T cells contribute to the control and resolution of inflammatory lesions in the cornea caused by herpes simplex virus (HSV) infection. Our results demonstrate that the expression of the IL-18R by regulatory T cells (Treg) was a pivotal event that influenced lesion pathogenesis. The engagement of IL-18R with its cytokine ligand resulted in Amphiregulin expression a molecule associated with tissue repair. In support of this scheme of events, lesion severity became more severe in animals unable to express the IL-18R because of gene knockout and were reduced in severity when IL-18 was overexpressed in the cornea. These changes in lesion severity correlated with the frequency of Treg that expressed Amphiregulin. Additional experiments indicated that IL-12 and IL-18 acted synergistically to enhance Amphiregulin expression, an event partly dependent on P38 MAPK activity. Thus, overall our results imply that Treg participate in controlling the severity of SK and contribute to tissue repair by converting into cells that produce Amphiregulin.

Introduction

Viruses may cause disease in many ways but few do so solely by their uncontrolled replication . More often lesions are the consequence of host inflammatory reactions to the infection and this can lead to chronic tissue damage. Resolving chronic reactions is problematic and these may persist even after the inciting virus is no longer replicating. Resolution of chronic lesions may require a change in the balance of cellular participants along with a change in the cytokines that dominate lesions . Cell types involved in limiting tissue damage include CD4 T cells that express the Foxp3 transcription factor (regulatory T cells -Treg) . Such Treg express a range of regulatory functions and can act against several targets in inflammatory responses . Indeed, there is a spectrum of Treg in terms of functional activities and the spectrum may differ according to location in the body and the stage of lesion development . Additionally, Treg function may be unstable and under some circumstances the cells lose their regulatory activities and may even take on a pro-inflammatory role in tissues . An objective for control of chronic infections is to expand and maintain subsets of Treg with functions that counteract tissue damaging events and even contribute to lesion repair.

The idea that Treg can participate in the repair of damaged tissues was realized recently, but so far has received limited investigation. A critical report on the reparative function of Treg came from studies on a muscle damage model , where the Treg population present during muscle lesion repair was dominated by cells which produced Amphiregulin (Amp) . Amp is a ligand for the epidermal growth factor receptor expressed mainly on epithelial cells and stem cells and its binding can result in the activation of downstream signaling kinases resulting in growth, proliferation and migration of cells . The mechanism that drives the expression of Treg reparative molecules such as Amp involves cytokines produced by innate immune cells or epithelial cells. For instance, both IL-33 and IL-18 were shown to cause the expression of Amp by Treg . However, whereas the participation of IL-33 in tissue repair has been well established , the role played by IL-18 needs to be further substantiated.

IL-18 is a member of the IL-1 family and is mainly produced at barrier tissues and inflammatory sites when a variety of cell types, which includes epithelial and innate immune cells, are exposed to microbial products . Whereas, some reports advocate a pathogenic role of IL-18 during infections and autoimmunity , others demonstrate a tissue protective role such as occurs following intestinal and ocular injury . One potential mechanism for the tissue protective function of IL-18 involves Treg. Thus, expression of the IL-18 receptor (IL-18R) on Treg appeared necessary for their suppressive function . However the role of IL-18 induced signaling events in Treg involved in the tissue repair process requires to be clarified.

The present report focuses on events that result in the expression of IL-18R and how it's binding to IL-18 results in Amp expression in Treg. We also explored the participation of IL-18 and Amp expression by Treg during the course of an inflammatory response caused by herpes simplex virus (HSV) infection in the mouse cornea. We demonstrate that when lesions were at their peak the majority of Treg in the cornea expressed IL-18R along with several suppressive markers compared to Treg in lymphoid organs. The expression of IL-18R was independent of TCR stimulation but was dependent on the pro-inflammatory cytokine IL-12. IL-12 signaling in Treg resulted in reduced expression of the enzyme DNA methyltransferase 3a (DNMT3a), which correlated with enhanced expression of the IL-18R. Thus, knockdown of DNMT3a in CD4 T cells expanded the Treg population that became IL-18R expressers. In fact, IL-18 signaling led to the expression of Amp and, together with IL-12, synergistically enhanced the expression of Amp. Moreover, IL-18R knockout animals displayed enhanced corneal lesion severity and had far fewer Treg that were Amp producers. In contrast, overexpression of IL-18 caused reduced lesion severity, an effect which correlated with higher numbers of Amp expressing Treg. Taken together, our results indicate that IL-18 plays a tissue protective role in the cornea during SK acting via effects on Treg. This effect occurred by binding to the IL-18R and induced the expression of the tissue repair molecule - Amp. Consequently, IL-18 therapy could represent a valuable strategy to shorten the duration of chronic inflammatory reactions to a viral pathogen.

Results

Treg in cornea upregulate IL-18R and Amp expression

To evaluate the phenotypic and functional status of Treg at different locations after HSV infection, single cell suspensions of pooled corneas and individual DLN were collected at 15 days post infection (pi) and the cell populations were analyzed by flow cytometry for multiple phenotypic markers. Day 15 pi is the time when lesions caused by HSV in the cornea are fully developed and the inflammation is at its peak. Differences between the two populations were evident. While the majority of the Treg in corneas displayed activation and functional suppressive markers (which included Ki-67, CD44, GITR, OX40, Helios, Nrp1, CD25, CTLA-4) only a minority of the Treg in DLN expressed those markers (Fig 4.1A). Additionally, a higher proportion of corneal Treg expressed IL-33R (ST2) and IL-18R compared to the DLN Treg (Fig 4.1B). Since, the expression of IL-18R in the corneal Treg was greater than ST2, we focused on the potential relevance of IL-18R. We could show that around day 15pi 80% of corneal Treg expressed IL-18R compared to about 46% which expressed ST2 (Fig 4.1C).

The expression of the tissue repair molecule Amp was also measured in day 15 samples. About 50% of the corneal Treg were shown to express Amp, whereas less than 25% of DLN Treg were Amp positive (Fig 4.1D). Curiously, about 70% of the corneal Treg expressing Amp were also IL-18R positive (Fig 4.1E). Collectively, these data indicate that the Treg in the cornea are functionally more activated than the Treg in lymph nodes, and the expression of IL-18R by corneal Treg might play a role in driving the production of Amp.

IL-18R and Amp expressing Treg increase with duration of lesion development

To evaluate the potential relevance of IL-18R and Amp expression on Treg following ocular infection, corneas were isolated at different time points pi that included the time of early lesion development (D8), its peak (D15) and the time when most lesions were decreased in severity (D21). The isolated corneal cells were stimulated with PMA/Ionomycin followed by the ICS assay to enumerate Treg that expressed IL-18R and/or Amp. At day 8, approximately 60 % of the Treg population expressed IL-18R. This increased to about 80% by day 15pi. By day 21, the Treg that expressed IL-18R was reduced to about 60% (similar differences in number were also observed) (Fig 4.2A). In the case of Amp expressing Treg, at day 8 approximately 30% of corneal Treg expressed Amp, but Amp expressing Treg increased to about 50% by day 15 and remained the same at day 21 (Fig 4.2B). Whereas at day 15 the majority of Amp expressors were IL-18R positive, by day 21 the majority of Amp expressors no longer expressed IL-18R (Fig 4.2C). The results indicate that the population of IL-18R expressing Treg changes during the course of infection. The high frequency of Amp expressing Treg (IL-18R pos & neg) when lesions were declining might mean that such cells were participating in lesion repair.

IL-12 and IL-18 synergistically induce the expression of IL-18R and Amp

To account for the observed changes in Treg phenotype over time, various cytokines were measured by multiplex assay and ELISA in the corneas at different time points pi. While, cytokines such as IL-12, IL-6, TNF-α and IL-1β peaked at day 8 pi (Supp Fig. 4.1A), the levels of IL-18 peaked at day 15 pi and this was followed by a modest reduction at day 21pi (Fig 4.3A). We hypothesized that the expression changes in one or more of these cytokines might have influenced the expression of the IL-18R on Treg. To evaluate this, Treg were differentiated in vitro (iTreg) from naïve CD4 T cells isolated from uninfected C57BL/6 animals. Of note, a low percentage of those iTreg expressed the IL-18R (<5%). This iTreg population was used as the cell source to test the effects of changing the cytokine environment on the expression of the IL-18R. The population was stimulated with IL-2 in the presence or absence of different inflammatory cytokines known to be present in corneal lesions and anti-CD3+anti-CD28 to mimic TCR stimulation. These cytokines included IL-2, IL-18, IL-6, IL-12, IFN-g and IL-33 and after 5 days of exposure, the proportion of Treg that expressed IL-18R and Amp was measured. Surprisingly, of all the cytokines tested, only IL-12 caused a significant increase (from 3% to 20%) in the frequency of IL-18R positive Treg compared to controls (Fig 4.3B, Supp Fig 4.1B). Of note, stimulation with anti-CD3+CD28, or IL-18 alone, did not influence the frequency of Treg that expressed IL-18R (Fig 4.3B). However, when a combination of both IL-12 and IL-18 cytokines was used to stimulate Treg, the number of cells that became IL-18R positive was increased to 60%, well beyond the increase caused by IL-12 stimulation alone (20%) (Fig 4.3B). Additionally, while IL-12 alone stimulation did not increase the number of Treg that also expressed Amp, the combination of IL-12 and IL-18 caused a

large percentage of cells (approximately 4-fold) to become Amp positive (Fig 4.3C). Thus, the cytokines IL-12 and IL-18, whose levels were maximal in the cornea at day 8 and day 15 pi respectively, appeared to act synergistically to induce the expression of IL-18R and Amp by Treg.

DNMT3a can regulate the expression of Amp in CD4 T cells via IL-18R

To evaluate the potential mechanism by which IL-12 could induce the expression of IL-18R, the levels of STAT4 and DNMT3a enzymes were measured in Treg generated in vivo. This analysis was chosen since, previous observations with Th1 cells indicated that IL-12 stimulation induced STAT4 mediated down-regulation of DNA methyltransferase-3a (DNMT3a) . This resulted in demethylation of the IL-18R gene and hence the expression of IL-18R . In these experiments, iTreg were exposed to IL-2 with or without IL-12 for 3 days after which the levels of STAT4 phosphorylation were measured using flow cytometry. Additionally, mRNA levels of DNMT3a were quantified by QRT-PCR. The results showed that Treg exposed to IL-12 alone significantly induced the phosphorylation of STAT4 (Fig 4.4A), but reduced DNMT3a mRNA levels (Fig 4.4B) compared to Treg stimulated with IL-2 or IL-18 alone. However, Amp mRNA levels increased when exposed to IL-18 or IL-12 and IL-18 combined, but remained unchanged by exposure to IL-12 or IL-2 alone (Fig 4.4B).

To evaluate if DNMT3a could influence IL-18R and subsequently Amp expression in vivo, corneal lesion responses was compared following HSV infection in DNMT3a KO and WT animals. Pools of corneas were stimulated with PMA/Ionomycin at day 15pi and the proportion of Treg that expressed Amp was measured. The results indicate that the frequencies and numbers of Amp producing Treg and effector T cells were higher (2-3 fold) in the corneas of DNMT3aKO animals compared to the control animals (Fig 4.4C). In addition, the frequency and numbers of Amp expressing IL-18R pos Treg were higher in DNMT3a KO compared to WT animals (Fig 4.4D). Taken together, the results indicate that DNMT3a may negatively regulate IL-18R expression and subsequently Amp expression.

Amp induction by IL-12 and IL-18 is P38 MAP kinase dependent

To evaluate the possible mechanism by which IL-18 induced Amp expression, a lead was taken from previous studies on Th2, Th1 or NK cells where P38 MAP Kinase was involved in IL-18 induced expression of IL-5 and IFN-γ respectively . The levels of phosphorylated P38 MAP kinase (p-P38) were compared between IL-18R positive and negative Treg isolated from the DLN of day 15pi animals. As shown in Fig 4.5A, IL-18R positive Treg had 2-fold higher expression of p-P38 compared to IL-18R negative cells. Experiments were also done on in vitro generated Treg wherein iTreg were exposed to IL-2 in the presence or absence of IL-12, or IL-18, or together for 30 minutes followed by measurement of p-P38. As shown in Fig 4.5B, exposure of IL-12 and IL-18 together enhanced the expression of p-P38, while the levels of p-P38 remained unchanged when exposed either to IL-12 or IL-18, or IL-2 alone (Fig 4.5B). To evaluate whether activation of P38 MAP kinase was essential for IL-12 and IL-18 induced Amp expression, Treg were exposed to IL-12 and IL-18 for 5 days in the presence or absence of various doses of SB203580, a specific inhibitor of mitogen-activated protein kinase p38. The results indicated that SB203580 dose dependently inhibited Amp expression (Fig 4.5C) without influencing the survival of Treg (data not shown). Since IL-18 also induces NF-kB along with P38 MAPK, NF-kB was also inhibited using a cell permeable inhibitor (SN50) at

various concentrations. However, NF-kB inhibition did not influence Amp expression in Treg (Supp fig 4.1C). These data indicate that IL-12 and IL-18 induced Amp expression in Treg may require MAP kinase P38 phosphorylation.

IL-18 signaling is critical for controlling lesion severity

To further evaluate a role for IL-18 in driving the expression of Amp in vivo, IL18r1 knockout mice (IL-18R KO) were used wherein a subunit of the receptor-IL18R1 was deleted. Both WT (C57BL/6) and IL-18R KO mice were ocularly infected with HSV-1 and lesion severity was compared. The results indicate that IL-18R KO animals displayed enhanced lesion severity when compared to WT animals at day 8pi (Fig 4.6A). Pools of corneas were collected and evaluated from both groups to measure the frequency and number of Amp expressing Treg in the cornea. It was evident that the Treg population that was Amp positive was significantly decreased in the IL-18R KO populations (Fig 4.6B). Of note, no significant differences in the number and frequency of Th1 and Amp expressing Treg was observed in the DLN of WT and IL-18R KO animals (Fig 4.6C). In addition, the knockout of IL-18R did not influence the expression of various activation markers on Treg in the DLN that included GITR, CTLA4 and CD25 (Fig 4.6D). Together, these data indicate that the lack of IL-18R signaling can result in enhanced tissue damage and this was accompanied by a diminished number of Treg that expressed Amp.

Over-expression of IL-18 diminishes SK lesions and expand Amp Treg

Finally, the therapeutic potential of IL-18 in driving the generation of Amp expressing Treg in the cornea was evaluated. For this, an IL-18 overexpressing plasmid which was previously shown to inhibit the development of SK lesions in mice , was used. C57BL/6 animals were ocularly injected with the IL-18 overexpressing plasmid 4 and 2 days before ocular infection with HSV. Control animals received empty vector at the same time points. As reported previously , animals that received the IL-18 plasmid showed significantly reduced ($p<0.01$) SK lesions at day 15pi compared to controls (Fig 4.7A). Single cell suspensions of corneas were stimulated with PMA/Ionomycin at day 8 to compare with empty plasmid recipients the numbers of Treg that were Amp positive. As a consequence of IL-18 plasmid exposure all cell types was reduced in number. However, the frequency of Amp expressing Treg and effector CD4 T cells (CD4+ Foxp3-) were both significantly increased at day 8pi (Fig 4.7B) compared to the empty plasmid control group. Collectively, these data indicate that IL-18 may play a tissue protective role during ocular lesions and it may be acting by inducing the expression of Amp in Treg.

Discussion

Stromal keratitis is an inflammatory reaction that occurs in the cornea in response to HSV infection. Lesion severity is known to be influenced by the relative abundance of the pro-inflammatory, mainly CD4 type Th1 cells, and regulatory T cells . The later cell type appears to limit tissue damage caused by the activities of Th1 cells along with the cells recruited to the cornea such as neutrophils and macrophages . Currently, it is not clear how Treg exert their anti-inflammatory function, or if they actively contribute to tissue repair. However, the results in this report support the idea that the expression of the IL-18R by Treg is a relevant event and that the engagement of IL-18R with its cytokine ligand results in the expression of Amphiregulin, a molecule associated with tissue repair in several situations . Our results also show that when Treg were unable to express IL-18R,

SK lesions became more severe and that overexpression of IL-18 in the eye using an expression plasmid was an effective means of limiting lesions. The later outcome correlated with the increased proportion of Treg that were Amp producers. Thus, overall our results imply that Treg participate in controlling the severity of SK and contribute to tissue repair by converting into cells that produce Amphiregulin.

Past studies had clearly associated the presence of Treg with diminished tissue damage caused by ocular infection with HSV . Treg may express numerous regulatory functions and it is not clear which ones participate in limiting the corneal damage caused by the effects of T cells and other inflammatory cells. In addition to constraining the pro-inflammatory activities of several cell types, evidence accumulates from studies in other systems that Treg may also participate in the repair of tissue damage . Tissue repair is a particularly relevant topic with an organ whose function is totally dependent on maintaining tissue clarity along the visual axis from the cornea to the retina. Thus, it would be valuable to discover how any cell type could orchestrate repair of the damaged cornea. Corneal tissue repair involves numerous events and one of these could be Amphiregulin production . Amphiregulin engages the epidermal growth factor receptor expressed on corneal epithelial cells and stem cells and causes cell proliferation, differentiation, and migration to participate in tissue repair . Several cell types, such as innate lymphoid cells and mast cells can mediate repair of some tissues via their production of Amp , but neither of these cell types are prominent in corneal lesions. However, Treg are numerous in corneal lesions and, as was recently shown in repairing muscle and lung lesions , these Treg were in large part Amp-producers, unlike Treg at other non-inflamed sites. These observations on repairing muscle and lung inspired the present investigations to determine how Treg could participate in corneal repair in response to a chronic viral induced inflammatory event.

Our studies revealed that an essential event leading up to Amp production by Treg was expression of the IL-18R and engagement by its cytokine ligand IL-18. Previous studies by Rudensky and colleagues had noted that a consequence of triggering the IL-18R on Treg was their conversion to become Amp producers . Of many cytokines evaluated for inducing Amp, only IL-18 and IL-33 were effective. Our studies focused on the IL-18R since Treg that expressed this receptor were around two-fold more frequent that those that expressed the IL-33R. We could demonstrate that the frequency of Treg that expressed IL-18R increased as lesions progressed but then declined after lesions diminished. This raised the question of what caused Treg to express IL-18R. Many cytokines were tested but IL-12 appeared to be the most likely candidate. Prior studies had shown that IL-12 is prominently expressed during SK lesion development, perhaps driven by viral components with TLR ligand activity or by produces released by damaged cells. In addition to IL-12, we also showed that IL-12 along with IL-18 appeared to act together to cause more Treg to become IL-18R and Amp expressers but the detailed mechanism that explained this apparent synergism needs further study.

The mechanism by which IL-12 caused the expression of IL-18R was associated with STAT4 phosphorylation and down regulation of DNMT3a gene expression. Previous results supported a role for DNMT3a in controlling IL-18R gene expression with it acting by methylating the promoter region . Additionally, the knockdown of DNMT3a in CD4 T cells led to the enhancement of Amp and IL-18R expressing Treg in the cornea. Hence, inhibitors targeting DNA methyltransferases such as 5-Azacytidine could have potential

therapeutic implications to enhance both the suppressive function and tissue reparative function of Treg. In fact, we recently observed that 5-Azacytidine therapy did inhibit the progression of SK and acted by enhancing the activity of Treg . However, it remains to be evaluated whether 5-Azacytidine treatment was also associated with an increased expression of IL-18R and Amp by Treg. Another mechanism by which IL-18 induced Amp expression was activation of P38 MAPK kinase. Thus inhibition of MAP kinase activity using a specific inhibitor led to a dose dependent reduction in Amp expression in the presence of IL-18. These data did not come as a surprise since P38 MAPK activity is known to be required for IL-18 induced Th2 cytokines (IL-4 and IL-13) in basophils and IFN-gamma in NK and Th1 cells . Hence, it is possible that IL-18 and P38 MAPK play a cell specific role in orchestrating the production of cell specific cytokines.

A critical event for Treg to become Amp-producers and contribute to lesion resolution was the expression of IL-18R. Thus knockout mice unable to express IL-18R developed more severe SK lesions than did intact control animals and a major consequence of IL-18R KO was a significant reduction in the frequency of Treg that produced Amp. Since the IL-18R KO could still produce IL-33, this might argue that if the IL-33/IL-33R axis is also involved in Amp expression its role is likely to be minor.

A final approach which implicated a critical role for IL-18 in controlling lesion severity involved using an expression plasmid encoding IL-18. As reported previously , use of this plasmid inhibited the severity of SK lesions and in the present study we could show that a consequence of IL-18 plasmid therapy was expansion of the Treg population that were Amp producing cells. However, since IL-18 can have effects on immune cells other than Treg such as neutrophils and macrophages , studies using IL-18R flox and Amphiregulin flox mice are needed to further depict the role of IL-18 induced Amp expression by Treg.

In conclusion, our results strongly support the idea that the ongoing events that occur during HSV–induced ocular lesions serve to cause Treg to express IL-18R and this event is necessary to subsequently express Amp, a molecule involved in tissue repair. So far we have been unable to fully verify the concept since we lack access to mice which lack expression of Amp specifically in Treg. However, preliminary studies on mice with developing lesions given the Amp protein via the subconjunctival route have resulted in diminished lesions and such studies are still ongoing.

Materials and Methods

Mice and Virus

C57BL/6 mice (Female) were purchased from Envigo, Inc. (Indianapolis, IN), IL-18R Knockout, CD4 Cre mice were purchased from Jackson and DNMT3a flox mice were a kind gift from Dr.Igor Nasonkin (University of Pittsburg Medical center) all were kept in pathogen free facility where food, water, bedding and instruments were autoclaved. CD4 cre mice were bred with DNMT3a flox mice and cre mice homozygous for flox was used for the experiments as DNMT3aKO. All the animals were housed in American Association of Laboratory Animal Care–approved facilities at the University of Tennessee, Knoxville, Tennessee. All investigations followed guidelines of the Institutional Animal Care and Use Committee, and adhered to the ARVO Statement for the Use of Animals in Ophthalmic and Vision Research. HSV-I RE strain was used in all procedures. Virus was grown in

Vero cell monolayers (American Type Culture Collection, Manassas, VA), titrated, and stored in aliquots at −80°C until used.

HSV-1 ocular infection and clinical scoring

Ocular infections with HSV-1 was done as previously described . Briefly, mice were kept under deep anesthesia by administering an intra peritoneal (i.p) injection of tribromoethanol (Avertin). Later, the mice eyes were scarified with 27-gauge needle and and a 3-µl drop containing 1 x 104 plaque-forming units (PFU) of HSV-1 RE was applied to the eye. The eyes were examined on different days after infection for the development of clinical lesions by slit-lamp biomicroscope (Kawa Co., Nagoya, Japan), and the clinical severity of keratitis of individually scored mice was recorded by a blinded observer. The scoring system was as follows: 0, normal cornea; +1, mild corneal haze; +2, moderate corneal opacity or scarring; +3, severe corneal opacity but iris visible; +4, opaque cornea and corneal ulcer; +5, corneal rupture and necrotizing keratitis.

Flow Cytometric Analysis

Flow cytometric analysis on tissue and lymph node samples were described previously . Briefly, cornea were excised at indicated time points, pooled and digested with liberase (Roche) for 45 minutes at 37°C in a humidified atmosphere of 5% CO2. Single cell suspensions were made by grinding the digested tissue and stained for different cell surface molecules for fluorescence-activated cell sorting (FACS) analyses. Draining cervical lymph nodes were isolated from mice at indicated time points and single cell suspensions were used for FACS analyses. To determine the Amp producing T cells, single cell suspensions were stimulated with PMA (50ng) and Ionomycin (500ng) for 3 hours in the presence of brefeldin A (10 µg/mL) in U-bottom 96-well plates . After this period, Live/Dead staining was performed to gate out the dead population followed by cell surface and intracellular cytokine staining using Foxp3 intracellular staining kit (ebioscience) in accordance with the manufacturer's recommendations. The stained samples were acquired with a FACS LSR II (BD Biosciences, San Jose, CA) and the data were analyzed using FlowJo software (Tree Star, Inc., Ashland, OR).

Reagents and antibodies.

All the staining CD4 (RM4-5), CD45 (53-6.7), CD11b (M1/70), Ly6G (1A8), F4/80 (BM8), IFN-γ (XMG1.2), CD25 (PC61), CD44 (IM7), Foxp3 (FJK-16S), anti-CD3 (145-2C11), anti-CD28 (37.51), IL-18Ra (P3TUNYA) phosphor p38 (4NIT4KK) from Thermofisher. Phorbol myristate acetate (PMA) and Ionomycin from Sigma. Live/Dead staining kit (Life Technologies), anti-mouse Amphiregulin (R&D), GolgiPlug (brefeldin A) and Stat4 (pY693) from BD biosciences. Recombinant mouse IL-2, IL-12, IL-6, IFN-γ, IL-33, IL-18, Amphiregulin and TGF-β from R&D systems. P38 inhibitor-SB202190 (Tocris) and NF-kB inhibitor-SN50 (emdmillipore).

In vitro Treg differentiation and Treg cultures

Treg were generated in vitro as previously described . Briefly, 1×106 naïve CD4 T cells were cultured in the presence of plate bound anti-CD3/CD28 Ab (1 µg/ml) and complete RPMI media containing rmIL-2 (100 U/ml) and TGFβ (5ng/ml) for 5 days at 37°C in a 5% CO2 incubator. After 5 days, Foxp3, IL18Ra and Amp expression was determined by flow cytometry as described above. For inducing IL18Ra expression, in vitro generated Treg were cultured with either IL-12 (5ng/ml) or IL-18 (100ng/ml) orIL-33 (100ng/ml) or IFN-gamma (10ng/ml) or IL-6 (25ng/ml) for 24 hours. For Amp induction experiments, iTreg cells were cultured in the presence of IL-12 (5ng/ml) or IL-18 (100ng/ml) or together. For

P38 MAPK inhibitor experiments, iTreg were cultured in the presence of IL-12 (5ng/ml) and IL-18 (100ng/ml) in the presence or absence of SB 202190 (P38 inhibitor) at doses indicated. After 5 days cells were re-stimulated with PMA/Ionomycin and analyzed for Amp expression using flow cytometer.

Quantitative PCR (qPCR)

Taqman gene expression assays for DNMT3a from Applied Biosystems were performed on iTreg populations using 7500 Fast Real-Time PCR system (Applied Biosystems) as described previously .

Cytokine level measurements

Corneas were pooled (3 corneas per sample) and collected in PBS containing anti-protease cocktail. Corneas were homogenized with tissue homogenizer (Kontes Pellet Pestle mortar). Levels of IL-18 were measured using Mouse IL-18 ELISA (R&D); other cytokines were measured using multiplex analysis (Eve technologies).

Purification of CD4+ T cells

Naïve CD4+ T cells were purified using a mouse naïve CD4+ T cell isolation kit (Miltenyi Biotec, Auburn, CA). The purity was achieved at least to an extent of 90%.

Over-expression plasmid preparation

IL-18 over expression plasmid was kindly provided by Dr. Seong Kug Eo, Chonbuk National University and empty plasmid (PCDNA3.1) from Thermosfisher. Plasmid was cloned and purified using Qiagen Maxi kit and 5 µg/eye was administered at 4 and 2 days before infection.

Statistical Analysis

The statistical significance between the 2 groups was determined using unpaired, 1-tailed Student's t test. For experiments involving more than 2 groups, 1-way ANOVA with Tukey's multiple comparison tests was used to calculate the level of significance. GraphPad Prism software (GraphPad Software, La Jolla, CA, USA) was used to calculate the statistical significance.

References

1. Rouse BT, Sehrawat S (2010) Immunity and immunopathology to viruses: what decides the outcome? Nature Reviews Immunology 10: 514-526.
2. Ortega-Gómez A, Perretti M, Soehnlein O (2013) Resolution of inflammation: an integrated view. EMBO molecular medicine 5: 661-674.
3. Keynan Y, Card CM, McLaren PJ, Dawood MR, Kasper K, et al. (2008) The role of regulatory T cells in chronic and acute viral infections. Clinical infectious diseases 46: 1046-1052.
4. Veiga-Parga T, Sehrawat S, Rouse BT (2013) Role of regulatory T cells during virus infection. Immunological reviews 255: 182-196.
5. Foulsham W, Marmalidou A, Amouzegar A, Coco G, Chen Y, et al. (2017) The function of regulatory T cells at the ocular surface. The Ocular Surface.
6. Schmidt A, Oberle N, Krammer PH (2012) Molecular mechanisms of treg-mediated T cell suppression. Frontiers in immunology 3.
7. Panduro M, Benoist C, Mathis D (2016) Tissue Tregs. Annual review of immunology 34: 609-633.
8. Zhou X, Tang J, Cao H, Fan H, Li B (2015) Tissue resident regulatory T cells: novel therapeutic targets for human disease. Cellular & molecular immunology 12: 543-552.
9. Sakaguchi S, Vignali DA, Rudensky AY, Niec RE, Waldmann H (2013) The plasticity and stability of regulatory T cells. Nature Reviews Immunology 13: 461-467.
10. Bhela S, Varanasi SK, Jaggi U, Sloan SS, Rajasagi NK, et al. (2017) The plasticity and stability of regulatory T cells during viral-induced inflammatory lesions. The Journal of Immunology 199: 1342-1352.
11. Burzyn D, Benoist C, Mathis D (2013) Regulatory T cells in nonlymphoid tissues. Nature immunology 14: 1007-1013.
12. Burzyn D, Kuswanto W, Kolodin D, Shadrach JL, Cerletti M, et al. (2013) A special population of regulatory T cells potentiates muscle repair. Cell 155: 1282-1295.
13. Berasain C, Avila MA. Amphiregulin; 2014. Elsevier. pp. 31-41.
14. Avraham R, Yarden Y (2011) Feedback regulation of EGFR signalling: decision making by early and delayed loops. Nature reviews Molecular cell biology 12: 104-117.
15. Zaiss DM, Gause WC, Osborne LC, Artis D (2015) Emerging functions of amphiregulin in orchestrating immunity, inflammation, and tissue repair. Immunity 42: 216-226.
16. Arpaia N, Green JA, Moltedo B, Arvey A, Hemmers S, et al. (2015) A distinct function of regulatory T cells in tissue protection. Cell 162: 1078-1089.
17. Schmitz J, Owyang A, Oldham E, Song Y, Murphy E, et al. (2005) IL-33, an interleukin-1-like cytokine that signals via the IL-1 receptor-related protein ST2 and induces T helper type 2-associated cytokines. Immunity 23: 479-490.
18. Monticelli LA, Osborne LC, Noti M, Tran SV, Zaiss DM, et al. (2015) IL-33 promotes an innate immune pathway of intestinal tissue protection dependent on amphiregulin–EGFR interactions. Proceedings of the National Academy of Sciences 112: 10762-10767.

19. Liew FY, Girard J-P, Turnquist HR (2016) Interleukin-33 in health and disease. Nature Reviews Immunology 16: 676-689.
20. Schiering C, Krausgruber T, Chomka A, Fröhlich A, Adelmann K, et al. (2014) The alarmin IL-33 promotes regulatory T-cell function in the intestine. Nature 513: 564-568.
21. Dinarello CA, Novick D, Kim S, Kaplanski G (2013) Interleukin-18 and IL-18 binding protein. Frontiers in immunology 4.
22. Kaplanski G (2018) Interleukin-18: Biological properties and role in disease pathogenesis. Immunological reviews 281: 138-153.
23. Nowarski R, Jackson R, Gagliani N, de Zoete MR, Palm NW, et al. (2015) Epithelial IL-18 equilibrium controls barrier function in colitis. Cell 163: 1444-1456.
24. Boraschi D, Dinarello CA (2006) IL-18 in autoimmunity. European cytokine network 17: 224-252.
25. Sedimbi SK, Hägglöf T, Karlsson MC (2013) IL-18 in inflammatory and autoimmune disease. Cellular and molecular life sciences 70: 4795-4808.
26. Levy M, Thaiss CA, Zeevi D, Dohnalova L, Zilberman-Schapira G, et al. (2015) Microbiota-modulated metabolites shape the intestinal microenvironment by regulating NLRP6 inflammasome signaling. Cell 163: 1428-1443.
27. Holmkvist P, Pool L, Hägerbrand K, Agace WW, Rivollier A (2016) IL-18Rα-deficient CD4+ T cells induce intestinal inflammation in the CD45RBhi transfer model of colitis despite impaired innate responsiveness. European journal of immunology 46: 1371-1382.
28. Doyle SL, Ozaki E, Brennan K, Humphries MM, Mulfaul K, et al. (2014) IL-18 attenuates experimental choroidal neovascularization as a potential therapy for wet age-related macular degeneration. Science translational medicine 6: 230ra244-230ra244.
29. Salcedo R, Worschech A, Cardone M, Jones Y, Gyulai Z, et al. (2010) MyD88-mediated signaling prevents development of adenocarcinomas of the colon: role of interleukin 18. Journal of Experimental Medicine: jem. 20100199.
30. Kim B, Lee S, Suvas S, Rouse BT (2005) Application of plasmid DNA encoding IL-18 diminishes development of herpetic stromal keratitis by antiangiogenic effects. The Journal of Immunology 175: 509-516.
31. Oertli M, Sundquist M, Hitzler I, Engler DB, Arnold IC, et al. (2012) DC-derived IL-18 drives Treg differentiation, murine Helicobacter pylori–specific immune tolerance, and asthma protection. The Journal of clinical investigation 122: 1082.
32. Harrison O, Srinivasan N, Pott J, Schiering C, Krausgruber T, et al. (2015) Epithelial-derived IL-18 regulates Th17 cell differentiation and Foxp3+ Treg cell function in the intestine. Mucosal immunology 8: 1226-1236.
33. Yu Q, Thieu VT, Kaplan MH (2007) Stat4 limits DNA methyltransferase recruitment and DNA methylation of the IL-18Rα gene during Th1 differentiation. The EMBO journal 26: 2052-2060.
34. Pham D, Yu Q, Walline CC, Muthukrishnan R, Blum JS, et al. (2013) Opposing roles of STAT4 and Dnmt3a in Th1 gene regulation. The Journal of Immunology 191: 902-911.

35. Kroeger KM, Sullivan BM, Locksley RM (2009) IL-18 and IL-33 elicit Th2 cytokines from basophils via a MyD88-and p38α-dependent pathway. Journal of leukocyte biology 86: 769-778.
36. Yang J, Zhu H, Murphy TL, Ouyang W, Murphy KM (2001) IL-18–stimulated GADD45β required in cytokine-induced, but not TCR-induced, IFN-γ production. Nature immunology 2: 157-164.
37. Mavropoulos A, Sully G, Cope AP, Clark AR (2005) Stabilization of IFN-γ mRNA by MAPK p38 in IL-12–and IL-18–stimulated human NK cells. Blood 105: 282-288.
38. Biswas PS, Rouse BT (2005) Early events in HSV keratitis—setting the stage for a blinding disease. Microbes and infection 7: 799-810.
39. Rajasagi NK, Rouse BT (2018) Application of our understanding of pathogenesis of herpetic stromal keratitis for novel therapy. Microbes and Infection.
40. Varanasi SK, Reddy PB, Bhela S, Jaggi U, Gimenez F, et al. (2017) Azacytidine treatment inhibits the progression of herpes stromal keratitis by enhancing regulatory T cell function. Journal of virology 91: e02367-02316.
41. Gaddipati S, Estrada K, Rao P, Jerome AD, Suvas S (2015) IL-2/Anti–IL-2 Antibody Complex Treatment Inhibits the Development but Not the Progression of Herpetic Stromal Keratitis. The Journal of Immunology 194: 273-282.
42. Ljubimov AV, Saghizadeh M (2015) Progress in corneal wound healing. Progress in retinal and eye research 49: 17-45.
43. Zieske JD, Takahashi H, Hutcheon AE, Dalbone AC (2000) Activation of epidermal growth factor receptor during corneal epithelial migration. Investigative ophthalmology & visual science 41: 1346-1355.
44. Morita S-i, Shirakata Y, Shiraishi A, Kadota Y, Hashimoto K, et al. (2007) Human corneal epithelial cell proliferation by epiregulin and its cross-induction by other EGF family members.
45. Peterson JL, Phelps ED, Doll MA, Schaal S, Ceresa BP (2014) The Role of Endogenous Epidermal Growth Factor Receptor Ligands in Mediating Corneal Epithelial HomeostasisEGFR Ligands in Corneal Wound Healing. Investigative ophthalmology & visual science 55: 2870-2880.
46. Monticelli LA, Sonnenberg GF, Abt MC, Alenghat T, Ziegler CG, et al. (2011) Innate lymphoid cells promote lung-tissue homeostasis after infection with influenza virus. Nature immunology 12: 1045-1054.
47. Okumura S, Sagara H, Fukuda T, Saito H, Okayama Y (2005) FcεRI-mediated amphiregulin production by human mast cells increases mucin gene expression in epithelial cells. Journal of allergy and clinical immunology 115: 272-279.
48. Kumaraguru U, Rouse B (2002) The IL-12 response to herpes simplex virus is mainly a paracrine response of reactive inflammatory cells. Journal of leukocyte biology 72: 564-570.
49. Yano T, Nozaki Y, Kinoshita K, Hino S, Hirooka Y, et al. (2015) The pathological role of IL-18Rα in renal ischemia/reperfusion injury. Laboratory Investigation 95: 78-91.
50. Varanasi SK, Donohoe D, Jaggi U, Rouse BT (2017) Manipulating Glucose Metabolism during Different Stages of Viral Pathogenesis Can Have either Detrimental or Beneficial Effects. The Journal of Immunology 199: 1748-1761.

APPENDIX

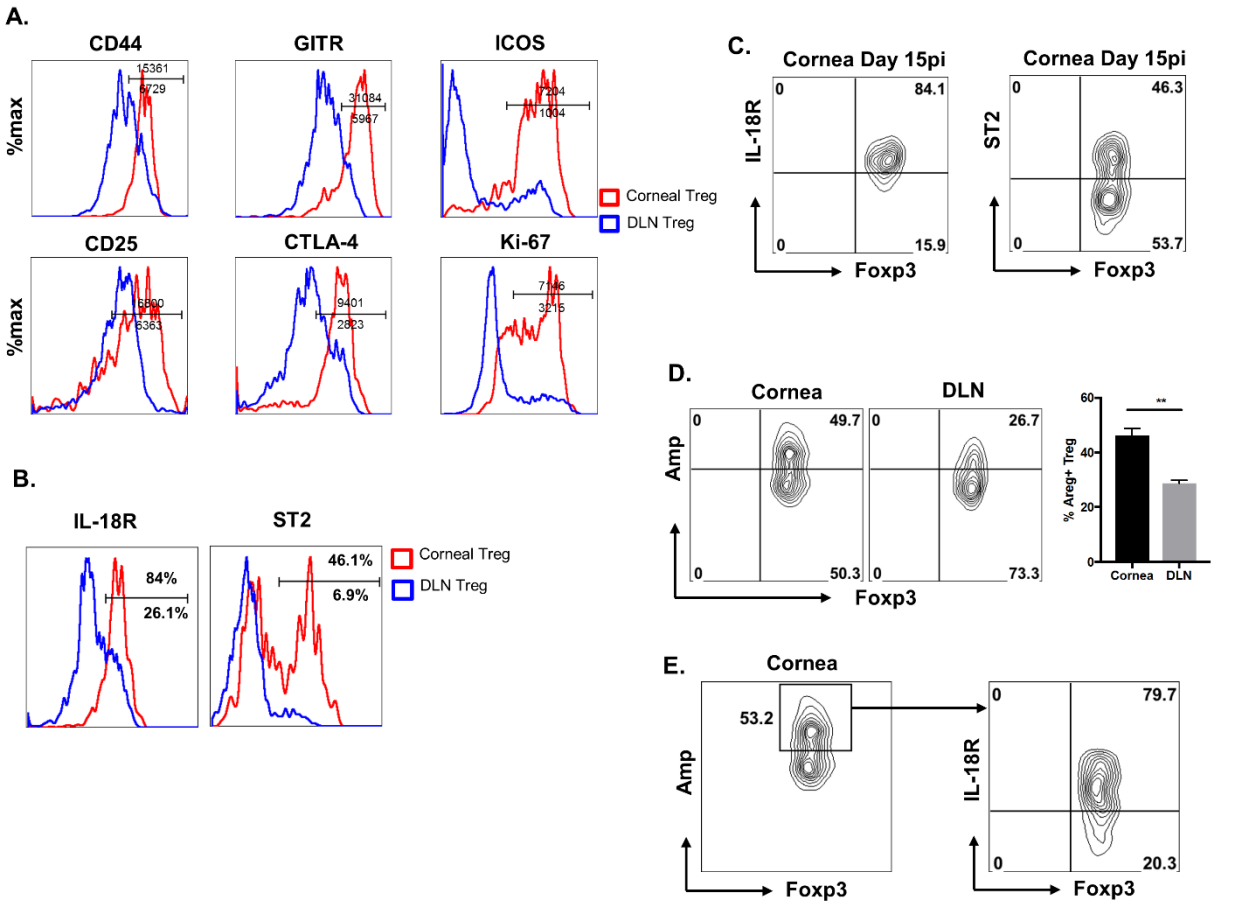

Figure 4.1. Corneal Treg have higher functional markers including IL-18R and Amphiregulin.

C57BL/6 animals were infected with 1 x 10^4 PFU of HSV-RE and at day 15 pi, of individual draining Lymph nodes (dLN) and pooled corneas were stained for flow cytometric analysis. (A-B) Representative histograms depicting the expression of markers related to Treg (CD4+ Foxp3+) function and activation on corneal Tregs and dLN Tregs (blue). (C) Representative flow plots showing the expression of IL-18R and ST2 (IL-33R) on corneal Treg at day 15pi. (D-E) Single cells suspension of dLN and cornea were stimulated with PMA/Ionomycin, (D) representative flow cytometry plots and histogram showing the Amphiregulin (Amp) expression in corneal and dLN Treg. (E) Representative flow cytometry plots showing the IL-18R expression on Amphiregulin (Amp) expressing Treg (gated on live cells). Data represents the mean±SEM of 3 independent experiments (n=3 mice/group). P≤0.01 (**).

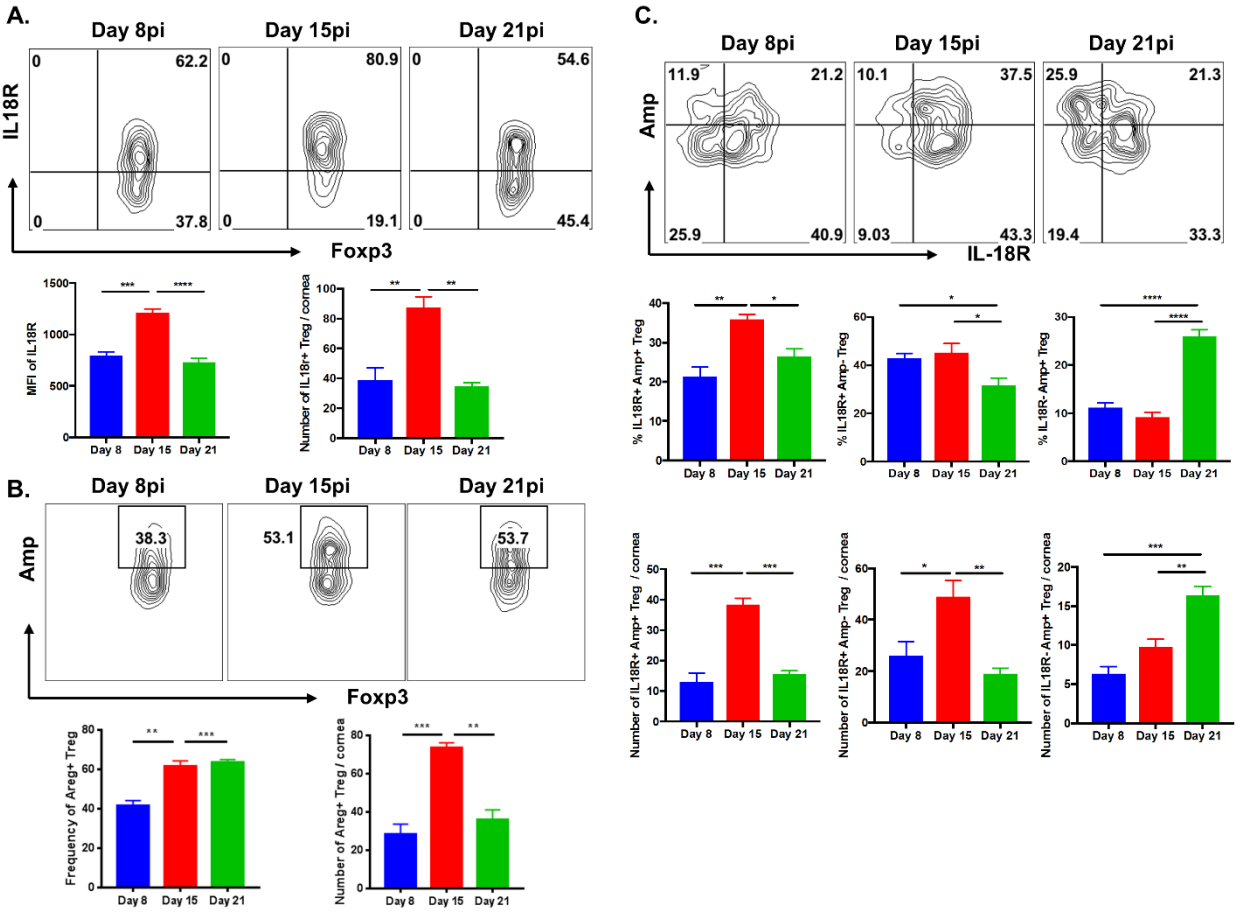

Figure 4.2. IL-18R and Amphiregulin expression on Treg change over the course of infection.

C57BL/6 animals were infected with 1 x 10^4 PFU of HSV-RE and at various time points post infection (Day 8, 15, 21) single cell suspension of pooled corneas were stimulated with PMA/Ionomycin. (A-C) Representative Flow cytometry plots and bar graphs showing frequency and number of (A) IL-18R expressing Treg or (B) Amphiregulin (Amp) expressing Treg or (C) both IL-18R and Amp expressing Treg. Data represents the mean±SEM of 3 independent experiments (n=3 mice/group). P≤ 0.0001 (****), P≤0.001(***), P≤0.01 (**), P≤0.05(*).

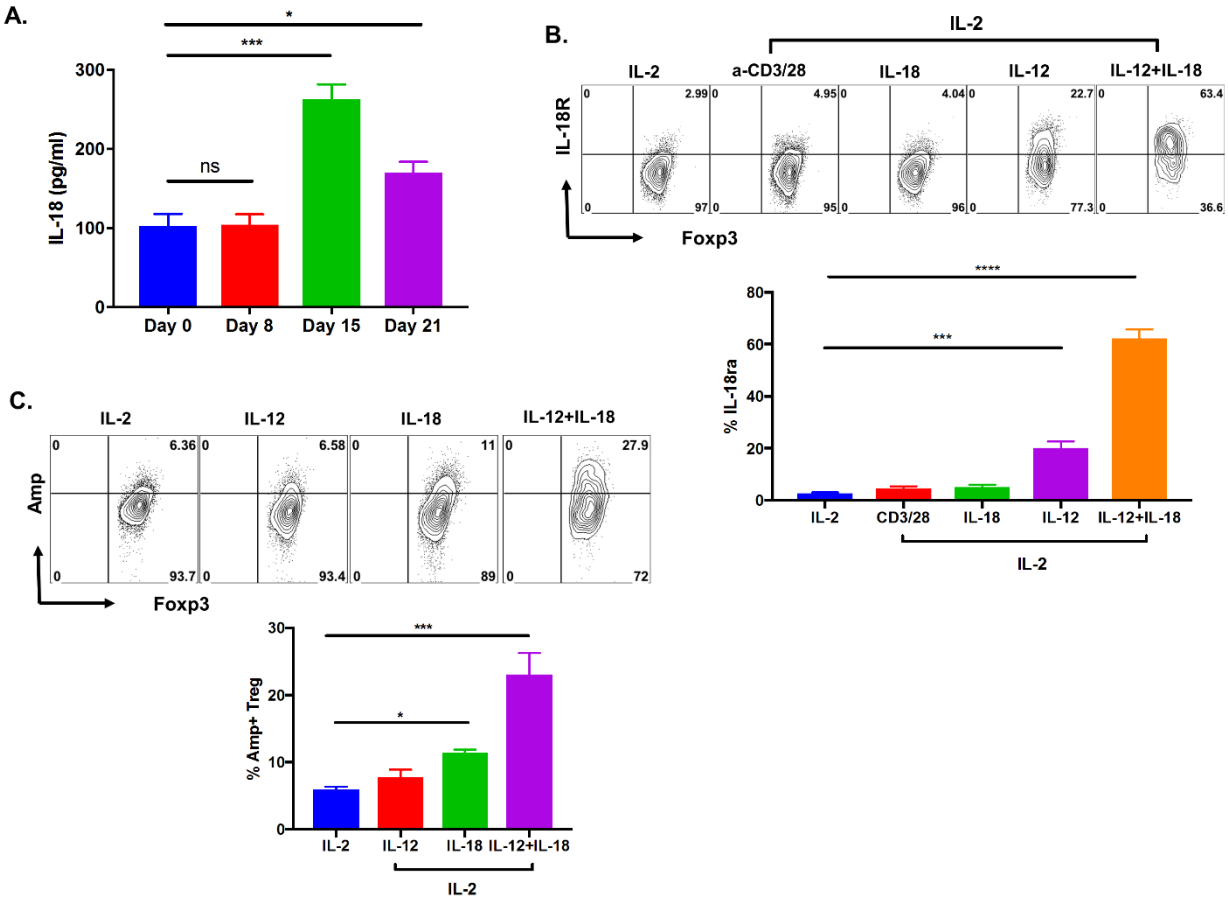

Figure 4.3. IL-18 and IL-12 synergistically induce the expression of Amphiregulin in Treg.

(A) C57BL/6 animals were infected with 1 x 10^4 PFU of HSV-RE. Bar graphs showing IL-18 protein levels in the corneas at various time points post infection (Day 0, 8, 15, 21) quantified by ELISA. (B, C) iTreg were differentiated from naïve CD4 T cells followed by culturing with either IL-2 alone or with IL-2 in combination with indicated cytokines for 5 days. Representative flow cytometry plots and bar graph showing frequency of (B) IL-18R expressing or (C) Amphiregulin (Amp) expressing Treg (gated on live CD4+ Foxp3+). Data represents the mean±SEM of 2 independent experiments for (A) or at least 3 independent experiments for (B,C) where n= 3-4 samples/group). P≤ 0.0001 (****), P≤0.001(***),P≤0.05(*).

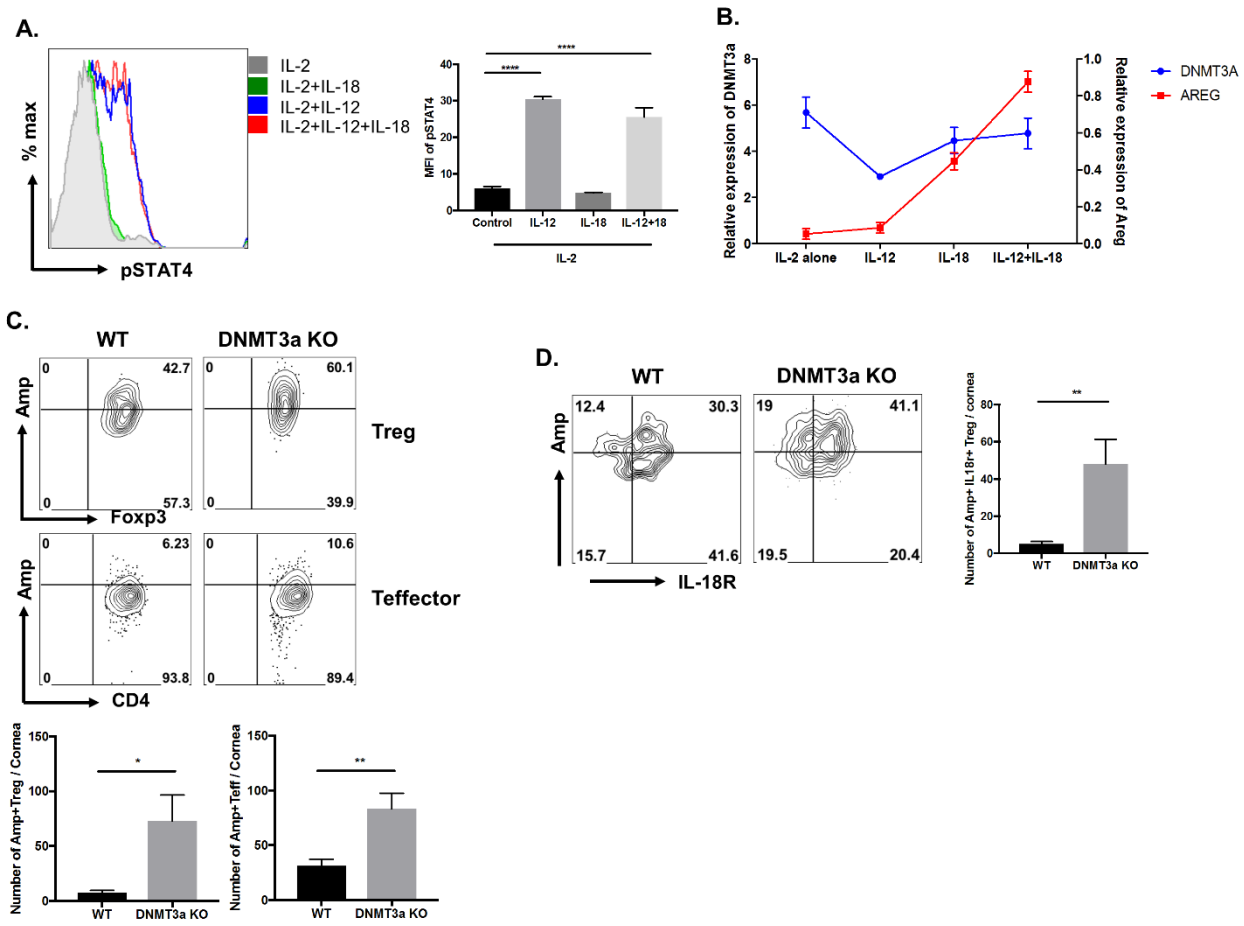

Figure 4.4. DNMT3a may regulate IL-18R expression in Treg.
(A,B) iTreg were differentiated from naïve CD4 T cells followed by culturing with either IL-2 alone or with IL-2 in combination with indicated cytokines for 5 days. (A) Representative flow cytometry plots and bar graphs showing phosphorylated STAT4 levels in Treg (gated on live CD4+Foxp3+). (B) Representative line graph showing relative gene expression levels of DNMT3a and Amp compared to beta-actin, quantified by QRT-PCR. (C, D) WT (DNMT3a flx/flx) and DNMT3a KO (CD4 Cre+DNMT3a flx/flx) mice were ocularly infected with HSV-RE and at day 8pi corneas were collected. Single cell suspensions of pooled corneas were stimulated with PMA/Ionomycin followed by ICS assay. (C) Representative flow cytometry plots and bar graph showing the frequency and number of Amphiregulin expressing Treg (gated on Live CD4+ Foxp3+) and effector T cells (gated on Live CD4+ Foxp3-). (D) Representative flow cytometry plots and bar graphs showing frequency and number of Treg double positive for IL-18R and Amp. Data represents the mean±SEM of 3 independent experiments where n= 3 samples/group. P≤ 0.0001 (****),P≤0.01 (**), P≤0.05(*).

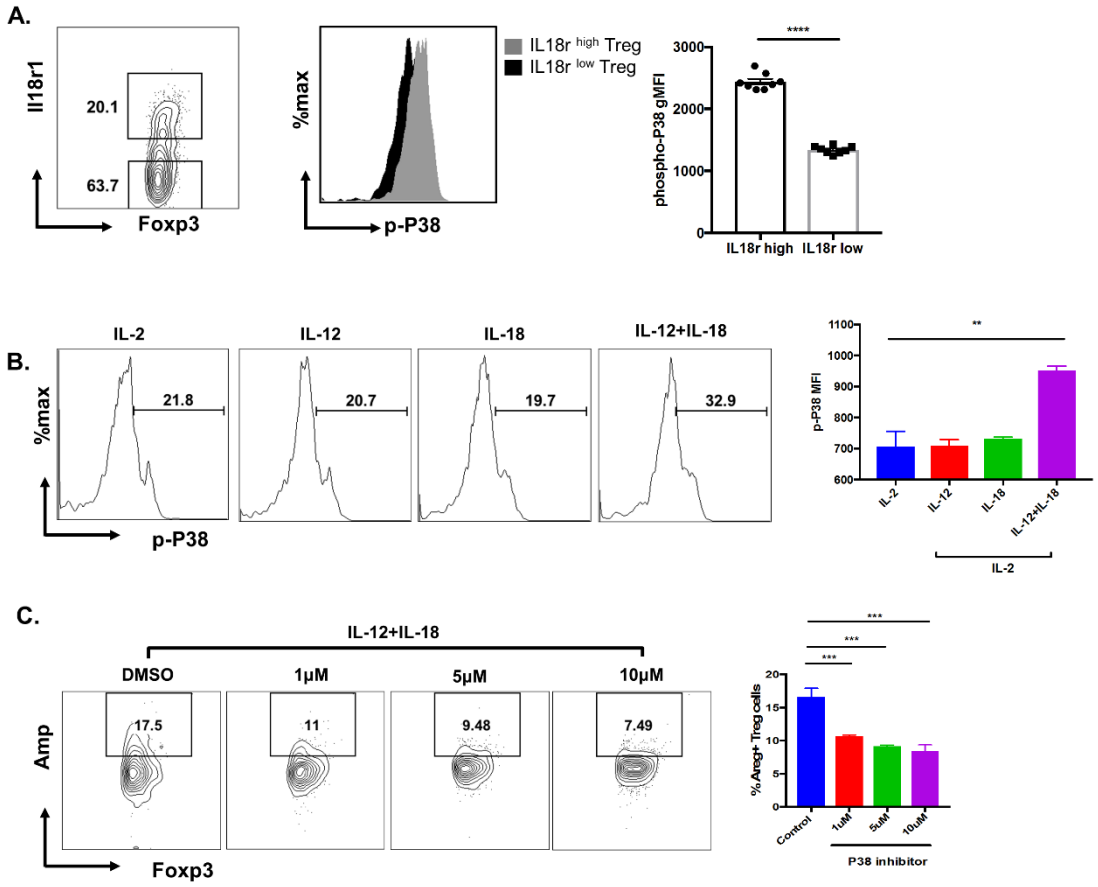

Figure 4.5. IL-12 and IL-18 induced Amphiregulin expression may be P38 MAPK dependent.

(A) C57BL/6 animals were infected with 1 x 10^4 PFU of HSV-RE and dLN were isolated at day 15pi. Representative flow cytometry plots and bar graph showing gating strategy and MFI of phosphorylated P38 in IL-18R high and IL-18R low Treg (gated on Live CD4+Foxp3+) in dLN. (B) iTreg were differentiated from naïve CD4 T cells followed by culturing with either IL-2 alone or with IL-2 in combination with indicated cytokines for 30 minutes. Representative histograms and bar graphs showing phopsho-P38 levels and phosphor-P38 MFI respectively. (C) iTreg were cultured with IL-12 and IL-18 for 5 days in the presence or absence of P38 inhibitor SB 202190 at different concentrations and DMSO as control. Representative flow cytometry plots and bar graph showing the frequency of Areg expressing Treg. Data represents the mean±SEM of 3 independent experiments where n= 3 samples/group. P≤ 0.0001 (****),P≤0.01 (**), P≤0.05(*).

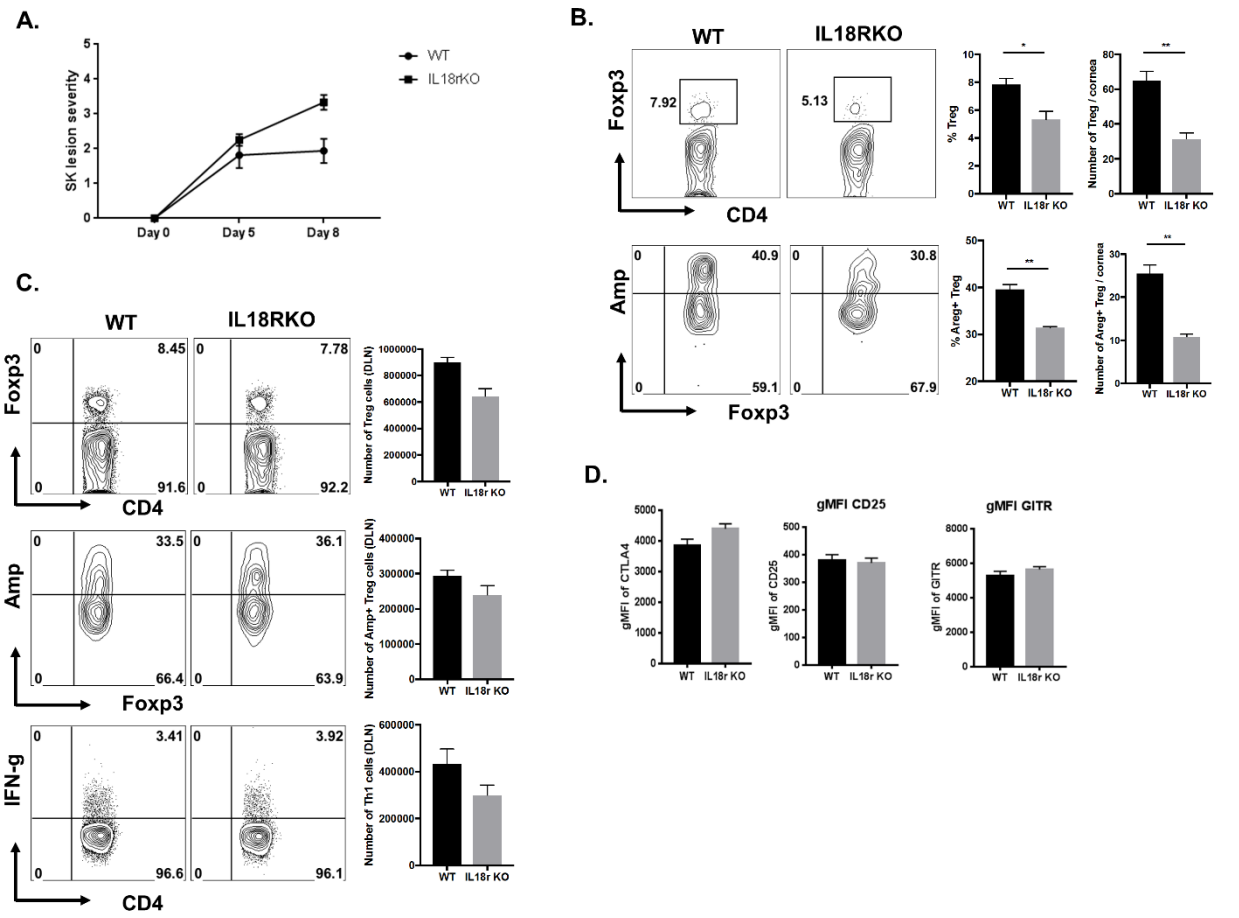

Figure 4.6. IL-18R KO animals show higher lesion severity and reduced Amp Treg in cornea.

(A-D) WT(C57BL/6) and IL18RKO animals were infected with 1 x 10^4 PFU of HSV-RE (A) line graph showing comparison of SK lesion severity scores at different time points day 5 and day 8 post infection between WT and IL18RKO. (B-C) Representative FACS plots and histogram showing frequency and number of Treg, Amp Treg cells in cornea (B) and Amp Treg and Th1 cells in DLN (C) at day 8 pi. (D) Histogram showing MFI of key suppressor molecules CTLA4, GITR and CD25 in DLN of WT and IL18RKO animals at day 8pi. Data represents the mean±SEM of 3 independent experiments where n= 8 samples/group (A), n= 3 samples/group (B-D). P≤0.01 (**), P≤0.05(*).

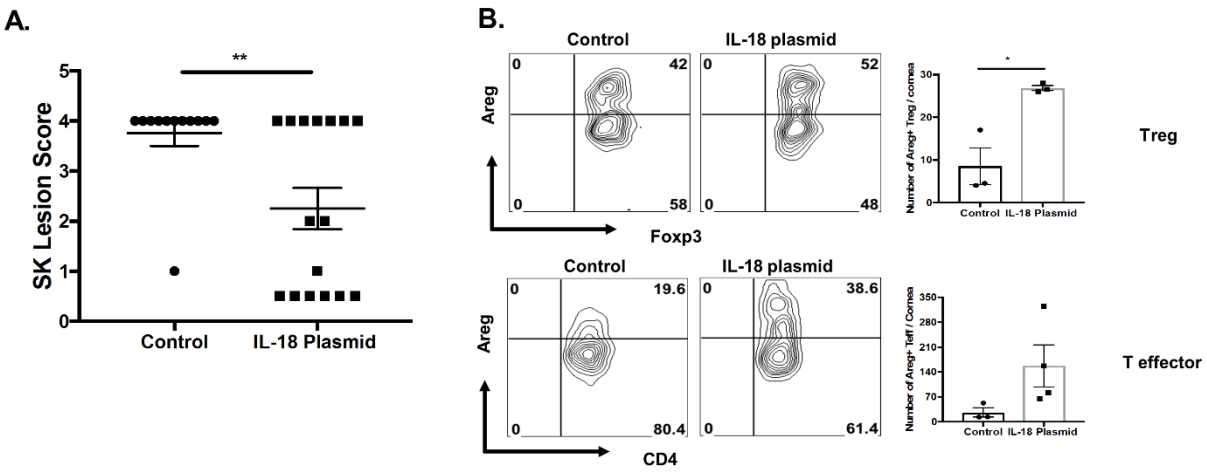

Figure 4.7. IL-18 expression plasmid increases the resolution of SK lesions and Amp Treg in cornea.

(A-B) C57BL/6 mice were ocularly infected with HSV-1 after administering IL-18 expressing plasmid 4 and 2 days before infection. (A) SK lesion severity scores as measured at day 15pi. (B) Representative FACS plots and bar graph showing Amp expressing Treg and Amp expressing effector T cells at day 8pi. Data represents the mean ± SEM of 3 independent experiments, where n=8 samples/group (A) and n=4 samples/group (B) P≤0.01 (**), P≤0.05(*).

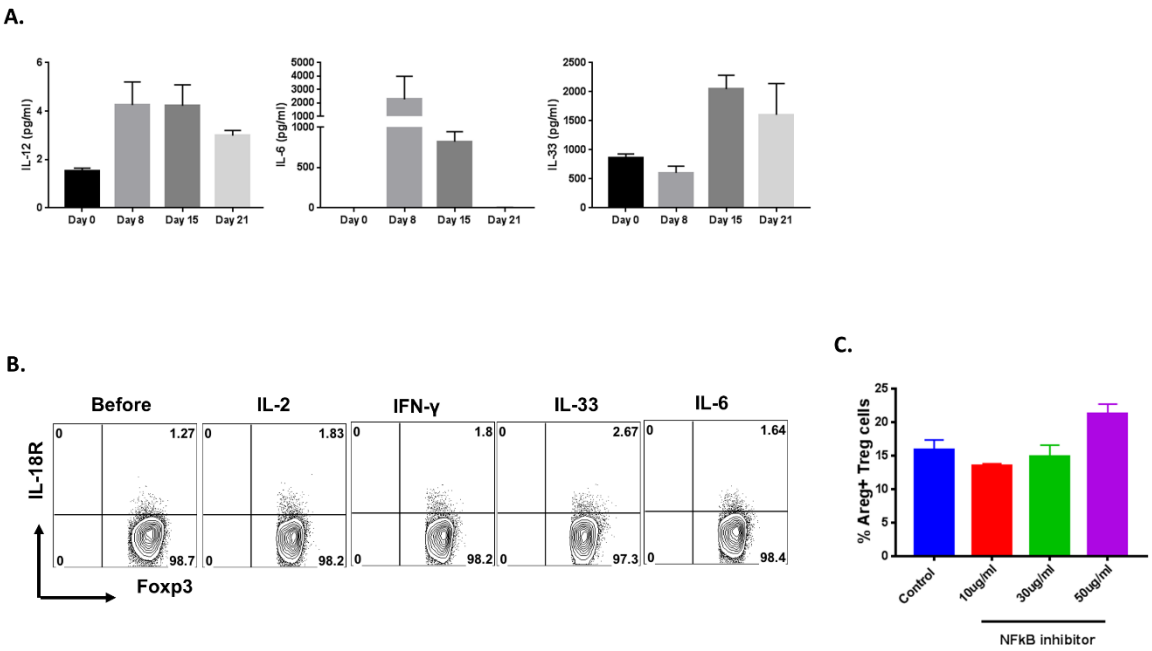

Figure S4.1.
(A) C57BL/6 animals were infected with 1 x 10^4 PFU of HSV-RE. Bar graphs showing IL-12, IL-6 and IL-33 protein levels in the corneas at various time points post infection (Day 0, 8, 15, 21) quantified by multiplex assay. (B) iTreg were cultured with IL-2 alone or in combination with either IFN-g, IL-6 or IL-33 for 5 days. Representative flow cytometry plots and bar graph showing frequency of IL-18R expressing Treg. (C) iTreg were cultured with IL-12 and IL-18 for 5 days in the presence or absence of NF-kB inhibitor SN50 at different concentrations and DMSO as control. Bar graph showing the frequency of Areg expressing Treg. Data represents the mean±SEM of 3 independent experiments where n= 3-5 samples/group.

CHAPTER 5
MANIPULATING GLUCOSE METABOLISM DURING DIFFERENT STAGES OF VIRAL PATHOGENESIS CAN HAVE EITHER DETRIMENTAL OR BENEFICIAL EFFECTS

Research described in this chapter is reproduced from a publication accepted in Journal of Immunology by Siva Karthik Varanasi, Dallas Donohoe, Ujjaldeep Jaggi, Barry T Rouse

Abstract

This report deals with physiological changes and their implication following ocular infection with herpes simplex virus (HSV). This infection usually results in a blinding inflammatory reaction in the cornea orchestrated mainly by pro-inflammatory CD4 T cells and constrained in severity by regulatory T cells (Treg). In the present report, we make the unexpected finding that blood glucose levels change significantly during the course of infection. Whereas levels remained normal during the early phase of infection when the virus was actively replicating in the cornea, they increased around two fold during the time when inflammatory responses to the virus was occurring. We could show that glucose levels influenced the extent of induction of the inflammatory T cell subset in vitro that mainly drives lesions, but not regulatory T cells. Additionally, if glucose utilization was limited in vivo as a consequence of therapy in the inflammatory phase with the drug 2DG, lesions were diminished compared to untreated infected controls. In addition, lesions in 2DG treated animals contained less pro-inflammatory effectors. Glucose metabolism also influenced the acute phase of infection when replicating virus was present in the eye. Thus, therapy with 2DG to limit glucose utilization caused mice to become susceptible to the lethal effects of HSV infection, with virus spreading to the brain causing encephalitis. Taken together, our results indicate that glucose metabolism changed during the course of HSV infection and that modulating glucose levels can influence the outcome of infection, being detrimental or beneficial according to the stage of viral pathogenesis.

Introduction

Virus infections cause tissue damage in several ways one of which is to induce an inflammatory reaction orchestrated by T cells that respond to viral antigens. One such example is the blinding immuno-inflammatory reaction called stromal keratitis (SK), which occurs in the cornea of the eye following infection with herpes simplex virus (HSV) (1, 2). In such reactions, the pro-inflammatory effector T cells may be more tissue damaging if regulatory components of immunity, such as certain cytokines or cells with regulatory functions, are deficient (3-6). Thus, one aim of therapy with these usually chronic tissue damaging lesions is to shift the balance of different components involved in the immune response to the infection. Few if any effective therapies are readily available to achieve this objective. However, recent studies in the field of cellular metabolism have drawn attention to the fact that nutrient uptake and their utilization may differ among cell types involved in immune responses (7-9). Moreover, it has become evident that manipulating metabolic pathways represents a potential means of rebalancing immune responses and this approach is being mainly explored in the cancer and autoimmunity fields where the imbalance largely involves different subsets of T cells (10-14).

Application of the metabolic reprogramming approach has focused on manipulating glucose and fatty acid metabolism, which can show major differences between immune cells involved in reactions (15). However, few if any studies so far, have focused on infectious diseases, but this topic is highly relevant since many chronic tissue damaging infections are not subject to control by effective vaccines, or by readily acceptable (or affordable) means of therapy. In fact, targeting metabolic events represents a logical approach to pathogen control since many cause major changes in

metabolism not only in cells they infect, but also impact on the function of distant uninfected organs such as the liver, kidney, cardiovascular system and even the brain (16). Some of the general physiological consequences of systemic infections has been highlighted by recent studies (16, 17). However, the general topic of how virus infections, particularly those that cause local infections, influences physiological responses is still poorly understood. Our present studies record some metabolic consequences of local infections in the eye with HSV.

Our results show that ocular HSV infection in mice led to increased fed and fasted blood glucose levels at the time when virus no longer persists in ocular tissues. In addition, CD4 T cells from infected mice showed increased glucose uptake both at the corneal lesion site and in the draining lymph node. The CD4 T cells from HSV infected animals were highly metabolically active and displayed increased glucose uptake in vitro compared to T cells from naïve animals. In vitro experiments also indicated that the effector function of inflammatory T cells was dependent on glucose concentration. Moreover, inhibition of glucose uptake by 2DG limited the differentiation of effector T cells in vitro. In contrast, regulatory T cells (Treg) were unaffected by 2DG in vitro. Finally, and of potential therapeutic relevance, in vivo administration of 2DG resulted in diminished SK lesions, a consequence of reduced effector T cell responses. Taken together, we show that local infection with HSV results in changes in glucose homeostasis causing increased blood glucose levels, which may act to stimulate the generation and sustenance of inflammatory CD4 effector T cells, which, in the special environment of the eye, can result in damaging consequences. Although changes in blood glucose levels were not evident during the acute phase of ocular infection, therapy with 2DG during that phase resulted in death from herpes encephalitis in many animals. Possible explanations for these findings are discussed.

Results

HSV-1 infection increases blood glucose levels

To ascertain if ocular infection with HSV led to changes in glucose metabolism, blood glucose levels were measured in control and infected animals up to 15 days post infection (pi), the time when inflammatory responses to the ocular infection were at their peak. Elevated blood glucose levels were not observed in the initial period after infection when replicating virus was present in the eye. However, a moderate increase (about 1.5 to 2 fold) in blood glucose levels occurred in samples from days 8, a time when ocular inflammatory lesions first become evident in the corneal stroma, as well as at day 15 pi (Fig.5.1A). However, at the latter time point the effect was more variable and differences were not significant in some experiments. At day 15, comparisons of blood glucose levels were also made between infected and uninfected animals following a 16-hour fasting period. Once again glucose levels were significantly higher ($p<0.01$) in the infected animals compared to uninfected controls in both the fed and fasting states. (Fig. 5.1B).

Previous studies indicated that low-grade inflammation can affect systemic glucose levels by inducing gene expression changes in the liver (25, 26). Accordingly, pro-inflammatory cytokine levels in the serum were measured at different time points pi. The results indicated that IL-6, TNF-α and IFN-γ cytokine levels were significantly increased in serum samples of day 4 pi animals compared to uninfected controls (Fig.

1C). Measurement of gene expression changes in the liver at different time points pi indicated a significant increase in the expression of genes in the signaling pathways of pro-inflammatory cytokines at day 8 pi (about 3 fold) which included Il6ra, Tnfr2, Ifnγr1 and Stat3 (Fig. 5.1D). A recent report suggests that systemic inflammation suppressed CYP7A1 (Cholesterol 7 alpha-hydroxylase), the rate-limiting enzyme of the bile acid biosynthesis in the liver (25). This led to the accumulation of intermediate metabolites of the mevalonate pathway, resulting in stabilization of RHOC, a small GTPase induced by inflammation. The outcome was fasting hyperglycemia. We also quantified the expression of both CYP7A1 and RHOC in the liver at day 8 pi the time when blood glucose was at its peak. While the expression of CYP7A1 was significantly reduced, the expression of RHOC was higher in the livers at day 8 pi (Fig. 5.1E). These data indicate that ocular infection with HSV-1 results in a change in glucose metabolism likely by effects on the liver mediated by responses to inflammatory cytokines.

CD4 T cells display enhanced glucose uptake and glycolysis

As the inflammatory response in the eye to HSV infection is mainly orchestrated by CD4+ T cells (1), changes in glucose uptake and glycolytic events was measured in CD4 T cells of animals with SK lesions and compared to CD4 T cells in uninfected animals. The first series of experiments compared glucose uptake in control uninfected and animals with lesions (day 15 pi), following the administration of a fluorescently labeled glucose analog 2-NBDG (2-(N-(7-Nitrobenz-2-oxa-1,3-diazol-4-yl) Amino)-2-Deoxyglucose). One hour later, the draining lymph nodes (DLN) were collected and the fraction of CD4+ T cells that took up 2-NBDG was measured by flow cytometry. The results indicated that the CD4+ T cells from mice with ocular lesions had significantly more cells (approximately 6-fold) that took up the glucose compared to uninfected controls (Fig. 5A, B). Of note, compared to uninfected animals, CD4+ T cells from infected mice contained 4-fold more cells with the effector memory phenotype and 7-fold more cells that produced IFN-γ when stimulated *in vitro* with PMA and Ionomycin (Supp. Fig. S5.1). The glucose uptake receptor GLUT1, as measured by flow cytometry was also increased in CD4 T cells at day 15 pi compared to cells from uninfected controls (Fig. 5.2C).

Given that the CD4+ T cells from infected animals exhibited enhanced glucose uptake, a second set of experiments measured if these CD4+ cells also had changes in glucose metabolism. This was done using seahorse technology by determining the extracellular acidification rate (ECAR), which serves as an indicator of lactate production and glycolytic activity (21). CD4+ T cells isolated from the DLN of infected animals (day 15 pi) had a higher basal and maximal glycolytic rate (>3-fold) compared to CD4+ T cells from uninfected animals (Fig. 5.2D). Of note, measurements of basal oxygen consumption rate (OCR), which serves as an indicator mitochondrial respiration (21), indicated that the ratio of OCR to ECAR was significantly reduced ($p<0.05$) in cells from infected animals. This result may indicate cellular preference for glycolysis over mitochondrial respiration (Fig. 5.2E). These results imply that upon infection with HSV-1, CD4+ T cells increase glucose uptake and glucose utilization (glycolysis), which might be supported by higher glucose levels observed in animals with inflammatory lesions.

Treg and effector cells differentially use glucose

Since different T cell subsets participate in SK reactions (1), it was of interest to determine the type of T cell subset in which changes in glucose metabolism was

occurring. The focus was on CD4 effector and regulatory T cells since these are the two major subsets which influence the extent of SK lesions (3, 4). The two cell types were isolated from the DLN of day 15 infected mice, separating them based on their expression levels of the IL-2 receptor CD25 with cells that were CD25+ taken to be mainly Treg. Thus in separate experiments, we could show that on average ~93% of the CD25+ T cells were Foxp3+ on day 15 pi, The CD4+CD25- population was considered to be predominantly effector T cells (Supp. Fig. S5.2). The uptake of 2NBDG was significantly higher in the CD25- population (mainly effector T cells) as compared to the CD25+ population (mainly Treg) (Fig 5.3A).

Since, the mTOR pathway is also involved in the control of glucose uptake and glycolysis in T cells (27), mTOR activity was compared in the two subsets. This was done by measuring the phosphorylation of S6 kinase (a component of the mTOR down-stream signaling cascade) (28). Higher glucose uptake in the CD25- CD4 effector population was also associated with higher mTOR activity compared to the activity of the CD25+ CD4 Treg population (Fig. 5.3B).

To further determine if glucose requirements differed between the Th1 effector and Treg subsets, experiments were done in vitro to generate Treg and Th1 populations from naïve DLN populations. The populations obtained were approximately 80% enriched for each subset. After 5 days, levels of glycolysis were compared in the two populations by using a glycolysis stress test which measures extracellular flux analysis (ECAR). As shown in Fig 5.3C, the basal ECAR levels were elevated in the Th1 population compared to the Treg population (2.8-fold). In addition, the glycolytic capacity, as measured by an increase in ECAR levels following inhibition of ATP synthase (using oligomycin) (21), was around 3 fold higher in Th1 compared to the Treg cells (Fig. 5.3C). Accordingly, the two major populations of CD4 T cells involved in SK lesions had distinct differences in glucose metabolism, a pattern of events noted in some autoimmune and neoplastic diseases (11, 13).

Glucose availability affects Th1 differentiation in vitro

To begin to approach the question of the potential relevance of raised glucose levels during the inflammatory response to HSV infection, in vitro experiments were done to measure the influence of glucose levels on the efficiency of Th1 and Treg cell differentiation, cell types critically involved in SK reaction (1, 4). For this naïve CD4 T cells were TCR stimulated under either Treg or Th1 inducing conditions after which the effect of supplementing cultures with different concentrations of glucose was measured. Levels of glucose evaluated varied from below physiological levels to hyperglycemic (0.5mM to 20mM). As shown in the Fig 5.4A, B, increasing glucose levels elevated the magnitude of Th1 responses, but had no significant influence on Treg responses, as noted previously (29, 30). Curiously, increasing glucose from physiological levels (about 5mM) to that observed in vivo in the infected mice at day 8 pi (maximum of 10mM) led to a significant increase ($P<0.05$) in Th1 differentiation. (Fig. 5.4C). The above observation supports the hypothesis that, a two-fold increase in the physiological levels of glucose in the periphery might be relevant in terms of enhancing the generation of Th1 cells in vivo.

Inhibition of glucose utilization using 2-deoxyglusose inhibits the glycolysis

To further measure the influence of glucose levels during the inflammatory response to HSV infection, experiments were done in vitro to measure the effect of the molecule 2DG, which inhibits glucose utilization and hence glycolysis. Naïve CD4 T cells

were activated in the presence of 2DG for 72 hours followed by measurement of basal glycolysis using extracellular flux analysis The data indicated a 3-fold reduction in basal ECAR levels indicating a decrease in basal glycolysis in cells activated in the presence of 2DG when compared to control activated cells (Fig. 5.5A). Of note, no difference in cell death was observed at the concentration of 2DG used (data not shown). Collectively, the above results support the hypothesis that activated T cells upregulate glycolysis which can be inhibited by 2DG.

Additional experiments were done to measure the expression of key genes involved in the glycolytic pathway both in the presence or absence of 2DG. Naïve CD4 T cells were activated in vitro by stimulating them with anti-CD3/CD28 for 24 hours and the effect of 2DG (250μM) on gene expression changes was recorded. Compared to naïve CD4 T cells, activated CD4 T cells expressed higher levels of several genes involved in glycolysis. These included Hexokinase-1 (2-fold), Hexokinase-2 (20-fold) and Glut1 (4-fold) (Fig. 5.5). However, when CD4 T cells were activated in the presence of 2DG, the genes involved in glycolysis remained at the levels or even below those observed in non-activated control cells. (Fig. 5.5B). The presence of 2DG in the cultures also served to switch off the raised mTOR activity, as measured by levels of phosphorylated S6 kinase using flow cytometry (Fig. 5.5C).

To measure the effect of inhibition of glycolysis on differentiation of the two CD4 T cell subsets of interest (Th1 and Treg), naïve CD4+ T cells were cultured in Treg or Th1 differentiating conditions for 5 days in the presence or absence of 2DG (250μM). Although, the differentiation of Treg was unaffected at the dose of 2DG used, a 20-fold reduction in the numbers of Th1 cells induced was observed in the presence of 2DG (Fig. 5.6). These results support the above findings that effector T cell use glycolysis to a higher extent than Treg. The results may also mean that 2DG therapy could be therapeutically useful against SK by inhibiting T effectors but leaving Treg function intact. This notion is tested in the next section.

Inhibition of glucose utilization limits SK lesion severity and diminishes effector T cell responses

To measure the therapeutic potential of 2DG against SK, HSV infected animals were given daily administrations of either 2DG or PBS (control) starting at day 5 pi. This is the time point when there is at best minimal replicating virus detectable in the infected corneas and early inflammatory reactions start to become evident. Animals were examined at day 15 pi to record and compare the severity of SK lesions. The results were clear cut with animals receiving 2DG therapy showing significantly reduced SK lesion severity ($P<0.01$) compared to PBS treated control animals (Fig. 5.7A). At day 15 pi, around 12% of 2DG treated animals showed a lesion score of ≥ 3.0 compared to 50% in control treated animals. At the termination of experiments on day 15 pi, pools of corneas were collected and processed to identify their cellular composition by FACS analysis. There was a reduction in the number of total CD4 T cells (~10 fold) infiltrating the corneas of 2DG treated animals compared to control animals (Fig. 5.7B).

In parallel experiments of similar design, pools of corneas, DLN and spleen were collected at 15 days pi from 2DG treated and control animals. Single cell suspensions were stimulated in vitro with PMA and ionomycin to activate T cells and to record the numbers of cells that were either IFN-γ producers or expressed the transcription factor Foxp3. In the corneas, the number of CD4 T cells expressing IFN-γ was reduced

approximately 8-fold in 2DG compared to untreated controls (Fig. 5.7C). In the DLN and spleen, 2DG treatment resulted in reduced frequency and numbers of IFN-γ producing CD4 T cells by about 2-fold. Although the frequency of Tregs in the DLN remained the same, their number decreased significantly. This might be explained by reduced inflammatory responses in treated animals. However, the number and frequency of Treg in the spleens of 2DG treated animals remained unchanged (Fig. 5.7D).

Taken together, our results indicate that daily administration of 2DG starting at day 5 pi significantly diminished HSV-1 induced immunopathology along with a reduction in effector T cell numbers in both the cornea and lymphoid organs, which could in part contribute to reduced lesion severity.

Inhibiting of glucose utilization is lethal in the acute phase of HSV infection

Although, we found no evidence for hyperglycemia in the acute phase of HSV infection, experiments were done to measure the effects of 2DG therapy at the time when virus was actively replicating in the infected cornea. Animals were ocularly infected with HSV-1 and were either treated daily with 2DG or PBS control, starting from the day of infection. Under the infection conditions used, HSV infection of untreated animals failed to cause detectable illness or signs of encephalitis. However, in the 2DG treated animals around 40–50% (in three separate experiments) of 2DG treated animals developed encephalitis and most had to be terminated by day 10 pi (Fig. 5.8A). By 8 days pi, affected animals became lethargic, lost weight, showed ruffled fur and hunched appearance along with signs of incoordination. Brains were collected from encephalitic 2DG treated animals, to quantify levels of virus present. High virus levels of HSV were detectable (>4 log) in brain homogenates in all animals that showed signs of encephalitis by day 10 pi (Fig. 5.8B). These animals also had detectable virus in ocular swabs at day 6 pi which is one day beyond the time when virus is regularly present in untreated infected animals. Additionally, levels of virus in ocular swabs were around tenfold higher than in untreated mice (Fig. 5.8C). Of note, virus could not be detected in the brains at day 10 pi or in the ocular tissue at day 6 pi in the control animals when infected with the same dose of virus that caused encephalitis in the 2DG treated animals.

The reduction in antiviral inflammatory cells or mediators could explain the increased viral burden in the animals treated with 2DG. To test this possibility, pools of corneas were isolated from animals treated with 2DG or PBS controls at day 2 pi and were evaluated for the abundance of macrophages and neutrophils. In addition, the effector function of macrophages and neutrophils was measured by the expression of pro-IL-1β using flow cytometry. While the number and frequency of pro-IL-1beta expressing neutrophils remained unchanged with 2DG treatment (Supp. Fig S5.3), the frequency and the number of pro-IL-1beta expressing macrophages in the cornea were significantly reduced in 2DG treated animals (>3-fold) (Fig. 5.8D). This might account for the failure to stop the spread of virus to the CNS. To assess if molecules involved in antiviral responses were affected upon 2DG treatment, the expression of IFN-β, IL-1α and TNF-α genes was determined in the corneas of both control and 2DG treated animals at day 2pi. The results indicated no significant differences in the expression of these molecules (Fig. 5.8E). Taken together, the increase in viral load in the cornea as well as the failure to stop the spread of virus to the brain could be in part explained by reduction in the innate effector function of macrophages which also require glucose for their function as demonstrated in the next section.

2DG reduces the macrophage activation in the presence of LPS

Macrophages are reported to play an important role in early stages of infection by controlling HSV-1 replication and dissemination within the TG (31). Hence, effects of 2DG on macrophage activation were measured using LPS stimulation of bone marrow derived macrophages (BMDM). BMDM's were stimulated with LPS in the presence or absence of 2DG (250μM) for 24 hours, followed by measurement of pro-IL-1β expression using flow cytometry. The results indicated that stimulation of macrophages with LPS in the presence of 2DG resulted in a 2-fold reduction in both the frequency of macrophages expressing pro-IL-1β and expression of pro-IL-1β per cell basis (MFI) as compared to LPS stimulation alone (Fig. 5.8F), supporting the previous reports (32). In conclusion, inhibition of glucose utilization in macrophages inhibited the effector function of macrophages, which might partially explain the high viral burden in the animals treated with 2DG.

Discussion

Inflammatory reactions are likely to be prolonged and cause excessive tissue damage when the activity of the principal orchestrators, usually either CD4 or CD8 T cells, are not constrained by inhibitory molecules or by cells that function as regulators (3-6). This is the state of affairs in the viral infection model we have used in this report wherein CD4 T cell driven inflammatory reactions in the eye cause a chronic vision-impairing lesion called stromal keratitis. The challenge with SK is to understand the events that result in lesions and to find therapies that limit the severity and duration of ocular damage. In the present report, we make the unexpected finding that blood glucose levels change significantly during the course of infection. Whereas levels remained normal during the early phase of infection when the virus was actively replicating in the cornea, they increased around two fold during the time when inflammatory responses to the virus was occurring. We could show that glucose levels influenced the extent of induction of the inflammatory T cell subset in vitro that mainly drives SK lesions, but not regulatory T cells. Additionally, if glucose utilization was limited in vivo as a consequence of therapy in the inflammatory phase with the drug 2DG, lesions were diminished compared to untreated infected controls. In addition, lesions in 2DG treated animals contained less pro-inflammatory effectors. Glucose metabolism also influenced the acute phase of infection when replicating virus was present in the eye. Thus, therapy with 2DG to limit glucose utilization caused mice to become susceptible to the lethal effects of HSV infection, with virus spreading to the brain causing encephalitis. Taken together, our results indicate that glucose metabolism changed during the course of HSV infection and that modulating glucose levels can influence the outcome of infection, being detrimental or beneficial according to the stage of viral pathogenesis.

Few reports have noted any changes in blood glucose levels in response to virus infections except in experimental situations where infection can set off diabetes mellitus (33, 34). Moreover, in the situation we described the mild hyperglycemia was absent during the time when virus was actively replicating in the eye or elsewhere in the body. Instead, the hyperglycemia only occurred during the inflammatory reaction to the virus, which in the case of HSV ocular infection becomes a vision-impairing lesion referred to as stromal keratitis. Moreover, SK is a local lesion in the eye accompanied by an inflammatory response in the innervating trigeminal ganglion (35). Two relevant questions

emerge. These are, what accounts for the mild hyperglycemia and does the event have any consequence.

With regard to causation, the likeliest explanation could be the production of factors from the inflammatory site that caused the liver to change its level of glucose production. Candidates could include hormones, cytokines, or the release of lipid mediators from inflammatory cells (36-39). In a complex model of sustained inflammation induced by LPS, elevated blood glucose levels were observed and these were shown to be mediated by TNF-α (25). This cytokine acted on the liver to suppress the expression of the bile acid biosynthesis enzyme CYP7A1 that normally functions to influence glucose production by acting on the hepatic mevalonate pathway, resulting in the inhibition of insulin signaling (25). In our system, components of the virus with Toll-like receptor components would likely not be involved since virus is absent in the blood stream especially at the time of raised glucose levels. However, we did observe increased blood levels of some cytokines, which included TNF-α, IL-6 and IFN-γ at day 4 pi, as well as an increase in the expression of their receptors in the liver at day 8 pi. Moreover, we could show that animals with high blood glucose levels had reduced levels of CYP7A1, which could mean that the mechanism inducing the hyperglycemia was similar to that described by the Medzhitov group (25). Additional experiments are underway to further evaluate potential mechanisms that could cause raised glucose levels in our system, which differs from the systemic model used by the Medzhitov group (25) in being only a local inflammatory lesion in a small organ, the eye.

The second question about the hyperglycemia observed was the issue of its potential relevance. Two lines of indirect evidence implied that the effect could have relevance. Firstly, the change of glucose levels was about two-fold and whether this change in glucose concentration was potentially meaningful was tested in an in vitro induction system. In this system, the levels of CD4 Th1 effector cells generated from naïve precursors were compared using media with controlled concentrations of glucose. Curiously increasing the glucose concentrations from physiological levels to the levels observed in infected animals significantly increased the number of effector Th1 cells induced and had no effect on the levels of Treg induction, confirming the previous observations (29, 30). This could mean that the 2-fold increase in blood glucose observed in vivo might also serve to enhance Th1 differentiation, but further studies are needed to verify this possibility.

Another indirect approach also indicated that the change in glucose levels might help drive the inflammatory T cell response. Accordingly, when glucose utilization was suppressed by treating mice with 2DG from the time of onset of ocular inflammation, SK lesions were significantly reduced in magnitude. Along with this, the composition of the cellular constituents involved in ocular lesions was markedly changed with reduced numbers of CD4 effectors. Other reports have also shown that 2DG therapy (13, 14) can control both auto-inflammatory lesions and GVHD inflammatory reactions. However, in these inflammatory models, therapy with 2DG alone was usually non-effective and additional antimetabolite therapies such as metformin (13) and 6-Diazo-5-oxo-L-norleucine - DON (14) were needed to be used in combination to counteract lesions. The fact that 2DG alone was highly effective therapy against SK, could relate to the less chronic nature of the SK lesion since viral antigen does not persist to drive lesions.

However, in the autoimmune disease and GvHD system the inflammatory cells in the lesions are under consistent activation.

One issue yet to be explained was the discrepancy with the dose of 2DG used to achieve therapeutic effects in vivo with that found to selectively inhibit inflammatory T cell responses in vitro. However, we could not measure the absolute concentrations of 2DG in the blood and DLN after in vivo administration, and it is well known that 2DG is rapidly metabolized in vivo (40). Another perplexing issue was the observation that 2DG could inhibit the effects of glucose in vitro when the later was far in excess of 2DG concentrations. Some data from studies with yeast at least partially explain such observations. Thus 2DG may inhibit the function of glucose transporters (41) and it is conceivable that 2DG has additional off target effects not mediated by glucose itself (42). These issues needs to be further clarified.

Another unexpected observation made in this report was the dramatic consequence of 2DG therapy administered during the acute phase of ocular HSV infection. In such experiments, many of the animals succumbed to lethal consequences with virus spreading to and replicating in the CNS. Herpetic encephalitis (HSE) is a very rare outcome of HSV infections in adult humans unless they are genetically compromised in some immune component (43-46). In animal models for HSV infection, HSE is a more common event and can occur at higher doses of infection, or with some virulent strains of virus, or if animals have one of several defects of either innate or adaptive immunity (22, 47-50). We strongly suspect that the lethal consequences of HSV infection in 2DG treated mice could be the result of impaired function of a protective component of innate immunity. So far we have minimal support for this idea, but could show that the number of IL-1β expressing macrophages but not neutrophils was reduced at the site of infection as a consequence of 2DG therapy. In addition, that animals can suffer lethal consequences when treated with 2DG as was noted with another viral model (16). Accordingly, with influenza, the lethal effects were attributed to the increased expression of the ER-stress-induced transcription factor CHOP protein and its target gene Gadd34 in the hindbrains of mice treated with 2DG. The increased expression of CHOP protein caused apoptosis of neurons leading to neuronal dysfunction and death. This phenomenon has yet to be evaluated in our HSE model, but we suspect to find differences since HSV replication occurs in the CNS and can be very destructive resulting from both direct viral and immune-pathological destructive events (22, 48, 49).

This study is one of the first to evaluate the use of a drug which influences metabolic processes used by different immune components responding to an infection. We show that modulating the main energy generating component of inflammatory T cells has value to modulate the extent of viral immune inflammatory lesions. In our system, the effect was particularly effective since 2DG therapy inhibited pro-inflammatory T effectors but had no direct effect on cells such as Treg that play a protective function in SK lesions. Our results also indicate that using metabolic modifying drugs should be used with caution especially during virus infections. Thus when 2DG therapy was used when the virus was still replicating, the viral replication was enhanced and this could have had lethal consequences as a result of virus spreading to the brain.

Materials and Methods

Mice and Virus

Female C57BL/6 mice were purchased from Harlan Sprague-Dawley, Inc. (Indianapolis, IN), BALB/c DO11.10 RAG2-/- mice were purchased from Taconic and kept in pathogen free facility where food, water, bedding and instruments were autoclaved. All the animals were housed in American Association of Laboratory Animal Care–approved facilities at the University of Tennessee, Knoxville, Tennessee. All investigations followed guidelines of the Institutional Animal Care and Use Committee, and adhered to the ARVO Statement for the Use of Animals in Ophthalmic and Vision Research. HSV-I RE strain was used in all procedures. Virus was grown in Vero cell monolayers (American Type Culture Collection, Manassas, VA), titrated, and stored in aliquots at −80°C until used.

HSV-1 ocular infection and clinical scoring

Corneal infections of C57BL/6 were conducted under deep anesthesia induced by intra peritoneal (i.p) injection of tribromoethanol (Avertin). Mice were scarified on cornea with a 27-gauge needle, and a 3 μl drop containing $1x10^4$ PFU of HSV-1 was applied to the eye. The eyes were examined on different days post infection (dpi) with a slit-lamp biomicroscope (Kowa Company, Nagoya, Japan), and the clinical severity of keratitis of individually scored mice was recorded as previously described (18). Briefly, the scoring system was as follows: 0, normal cornea; +1, mild corneal haze; +2, moderate corneal opacity or scarring; +3, severe corneal opacity but iris visible; +4, opaque cornea and corneal ulcer; +5, corneal rupture and necrotizing keratitis. The naïve-uninfected mice were scarified on cornea with a 27-gauge needle without addition of any virus.

2DG Administration

The 2-deoxy-glucose (2DG) (sigma) was dissolved in PBS and administered intraperitoneally at 500mg/kg twice a day starting from either day 0 or day 5 pi until day 14 after infection. The control group either received an equal volume of PBS or left untreated. The dose of 2DG was based on preliminary dose titrations.

Blood Glucose and cytokine quantification

Blood glucose levels were measured from tail blood at different time point pi using Bayer Contour glucose meter and compared to naïve un-infected animals. For Fasting blood glucose levels animals were fasted for 16 hours in a clean cage with water followed by measurement of glucose levels in the blood from tail. For cytokine measurements, serum was isolated from the blood collected using Retro-orbital bleeding. At least 10 mouse cytokines were profiled using a multiplex platform and data were extracted based on cytokine-specific standards by Eve Technologies (Calgary). Five independent serum samples were used from mice at different time points pi. Serum from control uninfected after 4 days of scarification was used as control.

Flow Cytometric Analysis

At day 15 pi, corneas were excised, pooled group-wise, and digested with liberase (Roche Diagnostics Corporation, Indianapolis, IN) for 45 minutes at 37°C in a humidified atmosphere of 5% CO2. After incubation, the corneas were disrupted by grinding with a syringe plunger on a cell strainer and a single-cell suspension was made in complete RPMI 1640 medium. The single-cell suspensions obtained from corneal samples were stained for different cell surface molecules for fluorescence-activated cell sorting (FACS) analyses. Draining cervical lymph nodes were obtained from mice sacrificed at 15 dpi and

single cell suspensions were used. All steps were performed at 4°C. Briefly, cells were stained with respective surface fluorochrome-labeled Abs in FACS buffer for 30 minutes, then stained for intracellular Abs. Finally, the cells were washed three times with FACS buffer and resuspended in 1% paraformaldehyde. The stained samples were acquired with a FACS LSR II (BD Biosciences, San Jose, CA) and the data were analyzed using FlowJo software (Tree Star, Inc., Ashland, OR). To determine the number of IFN-γ producing T cells, intracellular cytokine staining was performed. In brief, corneal cells were either stimulated with PMA (50ng) and Ionomycin (500ng) for 4 hours in the presence of brefeldin A (10 μg/mL) in U-bottom 96-well plates (18). After this period, Live/Dead staining was performed followed by cell surface and intracellular cytokine staining using Foxp3 intracellular staining kit (ebioscience) in accordance with the manufacturer's recommendations. Dead cells were gated out using Live/Dead staining. Cells are mentioned as Th1 if they are CD4+ IFN-γ+ and Treg if they are CD4+ Foxp3+. For 2-NBDG uptake in vivo, mice were injected i.v. with 100 μg 2-NBDG/mouse diluted in PBS to either naïve C57BL/6 animals or day 15 pi animals. 15 min following the injection cervical DLNs were collected and single cell suspensions were stained as described above and analyzed using flow cytometry (19).

Reagents and antibodies.

CD4 (RM4-5), CD45 (53-6.7), CD11b (M1/70), Ly6G (1A8), F4/80 (BM8), IFN-γ (XMG1.2), CD25 (PC61), CD44 (IM7), Foxp3 (FJK-16S), anti-CD3 (145-2C11), anti-CD28 (37.51), GolgiPlug (brefeldin A) and anti-pro-IL-1 beta (NJTEN3) from either ebiosciences or BD biosciences. Anti-Mouse phospho-S6 Ribosomal (D57.2.2E) from Cell signaling and hGlut1 from R&D. Phorbol myristate acetate (PMA) and Ionomycin from sigma. Live/Dead staining kit and 2-NBDG from Life Technologies. Recombinant IL-2, IL-12, IL-6 and TGF-β from R&D systems. Glucose free RPMI media (life technologies) was prepared using dialyzed FBS and glucose (sigma) was added at concentrations (0.1-20mM).

Quantitative PCR (qPCR)

At day 2 post ocular infection with HSV-1, the corneas were isolated and two corneas were pooled per sample/group. Naïve CD4 T cells or cells activated in vitro with or without 2DG were taken at least 100,000 cells/sample. Total RNA from corneal and isolated T cell populations was isolated using mirVana miRNA isolation kit (Ambion). Liver (≤30mg) was isolated at day 0, day 4, day 8 and day 15 pi and total RNA was extracted using RNeasy® Fibrous Tissue Mini Kit (Qiagen) as per manufacturer's recommendation. cDNA was made with 500ng of RNA (corneal samples) and entire RNA (isolated T cells) by using oligo(dT) primer and ImProm-II Reverse Transcription system (Promega). Taqman gene expression assays for Glut-1 (SLC2A1), HK1 (Hexokinase 1), HK2 (Hexokinase 2), Il6ra, Tnfrsf1b, Stat3, Ifngr1, Cyp7a1, Rhoc, Il1a, Ifnb, Tnfa and Il1b were purchased from Applied biosystems and quantified using 7500 Fast Real-Time PCR system (Applied Biosystems). The expression levels of different molecules were normalized to β-actin using ΔCt calculation. Relative expression between control and experimental groups was calculated using the $2^{-\Delta\Delta Ct}$ X 1000 formula.

Purification of CD4+ T cells.

CD4+ T cells (total or naïve) were purified from single cell suspension of pooled draining cervical lymph nodes (DLNs) and spleen from HSV-infected or naïve C57BL/6 mice using manufacturer's instructions (Miltenyi Biotec).

In vitro Treg and Th1 differentiation

For glycolysis measurements using seahorse extracellular flux analyzer, naïve CD4 T cells were used in Treg and Th1 differentiation. For experiments evaluating the effects of glucose concentrations or effects of 2DG, splenocytes from naïve DO11.10 RAG2 -/- mice were used as a precursor population for the induction of Treg and Th1 cells as previously described (18). Briefly, 1×10^6 splenocytes after RBC lysis and several washings or 1 million naïve CD4 T cells were cultured in 1ml glucose sufficient RPMI media or glucose free-RPMI media (dialyzed serum) containing rIL-2 (100 U/ml) and TGFβ (1-5ng/ml) in the presence or absence of various concentrations of Glucose (0.5-20mM) with plate bound anti-CD3/CD28 Ab (1 µg/ml) for 5 days at 37°C in a 5% CO2 incubator. After 5 days, samples were characterized for Foxp3 intracellular staining (ebioscience staining kit) analyzed by flow cytometry. For Th1 differentiation, cells were cultured in the presence of recombinant mouse IL-12 (5-10ng/ml) and anti-IL-4 (10 µg/ml). After 5-days samples were re-stimulated with PMA/Ionomycin and analyzed for the production of IFN-γ by intracellular cytokine staining kit (BD biosciences) using flow cytometer. 250µM-2DG dose was chosen based on the preliminary dose response experiments and previous reports (20).

OCR and ECAR measurement

OCR and ECAR values were measured using a Seahorse XF24 metabolic analyzer. Briefly, total CD4 T cells were purified from either infected or naïve female B6 mice or Treg/Th1 cells were differentiated and expanded from naïve CD4 T cells in vitro as described above. 1×10^6 cells per well were plated on XF24 plate (Seahorse Bioscience) pre-coated with 0.5 mg/ml poly-D lysine (Sigma). Cells were maintained in RPMI media (corning) supplemented with 1mM sodium pyruvate (Sigma) and 10% FBS. Before analyzing, cells were spun down and 530ul of XF media (with or without glucose) was added to each well, followed by incubation for 30 minutes in CO2-free incubator at 37°C. Seahorse analyzer was then run per manufacture's protocol with oligomycin (1uM), FCCP (1uM), and antimycin A (1uM) injected through ports A, B, and C respectively for mitochondrial stress test and glucose (10mM), oligomycin (1uM) and 2DG(10mM) for glycolysis stress test (21).

Viral Plaque Assay

Virus titers were measured in the brain and corneas of HSV infected mice as described previously by others (22). Virus titers in all samples were measured using standard plaque assay as described previously (22, 23).

Cell Culture

Female C57BL/6 mice were used at 8–16 weeks of age. BMDMs were generated as described previously (24) and grown in RPMI 1640 with 10% FCS. The media was supplemented with macrophage-colony-stimulating factor (10 ng/ml). Cells were 98% pure for macrophages (CD45+ CD11b+ F4/80+) and plated out on day 10 at 100,000 cells/well and stimulated with LPS (20ng/ml) for 24 hours.

Statistical Analysis

Statistical significance was determined by either Student's t-test (comparing two groups) or One-way ANOVA (comparing three or more groups). A P-value of <0.05 was regarded as a significant difference between groups: $^*P \le 0.05$, $^{**}P \le 0.01$, $^{***}P \le 0.001$. GraphPad Prism software (GraphPad Software, Inc., La Jolla, CA) was used for statistical analysis.

References

1. Biswas, P. S., and B. T. Rouse. 2005. Early events in HSV keratitis—setting the stage for a blinding disease. *Microbes and Infection* 7: 799-810.
2. Rowe, A., A. S. Leger, S. Jeon, D. Dhaliwal, J. Knickelbein, and R. Hendricks. 2013. Herpes keratitis. *Progress in retinal and eye research* 32: 88-101.
3. Veiga-Parga, T., S. Sehrawat, and B. T. Rouse. 2013. Role of regulatory T cells during virus infection. *Immunological reviews* 255: 182-196.
4. Suvas, S., A. K. Azkur, B. S. Kim, U. Kumaraguru, and B. T. Rouse. 2004. CD4+ CD25+ regulatory T cells control the severity of viral immunoinflammatory lesions. *The Journal of Immunology* 172: 4123-4132.
5. Sarangi, P. P., S. Sehrawat, S. Suvas, and B. T. Rouse. 2008. IL-10 and natural regulatory T cells: two independent anti-inflammatory mechanisms in herpes simplex virus-induced ocular immunopathology. *The Journal of Immunology* 180: 6297-6306.
6. Tumpey, T. M., V. M. Elner, S.-H. Chen, J. E. Oakes, and R. N. Lausch. 1994. Interleukin-10 treatment can suppress stromal keratitis induced by herpes simplex virus type 1. *The Journal of Immunology* 153: 2258-2265.
7. O'Sullivan, D., and E. L. Pearce. 2015. Targeting T cell metabolism for therapy. *Trends in immunology* 36: 71-80.
8. O'Neill, L. A., R. J. Kishton, and J. Rathmell. 2016. A guide to immunometabolism for immunologists. *Nature Reviews Immunology*.
9. MacIver, N. J., R. D. Michalek, and J. C. Rathmell. 2013. Metabolic regulation of T lymphocytes. *Annual review of immunology* 31: 259-283.
10. Pearce, E. L., M. C. Walsh, P. J. Cejas, G. M. Harms, H. Shen, L.-S. Wang, R. G. Jones, and Y. Choi. 2009. Enhancing CD8 T-cell memory by modulating fatty acid metabolism. *Nature* 460: 103-107.
11. Chang, C.-H., J. D. Curtis, L. B. Maggi, B. Faubert, A. V. Villarino, D. O'Sullivan, S. C.-C. Huang, G. J. van der Windt, J. Blagih, and J. Qiu. 2013. Posttranscriptional control of T cell effector function by aerobic glycolysis. *Cell* 153: 1239-1251.
12. Chang, C.-H., J. Qiu, D. O'Sullivan, M. D. Buck, T. Noguchi, J. D. Curtis, Q. Chen, M. Gindin, M. M. Gubin, and G. J. van der Windt. 2015. Metabolic competition in the tumor microenvironment is a driver of cancer progression. *Cell* 162: 1229-1241.
13. Yin, Y., S.-C. Choi, Z. Xu, D. J. Perry, H. Seay, B. P. Croker, E. S. Sobel, T. M. Brusko, and L. Morel. 2015. Normalization of CD4+ T cell metabolism reverses lupus. *Science translational medicine* 7: 274ra218-274ra218.
14. Lee, C.-F., Y.-C. Lo, C.-H. Cheng, G. J. Furtmüller, B. Oh, V. Andrade-Oliveira, A. G. Thomas, C. E. Bowman, B. S. Slusher, and M. J. Wolfgang. 2015. Preventing allograft rejection by targeting immune metabolism. *Cell reports* 13: 760-770.
15. Gerriets, V. A., and J. C. Rathmell. 2012. Metabolic pathways in T cell fate and function. *Trends in immunology* 33: 168-173.
16. Wang, A., S. C. Huen, H. H. Luan, S. Yu, C. Zhang, J.-D. Gallezot, C. J. Booth, and R. Medzhitov. 2016. Opposing effects of fasting metabolism on tissue tolerance in bacterial and viral inflammation. *Cell* 166: 1512-1525. e1512.
17. Rao, S., A. M. P. Schieber, C. P. O'Connor, M. Leblanc, D. Michel, and J. S. Ayres. 2017. Pathogen-Mediated Inhibition of Anorexia Promotes Host Survival and Transmission. *Cell* 168: 503-516. e512.

18. Varanasi, S. K., P. B. Reddy, S. Bhela, U. Jaggi, F. Gimenez, and B. T. Rouse. 2017. Azacytidine treatment inhibits the progression of Herpes Stromal Keratitis by enhancing regulatory T cell function. *Journal of Virology* 91: e02367-02316.
19. O'Sullivan, D., G. J. van der Windt, S. C.-C. Huang, J. D. Curtis, C.-H. Chang, M. D. Buck, J. Qiu, A. M. Smith, W. Y. Lam, and L. M. DiPlato. 2014. Memory CD8+ T cells use cell-intrinsic lipolysis to support the metabolic programming necessary for development. *Immunity* 41: 75-88.
20. Gerriets, V. A., R. J. Kishton, A. G. Nichols, A. N. Macintyre, M. Inoue, O. Ilkayeva, P. S. Winter, X. Liu, B. Priyadharshini, and M. E. Slawinska. 2015. Metabolic programming and PDHK1 control CD4+ T cell subsets and inflammation. *The Journal of clinical investigation* 125: 194-207.
21. van der Windt, G. J., C. H. Chang, and E. L. Pearce. 2016. Measuring Bioenergetics in T Cells Using a Seahorse Extracellular Flux Analyzer. *Current Protocols in Immunology*: 3.16 B. 11-13.16 B. 14.
22. Bhela, S., S. Mulik, P. B. Reddy, R. L. Richardson, F. Gimenez, N. K. Rajasagi, T. Veiga-Parga, A. P. Osmand, and B. T. Rouse. 2014. Critical role of microRNA-155 in herpes simplex encephalitis. *The Journal of Immunology* 192: 2734-2743.
23. Reddy, P. B., S. Sehrawat, A. Suryawanshi, N. K. Rajasagi, S. Mulik, M. Hirashima, and B. T. Rouse. 2011. Influence of galectin-9/Tim-3 interaction on herpes simplex virus-1 latency. *The Journal of Immunology* 187: 5745-5755.
24. Gonçalves, R., and D. M. Mosser. 2008. The isolation and characterization of murine macrophages. *Current protocols in immunology*: 14.11. 11-14.11. 16.
25. Okin, D., and R. Medzhitov. 2016. The effect of sustained inflammation on hepatic mevalonate pathway results in hyperglycemia. *Cell* 165: 343-356.
26. Masri, S., T. Papagiannakopoulos, K. Kinouchi, Y. Liu, M. Cervantes, P. Baldi, T. Jacks, and P. Sassone-Corsi. 2016. Lung adenocarcinoma distally rewires hepatic circadian homeostasis. *Cell* 165: 896-909.
27. Ray, J. P., M. M. Staron, J. A. Shyer, P.-C. Ho, H. D. Marshall, S. M. Gray, B. J. Laidlaw, K. Araki, R. Ahmed, and S. M. Kaech. 2015. The interleukin-2-mTORc1 kinase axis defines the signaling, differentiation, and metabolism of T helper 1 and follicular B helper T cells. *Immunity* 43: 690-702.
28. Nojima, H., C. Tokunaga, S. Eguchi, N. Oshiro, S. Hidayat, K.-i. Yoshino, K. Hara, N. Tanaka, J. Avruch, and K. Yonezawa. 2003. The mammalian target of rapamycin (mTOR) partner, raptor, binds the mTOR substrates p70 S6 kinase and 4E-BP1 through their TOR signaling (TOS) motif. *Journal of Biological Chemistry* 278: 15461-15464.
29. Cham, C. M., and T. F. Gajewski. 2005. Glucose availability regulates IFN-γ production and p70S6 kinase activation in CD8+ effector T cells. *The Journal of Immunology* 174: 4670-4677.
30. Michalek, R. D., V. A. Gerriets, S. R. Jacobs, A. N. Macintyre, N. J. MacIver, E. F. Mason, S. A. Sullivan, A. G. Nichols, and J. C. Rathmell. 2011. Cutting edge: distinct glycolytic and lipid oxidative metabolic programs are essential for effector and regulatory CD4+ T cell subsets. *The Journal of Immunology* 186: 3299-3303.
31. Kodukula, P., T. Liu, N. Van Rooijen, M. J. Jager, and R. L. Hendricks. 1999. Macrophage control of herpes simplex virus type 1 replication in the peripheral nervous system. *The Journal of Immunology* 162: 2895-2905.

32. Tannahill, G., A. Curtis, J. Adamik, E. Palsson-McDermott, A. McGettrick, G. Goel, C. Frezza, N. Bernard, B. Kelly, and N. Foley. 2013. Succinate is an inflammatory signal that induces IL-1 [bgr] through HIF-1 [agr]. *Nature* 496: 238-242.
33. Filippi, C. M., and M. G. von Herrath. 2008. Viral trigger for type 1 diabetes. *Diabetes* 57: 2863-2871.
34. Coppieters, K. T., T. Boettler, and M. von Herrath. 2012. Virus infections in type 1 diabetes. *Cold Spring Harbor perspectives in medicine* 2: a007682.
35. Khanna, K. M., A. J. Lepisto, V. Decman, and R. L. Hendricks. 2004. Immune control of herpes simplex virus during latency. *Current opinion in immunology* 16: 463-469.
36. Chen, L., R. Chen, H. Wang, and F. Liang. 2015. Mechanisms linking inflammation to insulin resistance. *International journal of endocrinology* 2015.
37. Glass, C. K., and J. M. Olefsky. 2012. Inflammation and lipid signaling in the etiology of insulin resistance. *Cell metabolism* 15: 635-645.
38. Shoelson, S. E., J. Lee, and A. B. Goldfine. 2006. Inflammation and insulin resistance. *The Journal of clinical investigation* 116: 1793-1801.
39. McGuinness, O. P. 2005. Defective glucose homeostasis during infection. *Annu. Rev. Nutr.* 25: 9-35.
40. Gounder, M. K., H. Lin, M. Stein, S. Goodin, J. R. Bertino, A. N. T. Kong, and R. S. DiPaola. 2012. A validated bioanalytical HPLC method for pharmacokinetic evaluation of 2-deoxyglucose in human plasma. *Biomedical Chromatography* 26: 650-654.
41. O'Donnell, A. F., R. R. McCartney, D. G. Chandrashekarappa, B. B. Zhang, J. Thorner, and M. C. Schmidt. 2015. 2-Deoxyglucose impairs Saccharomyces cerevisiae growth by stimulating Snf1-regulated and α-arrestin-mediated trafficking of hexose transporters 1 and 3. *Molecular and cellular biology* 35: 939-955.
42. Ralser, M., M. M. Wamelink, E. A. Struys, C. Joppich, S. Krobitsch, C. Jakobs, and H. Lehrach. 2008. A catabolic block does not sufficiently explain how 2-deoxy-D-glucose inhibits cell growth. *Proceedings of the National Academy of Sciences* 105: 17807-17811.
43. de Diego, R. P., V. Sancho-Shimizu, L. Lorenzo, A. Puel, S. Plancoulaine, C. Picard, M. Herman, A. Cardon, A. Durandy, and J. Bustamante. 2010. Human TRAF3 adaptor molecule deficiency leads to impaired Toll-like receptor 3 response and susceptibility to herpes simplex encephalitis. *Immunity* 33: 400-411.
44. Zhang, S.-Y., E. Jouanguy, S. Ugolini, A. Smahi, G. Elain, P. Romero, D. Segal, V. Sancho-Shimizu, L. Lorenzo, and A. Puel. 2007. TLR3 deficiency in patients with herpes simplex encephalitis. *science* 317: 1522-1527.
45. Casrouge, A., S.-Y. Zhang, C. Eidenschenk, E. Jouanguy, A. Puel, K. Yang, A. Alcais, C. Picard, N. Mahfoufi, and N. Nicolas. 2006. Herpes simplex virus encephalitis in human UNC-93B deficiency. *Science* 314: 308-312.
46. Sancho-Shimizu, V., R. P. de Diego, E. Jouanguy, S.-Y. Zhang, and J.-L. Casanova. 2011. Inborn errors of anti-viral interferon immunity in humans. *Current opinion in virology* 1: 487-496.
47. Sancho-Shimizu, V., S.-Y. Zhang, L. Abel, M. Tardieu, F. Rozenberg, E. Jouanguy, and J.-L. Casanova. 2007. Genetic susceptibility to herpes simplex virus 1 encephalitis in mice and humans. *Current opinion in allergy and clinical immunology* 7: 495-505.
48. Lundberg, P., C. Ramakrishna, J. Brown, J. M. Tyszka, M. Hamamura, D. R. Hinton, S. Kovats, O. Nalcioglu, K. Weinberg, and H. Openshaw. 2008. The immune

response to herpes simplex virus type 1 infection in susceptible mice is a major cause of central nervous system pathology resulting in fatal encephalitis. *Journal of virology* 82: 7078-7088.
49. Wang, J. P., G. N. Bowen, S. Zhou, A. Cerny, A. Zacharia, D. M. Knipe, R. W. Finberg, and E. A. Kurt-Jones. 2012. Role of specific innate immune responses in herpes simplex virus infection of the central nervous system. *Journal of virology* 86: 2273-2281.
50. Kurt-Jones, E. A., M. Chan, S. Zhou, J. Wang, G. Reed, R. Bronson, M. M. Arnold, D. M. Knipe, and R. W. Finberg. 2004. Herpes simplex virus 1 interaction with Toll-like receptor 2 contributes to lethal encephalitis. *Proceedings of the National Academy of Sciences of the United States of America* 101: 1315-1320.

APPENDIX

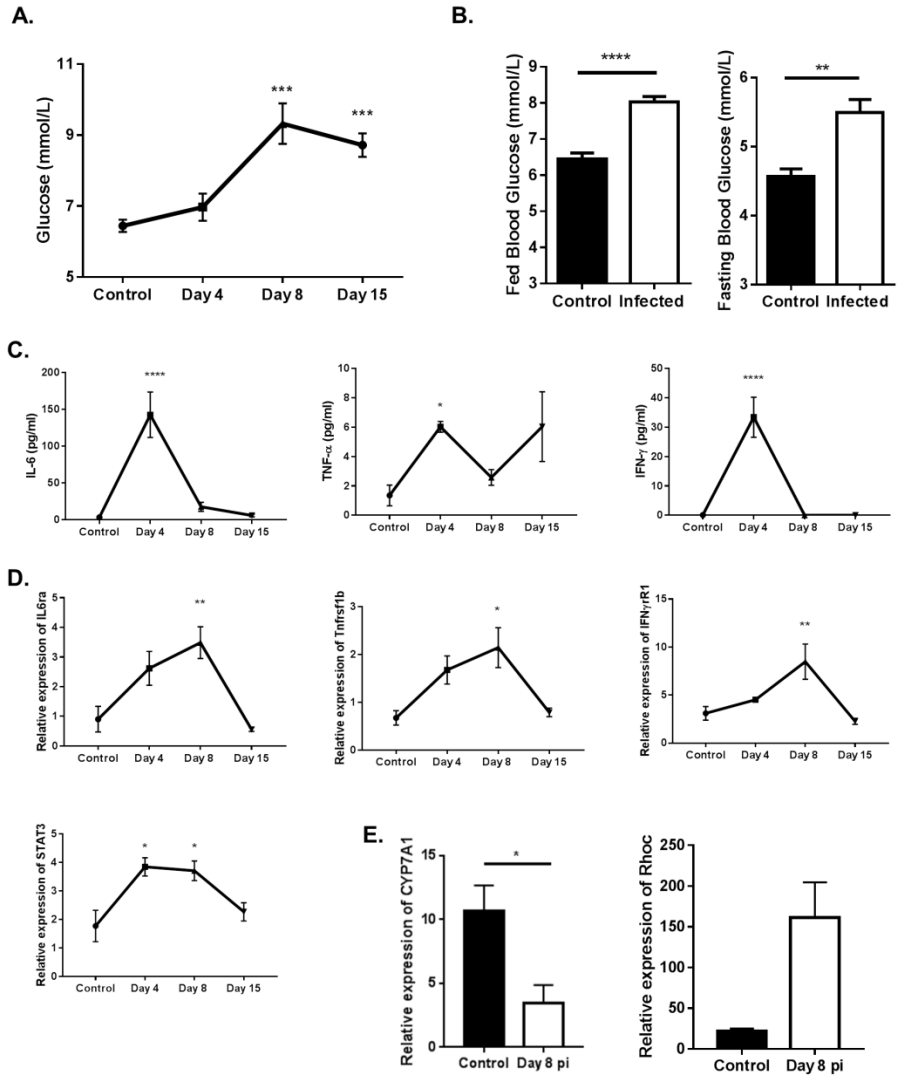

Figure 5.1. Blood glucose levels increase upon infection with HSV-1.
C57BL/6 animals were either infected with 1 x 10^4 PFU of HSV-RE or left alone. (A,B) Blood glucose levels were measured at time points indicated post infection. (A) Line graph showing kinetics of blood glucose levels (fed state) in control, day 4, day 8 and day 15 pi. (B) Histogram showing fed state and fasting state blood glucose levels at day 15 pi. (C) Line graph showing changes in serum cytokine levels at different time points pi. (D) Line graph showing changes in gene expression in the liver at different time points pi. (E) Histogram representing the expression of CYP7A1 and RHOC in liver of naïve and day 8 pi animals. Data represents the mean ± SEM of more than 8 independent experiments for A, B (n = 5-8 mice/group) and 2 independent experiments for C-E (n=4-5 mice/group). Data were analyzed with One-way ANOVA for A, C & D compared to the control or student's t-test for B & E. P≤ 0.0001 (****), P≤0.001(***), P≤0.01(**), P≤0.05(*).

Figure 5.2. Glucose uptake in CD4 T cells increases at day 15 post infection.
(A-E) C57BL/6 animals were either infected with 1 x 10^4 PFU of HSV-RE or left uninfected. (A, B) At day 15 pi animals showing SK lesions and naïve un-infected animals were administered with 2-NBDG (i.v) and glucose uptake by CD4 T cells was measured in DLNs. (A) Representative FACS plots and histogram (MFI) showing the 2-NBDG uptake by CD4 T cell from day 15 pi or naïve animals. For fluorescence minus one (FMO), mice were not injected with 2-NBDG. Cells were gated on live CD4+ T cells (B) Histogram number of CD4 T cells in DLNs with 2-NBDG uptake. (C) DLN from naïve and day 15 pi were stained with CD4 and Glut1 or Isotype. Representative FACS plots with Isotype control and Histogram (MFI) showing GLUT-1 expression by CD4 T cells. Cells were gated on live CD4+ T cells (D, E) Total CD4 T cells were purified from naïve and day 15 pi mice showing SK lesions and equal number of cells were used of extracellular flux analysis (D) Line graph showing changes in Extracellular acidification rates (ECAR) by CD4 T cells following addition of glucose, oligomycin and 2DG and Histograms showing basal glycolysis, glycolytic capacity (E) Histogram showing the ratio of OCR to ECAR. Data represents the mean ± SEM of more than 3 independent experiments for A-C (n=3-5 mice/group) and 2 independent experiments for D & E (n=5 replicates/group). All the data were analyzed with student's t test. P≤ 0.0001 (****), P≤0.01(**), P≤0.05(*)

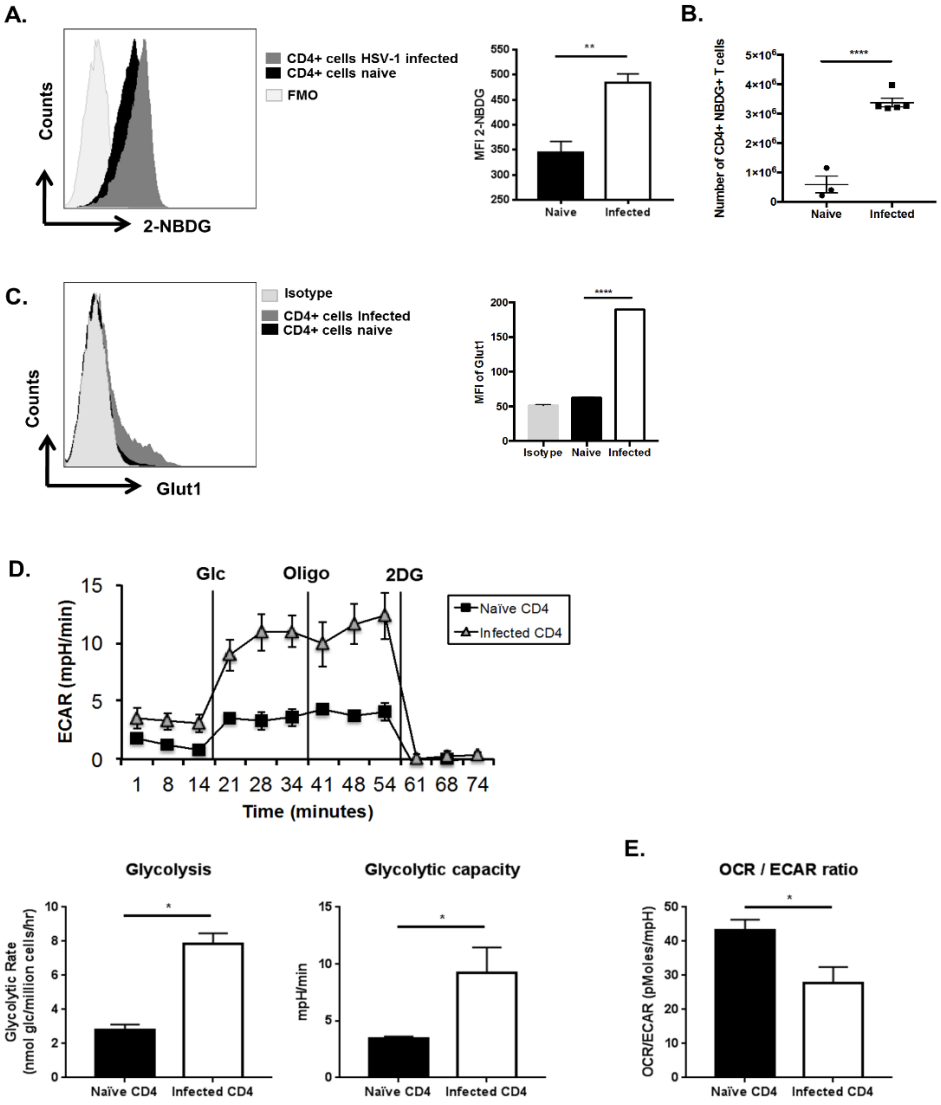
A.
Counts
2-NBDG
CD4+ cells HSV-1 infected
CD4+ cells naive
FMO
MFI 2-NBDG
Naive
Infected
B.
Number of CD4+ NBDG+ T cells
Naive
Infected
C.
Counts
Glut1
Isotype
CD4+ cells Infected
CD4+ cells naive
MFI of Glut1
Isotype
Naive
Infected
D.
Glc
Oligo
2DG
ECAR (mpH/min)
Time (minutes)
Naïve CD4
Infected CD4
E.
Glycolysis
Glycolytic Rate (nmol glc/million cells/hr)
Naïve CD4
Infected CD4
Glycolytic capacity
mpH/min
OCR / ECAR ratio
OCR/ECAR (pMoles/mpH)

Figure 5.3. CD4 T cells from infected and naïve animals have different glucose metabolism.
(A) C57BL/6 animals were infected with 1 x 10^4 PFU of HSV-RE and at day 15 pi animals showing SK lesions were administered with 2-NBDG (i.v) and glucose uptake by different CD4 T cell subsets was measured in DLNs. Representative FACS plots and histogram (MFI) showing the 2-NBDG uptake in Live cells of Treg (CD4+CD25+) cells and Teff (CD4+CD25-) cells as measured in DLNs at day15 pi. (B) DLNs at day 15 pi were stimulated PMA/Ionomycin followed by ICS assay. Representative FACS with Isotype control and histogram (MFI) of S6P in Treg (CD4+ Foxp3+) and Th1 (CD4+ IFN-γ+) cells. Dead cells were gated out using Live/Dead staining. Data represents the mean ± SEM of more than 3 independent experiments (n=3-5 mice/group) (C) Naive CD4 T cells purified from C57BL/6 mice were cultured in either Treg or Th1 differentiating conditions. After 5 days, equal number of cells were used of extracellular flux analysis. Line graph showing changes in extracellular acidification rates (ECAR) by CD4 T cells following addition of glucose, oligomycin and 2DG and Histograms showing basal ECAR and glycolytic capacity. Data represent the mean values ± SEM of two independent experiments of n=4. The level of significance was determined by Student's t test (unpaired). P≤ 0.0001 (****)

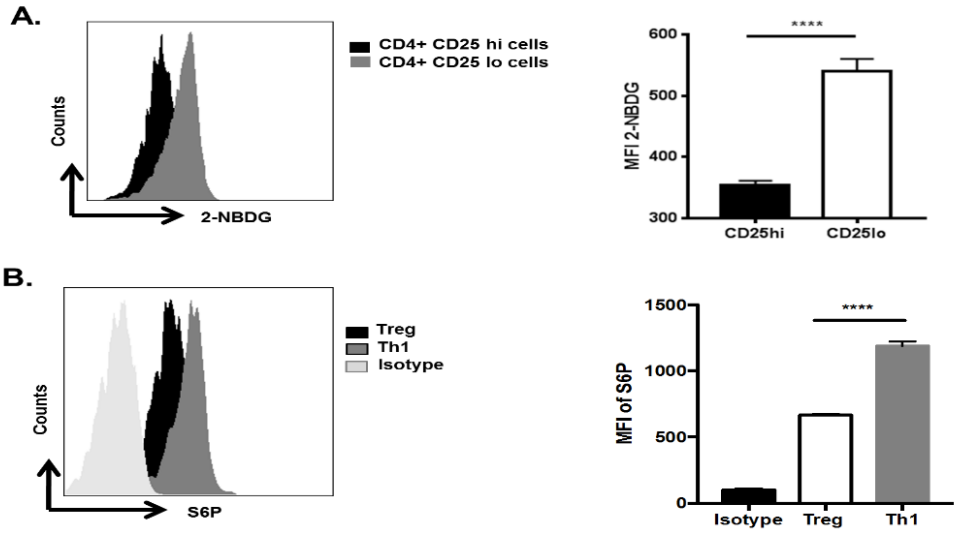
A.
CD4+ CD25 hi cells
CD4+ CD25 lo cells
Counts
2-NBDG
****
MFI 2-NBDG
600
500
400
300
CD25hi
CD25lo
B.
Treg
Th1
Isotype
Counts
S6P
****
MFI of S6P
1500
1000
500
0
Isotype
Treg
Th1

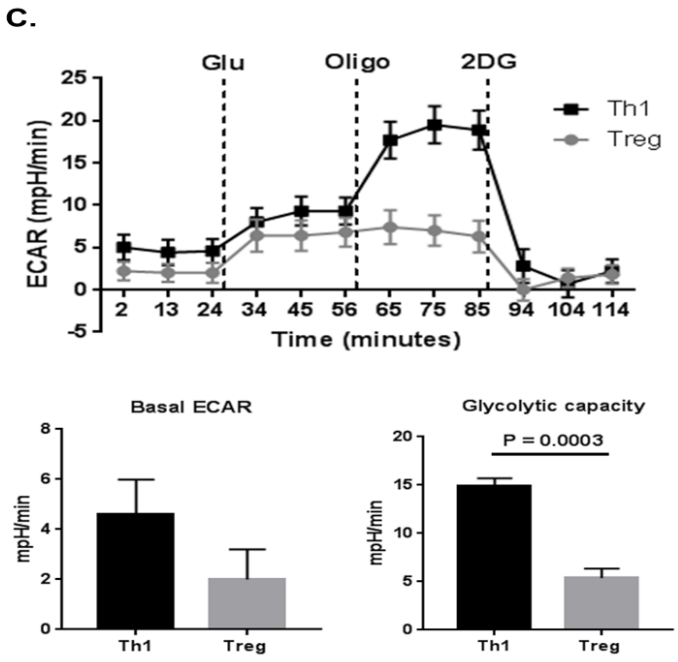
C.
Glu
Oligo
2DG
Th1
Treg
ECAR (mpH/min)
25
20
15
10
5
0
-5
2
13
24
34
45
56
65
75
85
94
104
114
Time (minutes)
Basal ECAR
mpH/min
8
6
4
2
0
Th1
Treg
Glycolytic capacity
P = 0.0003
mpH/min
20
15
10
5
0
Th1
Treg

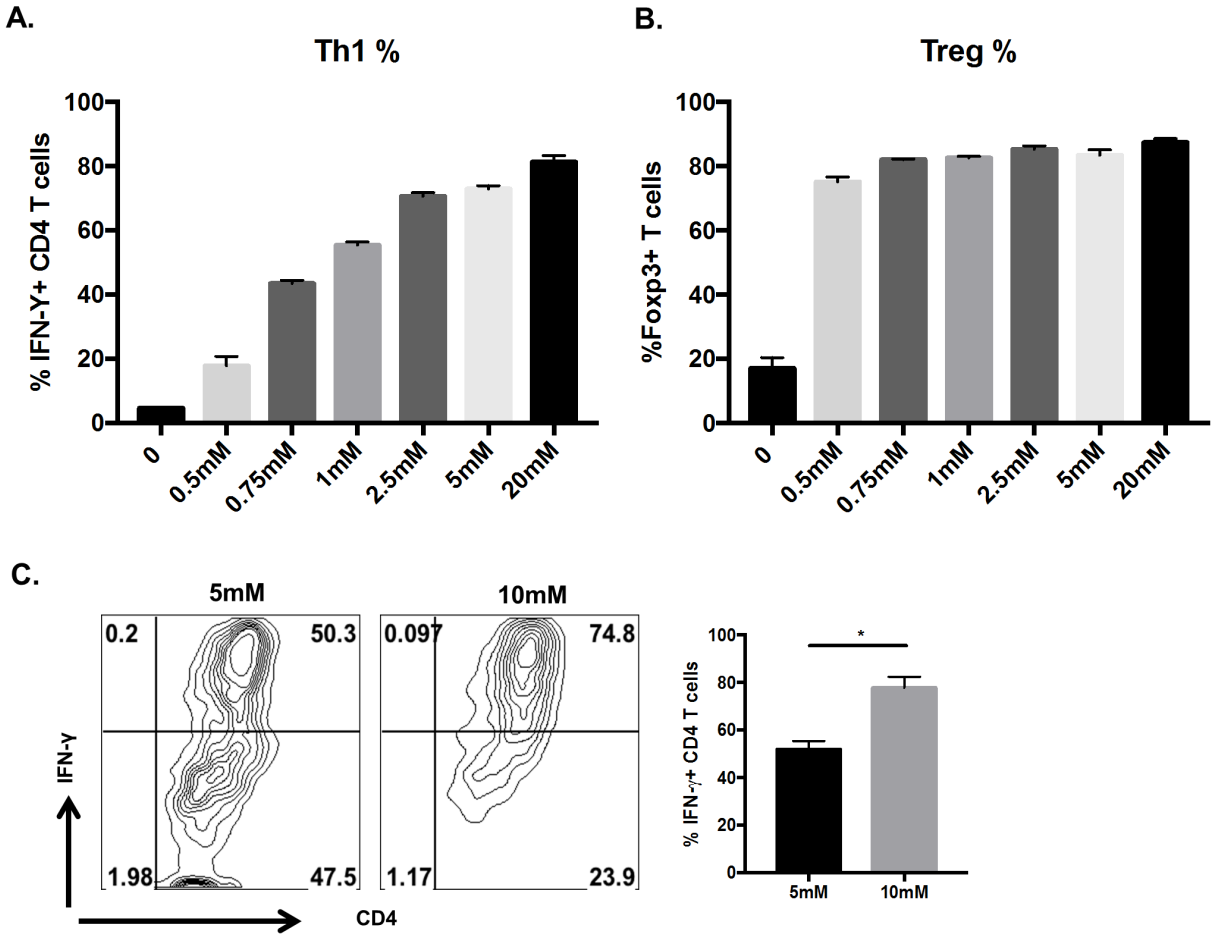

Figure 5.4. Increasing glucose levels increases Th1 but not Treg differentiation. Splenocytes from DO11.10 RAG2−/− mice were cultured (1 million cells) in the presence of 1 µg/ml of anti-CD3/CD28 antibody with either 100 U/ml of recombinant IL-2, 1ng/ml TGF-β (Treg differentiating conditions) or IL-12 (5ng/ml), anti-IL-4 (10 µg/ml) (Th1 differentiating conditions) with increasing concentrations of glucose(0.5mM-20mM) in glucose free conditions (A) Histogram showing frequency of IFN-γ during Th1 differentiation or (B) Foxp3 expression during Treg differentiation with increasing glucose concentrations (C) Representative FACS plots and histogram showing IFN-γ expression under Th1 differentiating conditions in the presence of glucose concentrations (5mM and 10mM). Cells were gated on live CD4+ T cells. Data represents means ± SEM from three independent experiments (n=3/group). The level of significance was determined by Student's t test (unpaired) P≤0.05(*).

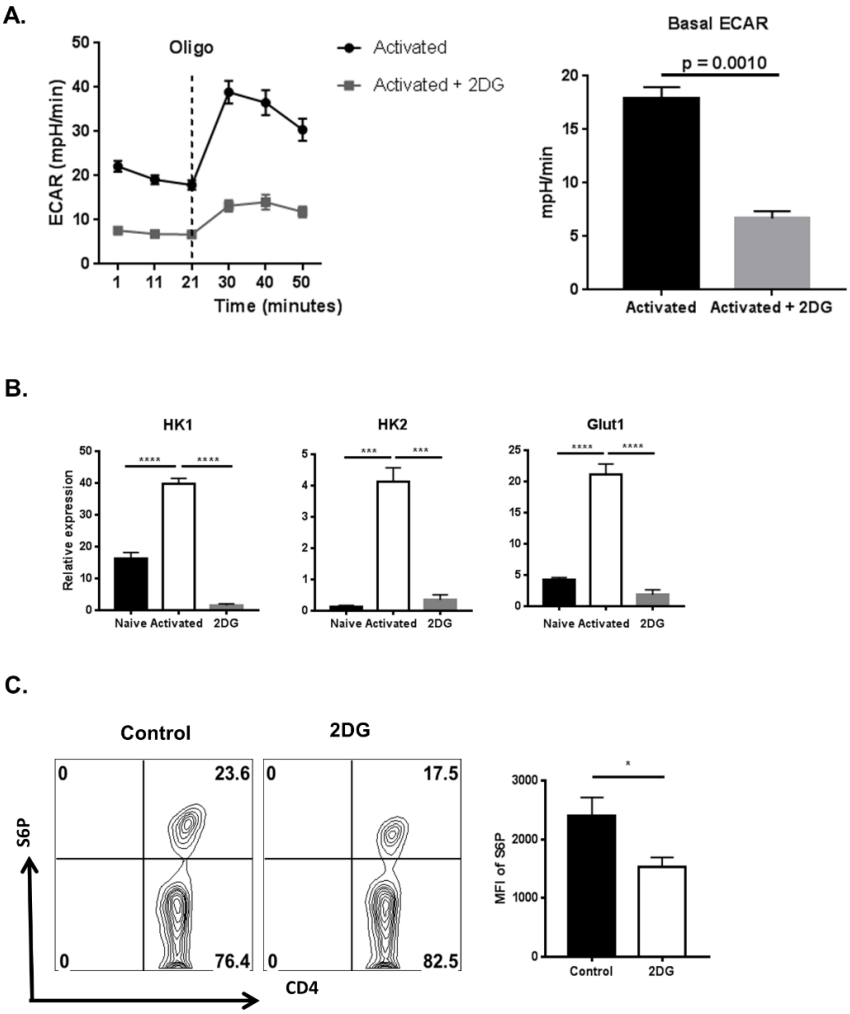

Figure 5.5. 2DG inhibits the metabolic reprogramming of CD4 T cells following activation.

(A) Naive CD4 T cells purified from C57BL/6 mice were cultured (500,000 cells/well) with 100U/ml IL-2, 1μg/ml anti-CD3/CD28 and in the presence or absence of 250μM 2DG for 3 days followed by extracellular flux analysis. Line graph showing changes in Extracellular acidification rates (ECAR) by CD4 T cells following addition of oligomycin and Histograms showing basal ECAR levels. (B) Naive CD4 T cells purified from C57BL/6 mice were cultured (100,000 cells/well) with 1μg/ml anti-CD3/CD28 and in the presence or absence of 250μM 2DG for 24 hours followed by gene expression analysis by QRT-PCR compared to beta-actin. Histogram representing expression of genes involved in glucose metabolism such as HK1, HK2 and Glut1 in naïve, activated and Activated in the presence of 2DG (2DG). (C) Naïve CD4 T cells were cultured (100,000 cells/well) with 1μg/ml anti-CD3/CD28 in the presence or absence of 250μM 2DG for 24 hours followed by measurement of Phosphorylation of S6 using flow cytometry. Representative FACS plots and histogram (MFI of S6P) of live CD4 T cells. Data represents means ± SEM from two independent experiments (n=3/group) and the level of significance was determined by Student's t test (unpaired) for A & C and One-way ANOVA for B. P≤ 0.0001 (****), P≤0.001(***), P≤0.01(**), P≤0.05(*).

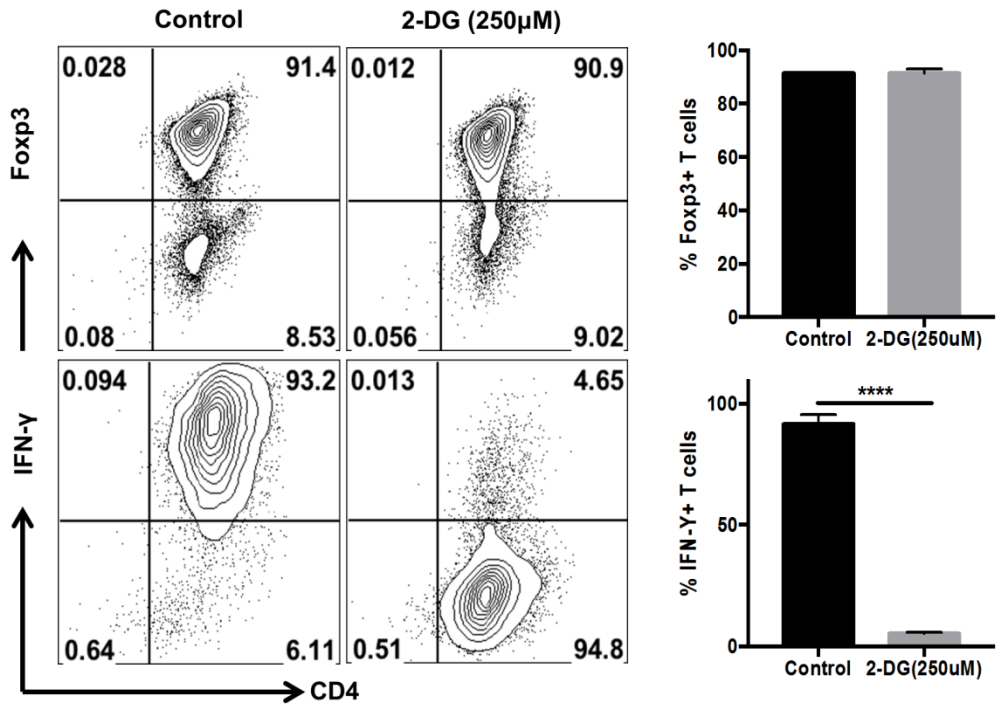

Figure 5.6. Effect of 2DG treatment on glycolysis and T cell differentiation.
Splenocytes from DO11.10 RAG2−/− mice were cultured (1 million cells) in the presence of 1 µg/ml of anti-CD3/CD28 antibody with either 100 U/ml of recombinant IL-2, 5ng/ml TGF-β (Treg differentiating conditions) or IL-12 (5ng/ml), anti-IL-4 (10 µg/ml) (Th1 differentiating conditions) with or without 2DG (250µM). After 5 days of culture, cells were analyzed for the expression of IFN-γ and Foxp3 on CD4 T cells. Representative FACS plots and histogram showing the frequency of Th1 and Treg. Cells were gated on live CD4+ Foxp3+ T cells (Treg) and live CD4+ IFN-γ + T cells (Th1). Data represents means ± SEMs of three independent experiments with n=3/group. Statistical significance was calculated by Student's t test (unpaired) P≤ 0.0001 (****).

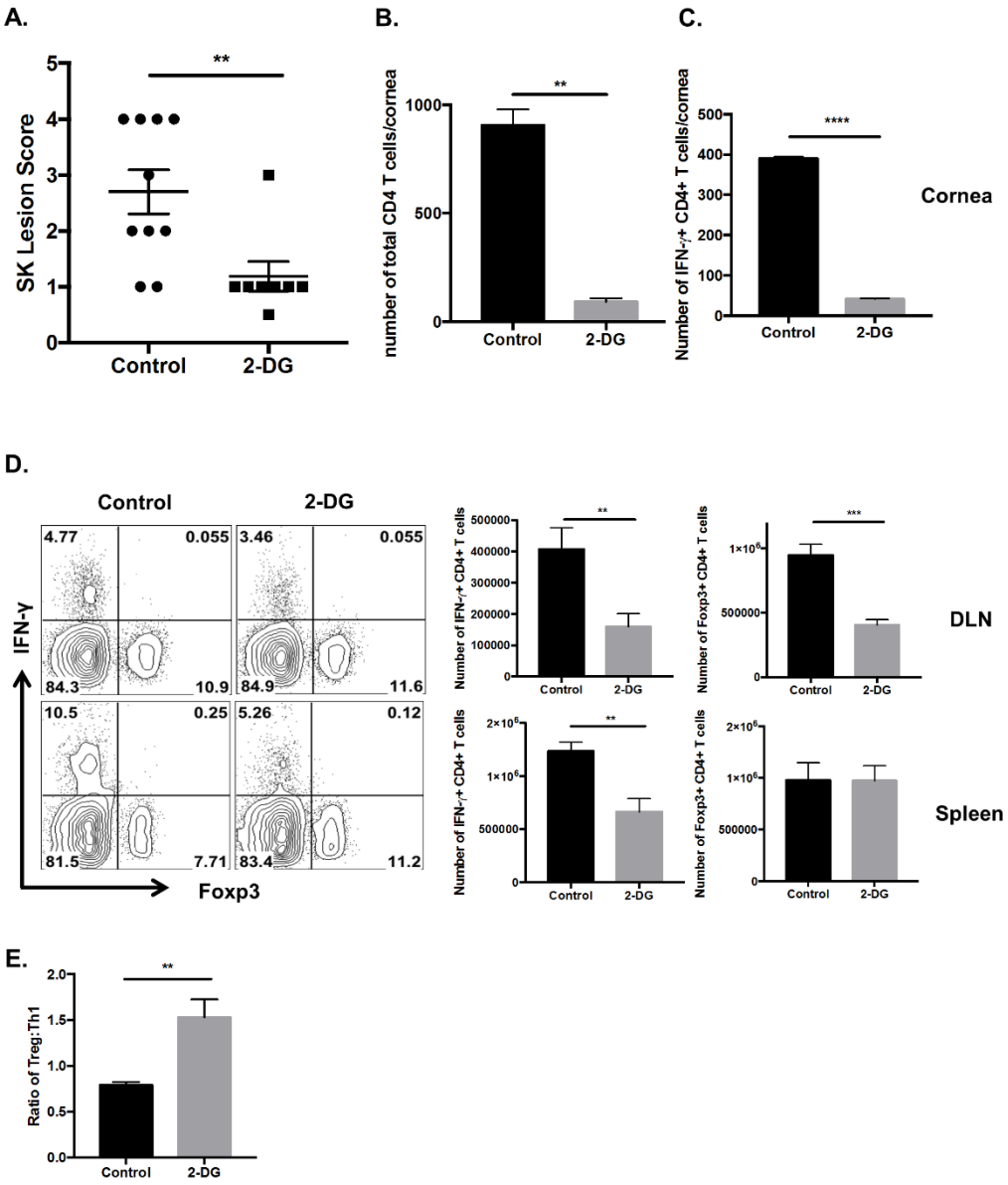

Figure 5.7. Therapeutic administration of 2DG diminishes SK severity.
C57BL/6 animals infected with 1 x 10^4 PFU of HSV-RE were given either 2DG or PBS from day 5 pi to day 14 pi. The disease progression was analyzed in a blinded manner using a scale described in materials and methods. (A) Individual eye scores of SK lesion severity on day 15 pi. (B) Representative histogram showing the number of total $CD4^+$ T cells infiltrating the cornea at day 15 p.i (C) Pool of corneas were stimulated with PMA/Ionomycin, representative histogram showing the number of Th1 (Live CD4+ IFN-γ) cells in the cornea at day 15 pi. (D) DLN and Spleen were stimulated with PMA/Ionomycin, representative FACS plots and histogram showing frequency and number of Treg (live CD4+ Foxp3+) and Th1 (live CD4+ IFN-γ). (E) Histogram representing Treg to Th1 ratio in the spleen at day15 pi. Data represents the mean ± SEM of more than 3 independent experiments (n=3-10 mice/group). All the data were analyzed with student's t test. P≤ 0.0001 (****), P≤0.001(***), P≤0.01(**).

Figure 5.8. 2DG administration during early HSV infection is lethal.
C57BL/6 animals infected with 1 x 10^4 PFU of HSV-RE were given either 2DG or PBS from day 0 pi to day 15 pi. (A) Survival of 2DG and control treated was established over 15 days. (B) Brains were harvested from 2DG treated and control mice at day 10 pi and homogenized, centrifuged, and the supernatants were tested for virus titers using plaque assay. (C) The presence of virus in the cornea was measured at day 6 pi by swabbing the HSV infected eye with a sterile swab and assaying for the virus by plaque assay. (D) Corneas were isolated at day 2 pi from control and 2DG treated animals and inflammatory macrophages (CD45+ CD11b+ F4/80+ Pro-IL-1β+) were identified using flow cytometry. Representative FACS plots and histogram showing MFI of pro-IL-1β, frequency and number of inflammatory macrophages in corneas of 2DG treated and control animals at day 2 pi. (E) Corneas were isolated from control and 2DG treated animals at day 2 pi and RNA was isolated followed by gene expression analysis by QRT-PCR. Histogram representing the gene expression of IL-1α, IFN-β and TNF-α. (F) Bone marrow derived macrophages (BMDM) were differentiated from naïve bone marrow progenitor cells (as described in materials and methods). BMDMs were stimulated with LPS (20ng/ml) in the presence or absence of 2DG (250μM) for 24 hours. Representative FACS plots and histogram showing frequency of BMDM expressing Pro-IL-1β (CD45+ CD11b+ F4/80+ Pro-IL-1β+). Data represents mean values ± SEM (n = 4–8 mice/group) for A-F. Experiments were repeated at least three times. The level of significance was determined by Student's t test (unpaired). P≤ 0.0001 (****), P≤0.01(**), P≤0.05(*).

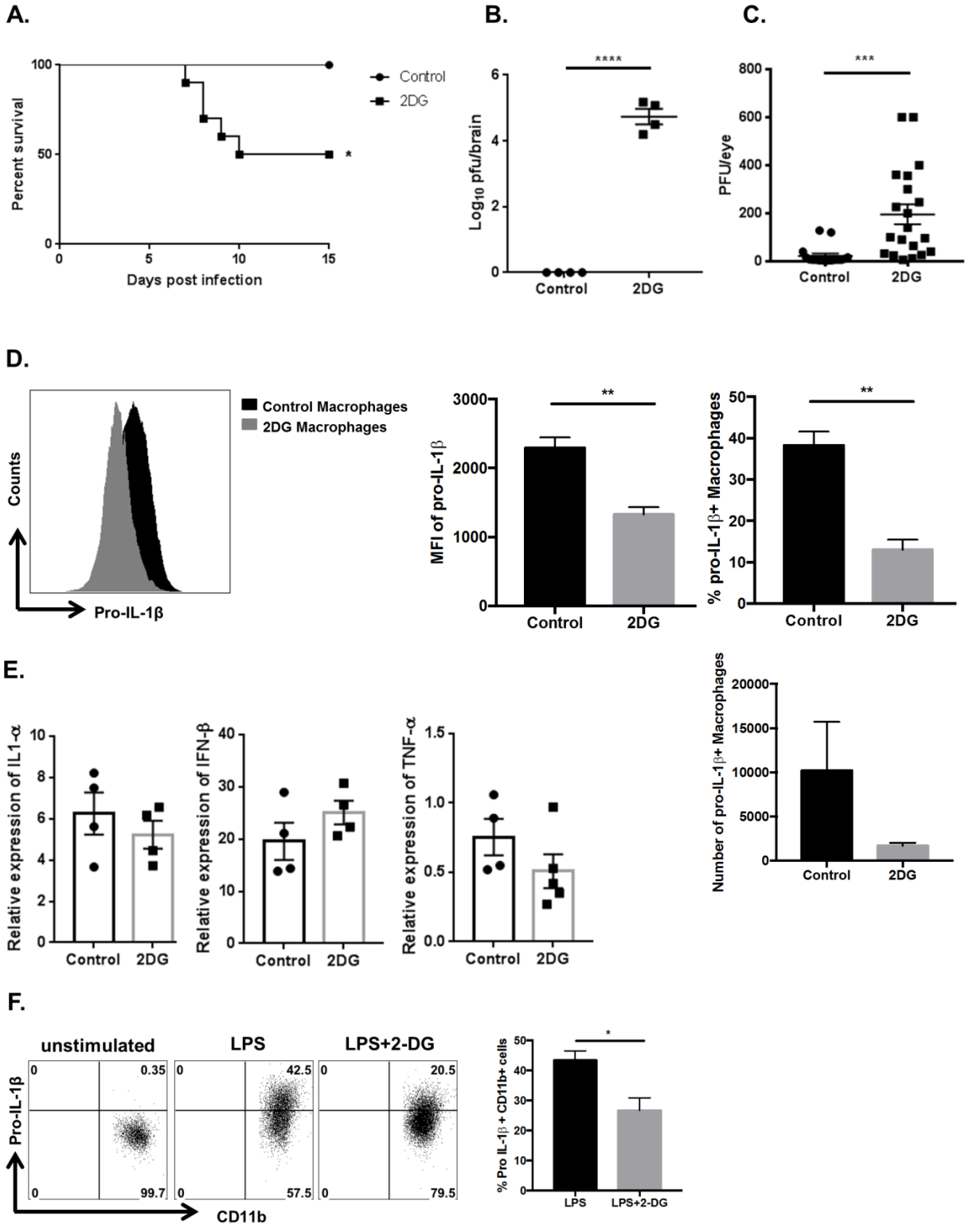
A.
Percent survival
Days post infection
Control
2DG
*
B.
Log10 pfu/brain
****
Control
2DG
C.
PFU/eye
***
Control
2DG
D.
Counts
Pro-IL-1β
Control Macrophages
2DG Macrophages
MFI of pro-IL-1β
**
Control
2DG
% pro-IL-1β+ Macrophages
**
Control
2DG
E.
Relative expression of IL1-α
Control
2DG
Relative expression of IFN-β
Control
2DG
Relative expression of TNF-α
Control
2DG
Number of pro-IL-1β+ Macrophages
Control
2DG
F.
unstimulated
LPS
LPS+2-DG
Pro-IL-1β
CD11b
0.35
99.7
42.5
57.5
20.5
79.5
% Pro IL-1β + CD11b+ cells
*
LPS
LPS+2-DG

CHAPTER 6
HEXOKINASE II MAY BE DISPENSABLE FOR CD4 T CELL RESPONSES AGAINST A VIRUS INFECTION.

Research described in this chapter is reproduced from a publication accepted in PLoS ONE by Siva Karthik Varanasi, Ujjaldeep Jaggi, Nissim Hay, Barry T Rouse

Abstract

Activation of CD4 T cells leads to their metabolic reprogramming which includes enhanced glycolysis, catalyzed through hexokinase enzymes. Studies in some systems indicate that the HK2 isoform is the most up regulated isoform in activated T cells and in this report the relevance of this finding is evaluated in an infectious disease model. Genetic ablation of HK2 was achieved in only T cells and the outcome was evaluated by measures of T cell function. Our results show that CD4 T cells from both HK2 depleted and WT animals displayed similar responses to in vitro stimulation and yielded similar levels of Th1, Treg or Th17 subsets when differentiated in vitro. A modest increase in the levels of proliferation was observed in CD4 T cells lacking HK2. Deletion of HK2 led to enhanced levels of HK1 indicative of a compensatory mechanism. Finally, CD4 T cell mediated immuno-inflammatory responses to a virus infection were similar between WT and HK2 KO animals. The observations that the expression of HK2 appears non-essential for CD4 T cell responses against virus infections is of interest since it suggests that targeting HK2 for cancer therapy may not have untoward effects on CD4 T cell mediated immune response against virus infections.

Introduction

Recently it has become evident that cells of the immune system show distinct differences in the metabolic pathways they use [1,2]. This opens up the prospect of manipulating metabolism to shape the nature of immunity. A well-studied metabolic difference between cell types has been the glucose metabolic pathway by which T cells mainly derive their energy [3]. Thus, some subsets of T cells generate their ATP mainly by oxidative glycolysis, whereas others mainly use mitochondrial respiration [4]. With regard to oxidative glycolysis, the process is critically influenced by enzymes which include at least 4 hexokinase isoforms to generate glucose 6-phosphate from glucose (the first rate limiting step of glycolysis). Of the 4 isoforms, mainly two, HK1 and HK2, are expressed by T cells [5,6]. In addition, when T cells are activated, as occurs in some autoimmune diseases, the fold change in expression of HK2 far exceeds that of HK1 when compared to resting cells [6,7]. Moreover, HK2 has two tandem catalytically active domains whereas HK1 has only one catalytically active domain [8]. Taken together this could mean that HK2 may be more relevant than HK1 for T cell function, although this possibility has not been substantiated, particularly in vivo.

In an attempt to evaluate if HK2 is more relevant than HK1 in activated T cells, we bred appropriate mice strains that would delete HK2 specifically in T cells from the onset of the development. We could readily show that overall CD4 and CD8 T cell numbers were unaffected by HK2 deletion and that the function of CD4 T cells in vivo in a virus immunopathology model was basically unchanged. Nevertheless, some modest differences in responsiveness were shown in vitro such as proliferative responses to T cell receptor stimulation. However, overall the absence of HK2 had no major effect on CD4 T cell functions. Moreover, expression of HK1 was upregulated in the absence of HK2 which was likely compensating for HK2 deletion. The systemic deletion of HK2 in adult mice does not elicit adverse physiological consequences but inhibits tumor development in mouse models of cancers, where HK2 is highly expressed compared to

normal cells [9]. The results presented here suggest that the systemic deletion of HK2 will not interfere with the immune response towards such tumor cells.

Results and discussion

As mentioned, previous studies showed that in activated T cells HK2 is up-regulated more than other hexokinases which could mean it is more relevant for T cell function. We confirmed this observation using real time PCR showing that upon TCR activation of CD4 T cells, the expression of HK2 was up-regulated 25-40 fold compared to naïve cells, whereas HK1 was up-regulated only about 3 fold (Fig 6.1B). However, the absolute expression level of HK1 in activated cells was still higher than HK2. The other isoforms HK3 and HK4 were barely detectable either in resting or activated T cells. Of note, resting T cells showed only minimal levels of HK2, whereas, the expression of HK1 was readily detectable (Fig. 6.1A).

To ascertain if the dramatic up regulation of HK2 in activated T cells had physiological relevance compared to other hexokinases, mice were bred to delete the expression of the HK2 isoform specifically in T cells. The deletion was achieved by breeding CD4 Cre mice to HK2 flox/flox and homozygous pups (HK2 KO) were raised to maturity to evaluate and compare T cell responses to HK2 flox/flox animals (WT). The deletion of HK2 was confirmed by the absence of HK2 expression in enriched CD4 T cell populations after TCR stimulation in vitro as measured by RT-PCR (Fig. 6.1C). Interestingly, deletion of HK2 also resulted in elevated levels of HK1 mRNA (~3 fold) in resting cells. Additionally, the expression of HK3 also increased although levels were still minimal (Fig. 6.1C). These results were unexpected, since deletion of HK2 in several tumors did not result in elevated HK1 [9] indicating that T cells might depend less on HK2 and have compensatory mechanisms distinct from cancer cells.

Experiments were also done to measure the impact of HK2 deletion in T cell development and function. HK2 deletion showed no major effect on CD4 T cell development, as the number of single positive (SP) CD4 and Treg in the HK2 KO and WT mice in both the thymus and spleen showed no statistically significant differences (Fig. 6.2A, C). The number of SP CD8 T cells was only minimally increased in the thymus and not in the spleen. However, no significant difference in expression of TCR beta on SP CD8 T cell thymocytes was observed (Fig. 6.2B). Hence, HK2 might be dispensable for CD4 T cell development. It remains to be known why HK2 deletion has resulted in minimal changes in CD8 T cell numbers in the thymus. Curiously the deletion of HK2 in some other tissue does have consequences to their development. These tissues include heart, muscle and adipose tissue [10,11].

Additional experiments were done to measure the functional and metabolic consequences of HK2 deletion. Isolated CD4 T cells from KO and WT were TCR stimulated in vitro and responses were compared. Some modest differences were observed. Thus KO CD4 T cells generated approximately 1.5 fold greater proliferative responses to TCR stimulation compared to WT T cells (Fig. 6.3A). However, the response to activation measured by induction of phosphorylated AKT and the phosphorylation of S6 kinase (indicative of mTOR activity) revealed no significant differences between WT and KO cells (Fig. 6.3B, C). In addition, no significant differences were observed when

cells from KO and WT were differentiated in vitro into Th1, Th17 and Treg populations (Fig. 6.3D).

The explanation for the higher proliferative response in KO CD4 T cells was not resolved but it could relate to suppressive effects that HK2 may have on mitochondrial function. Thus, activated T cells from HK2 KO animals displayed around 2-fold higher mitochondrial ROS (mROS) production without affecting cellular ROS levels (Fig. 6.4A, B). Also, the increased mitochondrial ROS is associated with only moderate increase in mitochondrial membrane potential as measured my MitoTracker Red CM-H2Xros with little or no change in mitochondrial mass as measured by MitoTracker green (Fig 6.4C). This is in line with the observation in some cell lines and neurons that HK2 binds to mitochondria via voltage-dependent anion channels and control mitochondrial function by inhibiting mROS generation [12,13]. Moreover, T cells that lack the ability to generate mROS display reduced proliferation and activation [14]. In conclusion, deletion of HK2 induced mROS which might have led to a modest increase in the proliferation of CD4 T cells. Since intact mitochondrial function is critical for effective memory T cell responses [15], the effects of HK2 deletion on established memory T cells needs to be evaluated using an inducible Cre system in adult mice with existing memory responses.

With regard to metabolism, activated CD4 T cells from WT and HK2 KO mice showed similar levels of glycolysis and glycolytic capacity as measured by extracellular flux analysis (Fig. 6.4D). These data likely mean that the absence of HK2 was being compensated by other hexokinase isoforms. This finding was in contrast to the findings in some cancer cells where, deletion of HK2 did result in reduced proliferation and glycolysis [9,16]. Although, the mechanistic reasons for such disparities were not evaluated in this report, we speculate that HK1, whose levels were elevated in the absence of HK2 could compensate for the function that HK2 was performing in activating CD4 T cells.

Finally, the effects of HK2 deletion on the outcome of CD4 T cell function in vivo were assessed. Age and sex matched WT and HK2 KO animals were ocularly infected with HSV-1 and the severity of lesions of stromal keratitis were compared. The results revealed no significant differences in responses in the two groups. Thus lesions were of comparable severity and the number of T cells present in lesions was basically the same including the proportion of infiltrating Th1 and Treg. (Fig. 6.5A-C). Similar to the in vitro data, the number and frequency of Treg and IFN-γ producing CD4 T cells in the DLN were not significantly different, despite some increased proliferation of both of CD4 T cell subsets (effectors and regulators) as measured by Ki-67 staining (Fig. 6.5D, E). Conceivably, the disparity between increased proliferation, yet similar inflammatory reactions could mean that some of the proliferating T cells of HK2 KO animals were undergoing apoptosis, an issue that is being further evaluated. Of note, the frequency and the number of CD44 and CD62L expressing CD4 T cells in the DLN at day 15 pi remained unchanged (Fig. 6.6A). To measure if HK2 deletion had an effect on HSV-1 specific CD8 T cell responses (a CD4 helper cell dependent response)[17], a well-established footpad immunization model was used [18]. Cell suspensions of draining lymph nodes were stimulated with a gB peptide, which is the immuno-dominant peptide recognized by B6 mice [19]. The results, measured by the ICS assay for HSV specific IFN-gamma producing CD8 T cells, revealed no significant differences in responses by WT and HK2 KO animals (Fig. 6.6B). In addition since HK2 deletion was done using CD4

Cre mice, CD8 T cells and some subsets of APC would also be deficient of HK2. However, such potential effect did not affect the outcome of a virus specific CD8 T cell response.

Concluding Remarks

Our finding that HK2 function can be dispensed with for CD4 T cell function could come as welcome news to the cancer therapy field. Thus for some cancers targeting HK2 with inhibitory drugs is an objective [20]. Our results would argue that such therapy may not be accompanied by negative effects on CD4 T cell functions which are necessary for anti-microbial protection and in some cases for anti-tumor effects as well.

Materials and Methods

Ethics statement

This study was carried out in strict accordance with the recommendations in the Guide for the Care and Use of Laboratory Animals of the National Institutes of Health and guidelines of the Institutional Animal Care and Use Committee, and adhered to the ARVO Statement for the Use of Animals in Ophthalmic and Vision Research. The protocol was approved by the University of Tennessee Animal Care and Use committee (IACUC) (protocol approval numbers 1244). All procedures were performed under Tribromoethanol (Avertin) anesthesia, and all efforts were made to minimize suffering.

Mice and Virus

Female C57BL/6 mice were purchased from Harlan Sprague-Dawley, Inc. (Indianapolis, IN), CD4 Cre mice (C57BL/6 background) mice were purchased from Jackson laboratories and HK2 flox/flox (C57BL/6 background) were a kind gift from Dr. Nissim Hay (University of Illinois, Chicago)[9]. CD4 Cre mice were bred to HK2 flox/flox mice and the pups that were positive for Cre and homozygous for HK2flox/flox (confirmed by genotyping) were used as HK2 KO and mice that were homozygous for only HK2flox/flox and negative for Cre were used as WT controls for all the experiments. HSV-l RE strain was used in all procedures.

HSV-1 ocular infection and clinical scoring

Corneal infections of 5-6 week old mice were conducted as previously described [21]. Briefly, mice were anesthetized by intra peritoneal (i.p) injection of Tribromoethanol (Avertin). Mice were scarified on cornea with a 27-gauge needle, and a 3 μl drop containing $1x10^4$ PFU of HSV in 3μl volume was applied to the eye. The eyes were examined on different days post infection (dpi) with a slit-lamp biomicroscope (Kowa Company, Nagoya, Japan), and the clinical severity of keratitis of individually scored mice was recorded as previously described [21].

Footpad Infection with HSV-1

Footpad infections on WT and HK2 KO (5-6 week old) animals were done as previously described [22]. Briefly, mice were deep anesthetized as described above and 30μl of $4x10^5$ PFU HSV-1 KOS was subcutaneously injected in each hind footpad. Mice were sacrificed 4 days post infection and the draining popliteal lymph nodes for isolated for ICS assay.

Flow Cytometric Analysis

The single-cell suspensions obtained from corneal samples, draining cervical lymph nodes, Thymus and Spleen were stained for different cell surface molecules for fluorescence-activated cell sorting (FACS) analyses as described previously [23]. Proliferation assays were performed using Cell Trace Violet (CTV) labelled naïve CD4 T

cells (2 X 10^5 cells/well) from WT and HK2 KO stimulated with plate bound anti-CD3/CD28 Ab (1 µg/ml or 5 µg/ml) for 3 days. Naïve CD4 T cells (2 X 10^5 cells/well) were stimulated for 72 hours in the presence of IL-2 and later labelled with MitoSOX (5µM), CM-H2DCFDA (1.25µM), MitoTracker Red CM-H2Xros (100nM) or MitoTracker green (100nM) and incubated for 30 min followed by live/dead staining and cytometric measurement. For HSV-1 specific CD8 T cells responses, 1x10^6 single cell suspensions popliteal lymph node were stimulated in a 96 well U-bottom plate. Cell were either left unstimulated or stimulated with SSIEFARL peptide (1µg/ml), for 5 h at 37°C in 5% CO2 in the presence of Brefeldin A (10µg/ml) followed by ICS assay.

Reagents and antibodies.

CD4 (RM4-5), IFN-γ (XMG1.2), CD25 (PC61, 7D4), CD44 (IM7), Annexin-V, Foxp3 (FJK-16S), anti-CD3 (145-2C11), anti-CD28 (37.51), GolgiPlug (Brefeldin A) from either ebiosciences or BD biosciences. P-AKT (S473-SDRNR) from ebiosciences and P-S6 (S235/236-D57.2.2E) from cell signaling. Phorbol 12-myristate 13-acetate (PMA) and Ionomycin from sigma. Cell Trace Violet, Live/Dead Fixable Violet Dead Cell Stain Kit, MitoTracker Red CM-H2Xros, MitoTracker Green, MitoSOX and CM-H2DCFDA from Life Technologies. Recombinant IL-2, IL-12, IL-6 and TGF-β from R&D systems. Glucose free RPMI media (life technologies) was prepared using dialyzed FBS. HSV-1 gB498–505 peptide (SSIEFARL) was from Genscript.

Quantitative PCR (qPCR)

Taqman gene expression assays for HK1 (Hexokinase 1), HK2 (Hexokinase 2), HK3 (Hexokinase 3) and HK4 (Hexokinase 4) from Applied Biosystems were performed on using 7500 Fast Real-Time PCR system (Applied Biosystems) as described previously (18).

Purification of CD4+ T cells.

Naïve CD4+ T cells were purified using a mouse naïve CD4+ T cell isolation kit (Miltenyi Biotec, Auburn, CA). The purity was achieved at least to an extent of 90%.

In vitro Treg, Th17 and Th1 differentiation assays

Naïve CD4 T cells were isolated from splenocytes of WT and HK2 KO mice as described above. Th1, Th17 and Treg cells were differentiated as described previously with some modifications [21,24]. Briefly, 1×10^6 cells were cultured with plate bound anti-CD3/CD28 Ab (1 µg/ml) containing either Treg differentiating conditions: rIL-2 (100 U/ml) and TGFβ (5ng/ml) or Th1 differentiating conditions: IL-12 (5ng/ml) and anti-IL-4 (10 µg/ml) or Th17 differentiating conditions: IL-6 (25ng/ml) and TGFβ (5ng/ml) with anti-IL-4 (10 µg/ml) and anti-IFN-γ (10 µg/ml) for 5 days at 37°C in a 5% CO2 incubator. After 5 days, samples were re-stimulated with PMA and Ionomycin to measure Foxp3 expressing, IFN-γ and IL-17A producing CD4 T cells using flow cytometry.

OCR and ECAR measurement

Naïve CD4 T cells from WT and HK2 KO were activated for 3 days in the presence of anti-CD3/CD28 (1 µg/ml). 1×10^6 cells per well were plated on XF24 plate (Seahorse Bioscience). ECAR values were measured for glycolysis stress test using a Seahorse XF24 metabolic analyzer as previously described [23].

Statistical Analysis

Statistical significance was determined by Student's t-test. A P-value of <0.05 was regarded as a significant difference between groups: *P ≤ 0.05, **P ≤ 0.01, ***P ≤ 0.001. GraphPad Prism software (GraphPad Software) was used for statistical analysis.

References

1. Buck MD, O'Sullivan D, Pearce EL (2015) T cell metabolism drives immunity. Journal of Experimental Medicine 212: 1345-1360.
2. O'Neill LA, Kishton RJ, Rathmell J (2016) A guide to immunometabolism for immunologists. Nature Reviews Immunology.
3. Palmer CS, Ostrowski M, Balderson B, Christian N, Crowe SM (2015) Glucose metabolism regulates T cell activation, differentiation, and functions. Frontiers in immunology 6.
4. Michalek RD, Gerriets VA, Jacobs SR, Macintyre AN, MacIver NJ, et al. (2011) Cutting edge: distinct glycolytic and lipid oxidative metabolic programs are essential for effector and regulatory CD4+ T cell subsets. The Journal of Immunology 186: 3299-3303.
5. Marjanovic S, Eriksson I, Nelson BD (1990) Expression of a new set of glycolytic isozymes in activated human peripheral lymphocytes. Biochimica et Biophysica Acta (BBA)-Gene Structure and Expression 1087: 1-6.
6. Gerriets VA, Kishton RJ, Nichols AG, Macintyre AN, Inoue M, et al. (2015) Metabolic programming and PDHK1 control CD4+ T cell subsets and inflammation. The Journal of clinical investigation 125: 194-207.
7. Shi LZ, Wang R, Huang G, Vogel P, Neale G, et al. (2011) HIF1α–dependent glycolytic pathway orchestrates a metabolic checkpoint for the differentiation of TH17 and Treg cells. Journal of Experimental Medicine 208: 1367-1376.
8. Ardehali H, Yano Y, Printz RL, Koch S, Whitesell RR, et al. (1996) Functional Organization of Mammalian Hexokinase II RETENTION OF CATALYTIC AND REGULATORY FUNCTIONS IN BOTH THE NH-AND COOH-TERMINAL HALVES. Journal of Biological Chemistry 271: 1849-1852.
9. Patra KC, Wang Q, Bhaskar PT, Miller L, Wang Z, et al. (2013) Hexokinase 2 is required for tumor initiation and maintenance and its systemic deletion is therapeutic in mouse models of cancer. Cancer cell 24: 213-228.
10. Fueger PT, Heikkinen S, Bracy DP, Malabanan CM, Pencek RR, et al. (2003) Hexokinase II partial knockout impairs exercise-stimulated glucose uptake in oxidative muscles of mice. American Journal of Physiology-Endocrinology and Metabolism 285: E958-E963.
11. Katzen HM, Schimke RT (1965) Multiple forms of hexokinase in the rat: tissue distribution, age dependency, and properties. Proceedings of the National Academy of Sciences 54: 1218-1225.
12. Cheung EC, Ludwig RL, Vousden KH (2012) Mitochondrial localization of TIGAR under hypoxia stimulates HK2 and lowers ROS and cell death. Proceedings of the National Academy of Sciences 109: 20491-20496.
13. da-Silva WS, Gómez-Puyou A, de Gómez-Puyou MT, Moreno-Sanchez R, De Felice FG, et al. (2004) Mitochondrial bound hexokinase activity as a preventive antioxidant defense steady-state ADP formation as a regulatory mechanism of membrane potential and reactive oxygen species generation in mitochondria. Journal of Biological Chemistry 279: 39846-39855.

14. Sena LA, Li S, Jairaman A, Prakriya M, Ezponda T, et al. (2013) Mitochondria are required for antigen-specific T cell activation through reactive oxygen species signaling. Immunity 38: 225-236.
15. van der Windt GJ, O'Sullivan D, Everts B, Huang SC-C, Buck MD, et al. (2013) CD8 memory T cells have a bioenergetic advantage that underlies their rapid recall ability. Proceedings of the National Academy of Sciences 110: 14336-14341.
16. Anderson M, Marayati R, Moffitt R, Jen YJ (2016) Hexokinase 2 promotes tumor growth and metastasis by regulating lactate production in pancreatic cancer. Oncotarget.
17. Kumaraguru U, Suvas S, Biswas PS, Azkur AK, Rouse BT (2004) Concomitant helper response rescues otherwise low avidity CD8+ memory CTLs to become efficient effectors in vivo. The Journal of Immunology 172: 3719-3724.
18. Bonneau R, Jennings S (1989) Modulation of acute and latent herpes simplex virus infection in C57BL/6 mice by adoptive transfer of immune lymphocytes with cytolytic activity. Journal of virology 63: 1480-1484.
19. Hanke T, Graham FL, Rosenthal KL, Johnson DC (1991) Identification of an immunodominant cytotoxic T-lymphocyte recognition site in glycoprotein B of herpes simplex virus by using recombinant adenovirus vectors and synthetic peptides. Journal of virology 65: 1177-1186.
20. Ros S, Schulze A (2013) Glycolysis back in the limelight: systemic targeting of HK2 blocks tumor growth. Cancer discovery 3: 1105-1107.
21. Varanasi SK, Reddy PB, Bhela S, Jaggi U, Gimenez F, et al. (2017) Azacytidine treatment inhibits the progression of Herpes Stromal Keratitis by enhancing regulatory T cell function. Journal of Virology 91: e02367-02316.
22. Bhela S, Mulik S, Reddy PB, Richardson RL, Gimenez F, et al. (2014) Critical role of microRNA-155 in herpes simplex encephalitis. The Journal of Immunology 192: 2734-2743.
23. Varanasi SK, Donohoe D, Jaggi U, Rouse BT (2017) Manipulating Glucose Metabolism during Different Stages of Viral Pathogenesis Can Have either Detrimental or Beneficial Effects. The Journal of Immunology: ji1700472.
24. Jones LL, Alli R, Li B, Geiger TL (2016) Differential T Cell Cytokine Receptivity and Not Signal Quality Distinguishes IL-6 and IL-10 Signaling during Th17 Differentiation. The Journal of Immunology 196: 2973-2985.

APPENDIX

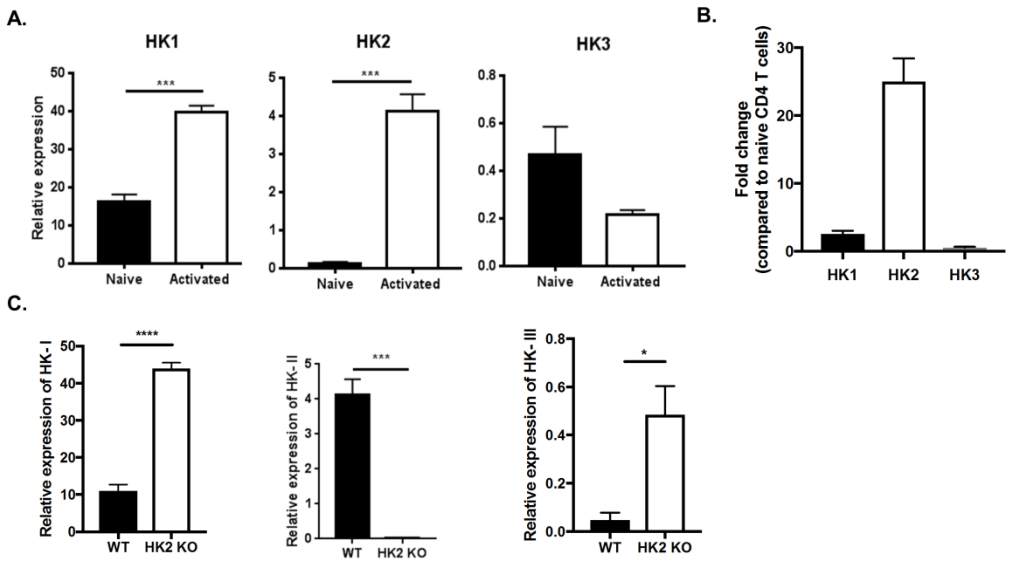

Figure 6.1. HK2 is up regulated upon CD4 T cell activation.
(A) Naive CD4 T cells purified from C57BL/6 mice were cultured (100,000 cells/well) with 1µg/ml anti-CD3/CD28 for 24 hours followed by gene expression analysis by QRT-PCR compared to beta-actin. Bar graph representing expression of HK1, HK2 and HK3 in naïve and activated cells. (B) Bar graph of fold change in gene expression in activated cells compared to naïve cells (C) Naïve CD4 T cells were purified from WT and HK2 KO mice were activated anti-CD3/CD28 for 24 hours. Bar graph representing gene expression of HK, HK2 and HK3 compared to beta-actin. Data represents means ± SEM from two independent experiments (n=3/group) P≤ 0.0001 (****), P≤0.001(***),P≤0.05(*).

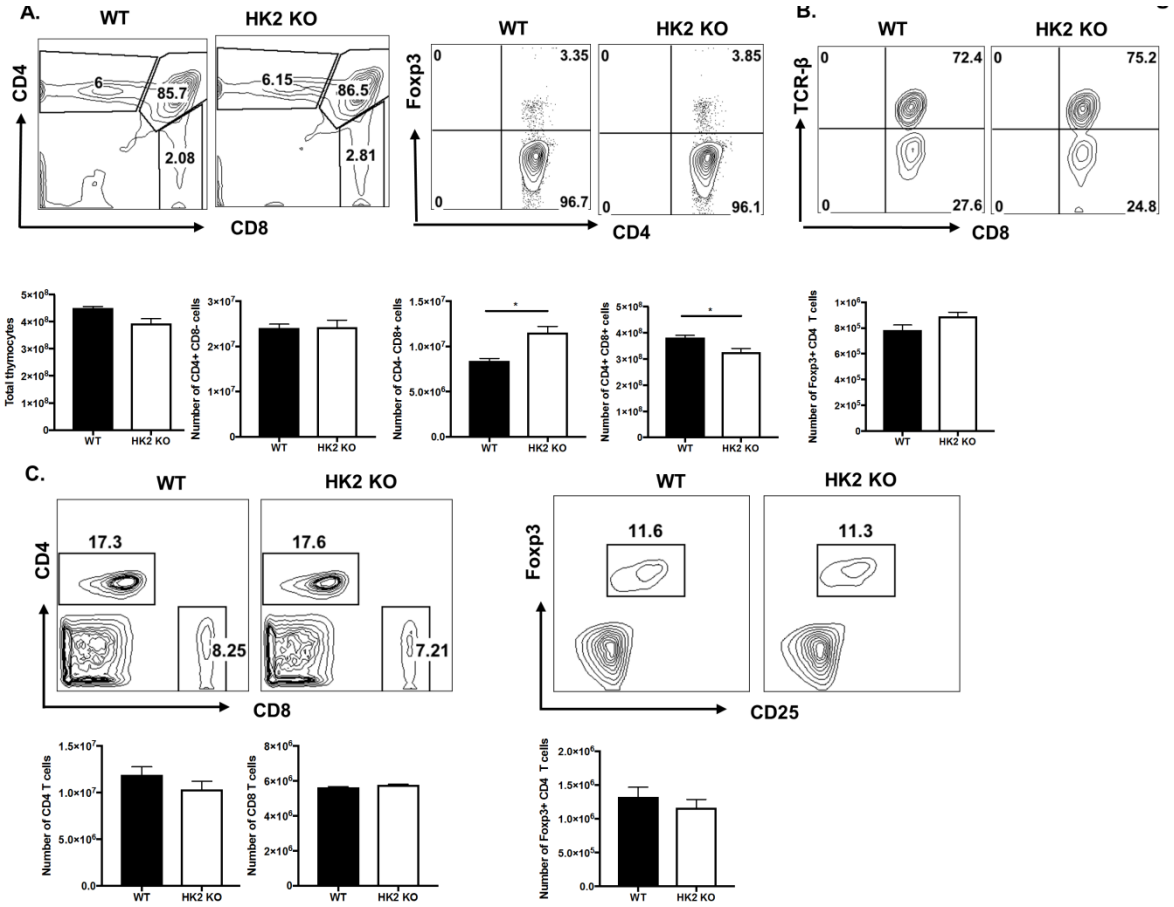

Figure 6.2. T cell specific HK2 deletion is dispensable for T cell development. Thymus and spleens from 5-6 week old naïve WT and HK2 KO animals were isolated. (A) Representative FACS plots and bar graph showing the frequency and number of total thymocytes, CD4+ CD8- T cells, CD4- CD8+ T cells, CD4+CD8+ T cells and CD4+CD8- Foxp3+ Treg cells in Thymus. (B) Representative FACS plot showing the TCR-beta expression gated on CD8+ CD4- T cells in the thymus. (C) Representative FACS plots and histogram showing the frequency and number of CD4+ CD8- T cells, CD4- CD8+ T cells and CD4+CD8- Foxp3+ Treg cells in Spleen. Gated on live cells. Data represents the mean ± SEM of more than 2 independent experiments (n=3 mice/group). P≤0.001(*)

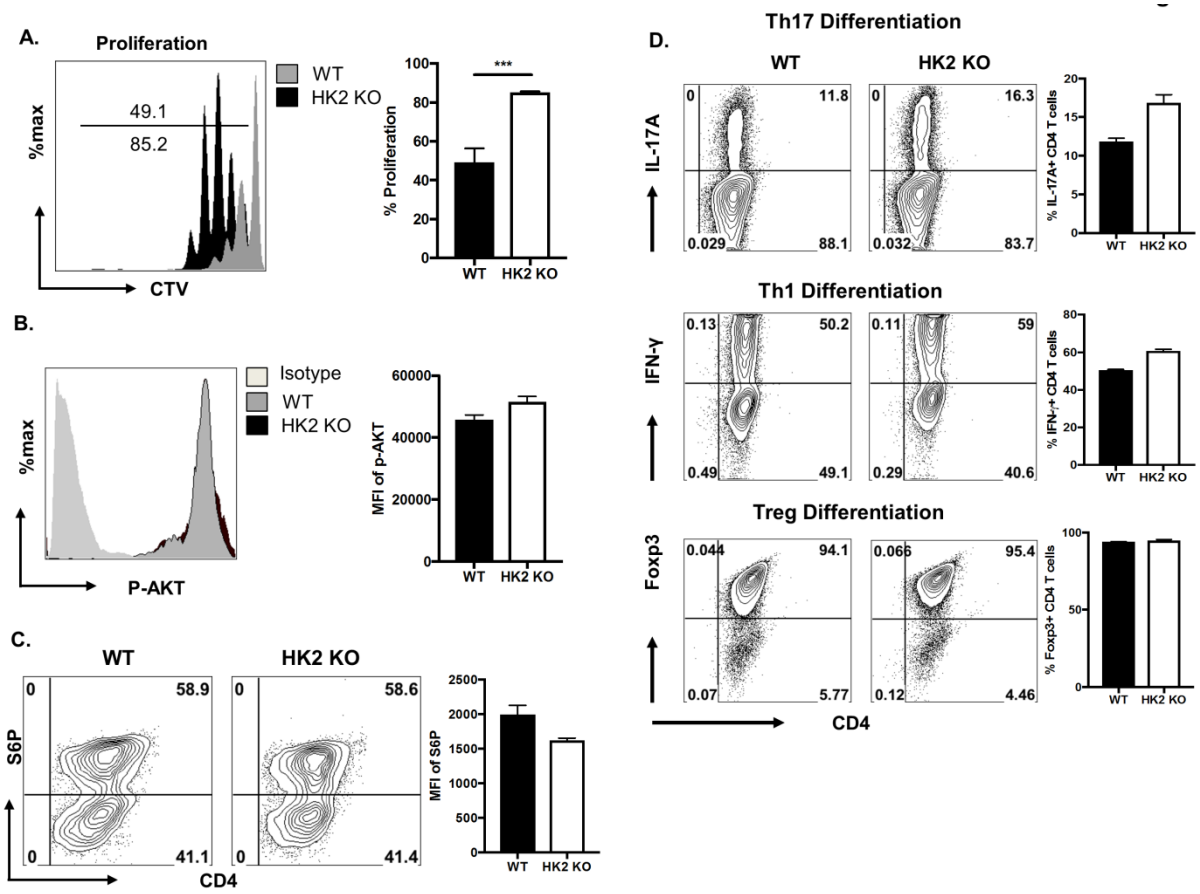

Figure 6.3. HK2 deletion increased CD4 T cell proliferation.
(A-C) Naïve CD4 T cells from WT and HK2 KO mice were CTV labelled and activated for 72 hours. (A) Representative FACS plots and bar graph indicating CTV dilution (as a measure of proliferation) gated on live CD4 T cells. Representative FACS plots and Histogram representing the levels of (B) phosphorylated–AKT and (C) Phosphorylated-S6 kinase. (D) Naïve CD4 T cells from WT and HK2 KO mice were cultured in the presence Treg or Th1 or Th17 differentiating conditions for 5 days followed by re-stimulation for 4 hours with PMA/Ionomycin. Histogram showing frequency of Th17, Th1 cells and Treg cells. All the measurements were made on live CD4 T cells. Data represents means ± SEM from two independent experiments (n=3/group) P≤0.001(***)

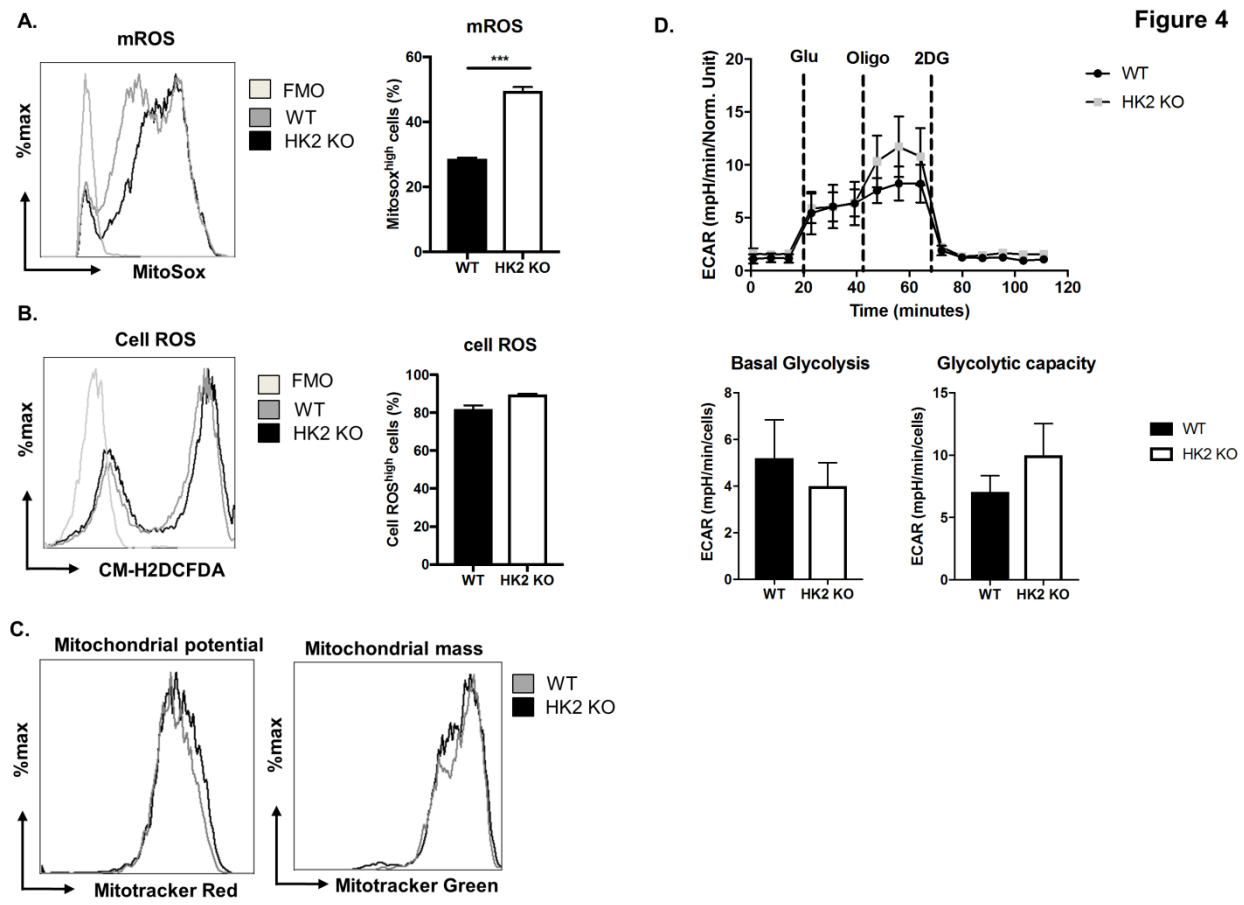

Figure 6.4. HK2 deletion in T cells had minimal effect on T cell glycolysis and T cell differentiation in vitro.

(A-C) Naïve CD4 T cells from WT and HK2 KO mice were activated for 72 hours. (A) mROS (MitoSOX high) producing cells, (B) Cellular ROS (CM-H2DCFDA) producing cells and (C) Mitrochondrial membrane potential (MitoTracker Red CM-H2Xros) and mitochondrial mass (MitoTracker Green). Data represents means ± SEM from three independent experiments (n=3/group). FMO, fluorescence minus one. (D) Naïve CD4 T cells were purified from WT and HK2 KO mice and cultured with 1µg/ml anti-CD3/CD28 for 72 hours. Line graph showing changes in Extracellular acidification rates (ECAR) following addition of glucose, oligomycin and 2DG and bar graph showing basal glycolysis, glycolytic capacity. n=6-8/group.

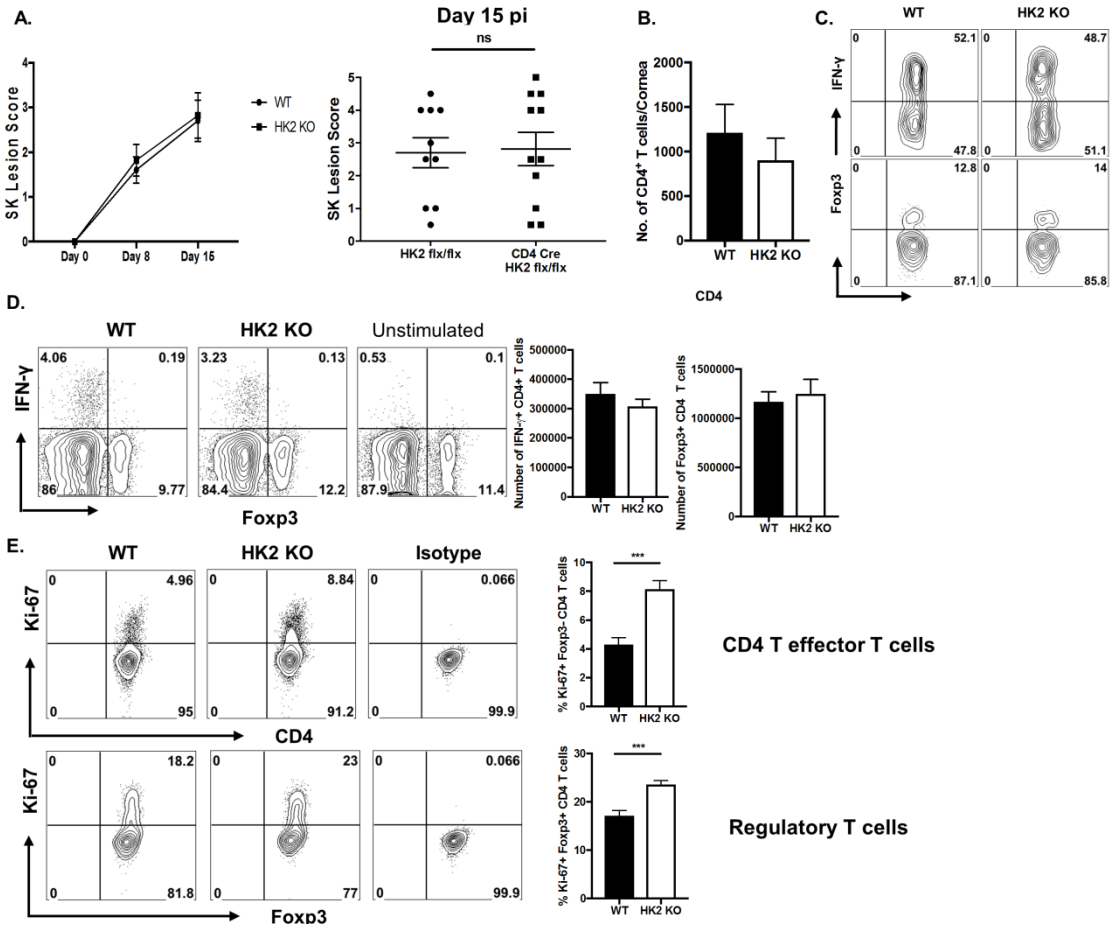

Figure 6.5. HK2 deletion displayed similar CD4 T cell responses upon ocular infection with HSV-1.

WT and HK2 KO animals were infected with 1 x 10^4 PFU of HSV-RE. (A) Individual eye scores of stromal keratitis lesion severity on day 15 pi. (B) Representative histogram showing the number of total CD4+ T cells infiltrating the cornea at day 15 p.i (C) Pool of corneas were stimulated with PMA/Ionomycin, representative histogram showing the number of Th1 (Live CD4+ IFN-γ) cells and Treg (Live CD4+ Foxp3) cells in the cornea at day 15 pi. (D) DLN were stimulated with PMA/Ionomycin, representative FACS plots and histogram showing frequency and number of Th1 (live CD4+ IFN-γ^{pos}) and Treg (live CD4+ $Foxp3^{pos}$). Gated based on the Unstimulated control. (E) Representative FACS plots and histogram showing frequency of proliferating (Ki-67^{pos}) effector (Live CD4+ $Foxp3^{neg}$) and regulatory T cells (Live CD4+ $Foxp3^{pos}$). Gated based on the Isotype. Data represents the mean ± SEM of more than 3 independent experiments (n=3-10 mice/group). P≤0.05(*).

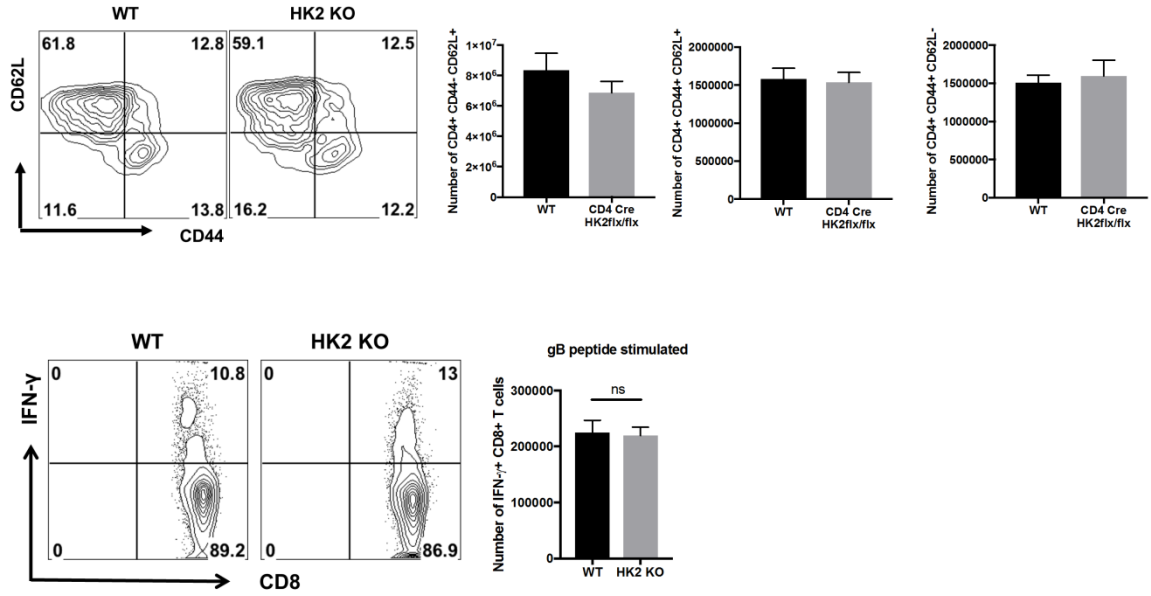

Figure 6.6. HK2 deletion in T cells had minimal effect on the expression of CD44 and CD62L on CD4 T cells after infection.

Representative FACS plots and bar graphs showing the frequency and number of activated (CD44+CD62L-), naïve (CD44-CD62L+) and memory CD4 T cells (CD44+CD62L+) in the DLN of WT and HK2 KO animals at day 15pi. Data represents means ± SEM from three independent experiments (n=3/group).

CHAPTER 7
CONCLUSIONS AND FUTURE DIRECTIONS

Herpetic stromal keratitis is the most common cause of infectious blindness in humans. Adaptive immune responses dominated by Th1 cells drives the immunopathology in the cornea whereas regulatory T cells (Treg) play a protective role. Thus approaches that rebalance the Treg to effector T cell ratio to emphasize Treg can have potential clinical benefits. However, the protection offered by Treg is often incomplete since they lose their regulatory functions, resulting in more severe lesions. Hence, we sought to trace the fate of the Treg phenotype and functionality after infection with HSV-1. Results indicated that upon ocular infection with HSV-1, Treg may become unstable and take on an effector phenotype. Thus about 50% of the Treg in the cornea that once expressed Foxp3 now became IFN-gamma or IL-17A expressing effector cells. The functional and phenotypic plasticity of Treg was observed predominantly by Treg that expressed low levels of the receptor for IL-2 (CD25). This plastic nature of CD25 low Treg can be explained by methylation changes which occurred in their TSDR region. The CD25 low Treg expressed a methylated TSDR region whereas CD25 hi Treg had a demethylated TSDR. Inhibiting methylation changes using DNA methyltransferase inhibitor-5-Azacytidine rescued the unstable Treg and the Treg population showed enhanced immunosuppressive functions. Consequently, treating animals with 5-Azacytidine from the time when lesions commenced resulted in reduced lesion severity.

We also show that Treg in the cornea are not only important for immune suppression but also are key components of tissue repair. Thus Treg in the cornea secreted a key tissue repair molecule called Amphiregulin (Amp). We identified that IL-18, a pro-inflammatory cytokine, can induce the expression of Amphiregulin by Treg. Moreover, enhancing levels of IL-18 in the cornea using an expression plasmid resulted in the increased representation of Amp Treg and more effective lesion control. Together these observations explain that enhancing Treg function and stability can be useful for better lesion control and repair.

Another novel approach to rebalance the Treg to effector ratio is by targeting their metabolic requirements. Results from our studies and others indicate that effector T cells, but not Treg mainly rely on glucose utilization for their function. Thus, inhibiting glucose utilization using 2-deoxy glucose (2DG) diminished the effector T cell responses, leaving Treg function intact and able to reduce lesion severity. However, when glucose utilization was inhibited from the time of infection, anti-viral immune responses, both innate and adaptive, were inhibited resulting in uncontrolled virus replication and death of animal. These observations highlight the importance of metabolic requirements especially glucose utilization by immune cells on the outcome of virus infection.

While our studies identified several new ways to control HSV induced immunopathology, future studies must focus on evaluating the effects of these inhibitors locally rather than systemic administrations. Local administration could reduce the off-target effects and unnecessary complications. Although the role of Amp in corneal tissue repair has been identified, the role of Treg specific Amp expression in cornea remains to be established. Thus, mice that lack Amp specifically in Treg could be used to evaluate such a role. In the current study, we highlighted the role of glucose utilization by immune cells during virus infections. However, future studies must focus on the understanding how other host metabolic pathways such as fatty acid and amino acid metabolism influence immune responses and thus the outcome of HSV infection.

Manipulating metabolism represents a viable new approach to control some virus infections. We have argued that metabolic differences between individuals can be one factor that explains the variable outcome of a virus infection. We also argue that manipulating metabolic events could be useful to influence the outcome of some virus infections. We also anticipate that the consequences of infection in each person may differ because of differential metabolic changes ongoing during infection. Should this be true then performing metabolic profiles on sick or perhaps even normal persons might help predict the outcome of their infection. If abnormal profiles are detected, especially in early infections or in uninfected persons as part of a personalized medicine workup, targeted therapies might be developed that restore normalcy. Finally, metabolic manipulation may find a place during vaccination. Accordingly, if optimal immunity depends on the magnitude of one or another component of immune memory, metabolic supplements might be used that shape induction of the required type of memory cells. We speculate that an approach worth exploring is to administer polyunsaturated fatty acids such as linoleic acid, a known FABP5 activator, at the vaccination site which would favor the expansion of TRM cells over the central memory population, a situation beneficial for mucosal infections. Just a note of caution: what is good to stop viruses may act in an opposite way against bacteria.

VITA

Siva Karthik Varanasi was born on April 29th, 1989, in Kuchipudi, India. He obtained his Bachelor of Science degree in Biotechnology from Osmania University, Hyderabad, India in 2009. He got his Master of Science in Biotechnology from Vellore Institute of Technology, Vellore, India in 2011. He then worked as a Research Associate in the Biological E Pvt Ltd, Hyderabad from 2012-2013. In 2013, he joined the lab of Dr. Barry T Rouse at University of Tennessee, Knoxville, TN and got his PhD in Genome Science and Technology in 2018.